

**PREDICTION OF WHOLE-BODY LIFTING KINEMATICS USING ARTIFICIAL NEURAL
NETWORKS**

Miguel A. Perez

Dissertation submitted to the faculty of the
Virginia Polytechnic Institute and State University
in partial fulfillment of the requirements for the degree of

DOCTOR OF PHILOSOPHY

In

Industrial and Systems Engineering

Dr. Maury A. Nussbaum, Chairman

Dr. Kari L. Babski-Reeves

Dr. Kevin P. Granata

Dr. Thurmon Lockhart

Dr. Michael L. Madigan

Dr. Xudong Zhang

August 15, 2005

Blacksburg, Virginia

Keywords: Kinematics Prediction, Lifting, Artificial Neural Network, Modeling

Copyright 2005, Miguel A. Perez

Prediction of Whole-body Lifting Kinematics using Artificial Neural Networks

Miguel A. Perez

(ABSTRACT)

Musculoskeletal pain and injury continue to be prevalent sources of disability for thousands of workers in the U.S. every year. Proactive approaches to the reduction of this incidence attempt to prevent the injury by effecting task design so that human capabilities and limitations are driving factors in the task design and analysis process. Knowledge about the posture and kinematics that might be employed by an individual in performing a task is an important element of these proactive approaches to task design and analysis, especially for manual materials handling (i.e., lifting) exertions. In turn, accurate models that predict posture and kinematics can reduce the need for empirical postural and kinematic data in this task development process. Artificial neural networks were used in this investigation to achieve these predictions. As input, these networks received information about lift characteristics (e.g. target location, movement duration) and returned a predicted set of joint angles. Two types of networks were created, one to predict static posture based on target position, the second to predict the time histories of several joint angles (i.e., kinematics) as an object is lifted or lowered. Initial networks were created for sagittally symmetric lifts (two dimensions), but the final set of networks was expanded to make predictions for symmetric and asymmetric lifts in three dimensions. Networks were trained and verified with an empirical set of non-cyclic lifting motions. Notably, the within-subject variability in these motions was similar in magnitude to the associated between-subjects variability. In general, the networks were able to assimilate the data relatively well, especially in predicting kinematics, where root mean square errors were typically smaller than 20 degrees. These errors were similar in magnitude to the levels of within-subject variability observed in the dataset. Network performance also compared favorably to other existing models, typically resulting in smaller prediction errors than these other approaches. In addition, the internal connections of trained networks were examined to infer hypothetical motor control strategies. Results of this examination showed that feedback was an important

component in providing kinematic predictions, whereas posture prediction benefited greatly from knowledge about individual anthropometry. Finally, potential improvements to increase prediction accuracy are discussed. Overall, these results support the use of artificial neural network models to predict posture and kinematics for lifting tasks.

DEDICATION

To God, for giving me life.

To my parents, for nurturing that life.

To my wife, for loving me as much as anybody possibly could, and in the process being a constant source of inspiration and strength.

To my friends, who I consider family.

To my father-in-law, for teaching me that I could enjoy life without working, because when you love your job, it is never work.

To people, because in understanding and explaining their individuality I find the constant challenge and inspiration that allow me to never have worked a day of my life.

ACKNOWLEDGMENTS

To Dr. Nussbaum, my committee chair, words cannot describe my level of appreciation for your guidance, encouragement, and commitment. I am honored to have you as an advisor, mentor, and friend.

My heartfelt thanks go to all the members of my advisory committee for their time and effort. The questions you posed served as an inspiration for much of this document and made this the most challenging and fruitful learning experience of my young career. You are not only wonderful scholars but also wonderful people, and I'm proud to be able to call you friends.

Thanks to the HUMOSIM laboratory of The University of Michigan and its director, Dr. Don Chaffin, for generously providing the data that was used in this investigation and a copy of the 3DSSPP™ software package. Special thanks go to Chuck Woolley, a researcher at the HUMOSIM laboratory, for quickly and patiently answering all my questions about the data.

I also want to thank Dr. Ulrich Raschke for providing the Industrial Ergonomics laboratory with a version of the Jack™ software package and for his comments on various versions of this document. Your willingness to give up some of your busy schedule to help me out is very much appreciated.

To all my friends (you know who you are), thanks for your encouragement, support, and comic relief when it was sorely needed. I cannot think of a better group of people to have shared this experience with. I will do my best to return the favor.

Myra, this would not have been possible without your love, sacrifice, support, and encouragement. I will spend the rest of my life thanking you for all of this, and be a happy man while doing so.

Finally, to the 20 people who gave of their time and effort in providing the data that was used to complete this investigation. Needless to say, none of this would have been possible without them.

TABLE OF CONTENTS

CHAPTER 1	INTRODUCTION.....	1
1.1	MOTIVATION.....	1
CHAPTER 2	LITERATURE REVIEW.....	5
2.1	OCCUPATIONAL MUSCULOSKELETAL INJURIES.....	5
2.1.1	<i>The challenging problem of musculoskeletal injuries.....</i>	5
2.1.2	<i>The relationship between motion characteristics and WMSDs as a function of body segment.....</i>	6
2.1.2.1	Neck and Shoulders.....	6
2.1.2.2	Upper Extremities.....	7
2.1.2.3	Low-Back.....	9
2.1.2.4	Other structures.....	10
2.1.3	<i>Theories on causes of musculoskeletal injury.....</i>	10
2.2	MODELING AS A TOOL TO PREDICT MUSCULOSKELETAL INJURY.....	13
2.2.1	<i>Neuromechanical Models.....</i>	13
2.2.2	<i>Risk allocation models.....</i>	15
2.2.3	<i>Past approaches to modeling motion.....</i>	16
2.2.3.1	Control Theory.....	18
2.2.3.2	Mechanical Models.....	21
2.2.3.3	Inverse Kinematics.....	22
2.2.3.4	Optimization.....	25
2.2.3.5	Optimization-aided Inverse Kinematics.....	28
2.2.3.6	Inverse Dynamics.....	31
2.2.3.7	Artificial Neural Networks (ANNs).....	31
2.2.3.8	Fuzzy Logic.....	34
2.2.3.9	Simulation environments.....	35
2.2.4	<i>Contrasting among previously used motion prediction approaches.....</i>	36
CHAPTER 3	LIFT MOTION MODIFIERS.....	39
3.1	BIOMECHANICAL MODIFIERS.....	39
3.1.1	<i>Lift Style.....</i>	40
3.1.2	<i>Lift Velocity and Lift Frequency.....</i>	41
3.1.3	<i>Lift Asymmetry.....</i>	43
3.1.4	<i>Other Lift Characteristics.....</i>	43
3.1.5	<i>Use of tools and other devices.....</i>	43
3.1.6	<i>Load magnitude.....</i>	44
3.1.7	<i>Distance to load.....</i>	45
3.1.8	<i>Injury.....</i>	45
3.2	PSYCHOLOGICAL FACTORS.....	45
3.2.1	<i>Training and experience.....</i>	46
3.2.2	<i>Behavioral approaches.....</i>	46
3.3	PSYCHOPHYSICAL FACTORS.....	47
3.4	ACCOUNTING FOR HUMAN VARIABILITY IN MOTION PREDICTION MODELS: A PRESCRIPTION FOR REALISTIC MODELS.....	48
3.4.1	<i>Inter- and intra-person variability in motion prediction models.....</i>	49
3.4.1.1	Inter-person variability.....	50
3.4.1.2	Intra-person variability.....	52
3.4.1.3	Implications of accounting for inter- and intra-person variability.....	54
3.5	STRATEGIES FOR INCLUSION OF LIFT MOTION MODIFIERS IN MOTION PREDICTION MODELS.....	55
CHAPTER 4	RESEARCH OBJECTIVES.....	57
CHAPTER 5	MOTION SIMULATION DATABASE.....	59
5.1	DATA PROCESSING.....	62
5.2	QUANTIFICATION OF INTER- AND INTRA-SUBJECT VARIABILITY WITHIN THE HUMOSIM DATABASE.....	64
5.2.1	<i>Two Dimensions.....</i>	64

5.2.2	<i>Three Dimensions</i>	70
5.3	SYNTHESIS OF DATABASE PROCESSING.....	77
CHAPTER 6	SIMULATING MOVEMENTS FOR AN INDIVIDUAL	80
6.1	PREDICTING JOINT POSITIONS	81
6.1.1	<i>Two-dimensions</i>	81
6.1.1.1	Determining the inputs of the ANNs.....	81
6.1.1.2	Creating the ANNs.....	82
6.1.1.3	Results	89
6.1.1.4	Training with more than one movement	92
6.1.2	<i>Three-dimensions</i>	92
6.1.2.1	Results	97
6.1.2.2	Training with more than one movement	101
6.1.3	<i>Implications of Results for an Unconstrained Network Structure</i>	101
6.2	PREDICTING JOINT ANGLES.....	102
6.2.1	<i>Two dimensions</i>	103
6.2.1.1	Results	105
6.2.1.2	Implications of results.....	111
6.2.1.3	Results for an extended training dataset.....	111
6.2.1.4	Implications of results – Training with an extended dataset	114
CHAPTER 7	PREDICTING INITIAL AND FINAL POSTURES.....	117
7.1	INTRODUCTION.....	117
7.2	METHODS	117
7.2.1	<i>Lift Modifier Factors</i>	117
7.2.1.1	Anthropometry	117
7.2.1.2	Biomechanical factors.....	118
7.2.1.3	Behavioral and psychophysical factors	119
7.2.2	<i>Two Dimensions</i>	119
7.2.3	<i>Three Dimensions</i>	123
7.3	RESULTS.....	125
7.3.1	<i>Two Dimensions</i>	125
7.3.2	<i>Three Dimensions</i>	131
7.4	MODEL CHARACTERIZATION	146
CHAPTER 8	SIMULATING MOVEMENTS ACROSS INDIVIDUALS	173
8.1	INTRODUCTION.....	173
8.2	METHODS AND RESULTS	173
8.2.1	<i>Two dimensions</i>	173
8.2.1.1	Results	176
First Training Set.....	176	
Second Training Set.....	180	
8.2.1.2	Implications of training dataset.....	186
8.2.2	<i>Three Dimensions</i>	188
8.2.2.1	Results	190
8.2.2.2	Implications of results for motions in three dimensions.....	201
8.3	MODEL CHARACTERIZATION	211
CHAPTER 9	CLOSING DISCUSSION.....	221
9.1	CONCLUSIONS AND FURTHER RESEARCH.....	230
CHAPTER 10	REFERENCES.....	234

LIST OF FIGURES

Figure 1. Inverse kinematics attempts to mathematically derive the set of angles θ_1 and θ_2 that would result in the end-effector reaching position \mathbf{x} .	23
Figure 2. Layers of artificial neurons, from the input layer to the output layer, are interconnected in an ANN.	32
Figure 3. Illustration of recursive connections in a recurrent ANN.	34
Figure 4. Stick figure representation of a posture. These representations were visually inspected to verify the appropriateness of start and stop points. All distances are in centimeters.	63
Figure 5. Joint angle time history for a movement that brings back the load from the lower near location. Each line represents a different participant.	66
Figure 6. Joint angle time history for the shoulder joint during a movement that brings back the load from the lower near location. The gray lines show individual traces for each subject.	67
Figure 7. Joint angle time history for the shoulder joint during a movement that brings back the load from the lower near location. Black lines show the average and standard deviation between-subjects; gray lines show the average and standard deviation within-subject.	69
Figure 8. Joint angle time history for a movement that brings back the load from the lower near location. Alpha and Beta represent the two Euler angles used to describe the posture of each joint.	71
Figure 9. Initial two-dimensional network structure, based on a Jordan-Elman network. Although all layers are fully interconnected, some connections are omitted for clarity. A detailed diagram of the connections within the dashed-line box is presented in Figure 10. Boxes with 'D' represent a single time delay.	83
Figure 10. Detail of connections for the joint locations layer. Note that this diagram represents a detail of Figure 9.	85
Figure 11. Time sequence for the first simulated movement. The sequence proceeds from left to right and top to bottom. Markers indicate the different joints and/or surface marker positions.	88
Figure 12. Error temporal pattern for the simulated movement.	89
Figure 13. Root mean square error by joint and direction of movement.	90
Figure 14. Root mean square error normalized for joint travel distance by joint and direction of movement.	91
Figure 15. Comparison of the predicted (stick figure) and input (hollow diamonds) end posture. Note that the network still simulates the training movement, even when the inputs to the network indicate a lower end location.	92
Figure 16. Initial three-dimensional network structure, based on a Jordan-Elman network. Although all layers are fully interconnected, some connections are omitted for clarity. A detailed diagram of the connections within the dashed-line box is presented in Figure 17.	93
Figure 17. Detail of connections for the joint locations layer. Note that this diagram represents a detail of Figure 16.	94
Figure 18. Time sequence for the first movement, which required overhead lifting. Markers indicate the different joints and/or surface marker positions.	95
Figure 19. Time sequence for the second movement, which required a lateral transfer. Markers indicate the different joints and/or surface marker positions.	96
Figure 20. Error temporal pattern for movement 1 (a) and movement 2 (b).	97

Figure 21. Root mean square error by joint and direction of movement. These data correspond to the first network.	98
Figure 22. Root mean square error corrected for joint travel distance by joint and direction of movement. These data correspond to the first network. Values for the left ball of foot are not presented as this joint was fixed in space throughout the trial.	99
Figure 23. Root mean square error by joint and direction of movement. These data correspond to the second network.	99
Figure 24. Root mean square error corrected for joint travel distance by joint and direction of movement. These data correspond to the second network. Values for the left ball of foot are not presented as this joint was fixed in space throughout the trial.	100
Figure 25. Comparison of the predicted (stick figure) and input (hollow diamonds) end postures for the first network. Note that the network still simulates the training movement, even when the inputs to the network indicate a lower end location.	101
Figure 26. Two-dimensional network structure using joint angles as the input and prediction basis. Although all layers are fully interconnected, some connections are omitted for clarity. Boxes with 'D' represent a single time delay. The 'x 10' next to two of the inputs indicates that each of these nodes represents ten different inputs (each corresponding to one of the outputs). The dashed box indicates components of a conversion process that was not coded within the network (see text for details).	104
Figure 27. Time sequences for the three movements used in network training. Note that the movements are qualitatively different in their requirements. Markers indicate the different joints and/or surface marker positions.	105
Figure 28. Error temporal pattern for movement 1 (a), movement 2 (b) and movement 3 (c)..	106
Figure 29. Root mean square error by joint and direction of movement. These data correspond to the first training movement.	107
Figure 30. Root mean square error by joint and direction of movement. These data correspond to the second training movement.	108
Figure 31. Root mean square error by joint and direction of movement. These data correspond to the third training movement.	108
Figure 32. Comparison of the predicted (stick figure) and input (hollow diamonds) end postures for the best (a) and worst (b) predicted novel movements.	110
Figure 33. Error temporal pattern for the 19 movements from the same participant that were used for training.	112
Figure 34. Root mean square error by joint and direction of movement for the 19 movements.	113
Figure 35. Time sequence for the same movement performed by two anthropometrically similar participants. Markers indicate the different joints and/or surface marker positions.	114
Figure 36. Network structure used for initial and final 2-D posture predictions.	120
Figure 37. Network structure used for initial and final 3-D posture predictions.	123
Figure 38. Comparison of predicted posture (stick figure) and actual posture (joint positions are represented by hollow diamonds) for training cases where maximum (a) and minimum (b) rmse levels were observed.	130
Figure 39. Comparison of predicted posture (stick figure) and actual posture (joint positions are represented by hollow diamonds) for training cases where maximum (a) and minimum (b) rmse levels were observed.	143
Figure 40. Joint angle predictions as a function of box position.	149

Figure 41. Joint angle predictions as a function of box position with a low strength input.	150
Figure 42. Joint angle predictions as a function of box position with a high strength input.	151
Figure 43. Joint angle predictions as a function of inferior-superior box position. The dashed line represents a low strength input (-4), the solid thin line a neutral strength input (0), and the solid wide line a high strength input (+4).	152
Figure 44. Joint angle predictions as a function of inferior-superior box position. The dashed line represents a low first anthropometry input (-8), the solid thin line a neutral one (0), and the solid wide line a high one (+8).	153
Figure 45. Joint angle predictions as a function of inferior-superior box position. The dashed line represents a low second anthropometry input (-4), the solid thin line a neutral one (0), and the solid wide line a high one (+4).	154
Figure 46. Joint angle predictions as a function of inferior-superior box position. The dashed line represents a low third anthropometry input (-4), the solid thin line a neutral one (0), and the solid wide line a high one (+4).	155
Figure 47. Joint angle predictions as a function of inferior-superior box position. The dashed line represents a low fourth anthropometry input (-4), the solid thin line a neutral one (0), and the solid wide line a high one (+4).	156
Figure 48. Comparison between target (light gray) and predicted (dark grey) between-subject variability. The shaded regions correspond to a ± 1 standard deviation region around the between-subjects mean for each group.	159
Figure 49. Comparison between target (light gray) and predicted (dark grey) between-subject variability. The shaded regions correspond to a ± 1 standard deviation region around the between-subjects mean for each group. The figure continues on the next page.	164
Figure 50. Comparison between target (light gray) and predicted (dark grey) between-subject variability. The shaded regions correspond to a ± 1 standard deviation region around the between-subjects mean for each group. The figure continues on the next page.	166
Figure 51. Comparison between target (light gray) and predicted (dark grey) between-subject variability. The shaded regions correspond to a ± 1 standard deviation region around the between-subjects mean for each group. The figure continues on the next page.	168
Figure 52. Two-dimensional network structure using joint angles as the input and prediction basis. Although all layers are fully interconnected, some connections are omitted for clarity. Boxes with 'D' represent a single time delay. The 'x 10' next to two of the inputs indicates that each of these nodes represents ten different inputs (each corresponding to one of the outputs). The 'x 4' next to the anthropometry modifier input indicates that there are four of those inputs in the network.	174
Figure 53. Root mean square error by joint and direction of movement. Training dataset.	177
Figure 54. Root mean square error by joint and direction of movement. Verification dataset.	178
Figure 55. Root mean square error by joint and direction of movement. Training dataset.	181
Figure 56. Root mean square error by joint and direction of movement. Verification dataset.	182
Figure 57. Root mean square error by joint and direction of movement. Verification dataset.	184
Figure 58. Root mean square error by joint and direction of movement. Verification dataset.	185
Figure 59. Comparison between target (light gray) and predicted (dark grey) between-subject variability. The shaded regions correspond to a ± 1 standard deviation region around the between-subjects mean for each group.	187
Figure 60. Three-dimensional network structure using joint angles as the input and prediction basis. Although all layers are fully interconnected, some connections are omitted for	

clarity. Boxes with ‘D’ represent a single time delay. The ‘x 36’ next to four of the inputs indicates that each of these nodes represents thirty-six different inputs (each corresponding to one of the outputs). 189

Figure 61. Root mean square error by joint and direction of movement. Training dataset. 192

Figure 62. Root mean square error by joint and direction of movement. Verification dataset. 194

Figure 63. Root mean square error by joint and direction of movement. Verification dataset. 195

Figure 64. Root mean square error by joint and direction of movement. Verification dataset. 197

Figure 65. Comparison between target (light gray) and predicted (dark grey) between-subject variability. The shaded regions correspond to a ± 1 standard deviation region around the between-subjects mean for each group. No Rotation. 203

Figure 66. Comparison between target (light gray) and predicted (dark grey) between-subject variability. The shaded regions correspond to a ± 1 standard deviation region around the between-subjects mean for each group. Medium Rotation..... 205

Figure 67. Comparison between target (light gray) and predicted (dark grey) between-subject variability. The shaded regions correspond to a ± 1 standard deviation region around the between-subjects mean for each group. High Rotation. 207

Figure 68. Comparison between target (light gray) and predicted (dark grey) between-subject variability. The shaded regions correspond to a ± 1 standard deviation region around the between-subjects mean for each group. No Rotation. 209

Figure 69. Hidden unit input distributions for inputs that are not delayed (Two dimensions).. 212

Figure 70. Hidden unit input distributions for inputs that have a single time-step delay (Two Dimensions). 213

Figure 71. Hidden unit input distributions for inputs that have a double time-step delay (Two Dimensions). 214

Figure 72. Hidden unit input distributions for inputs that are not delayed – Part 1 (Three dimensions). 215

Figure 73. Hidden unit input distributions for inputs that are not delayed – Part 2 (Three dimensions). 216

Figure 74. Hidden unit input distributions for inputs that have a single time-step delay (Three Dimensions). 217

Figure 75. Hidden unit input distributions for inputs that have a double time-step delay (Three Dimensions). 218

LIST OF TABLES

Table 1. Available anatomical locations.....	61
Table 2. Maximum standard deviation for each joint angle and movement location, calculated across time samples.....	67
Table 3. Maximum within-subject standard deviation for each joint angle, calculated across time samples. Italicized cells indicate smaller within-subject variability than between-subjects variability (as shown in Table 2).	68
Table 4. Maximum between-subjects standard deviation for each joint angle, calculated across time samples.....	73
Table 5. Maximum within-subject standard deviation for each joint angle, calculated across time samples. Italicized cells indicate smaller within-subject variability than between-subjects variability (as shown in Table 4).	75
Table 6. Statistical results for comparisons of maximum standard deviation across time samples for the 3-D case. Italicized p-values indicate significant effects.	77
Table 7. Strength coefficient parameters.	120
Table 8. Anthropometry coefficient parameters.	122
Table 9. Root mean square errors for the posture prediction network using the training and generalization postures.....	126
Table 10. Prediction root mean square errors by participant and joint. Italicized values are separated from the mean rmse for each joint by more than two standard deviations.	128
Table 11. Prediction root mean square errors by movement location and joint. Italicized values are separated from the mean error for each joint by more than two standard deviations. LL-Lower Location, MLL-Middle Lower Location, ML-Middle Location, MUL-Middle Upper Location, UL-Upper Location. Locations combine errors for both Deliver and Bring Back movements, since only static postures were considered.	129
Table 12. Root mean square error (in degrees) by subject, split in training and generalization groups.....	131
Table 13. Prediction root mean square errors for the posture prediction network using the training and three generalization datasets.	133
Table 14. Prediction root mean square errors by participant and joint. Italicized values are separated from the mean error for each joint by more than two standard deviations. The table is continued on the next three pages.	135
Table 15. Prediction root mean square errors by movement location and joint. Italicized values are separated from the mean error for each joint by more than two standard deviations. LL-Lower Location, MLL-Middle Lower Location, ML-Middle Location, MUL-Middle Upper Location, UL-Upper Location. Locations combine errors for both Deliver and Bring Back movements, since only static postures are considered. The table is continued on the next three pages.	139
Table 16. Root mean square error (in degrees) by subject, split in training and generalization groups.....	144
Table 17. Prediction root mean square errors for the posture prediction network and the 3DSSPP™ simulation environment.	145
Table 18. Prediction root mean square errors for the posture prediction network and the Jack™ simulation environment.	146

Table 19. Network rmse (calculated across joint, tasks, and subjects) in comparison to observed average between- and within-subject variability. Maximum values are italicized. All quantities are in degrees.....	157
Table 20. Network rmse (calculated across joint, tasks, and subjects) in comparison to observed average between- and within-subject variability. Maximum values are italicized. All quantities are in degrees.....	161
Table 21. Rmse levels across Movement Location. Training dataset.....	177
Table 22. Rmse levels across Movement Location. Verification dataset.....	179
Table 23. Root mean square error (in degrees) by subject, split in training and generalization groups.....	180
Table 24. Rmse levels across Movement Location. Training dataset.....	181
Table 25. Rmse levels across Movement Location. Verification dataset.....	183
Table 26. Rmse levels across Movement Location. Verification dataset.....	185
Table 27. Network root mean square error (first training set) in comparison to observed average between- and within-subject variability. All numbers are expressed in degrees. Maximum values are italicized.....	186
Table 28. Rmse levels across Movement Location. Training dataset.....	193
Table 29. Rmse levels across Movement Location. Verification dataset.....	194
Table 30. Rmse levels across Movement Location. Training dataset.....	196
Table 31. Rmse levels across Movement Location. Verification dataset.....	197
Table 32. Root mean square error (in degrees) by subject, split in training and generalization groups.....	198
Table 33. Average network error in comparison to observed average for the Jack™ simulation environment.....	200
Table 34. Average network error in comparison to observed average between- and within-subject variability. Maximum values are italicized.....	202

Chapter 1 INTRODUCTION

1.1 Motivation

The physical interaction of people with their surroundings is constant and complex. As people sit, walk, lift boxes, sleep, or perform any other task, they must consciously or unconsciously perform physical actions, in the form of movements, to interact with their surroundings. These actions typically consist of coordinated muscle activations that impact the positions, velocities, and accelerations of various body parts and, consequently, the overall human posture at each point in time (i.e. human motion or movement).

Predicting human motion has become increasingly important as new software packages attempt to simulate the physical interaction between humans and their environment. Programs such as Jack™ (EDS, 2001), Deneb/ERGO™ (Delmia, 2001), and ANTHROPOS™ (Tecmath, 2001) assist designers by providing humanoids that can be manipulated and animated in a virtual environment. These tools allow task- and work-designers to create a digital mockup of working situations and make a variety of virtual humans interact with these mockups. The goal of this process is to discover problems in the human interaction with the proposed designs before these designs are built, thus reducing the risk of costly redesign processes and workforce injury.

Musculoskeletal injuries remain one of the primary occupational injury classifications in the United States (Baker and Landrigan, 1990; Dempsey and Hashemi, 1999; National Research Council, 1999), with associated costs in the hundreds of billions of dollars per year. The high costs of the injuries, combined with their high potential for disabling productive individuals, has motivated an ongoing variety of research towards understanding the causes of various musculoskeletal injuries (National Research Council, 1999). If these causes, or risk factors, are identified, then the incidence of their resultant injury can be minimized.

Risk factors that have been associated with occupational musculoskeletal injury are numerous, and vary depending on the body part (e.g. low back, upper extremity, neck). These factors may be work-related, such as magnitude of loads handled, repetitiveness of work, or posture (Radwin and Lavender, 1999), or individual aspects, such as gender, physical conditions, or genetic composition (Faucett and Werner, 1999). These risk factors are very likely not independent, and some researchers have attempted to develop theories that describe their interactions (Kumar, 2001; Marras, 2000).

Among work-related risk factors, body posture and motion have been repeatedly identified in several investigations. Extreme postures have been recognized as a primary risk factor for musculoskeletal injuries in many different body parts, including the low back (Anderson et al., 1987; Brulin et al., 1998; Caboor et al., 2000; Granata and Wilson, 2001; Hoozemans et al., 1998; Keyserling, 2000a; Vingard et al., 2000), upper extremity (Armstrong, 1986; Armstrong et al., 1982; Burgess-Limerick et al., 1999; Keyserling, 2000b; Matias et al., 1998), and neck/shoulder (Arndt, 1983; Brulin et al., 1998; Ekberg et al., 1994). The importance of posture as a risk factor lies in its three-fold effect. First, posture affects the external moment at a joint by changing the moment arm of the load. Second, posture modifies the strength of a particular joint by changing both the force that a particular muscle is able to exert (through the length-tension relationship, An et al., 1989; Kaufman et al., 1989; Lieber et al., 1994; van Schaik et al., 1994) and the moment arm of the muscle (Jorgensen et al., 2003; Murray et al., 1995). Third, posture has direct effects on the geometry of internal structures and, thus, on the amount and distribution of the internal loads on these structures (Delisle et al., 1997).

Given the identification of posture as a risk factor for musculoskeletal diseases, researchers have attempted to describe it using a variety of methods, both quantitative and qualitative, with the goal of establishing relationships between particular postures and the risk of musculoskeletal injury (e.g. Neumann et al., 2001). However, these efforts act as ‘secondary’ prevention, as an individual must already be repeatedly performing a task, and thus, be exposed to injury. Furthermore, overall costs of ergonomics in the operation under study increase, since a new redesign investment must be added to the original corporate investment to create the operation.

Thus, a better approach in musculoskeletal injury prevention when postural issues are considered may be to apply a proactive prevention approach, where an individual’s sequence of postures (i.e. movement) is predicted for a particular set of environmental and task conditions. In addition to assisting with injury prevention efforts, a predictive approach has the potential of reducing design costs since fewer (or no) physical prototypes of design options have to be built. While previous research and commercial efforts have addressed various aspects of this problem, there are areas of movement prediction where further improvements are needed.

One area is the prediction of movement when lifting during manual materials handling (MMH) operations, where the most common injuries occur to the low back. If the prediction is

achieved via a software package, the particular software package employed must, given the characteristics of the individual and the task, predict a movement that is likely to be used by the population of individuals that complies with the input characteristics. Several algorithm types (e.g. Beck and Chaffin, 1992; Byun, 1991; Dysart, 1994; Dysart and Woldstad, 1994, 1996; Gundogdu, 2000; Hsiang and McGorry, 1997; Jung and Park, 1997; Woldstad, 1997) have been proposed and implemented to address this prediction problem in the past, with advantages and disadvantages particular to each approach and various degrees of success.

The fact that musculoskeletal diseases are common occupational injuries in the United States (Baker and Landrigan, 1990; Campbell, 1999; Richter, 1998) suggests that further improvements in the design of work have to be achieved. One direction for improvement is in the tools used for motion prediction in human simulation software, in the context of manual materials handling. This investigation will attempt to advance the state of lifting motion prediction tools by applying an Artificial Neural Network (ANN) approach. ANNs are mathematical structures that are capable of learning through the collective modification of weights that interconnect a series of nodes. These weights, combined with a variety of node output behaviors, allow neural networks to emulate, in theory at least, any dataset that exhibits some pattern of regularity.

In the process of constructing a lifting motion prediction modeling tool that is based on ANNs, this document examines in more detail the extent of the occupational musculoskeletal injury problem, the evolution of posture and movement prediction algorithms, and, within the context of variability sources, a number of motion and posture modifiers that should be considered by these algorithms in the context of lifting exertions. Advantages and disadvantages of employing ANNs as prediction tools are presented. The development work to create an ANN that predicts motion in a lifting context is also presented in its evolutionary phases. Through this development process, networks are evaluated based on various aspects of their performance. Structures within networks are also examined for any hypothetical higher order control mechanisms that may be inferred from the network's organization. Performance comparisons between the networks and other approaches are also considered. The goals of this investigation are to:

- Determine the important variables to consider for examination of lifting motions and obtain data of lifting exertions that vary subsets of these important variables.

- Define an artificial neural network structure that sufficiently predicts the available data.
- Create and train one or more networks that use the defined structure.
- Examine trained network architecture to develop hypotheses for generalized motor control.
- Compare the performance of best-performing networks against empirical data using novel performance indicators.

Chapter 2 LITERATURE REVIEW

2.1 Occupational musculoskeletal injuries

Despite considerable efforts to reduce the incidence of work-related musculoskeletal disorders (WMSDs) in the workplace, these injuries continue to result in the pain and suffering of thousands of Americans (BLS, 2003) and millions of people around the world. The World Health Organization reported that between 10% and 30% of the workforce in industrialized countries and between 50% and 70% of the workforce in developing countries may be exposed to a heavy physical workload or to poor ergonomic working conditions such as lifting and moving heavy items or repetitive manual tasks (WHO, 1995), which are primary causes for the development of WMSDs. While a decline in the number and incidence of work injuries has been reported, there were still hundreds of thousands of injuries due to repetitive trauma reported in the year 2002 (BLS, 2003). These numbers are staggering, and have served as the motivation for cataloguing the reasons for occurrence of these injuries and developing work design guidelines that result in their prevention and eventual elimination. The purpose of this section is to summarize what these reasons are, how they are theorized to relate to WMSDs, and how they can be used to predict the occurrence of these injuries.

2.1.1 *The challenging problem of musculoskeletal injuries*

Several reasons make the study of WMSDs a challenging field. First, the development of WMSDs is due to a variety of different factors that many times act concurrently, which limits the ability of researchers to pinpoint their relative contribution to the risk of WMSDs. Second, even if the onset of pain perception caused by a WMSD is sudden, its causal factors may not be. WMSDs may be a product of the gradual degradation of human tissue that results from repeated overuse of the tissue. Thus, the causal factors for the development of WMSDs may be temporally separated from the occurrence of the injury, which makes these factors hard to identify. Third, while a dose-response relationship between many risk factors and the risk of WMSD has been posited in numerous studies (e.g. Armstrong et al., 1993; Bernard et al., 1994; Bovenzi, 1994; Muggleton et al., 1999; Ohlsson et al., 1995), the relationship is usually weak and highly dependent on the type of body part and the risk factors under consideration. Only limited information is thus available to quantify the amount of risk each of these factors represents. Without such quantification, it is difficult for ergonomists to (1) allocate their limited resources into eliminating risk factors that cause the most harm, and (2) justify future

ergonomics improvement projects based on the economic savings that might be generated. Fourth, many different body parts can be affected by WMSDs, which results in a variety of clinical symptoms that can serve as indicators of WMSDs. Fifth, in some cases the particular cause of the pain cannot be determined. For example, in many cases of low-back pain, the anatomical structure or tissue that is responsible for the pain cannot be identified, even when using advanced imaging methods (Bogduk, 1995; Tulder et al., 1997). Three possibilities could account for this fact, possibly in interaction with each other. The first is that the visualization methods being used are not sensitive enough. The second possibility is that the measures are not observing the appropriate sources; the pain is being produced in a different body part that is not clinically suspected. The third possibility is that the reason for the pain may not be necessarily physical, but psychological. These three possibilities all represent active areas of WMSD research.

2.1.2 The relationship between motion characteristics and WMSDs as a function of body segment

The body segments where WMSDs are principally observed include the neck/shoulder area, the upper extremities, and the low back area. Each of these body parts has been the focus of a considerable degree of attention from the research community. Consequently, for each of these body parts there is a large body of literature describing the importance of various risk factors and suggesting potential alternatives for their elimination.

2.1.2.1 Neck and Shoulders

The neck and shoulders complex has received considerable attention, especially with the prevalence of visual display terminals (VDT) in some professions and the common use of these systems in households. Various reviews of the literature summarize the risk factors for occupational WMSDs for this region.

Sommerich et al. (1993), for example, identified several risk factors associated with particular shoulder pain syndromes. These factors include ‘awkward’ or static postures, heavy work, direct load bearing, repetitive arm movements, working with hands above shoulder height, and lack of rest. Linton (2000), in a review of psychological factors in neck pain, found a link between psychological variables and neck pain. The prospective studies they examined indicated that psychological variables such as stress, distress, anxiety, mood and emotions, cognitive

functioning, and pain behavior were statistically related to the onset of pain, and to acute, subacute, and chronic pain. Personality factors were not found to produce conclusive results.

In a systematic review of the risk factors for shoulder pain, Windt et al.(2000) found that heavy work load, ‘awkward’ postures, repetitive movements, vibration, and duration of employment were all potential risk factors for shoulder pain. While positively associated with shoulder pain, high psychological demands, poor control at work, poor social support, and job dissatisfaction failed to be consistent as risk factors. For the neck region, Ariens et al. (2001) found some evidence of a relationship between several psychosocial factors and neck pain. These factors included high physical job demands, low social (coworker) support, low job control, high and low skill discretion and low job satisfaction. In a survey of the available literature, Keyserling (2000b) concluded that posture was the main contributor to the feeling of discomfort and pain in the neck and shoulders area. Even small shoulder elevation angles and neck flexion can represent risk factors for WMSDs, if the exposure time is long enough.

Another comprehensive review was performed by the National Institute for Occupational Safety and Health (NIOSH, 1997), which involved a detailed review of over 600 epidemiologic studies. NIOSH classified the evidence for a relationship between various workplace factors and the development of WMSDs depending on the strength of association, consistency across different studies, temporality, exposure-response relationship, and coherence of evidence. The resulting classification scheme used the following categories: strong evidence of work-relatedness, evidence of work-relatedness, insufficient evidence of work-relatedness, and evidence of no effect of work factors. For the neck, posture showed strong evidence of work-relatedness, repetition and force showed evidence of work-relatedness, and vibration showed insufficient evidence of work-relatedness. For the shoulder, posture and repetition showed evidence of work-relatedness while force and vibration showed insufficient evidence of work-relatedness.

2.1.2.2 Upper Extremities

The varieties of manual tasks that are performed occupationally have resulted in the development of a wide array of different occupational upper extremity ailments. The regions of the upper extremity most commonly affected are the fingers and the wrist, since these are the anatomical structures most involved in dexterous and repetitive manual work. Muggleton et al. (1999) classified the various WMSDs of the upper extremity into vibration white finger and

related dysfunctions, nerve compression disorders, and tendon and tendon related disorders. Similar to the neck and shoulders region, some reviews of the literature summarize the risk factors for these body parts.

Vender et al. (1995) reviewed the relationship between upper extremity disorders and work activities. However, they found that most of the literature on the topic contained what appeared to be major validity flaws. These authors reached this conclusion based on their opinion that the works reviewed failed to incorporate sound medical diagnostic criteria in the definition and identification of upper extremity disorders. They found no study that established a causal relationship between distinct medical entities and work activities.

Other reviews have provided more conclusive results. Based on their review of the literature, Muggleton et al. (1999) found three main categories of work-related risk factors for WMSDs: load-related, posture-related, and environmental factors. Load-related factors included vibration, mechanical shocks, palmar and gripping loads, external loads, and hard/sharp edges. Posture-related factors included wrist flexion/extension, wrist ulnar/radial deviation, elbow movements, shoulder movements and posture, and repetitive movements (including exposure time). Environmental factors included temperature, humidity and psychological stress. Finally, Keyserling (2000b) described, in his review, a variety of risk factors considering data gathered from laboratory experiments and biomechanical models. These factors included forceful prehension exertions, exertions involving a flexed or extended wrist, exertions involving radial or ulnar deviation, exertions involving pinch grip posture or pressing with the finger tips, repetitive hand exertions, task duration/shift length, amount of displacement of task object, wrist acceleration, work with pneumatic tools, keyboard work, and work with gloves.

In their review of epidemiologic studies, NIOSH (1997) found evidence of a causal relationship between various work factors and upper extremity WMSDs. For the elbow, strong evidence of work-relatedness was found for a (vaguely defined) combination of factors, evidence of work-relatedness was observed for force, and insufficient evidence of work-relatedness was found for repetition and posture. For the hand and wrist, a breakdown based on disease type was used. A combination of factors exhibited a strong causal relationship with Carpal Tunnel Syndrome, while repetition, force and vibration showed causal relationship, and insufficient evidence of a causal relationship was observed for posture. A strong causal relationship was observed between a combination of factors and tendonitis, while repetition, force, and posture

showed a causal relationship. Vibration was observed to maintain a strong causal relationship with Hand-arm Vibration Syndrome.

2.1.2.3 Low-Back

Given their potential as a disabling injury, both occupationally and in daily activities, injuries to the low-back have received considerable attention. However, studies of low-back injuries stumble upon two problem areas. First, the region has a considerable number of degrees of freedom and anatomical complexity, which makes the determination of exact sources of pain difficult. Second, many injuries of the region occur without any apparent signs of tissue damage, which hinders efforts to determine cause-effect relationships, since the effect is not always visible (Kerry et al., 2002). Nevertheless, reviews of the literature point to a variety of factors that may increase the risk of suffering from an occupational low-back injury.

Fuortes et al. (1994), for example, reviewed workers' compensation records for back injury from a large university hospital. The majority of the claims were made for nurses and physical plant workers. From multivariate logistic regression modeling, these authors showed that prior non-back injury and the performance of combined lifting activities were statistically significant risk factors for back injury. Weight, or being overweight, approached significance. Ferguson and Marras (1997) concluded from their review that psychosocial risk factors were highly associated with chronic levels of low back pain.

Apart from discussing the advantages and disadvantages of various types of lifts, Hsiang et al. (1997) point a variety of potential risk factors for low-back injury in lifting exertions. These factors include position of the load with respect to the body, deviation from normal lumbar curvature, twisting, increases in lifting speed, and compound motions.

In a review of psychosocial factors and low-back injury, Hoogendoorn et al. (2000) linked low social support in the workplace and low job satisfaction to low-back pain. Support for other psychosocial factors such as high work pace, high qualitative demands, low job content, low job control, and psychosocial factors in private life was insufficient. Keyserling (2000a) examined the relationship between mechanical factors and low-back injury using the results of laboratory experiments and biomechanical models. The review identified several risk factors including trunk forward flexion, trunk rotation, one-handed lifting, lifting above shoulder height, lifting in restricted work postures, magnitude of lifting force, horizontal location of center-of-

gravity, availability of handles, task frequency/repetition, task duration/shift length, displacement of lifted object, and lift velocity.

NIOSH (1997), in their review of epidemiologic literature, determined that lifting/forceful movements and whole body vibration offered strong evidence of causality for low-back WMSDs. 'Awkward' posture and heavy physical work offered evidence of causality, while static work posture offered insufficient evidence of causality.

2.1.2.4 Other structures

Attention to other structures has received limited attention from an occupational standpoint. For example, Lavender and Andersson (1999) reviewed the research on lower limb injuries, and found it to be lacking. Using a sample of the military population, Ross (1993a; 1993b) identified several injuries in the lower limb and speculated as to their cause. However, the use of this very special population limits the applicability of these studies to the working population, both in terms of body characteristics and in terms of the tasks required.

While particular risk factors have been identified for these body structures, these factors can certainly be grouped into some broad areas. The resultant groupings can be used to construct hypotheses on how WMSDs occur, which have in turn led to some theories on the subject. The focus of the next section is to briefly discuss these groupings and theories.

2.1.3 Theories on causes of musculoskeletal injury

Hagberg et al. (1995, Chapter 4) established several general risk factor groupings for WMSDs: (1) fit, reach, and see, (2) cold, vibration, and local mechanical stresses, (3) postures, (4) musculoskeletal loads, (5) static loads, (6) task invariability, (7) cognitive demands, and (8) organizational and psychosocial work characteristics. Furthermore, the contribution of each of these factors can in turn be modulated by the location of the anatomical structure exposed to the risk factor (e.g. neck vs. low-back), the magnitude or intensity of the risk factor (e.g. lifting an object of high weight vs. one of low weight), the time variation of the risk factor (e.g. repetitiveness), and the duration of the risk factor.

Radwin and Lavender (1999) classify the biomechanical risk factors into external loading factors and workplace design factors. The effects of external loading are based on their generation of physical stresses in various anatomical structures. These physical stresses are characterized by the four physical quantities of motion, force, vibration, and temperature. The

effect of these stresses is modulated by the exertion magnitude, repetition, and duration. The workplace design factors include workplace layout, human interaction with objects, work scheduling, force requirements, and individual factors. This classification of biomechanical risk factors is complemented by the classification of non-biomechanical risk factors presented by Faucett and Werner (1999). These researchers group these remaining factors into medical conditions, body mass index, gender, wrist dimensions, age, general conditioning, genetics, and organizational issues.

Most recently, Kumar (2001) classified a large number of possible risk factors into genetic, morphological, psychological and biomechanical categories. Psychological and biomechanical factors are the two that can be more easily manipulated. Morphological factors are related to the age and the size and shape of anatomical structures and can be manipulated in some instances. Examples of these morphological factors include body size (within constraints, as this can be somewhat modified) and spinal canal size. Genetic factors cannot be manipulated and innately predispose an individual to certain ailments. For example, genes may, through changes in the encoded basic tissue composition, affect the propensity of spinal disks to injury and/or be linked with obesity. Genetic and morphological factors are, in most situations, not independent. For example, a certain genetic sequencing might, within a certain range of inherent variability (i.e. morphological factor), specify the size of a person's wrist. A researcher observing wrist size across individuals would not be able to separate the effects of genetic encoding and normal variation (i.e. morphology) on wrist size.

Psychological factors form the third category in Kumar (2001) and include concepts such as job dissatisfaction, anxiety, neurosis, and depression, among many others. Biomechanical factors, the last category described by this researcher, include strength relative to job demands, repetitiveness of the task, and duration of exposure.

The previous descriptions illustrate the complexity of the problem of predicting WMSDs. While there exists a general consensus on the types of factors that should be considered in determining whether a work task can result in a WMSD, there is little hard data on the interactions between these factors or their relative levels of importance. Furthermore, the various anatomical structures of the human body all react differently to different levels and combinations of these risk factors, mainly since these structures differ in their morphology, range of motion, and intended use. The influence of each of these factors in a WMSD can also vary

between mediating and causal depending on the specific situation. Because of these complexities, there has been little success in formally developing and presenting theories that summarize this knowledge into sets of basic principles that conceptually model how a WMSD is developed.

A comprehensive set of theories concerning WMSDs was recently developed by Kumar (2001), who recognizes that humans, as complex biological organisms, perform their functions based on a variety of variables that are affected by the biological, mechanical, and behavioral domains. Within this level of complexity, it is unlikely that a single mechanism of organism failure exists. Thus, the journey to injury can be completed through a variety of different paths. In his paper, Kumar (2001) describes four of these paths.

The first path is the Multivariate Interaction Theory of Musculoskeletal Injury Precipitation. This theory supposes that the precipitation of musculoskeletal injury is the result of an interactive process between genetic, morphological, psychosocial, and biomechanical factors. The interactions between each of these factors and the relative weights that each should be assigned still remain unknown.

The three remaining paths are explained by the constructs of fatigue (Differential Fatigue Theory), cumulative loading (Cumulative Load Theory) and overexertion (Overexertion Theory). Briefly, the Differential Fatigue Theory establishes that exertions that continue for prolonged periods and thus fatigue tissue may alter the joint kinematics and loading patterns from those that are optimum in terms of resistance to injury. The Cumulative Load Theory accounts for the possibility that a tissue's load bearing capacity may be diminished due to material fatigue, consequently increasing its propensity to injury. The Overexertion Theory accounts for those situations in which the injury is immediate due to the performance of an activity that exceeds the mechanical tolerance of the system, either in terms of its ultimate strength or the maximum tolerable strain rate. While Kumar (2001) provides justification for each of these paths, it appears as if they complement each other, and that it would be possible to construct a diagram considering all of them.

These theories in turn can serve as the basis for models that predict the risk of WMSDs from particular work activities based on a group of the aforementioned risk factors. With the intention of filling some of the gaps in the theories available, many researchers have developed such models. Given the wide variety of possible risk factors, and the lack of control that

researchers have over many of them, the possible approaches for the generation of these models are somewhat limited. In most instances, however, the models themselves serve as useful ergonomics tools.

2.2 Modeling as a tool to predict musculoskeletal injury

Prediction of musculoskeletal injury has been typically based on two types of modeling approaches. The first type of model, referred to here as a neuromechanical model, attempts to simulate various sections of the body using physiologically feasible data. Neuromechanical models produce predictions of tissue stresses that are then compared against population tissue tolerance data to estimate general risk probabilities. The second type of model, referred to here as a risk allocation model, takes known risk factors and known rates of injury and estimates the importance of each risk factor, independent of others, to the development of particular injuries. Risk allocation models are typically broader in focus, including factors from all the different categories discussed in the previous section.

2.2.1 Neuromechanical Models

Neuromechanical models exist for almost every imaginable body part. As the field of biomedical engineering has progressed, so has the understanding of the basic building blocks of the control and physiological processes involved in the generation of force and movement. Researchers continuously attempt to synthesize these basic building blocks into simulations of how humans operate. The assumption is that if the blocks are assembled in the correct way (i.e. the way they are assembled in the human body) they will generate outputs that parallel human responses. For example, a biomechanical modeler interested in generating a model of the elbow joint would take existing models of muscle operation, modify their properties to reflect the individual properties of each muscle modeled, and then virtually “arrange” these muscles so that their lines of action emulate the known lines of action of these muscles in humans. Assuming (perhaps presumptuously) that the correct neural input signals can be provided to the muscles in the model, the forces generated by these muscles and the resultant stresses in the elbow joint should be accurate representations of what would be measured (if it could be measured) in a real human. These predictions of forces and stresses are then compared to known tissue tolerances, which are known to vary between-individuals. Because of these variations, relative risks of injury can be estimated for the entire population of workers or segments of that population.

The main drawback of neuromechanical models is that they function based on mathematical relationships. If those mathematical relationships are not known, then they must be somehow estimated or assumed, which reduces the trustworthiness of the results. Furthermore, these estimates, while possible in many instances, are not necessarily supported by a known cause-effect mechanism. For example, many of the studies on low-back pain associate its occurrence with psychological aspects such as job satisfaction. The fact that this data is available means that job satisfaction can be regressed as a causal factor of low-back pain and a mathematical relationship between the two generated. However, the validity of such a cause-effect relationship is highly dubious without an understanding of the mechanisms through which the level of job satisfaction, the independent variable, generates pain, the dependent variable. In addition, the experimental control of these 'soft' independent variables is often difficult to achieve while maintaining a sufficient degree of external validity. This introduces confounding effects on the data, making results interpretation more difficult. For these reasons, neuromechanical models are typically limited to the consideration of biomechanical factors, which generally show more apparent cause-effect relationships and are easier to control in experimental situations.

Because of this limitation to biomechanical factors, these models are often not useful in many situations. While, for example, models that predict loads on the back during lifting exertions (e.g. McGill and Norman, 1986) are useful in situations involving high external forces acting on a human, they are of little use in predicting the risk of low-back pain in an office worker who spends the day seated and is not exposed to any large external forces. For the office worker, factors other than high loads may be at play or the tissues that are being stressed may not be reflected in typical models. In these situations, a model based on biomechanical factors and typical tissues may not be able to predict their risk of pain.

The main advantage of neuromechanical models is that, when applied to the correct type of situation, they provide the user with a variety of possible mechanisms for injury. Thus, a reason (or reasons) can be associated with an injury, which at the same time can be used to suggest work modifications. In essence, a hypothetical cause-effect relationship can usually be identified, either as a building assumption for the model (i.e. input) or as an abstraction of the resultant model structure (i.e. output). This relationship, in turn, can be used to predict dose-

response patterns. While the establishment of this relationship is also possible with risk allocation models, cause-effect mechanisms are seldom apparent in them.

2.2.2 Risk allocation models

Risk allocation models take as inputs information on job characteristics and the prevalence of disease under those characteristics (Armstrong et al., 1993; Cats-Baril and Frymoyer, 1991; Heecheon, 1999; Kumar, 1994; Malchaire et al., 1996; Matias et al., 1998; Nordstrom et al., 1997; Ohlsson et al., 1995; Punnett and Beek, 2000; Seth et al., 1999; Warren et al., 2000; Westgaard et al., 1993). The modeling process then identifies those factors that contribute significantly to the risk of developing a WMSD. Due to constraints with the types of data that are available for analysis (e.g. discrete instead of continuous), risk allocation models tend to be statistical in nature.

Most of the risk allocation models for WMSD in the literature take the form of either multivariate regressions or logistic regressions, depending on the entity to be predicted. To predict a continuous entity (e.g. rate of injury), multivariate regressions are used. To predict discrete entities (e.g. injury vs. no injury), logistic regressions are used. The classification performance of these models varies considerably across the literature but is generally considered adequate. However, the predictive validity of the models is seldom tested.

Another tool recently used to create risk allocation models are ANNs (Bishop et al., 1997; Chen et al., 2000; Vaughn et al., 2000). Excellent levels of classification performance have been attained with these tools. As for risk allocation models using multivariate or logistic regression, tests of predictive validity are seldom performed.

The main advantage of risk allocation models is that they can receive as input almost any type of data, as long as it is quantitative. These models do not make, or need to make, assumptions about cause-effect relationships or mechanisms for injury occurrence. Hence, psychological factors, psychosocial factors, and genetic factors can be readily implemented in the model as long as they can be quantified. One reason for this flexibility with inputs is that only relative quantifications of the inputs are typically sufficient. Thus, psychological factors whose values are based on a particular scale or questionnaire are perfectly acceptable, as long as that scale remains constant for all uses of the model.

These models are also very useful in establishing relationships between variables, albeit not at explaining how or why these relationships occur. To achieve this deeper understanding,

new hypotheses and experiments are usually developed as a result of risk allocation models. Once a relationship has been determined, researchers have a better idea of where to direct their efforts, either to prove the actual physiological mechanism through which the relationship operates or to find that the relationship is simply the result of high correlations to a third factor. This approach is also followed for epidemiological studies, which have provided a large amount of the knowledge available on WMSD risk factors.

The main disadvantage of risk allocation models is that they are restricted to operate within the limits of the data for which they were developed. Moving outside of this data envelope would require the model to extrapolate, which is typically not suggested for any type of statistical model. Although the use of neural networks alleviates some of this concern if the network is not over-trained (i.e. is able to generalize), extrapolating with these tools is also a risky proposition, since no possible verification of the accuracy of the results obtained is possible. The obvious alternative to circumvent this drawback is to include as much data as possible in the model. However, this process usually results in lower levels of performance, which are seldom justified based on the flexibility of use that is gained.

2.2.3 Past approaches to modeling motion

Previous sections have illustrated some of the issues that have to be considered in modeling the risk of WMSDs. There exist a variety of risk factors for WMSD, of which the postures selected during the motion are only one. To accurately predict the risk that a particular operation might result in the development of WMSDs, factors that cannot be measured or estimated have to be predicted or determined through an abstract model, either neuromechanical- or risk allocation-based. However, accurate motion prediction models still represent an important and worthy step in a long, complex journey to accurate musculoskeletal injury prediction.

The importance of dynamic models in the study of movement has been recognized for quite some time (Koozekanani et al., 1980). Extensive literature exists on the modeling of dynamic postures, which has been motivated by two goals. First, to achieve an understanding of the processes that the central nervous system uses to organize the redundant degrees of freedom in the human body. Second, employing motion prediction algorithms in human simulation models to evaluate work and aid in the investigation of occupational disorders. Accurate prediction of the sequence of postures in these contexts would assist in the quick design of work

tasks that pose minimal risk of injury for the worker. The literature discussed here illustrates the general techniques used in motion modeling, and provides a basis to discuss the advantages and limitations of the various approaches that are advocated by different researchers.

Throughout this document, no distinction is made between movement prediction and movement modeling. It is assumed that a motion prediction algorithm must also model as well, even if the modeling process is not interpretable or useful by itself. Thus, in this context motion prediction algorithms represent a subset of motion modeling, a distinction which is not always clear.

Presently, there exist two main areas of research in the field of motion prediction. Commercial approaches rely on recent developments in human animation and simulation software (Delmia, 2001; EDS, 2001; Tecmath, 2001), which have resulted in virtual environments in which work designers can cost-efficiently prototype their plans. These programs contain motion prediction algorithms that work in three dimensions using all the degrees of freedom in the human body. Despite some exceptions (Loczi and Dietz, 1999), verification of the predictions of these tools has either not been performed or is used as a competitive advantage and, thus, not published. On the other hand, academic or institutional research approaches are typically narrower in their goals, usually focusing on specific body parts (e.g. reach motions of the upper limb). These research efforts, however, are usually tested against empirical data to verify that the model predictions are accurately describing human behavior within a constrained set of conditions. Both research approaches have provided useful information, which is summarized herein. Before summarizing this information, however, two issues related to motion should be briefly discussed.

First, the end result of any motion prediction algorithm is a sequence of predicted joint angles, and errors in these angles will have an effect on the modeling that is being performed. Some researchers have suggested that errors above 10° should be avoided to achieve reasonably accurate 3-D modeling of static strength (Chaffin and Page, 1994). A particular limiting value for joint-angle prediction error, however, is not available, as several factors determine the sensitivity of any model to errors in a specific joint angle. These factors include the type of model, the type of prediction resulting from the model, the type of joint under consideration, the range of motion of the joint, and the position of the joint with respect to the section of the body under consideration. Nevertheless, the limiting value of 10° has been used in the past as a rule-

of-thumb in the empirical evaluation of motion prediction models (Beck and Chaffin, 1992) and will be used as such, with caution, in the following discussion. The reader should note that 10° errors can lead to substantial accumulated errors at the end of a kinematic chain.

Second, many slightly different definitions of posture within a movement exist, mainly because posture is difficult to compactly define and quantify given its functional, anatomical, and biomechanical components (Haslegrave, 1994). In the realm of lifting research, however, posture generally refers to the complete specification of the state of all the degrees of freedom of the human body in the plane or planes of interest. These degrees of freedom vary depending on the task, the number of dimensions being considered (2-D or 3-D), and the type of joint or joints under study. These characteristics, together with the type of prediction algorithm used, are used to classify existing models of lifting motion.

With these issues in mind, the following sections each present one of the different techniques currently employed in modeling dynamic postures. These approaches range from fully mathematical to fully empirical formulations and are mainly discussed in the context of their past predictive usefulness and effectiveness. The reader should note that in many cases the lines drawn between model types are very artificial, and particular models may fit in more than one category. This is illustrative of the multidimensional approach that has been taken to address the movement prediction problem.

2.2.3.1 Control Theory

Early models of movement control were mostly motivated by a desire for understanding of the processes employed by the central nervous control system in manipulating a motor system with considerable degrees of redundancy. Therefore, these models were usually based on control theory, an approach that is still in use by many researchers today.

Control theory models recognize the complex frequency and time patterns that are used by the human motor control system (e.g. Sato, 1981). These models initially tended to focus on the control of minimally-dynamic forms of human movement, usually a ‘static’ standing posture (e.g. Amblard et al., 1985; Barin, 1989; Koozekanani et al., 1983; Werness and Anderson, 1984), but this has changed considerably as more advanced models could be implemented.

The main objective of control theory models is to identify the mechanisms employed by humans (although animal studies are very common) in the control of movement. Thus, many theoretical frameworks have been developed. Hogan et al. (1987), for example, suggested that

motor control is organized in a hierarchy of increasing levels of abstraction, and complement this suggestion with several observations about posture control mechanisms. First, coordination is not a problem for movement alone; in a multi-articular system, even posture requires coordination and control. Second, muscles do not merely act reciprocally to generate forces about the joints; the net mechanical impedance of the limb may be controlled by synergistic activation of all muscles, including antagonists. Third, controlling dynamic behavior is a far more demanding task than controlling motion. Consequently, features of the neuromusculoskeletal system that appear to be redundant or unnecessary for static control can play a functional role in controlling dynamic behavior. Fourth, rather than representing a complication, redundancies in the musculoskeletal system may provide the central nervous system with easier control of complex aspects of motor behavior, such as controlling the apparent inertia of the limbs. Taga (1995a; 1995b) developed and evaluated a model of gait based on conceptual linkages between the neural and musculoskeletal systems. The musculoskeletal system was modeled via standard equations of body dynamics and muscle actions. The neural system was represented via neural oscillators that independently controlled the interplay of the various degrees of freedom necessary for gait. Sensory feedback was also included in the model. All of these inputs were integrated with impedance controllers and other inputs. The walking movements of the model could be compared with empirical evidence, and were robust to various perturbations (e.g. changes in load, uneven terrain).

Other control theories have also been presented. Frank and Earl (1990) suggested a schema for the coordination of posture and movement based on the main idea that the central nervous system somehow contains a model of body dynamics that is essential to anticipatory control of posture during movement. Schoner (1990) created a model of combined nonlinear oscillators, which could capture the coordination required by a rhythmic movement. They deduced that the central nervous system tends to synchronize the component movements, a tendency which gradually breaks down as the component movements become too different in term of their dynamic properties. Johansson and Magnusson (1991) discuss the importance of a control framework in motion modeling, based on the concept of the system feedback that the human somatosensory, vestibular, and visual systems provide. They suggest that the study of posture dynamics and stability entails the study of mechanical aspects of the human body, its sensory systems, and the principles governing coordination in motion control.

The use of control theory in motion prediction continues in more recent work. Developments in control models have, for example, special importance in the field of rehabilitation (Eom et al., 2000; Riener and Fuhr, 1998). If the human motion control mechanisms can be synthesized, then they can be used to assist individuals in recovering lost mobility. The concepts of systems theory have also recently been applied, specifically to the problem of coordination (Calvitti and Beer, 2000).

Given their generality, control models are also used to describe in broad terms particular theories to understanding how the motor control system operates. These theories have been grouped in the past into reflex, hierarchical, and dynamic systems (Rose, 1997). This order also roughly describes their historical development. Reflex theories consider the reflex as the primary component of motor control. Stimuli trigger a series of individual reflex circuits that produce a movement response. While the theory explains well simple movements, it fails to account for the concept of movement planning, which is evident in many human actions (e.g. sports). Furthermore, the theory fails to explain movements that are performed in the absence of sensory feedback. Hierarchical theories assume that all aspects of movement are planned in high level brain centers. These movement plans are then passed down to other lower level centers for execution. This execution is achieved through the transmission of ‘motor programs’ (i.e. sets of ‘learned’ motor commands). Feedback is optional, as movements can be planned in its absence. Dynamic systems theory mainly posits two arguments. First, that the environment in which an action is performed provides essential information for the planning of the movement. Second, that movement execution is the result of self-organization, implying that several subsystems (e.g. neurological and musculoskeletal) interact in the control and production of movement, with no specific one having priority over others. This theory combines, in part, elements of the reflex and hierarchical theories. Its distributed processing approach also suggests modeling approaches that are well suited to simulate this structural composition (e.g. ANNs).

Independent of the theory under which a control model can be classified, control models have the advantage of being mainly white box models, which means that their inner workings and assumptions are clearly specified. Thus, their goal is to completely predict human motion through an explicit understanding of the simplifying assumptions that the human central nervous system must make. If the modeling approach is successful in predicting human behavior during an empirical verification process, then the central idea or assumption that motivates the model is

supported. Given the mathematical nature of the models, they tend to be elegant and conceptually simple. However, since the mathematics required by this approach tend to be complex, and the number of assumed parameters large, these models have typically been limited to the upper limb and other structures with a limited number of degrees of freedom. Also, given the highly theoretical nature of these models, their support in the literature can always be questioned. For each proponent of a particular theory, there is always some opponent that has made empirical observations in which the theory is invalidated. Furthermore, the approaches are sometimes highly simplistic, as it is unlikely that systems as complex as humans are simply governed by only one or two organizing principles.

2.2.3.2 Mechanical Models

Mechanical models were one of the first tools used to attempt modeling of motion. These models tend to be fairly intuitive, as they are composed of sub-systems that engineers are familiar with (e.g. spring and damper systems) and for which accurate physical descriptions of behavior exist. Hogan (1985), for example, suggested a model for movement control that employed the “spring-like” behavior of muscles as its basis. Concepts of modification of inertia, muscle cocontraction, and impedance properties of a multi-joint system were explained based on this “muscles-as-springs” concept. A unified description of the posture and movement of a multi-joint system was also presented by defining a "virtual trajectory" of equilibrium positions for the limb that may be specified by the neuro-muscular system. No empirical verification of this model is provided, however. Yang et al. (1990b) studied kinematic patterns in gait using a planar model containing five rigid segments articulated at frictionless pin joints. The model was used to identify joint torque combinations that would successfully correct for an impulsive force disturbance applied at different points in the walking cycle. An experimental verification of the model showed that electromyographic readings from subjects generally supported the model predictions. Similar findings were obtained for a related model evaluating postural control while standing (Yang et al., 1990a). Newer, “uncontrolled” mechanical models have also been shown to simulate downhill-walking (Garcia et al., 1998).

Other mechanical models have applied the knowledge gained by control theory models to a set of mechanical components that simulate a multi-joint system. Jaeger (1986), for example, attempted to simulate quiet standing by the use of a single-link inverted pendulum model that used electrical activation of simulated muscles to provide balancing activation at the ankle joint

and stabilization of the knee and hip joints. Their initial simulations showed that the method had some potential to achieve quiet standing in paraplegic individuals subject to some constraints, the most important of which was the availability of the required torque. Other inverted pendulum models have also been suggested, especially in the analysis of gait, with good results (e.g. Lee and Patton, 1997; MacKinnon and Winter, 1993; Winter et al., 1993).

Bennett et al. (1992) constructed a time-varying system identification technique to analyze the phase changes in the elbow joint's mechanical response during arm movement. The mechanical properties were found to be time-varying, and well approximated by a quasi-linear second-order model. Gomi and Kawato (1997), based on a mathematical stiffness model, determined that the equilibrium point hypothesis, which implies that the brain controls posture through the control of stability, is not applicable in all situations. They conclude that the brain must consider some internal models of controlled objects in the determination of dynamic posture. These findings have been supported by some research (Gottlieb et al., 1997) but contradicted by others (Domen et al., 1999).

Mechanical approaches are very useful in simulating behavior, but their use in modeling behavior is limited. Thus, the effectiveness of these approaches depends mostly on the type of control theory that is implemented in the model, although some mechanical models don't strictly depend on control models. The advantages and disadvantages mentioned for control theory models also apply here. The main use of mechanical models is in the simulation of control theories. The abstraction of the musculoskeletal system that these models represent allows the virtual application of a control model, and the observations obtained can then be verified empirically. Control theory models lay out a set of principles or schemes that may be used by the central nervous system. Mechanical models allow the simulation of those control schemes using systems that approximate human musculoskeletal behavior.

2.2.3.3 Inverse Kinematics

While the previously discussed models are useful in understanding the kinematic behavior of simple mechanisms, some method of modeling the behavior of more complex mechanisms (e.g. whole body) is also required. Inverse kinematics involves using mathematical approximations to define the degrees of freedom of a kinematics chain given the expected final position of an end-effector (Figure 1). This concept of obtaining a set of segmental angles based on the data on a matrix describing the movement, which is the basic premise of inverse

kinematics, has been proposed as a modeling technique to achieve this goal, both in robots and in humans (Craig, 1989; McCarthy, 1990). One reason for this application is the geometrical simplicity of inverse kinematics when kinematic chains with few degrees of freedom, or those for which a few simplifying assumptions are made, are analyzed.

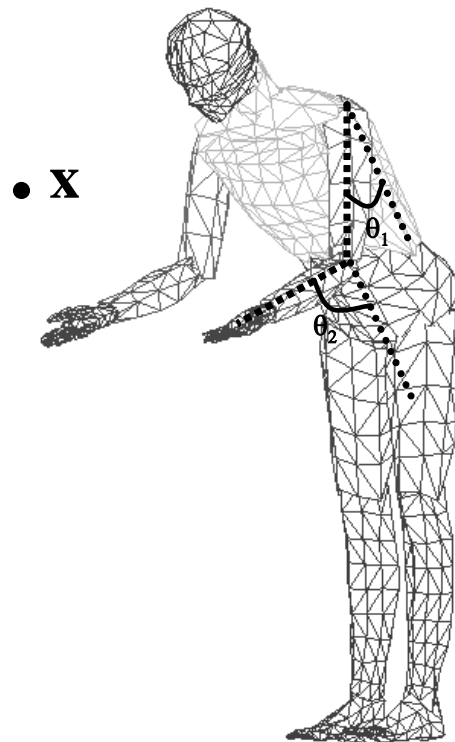


Figure 1. Inverse kinematics attempts to mathematically derive the set of angles θ_1 and θ_2 that would result in the end-effector reaching position \mathbf{x} .

The successful application of the inverse kinematics technique in robots, however, has not been fully realized in humans. One reason for this lack of success is the difference in degree of freedom properties between robots and humans. Whereas degrees of freedom in robots can be easily modified in number and type, human degrees of freedom are far more complex and typically not variable after an initial growth period (i.e. childhood) unless a catastrophic event occurs (e.g. paraplegia). The higher the redundancy of degrees of freedom in a kinematic chain, the more difficult it becomes to find a motion solution using inverse kinematics algorithms. The analytical solutions to the equations of motion that would yield data for the desired degrees of freedom are hard to find, so approximations to those solutions must be used (McCarthy, 1990). Even when these approximations are used and simplifying assumptions made, another problem

remains. Because of redundancies in the degrees of freedom, at each point in the movement several postures can be assumed with no change in the position of the endpoint of the kinematic chain, the accurate positioning of which is typically the goal (Zhao and Badler, 1994). Inverse kinematics algorithms can find any of these postures for any feasible endpoint location. The main problem lies in the ensuing selection process among the different postures. While robots can accept (within constraints of available joint torques and inertia issues) any solution provided by the inverse kinematics algorithm, humans may have “preferences” for certain postures. Inverse kinematics algorithms, by themselves, have no ability to determine what these “preferred” postures are. Therefore, some other method is necessary to assist the inverse kinematics algorithm in selecting a “preferred” posture from the solution set (Guez and Ahmad, 1990). Feasibility issues also plague inverse kinematics algorithms. While robots typically have unconstrained joints, range-of-motion limitations exist for all human joints. If these limitations are not provided to the algorithm, the prediction of unfeasible postures might result.

Nevertheless, numerous previous efforts have used inverse kinematics to predict human motion. To facilitate the computational process, the number of degrees of freedom in the human body is typically reduced by examining only a single plane of movement, usually the sagittal plane, or by examining only a particular area of the body, for example the upper limbs. In these previous efforts, the selection of a solution when multiple postures are possible within a movement segment has been achieved using a variety of approaches, optimization being the most common. These algorithms are discussed in a subsequent section.

A limited number of studies that employ inverse kinematics without any formal optimization exist. Beck & Chaffin (1992), for example, proposed a hybrid model where inverse kinematics provided an initial likely estimate for the posture at any particular movement stage and the user of the program could modify the resulting posture to make it closer to the posture that was being modeled, a heuristic process. Once any change in a joint’s position was made, the algorithm “froze” that joint, but recalculated (using inverse kinematics) any joint between the “frozen” joint and the endpoint of the kinematic chain. The process continued until the user obtained the desired posture. While certainly not predictive, this approach is indicative of the best possible situation when inverse kinematics is used unassisted by a formal optimization algorithm or other higher order constraints.

2.2.3.4 Optimization

In addition to being used as a selection tool in inverse kinematics motion prediction algorithms, optimization has been employed directly as a prediction method. In optimization-based approaches, a mathematical function (i.e. the objective function) is minimized or maximized subject to a series of constraints that are also expressed as mathematical functions. Similar to the inverse kinematics algorithms, the output of this process is a time-based series of predicted joint angles.

The concept that the human motor control system somehow determines a pattern of movement based on the optimization of one or more variables has existed for quite some time. Hogan (1984), in primate studies, suggested that the movement of a limb was determined based on the minimization of the rate of change of acceleration (jerk) of the limb. Nashner and McCollum (1985) suggested that the theoretically infinite number of combinations of muscle contractions and associated movement trajectories used for performing postural corrections could be limited by the adoption of a series of neural organizational hypotheses. Two of these hypotheses were implemented into a model that was qualitatively compared with observed motion patterns of various individuals, and conformance between model predictions and empirical observations was achieved. These hypotheses proposed that postural controls were organized to: (1) use the minimum number of muscles possible, and (2) minimize the necessary neural decision-making requirements, especially for frequently performed movements. More recently, Hatze (2000) has proposed the existence of special neural circuits that control the numerous individual controls that are required for movement, and that these special neural circuits likely obey certain optimality principles.

Lower limb research was perhaps the initial application of optimization to the prediction of motion. For example, the work of Pandy and colleagues (Pandy and Anderson, 2000; Pandy et al., 1992; Pandy et al., 1990) used an optimization-aided forward kinematics approach to simulate maximum-height jumps. These models have recently been expanded to simulate gait patterns (Anderson and Pandy, 2001). Note, however, that the work of Pandy and colleagues does not employ optimization by itself, but as a basis for forward dynamics modeling. In this sense, these models are optimization-based (or optimal control), rather than optimization-only.

In the realm of lifting, Wiker (1992) determined that subjects appear to minimize aerobic demands when performing a free-style lift at the expense of increasing mechanical stress in the

low back, thus suggesting the use of those objectives in optimization algorithms. This researcher found, across a range of participants, that the use of this strategy for free-style lifts was consistent and reliable.

Gundogdu (2000) developed a two-dimensional sagittally symmetric five-rigid-link human body model. The equations of motion for this mechanism were derived using a Newton-Euler formulation. Objective functions considering jerk, work, moment minimization, and a linear combination of these three were evaluated, with the linear combination objective function being the most effective. An additional consideration in this model is that moment cost functions considered dynamic joint strengths instead of static ones. No absolute performance results for trajectory prediction are provided.

Cruse and colleagues (Cruse et al., 1993b; Cruse et al., 1990) suggested that human body control follows the cost function hypothesis. A cost function, based loosely on the concept of comfort, is attached to each joint and this cost function defines a cost value for each joint angle. The posture configuration that provides the minimum total cost is chosen from the set of possible postures. Other researchers (Rossetti et al., 1994) have also suggested that maximization of comfort levels might also be employed in motion prediction. In a finger localization task, less posture variability was observed for those postures in which the comfort level was high.

Empirically verified models of motion have been constructed based on these objective function suggestions and on many others that have been previously presented in the literature. Lee (1988), in a study of sagittal-plane lifting, developed an optimization model that predicted five joint angles based on the principle of minimizing mechanical work done and the maximization of the utilization of all joints. Constraints due to the task, the joint mobility, the reach envelope, the workstation, angular acceleration, and jerk were used. Lee (1988) used a coefficient of inequality to evaluate model predictions, and absolute prediction errors are not provided outside of graphs. Inspection of those graphs reveals that errors of 20-30° are not uncommon. Even so, model performance is described as adequate. Soechting et al. (1995), based on an experiment to determine whether Donders' law (i.e. the idea that for any given postural endpoint there exists a unique three-dimensional orientation of the effector regardless of the starting position, originally observed in gaze) applies to the arm, developed an optimization algorithm to predict the shoulder and elbow angles of the arm based on initial and target postures. High correlations between predictions and empirical observations were obtained for an

objective function minimizing the work done to transport the arm from the starting location to the target. Estimates of error (derived from a figure in the paper) seem to average 10° - 15° .

More recently, Hsiang and others (Hsiang and Ayoub, 1994; Hsiang et al., 1999a, 1999b; Hsiang and McGorry, 1997) investigated the performance of three different objective functions: maximize the smoothness of the motion pattern of the external load (i.e. minimal hand jerk), minimize the sudden change of the center of gravity of the body-load system (i.e. minimal center of gravity jerk), and minimize the integration over time of the sum of the square of the ratio of the predicted joint moments to the corresponding joint strength during the course of lifting (i.e. minimal muscle utilization rate). The particular goal of these papers, to model human behavior after it is modified by a set of precise instructions, precludes its verification with the same data. Thus, no error measures are available. Recent work also reported satisfactory predictions using an objective function that minimizes the sum of the squares of the joint moments (Chang et al., 2001). Bernard et al. (1999) have modified this model to yield an objective function consisting of the squared ratio of joint moment to the moment strength at the joint. Since their intent was to predict joint moments, rather than joint angles, no data are provided regarding the efficacy of this approach in predicting correct kinematic patterns. Recent studies have combined control models and optimization (Schouten et al., 2001), although these predictions have not been verified. The goal of these models is to find optimization functions that emulate the operation of the assumed control structures in the human central nervous system.

Optimization techniques offer either a distinct optimal solution or a multitude of equally optimal solutions. The feasibility of the solutions obtained from the algorithm is assured by the constraints that are imposed as part of the problem. The limitation of the optimization approach lies in its requirement for the minimization or maximization of a goal. Similar to control models, the assumption that the central nervous system and the musculoskeletal system act according to one or two simplifying principles is required. Although it has been the focus of a considerable amount of research, an objective function that consistently explains postural behavior while lifting has remained elusive. Furthermore, convergence of the algorithm to a solution in a finite number of steps is not always assured, and situations can arise where the optimization problem is ill-posed. The next section further expands on some of these issues.

2.2.3.5 Optimization-aided Inverse Kinematics

In order to address some of the main limitations of inverse kinematics algorithms while exploiting their advantages, many approaches have attempted to combine the inverse kinematics methods with optimization methods. In essence, this approach takes advantage of the geometric simplicity of the inverse kinematics process while providing a solution for the singularities of the mathematics required by inverse kinematics when there are extra degrees of freedom.

Studies of lifting exertions represent the most common application of this method. Park (1973), for example, using an incrementation (i.e. quasi-dynamic) method, developed a motion prediction model for sagittal plane lifts. This researcher's selection criteria were the minimization of the balancing problem, minimization of relative torque loading, minimization of low back compression and minimization of external work done. The best optimization criterion, based on a comparison with empirical data, was the minimization of external work, with mean prediction errors below 5° for the lower leg angle, upper leg angle, and trunk angle. Byun (1991) proposed a model that employed both inverse kinematics and optimization to predict sagittal plane lifting motions. The model had four distinct components: (1) inverse kinematics to predict body posture for a predetermined location of the load and movement segment, (2) a kinetic model to calculate force, moment, and torque propagated from a joint to the next, (3) feasibility criteria to test the kinematic and biomechanical feasibility of a predicted body posture at each point in the motion, and (4) posture selection criteria to predict the most favorable body postures at each point in the motion. The posture selection criteria were the minimization of energy expenditure and the maximization of the load lifted. No data are provided regarding model verification, as these researchers conceptualize their research as a tool to indicate optimum lifting patterns rather than as a motion prediction tool.

Dysart and Woldstad (Dysart, 1994; Dysart and Woldstad, 1994, 1996) developed a motion prediction model that employed a whole-body sagittal plane representation of the worker that had five links and used inverse kinematics procedures to predict motions. Their model chose a final motion trajectory by optimizing an objective function using a nonlinear programming search. Three separate models, each using a different objective function, were developed. The objective functions were the minimization of total torque, minimization of percent strength (required strength per joint), and maximization of balance. The minimization of total torque resulted in the best predictions. Although the researchers point out that all prediction

errors were significantly greater than zero, no detailed indication of their magnitude is provided. Qualitative observation between the predicted and empirical data shows substantial differences. Woldstad (1997) reports better results with some changes to the model, including the use of two new objective functions based on the sum-of-cubed muscle intensities and the sum of squared joint torques, additional links to predict the head and neck posture, the addition of a line-of-sight constraint that requires each posture to allow the subject to see their hands, and improvements to the optimization procedures. For this set of objective functions, the best performance was obtained for the sum of squared joint torques function, although average errors in the 20° range were common.

Other studies using this method have focused on the kinematic patterns of the upper limb. Jung (1992) modeled each upper limb as a four-link system, consisting of trunk, upper arm, lower arm, and hand. Eight degrees of freedom were contained in this system. Inverse kinematics, specifically the resolved motion method, was used to predict the trajectory of multi-link segmental movement. Joint range availability was used as a performance function in order to guarantee local optimality of the final solution. Comparison of model predictions with empirical data showed average prediction errors near 10° for shoulder and elbow angles. A revised version of this model (Jung et al., 1995; Jung and Park, 1994) compared two cost functions, one based on posture discomfort (based on the previously employed joint range availability) and the second based on joint torque (minimizing the sum of the joint torques). The posture discomfort objective function had prediction errors in the range of 1° to 4°, while the errors for the biomechanical function ranged from 2° to 27°. Further developments of the discomfort functions have also resulted in small prediction errors (Jung and Choe, 1996; Jung and Park, 1997). While the errors produced by these techniques are relatively small, the reader should note that they refer only to a small number of joints with limited degrees of freedom.

Wang (1999) has developed a seven degree of freedom model of the arm in which the kinematic redundancy is solved by a series of heuristics. An optional optimization algorithm can be used in the model, with an objective function consisting of the sum of various weighted rotational velocities. The model was verified using elbow positions of participants performing a limited set of exertions. Differences between measured and predicted positions were less than 5.0 cm. in most cases. No data is provided regarding the prediction of segmental angles.

A possible problem with optimization can be whether a local or a global optimum is being determined and used. If discrete movement steps are analyzed, there is the possibility that the movement is optimized for each particular point in time, rather than for the movement as a whole. To address this potential problem, Zhang and colleagues have created an optimization-based differential kinematics model (Zhang et al., 1997; Zhang et al., 1998). In this method, instead of searching for a static set of solutions for the segmental angles at each point in time, a pseudo-inverse of the Jacobian is calculated. The Jacobian is a matrix formed by the partial derivatives of a number of functions (matrix rows) with respect to a number of variables (matrix columns). In this case the Jacobian consists of the equations for the x, y, and z coordinates of the hand as a function of the various arm joint angles. This pseudo-inverse requires the calculation of a set of weights that represent the participation (in the joint angular velocity, ω , domain) of each degree of freedom included in the model on the instantaneous effort that is performed. The estimation of these weights is based on the minimization of the time-averaged root mean square error for the difference between predicted angles and a set of empirical observations. A set of assumptions determines how many weights are calculated and whether the weights are time invariant or not. While the model is not fully predictive, as it requires empirical data in the determination of the weights, it does allow for formulation of hypotheses regarding the nature of the movement and the interactions between the various degrees of freedom involved. Recent modifications (Zhang and Chaffin, 2000) have verified the performance levels of a version of this model with synthesized weights, with a time averaged mean error of 5.2°.

Optimization-aided inverse kinematics algorithms combine the advantages and limitations of optimization and inverse kinematics algorithms. They represent the majority of the work that has been performed in terms of motion prediction for use in ergonomic models. These algorithms typically require a limited number of empirically obtained parameters. They are explicit in terms of the objective functions they optimize. Thus, an accurate optimization-based motion prediction algorithm places credibility on the objective function that is optimized. The problem with this concept is establishing a connection between that objective function and the central nervous system. How does the brain learn how to optimize, and how does it select what to optimize?

2.2.3.6 Inverse Dynamics

Inverse kinematics, discussed previously, focuses on the determination of joint kinematics based on endpoint position. Inverse dynamics uses a similar approach to determine joint kinetics based on a particular posture and movement characteristics (e.g. acceleration). There has been some considerable debate in the literature regarding the end goal of the motor control system (Kawato, 1999). If the end goal of the motor control system is to control kinetics, then kinematics is simply an intermediate step in that process (Jansen-Osmann et al., 2002; Thoroughman and Shadmehr, 1999). If the end goal, however, is to control kinematics, then kinetics are a tool to attain a certain movement.

More than philosophical, this debate has direct implications for the mechanics behind a particular model. This is particularly the case in models where optimization is used, as the parameter being optimized usually changes. Verification of inverse dynamics algorithms is also more difficult, as unobtrusive measurement of internal joint forces is difficult in most situations. Prediction of kinematics, the main goal of the current effort, is not a goal of these models. Thus, no detailed consideration of these models is presented in this review, given their different predictive goals.

2.2.3.7 Artificial Neural Networks (ANNs)

Rather than attempting to find answers to the questions of how the motor control system plans and controls movement, many researchers have approached the motion prediction problem by building virtual neural structures that function analogously to brain structures. If these structures are able to learn observed kinematic patterns, then it is possible that the brain is utilizing similar structures in the control of movement. Generally, these virtual neural structures are referred to as artificial neural networks (ANNs).

An ANN is an artificial representation of biological networks of neurons. ANNs consist of a group of individual processing units that are highly interconnected. Input variables are presented to an input layer, and signals from this layer are propagated through the rest of the network until the output layer is reached and an output signal is produced (Figure 2).

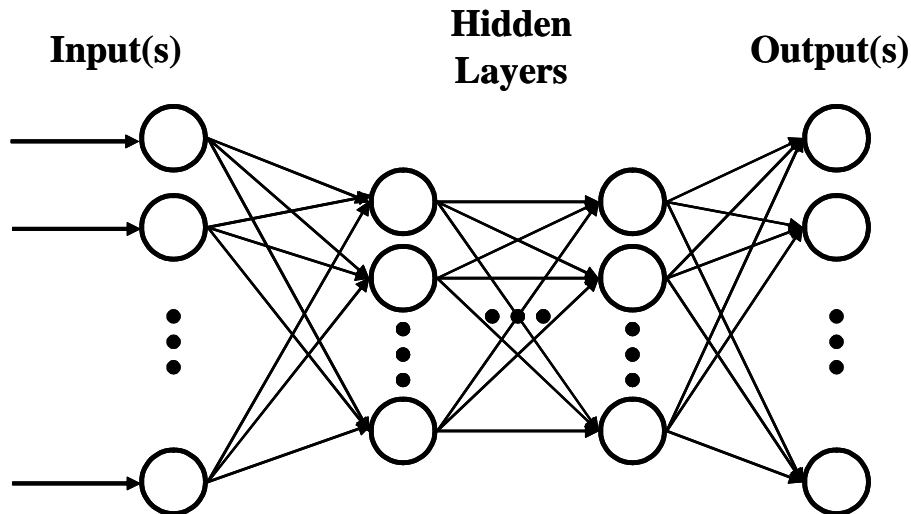


Figure 2. Layers of artificial neurons, from the input layer to the output layer, are interconnected in an ANN..

The ability of ANNs to simulate complex patterns based on highly interconnected entities has motivated its use as motion modeling algorithms. Furthermore, evidence towards the manipulation of motion control by collections of structures similar to neural networks seems to be increasing (Windhorst, 1996).

Massone and Bizzi (1989) evaluated the performance of an ANN in representing and generating unconstrained aiming movements of a limb. The training of the network was performed via simulated bell-shaped velocity trajectory profiles. Their results showed that the aiming task could be learned by a three-layer sequential network, which performed successful generalization and velocity profile adaptation.

Cruse et al. (1993a), in their study of arm motions and the cost functions associated with those motions, developed neural network simulations that learned to predict upper limb joint angles in reaching motions. The inputs of the model were the two dimensional target coordinates. The conclusion of Cruse and colleagues was that these networks had internalized the cost functions that had been observed, although no proof of this assertion is provided. Although the network outputs are described as angles, the error magnitudes are provided in centimeters, which makes the interpretation of error magnitude difficult.

Jung and Park (1994) evaluated the applicability of ANNs to the prediction of human reach motions. A feedforward-backpropagation neural network was used to predict the shoulder, elbow, and wrist three-dimensional positions given the three-dimensional positions of the target.

The starting position of the movement was implicitly included in the model, since all movements originated from the same position. While the units for the prediction errors are not provided, based on observation of the figures in the paper they seem to be small, and statistical tests found no difference between model simulation results and empirical observations. This approach, however, neglects the intermediate postures between beginning and endpoints of the movement and is not appropriate for real-time motion simulations. While arguably the hand coordinates could be subsequently altered very slightly to produce a set of intermediate postures between the beginning and the end of a movement, the network was not trained in these postures and, thus, would most likely perform poorly in predicting the motion generated between the starting and end postures.

Lim et al. (1996) created a feedforward-backpropagation neural network to predict the range of anatomical joint motions for the design/layout of workstation and tasks. The trained neural network was capable of predicting the maximum and minimum angles of joint motions associated with a range of workstation configurations. The average prediction accuracy was found to be around 10 degrees.

Most recently, Bellan and colleagues (Bellan et al., 1999; Bellan et al., 2000) developed a recurrent ANN structure that simulated three-dimensional reaches of the upper limb. Given start and end-points of a movement and a time frame, the model generated paths of endpoint motion that achieved remarkable similarity with empirical observations, as determined from figures in the papers.

These recurrent ANNs, which distinguish themselves from a traditional feedforward neural network (Figure 2) in that they have at least one feedback loop (Figure 3), are a relatively recent type of ANN (Elman, 1990; Pineda, 1987; Williams and Zipser, 1989) and may be ideally suited for predicting motion. The existence of a feedback loop may allow the ANN to process information about the current state of the system with respect to its previous states, thus yielding a series of intermediate predictions that build upon each other. Given that motion is dynamic, there should be a clear time-dependency in successive states; each subsequent system state is not independent of previous states.

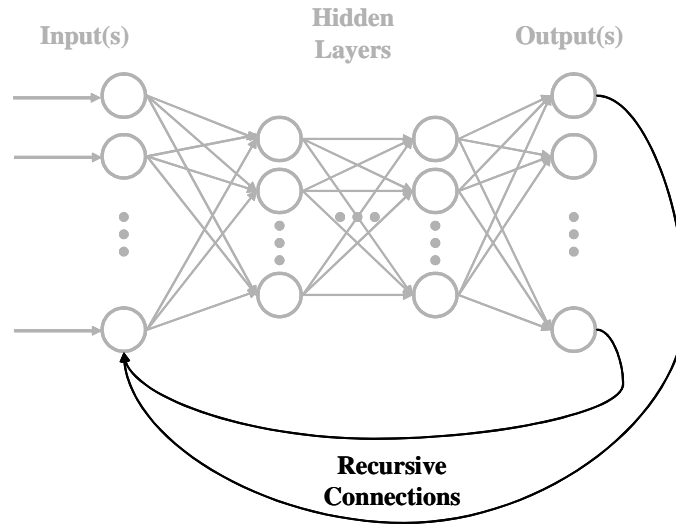


Figure 3. Illustration of recursive connections in a recurrent ANN.

Every type of artificial neural network shares some advantages and limitations. The main disadvantage of an ANN is the training process that is required to make the network learn the correct input/output associations. In order to provide useful results, the network has to be exposed to a series of input-output sets that allow it to modify its internal connections and adapt itself to represent the data that are presented. Thus, the training set that is presented to the network has to be carefully chosen. This supervised training approach can also limit the extent to which the network is considered predictive, as its outputs are usually based on some previously obtained empirical information. The main advantage of the ANN approach is that no assumptions are made with respect to functions that the body attempts to minimize or maximize or control principles that are used. The network simply determines, based on its training process, the most appropriate output for the sets of inputs presented. The physical feasibility of solutions can be assured through manipulations of the neuronal activation functions, and a trained network will always provide a solution.

2.2.3.8 Fuzzy Logic

While this approach has not been formally applied to the prediction of motion, Young (1995) developed a heuristic model that approximates a fuzzy logic algorithm. Given the location and orientation of a worker's hands relative to the shoulder, the model returned predictions for the upper limb posture at a particular point in time. The heuristic approach was implemented via a set of IF-THEN relationships or rules that predicted limb posture based on hand location and orientation. The combination of these relationships with their potential for

hazard was then used to select upper limb postures that minimized hazards. The results showed that 77% of the postures were predicted correctly, although the definition of ‘correctly’ is unclear. It is possible that in the future, successful neural networks techniques might be able to generate sets of fuzzy rules that result in the creation of motion prediction models based on fuzzy logic. These rules could also provide a summary of the control principles humans employ for motion control.

2.2.3.9 Simulation environments

While one or more of the techniques discussed above are central in a motion simulation environment, the level of complexity present in these environments requires the use of some unique approaches. Motion simulation environments are the result of the tremendous increases in computing power that occurred during the 1990’s, which allowed the development of three-dimensional virtual environments that designers could use to interact with virtual humans. One of these original models was MAN3D (Verriest et al., 1991). In MAN3D, only limb movement predictions were possible, and achieved through an algorithm that eliminated enough degrees of freedom from the limb as were necessary to obtain an analytical inverse kinematics solution. No empirical verification of this model was provided.

Jack™ is another one of these environments (Badler et al., 1993; EDS, 2001; Zhao and Badler, 1994). This three dimensional environment utilizes an inverse kinematics procedure to derive movement, which is constrained via a series of weighted functions. These constraints are ‘soft’ in the sense that some take precedence over others. If complying with one constraint requires the violation of another, then the most important constraint takes precedence. The end result, while providing postures that qualitatively appear realistic and that can be used interactively, does not necessarily result in movements that are likely or preferred. Verification of these motions has received little attention in the literature.

Another 3D environment is RAWMSDS™, which applies an optimization-driven inverse kinematics approach based on strength objective functions (Loczi and Dietz, 1999; Marach and Bubb, 2000; Seitz and Bubb, 1999). As with Jack™, limited verification of the model predictions has been conducted.

These environments are useful in predicting the feasibility of a workstation arrangement, allowing designers the quick and cost-effective creation of various prototypes. Since their models of motion have received little verification, however, their use as models of kinematic

behavior may be limited. Furthermore, care must be taken in interpreting the various ergonomic design variables that many of these environments estimate (e.g. L5/S1 compression loads) as these are highly dependent on particular postures assumed during the movement. If the posture that the environment assumes is incorrect, so will be the resulting estimate of the ergonomic variable.

2.2.4 Contrasting among previously used motion prediction approaches

Each of the methods discussed in the previous sections exhibits a variety of inherent advantages and disadvantages. These characteristics make each of the methods applicable under different situations and useful in different areas of motion prediction. While some model types are better suited for the simulation of motion, others serve as test-beds for control theories, and still other serve to verify whether particular control theories are used by the central nervous system. Thus, developments will likely continue in the future for each of these different motion modeling approaches. In the context of motion *prediction*, however, some of these modeling approaches are inherently more applicable.

Inverse kinematics, for example, has been widely used in the past for motion prediction, mainly because mathematical algorithms have been developed that efficiently invert the matrices that are necessary for the algorithm to converge. These approaches are not perfect, however, and when the algorithm fails to converge, an infinite number of solutions are possible. In the past, optimization techniques have been employed to select the “best” solution based on a particular function that is either minimized or maximized. In this respect, the inverse kinematics method also exhibits the advantages and disadvantages of optimization methods. The inverse kinematics method can also be computationally intensive, depending on the structure of the inputs that are fed into the solution algorithm. No assurance is made of the physical feasibility of the geometric solution provided by an inverse kinematics algorithm, unless artificial limits are imposed as part of the algorithm. Finally, performance of algorithms using this approach varies widely depending on the joint that is predicted and the optimization function or selection algorithm that is employed. In many cases, errors in applying these algorithms fall outside the 10° range suggested by Chaffin and Erig (1991).

Optimization techniques offer either a distinct optimal solution or a multitude of equally optimal solutions. The feasibility of the solutions obtained from the algorithm is assured by the constraints that are imposed as part of the problem. Optimization algorithms can be

computationally intensive depending on the type of function that is optimized (e.g. linear vs. non-linear) and the type and number of constraints that bound the problem. The main drawback of the optimization approach is the requirement that some function be minimized or maximized. There is always an assumption made when using any of these algorithms: that the central nervous system and the musculoskeletal system act as an optimal machine that continuously adapts itself to operate in the “best” possible way with respect to some criterion or series of criteria. Although it has been the focus of a considerable amount of research, an objective function that consistently explains postural behavior while lifting has remained elusive. Furthermore, as is the case with inverse kinematics, performance of optimization-based algorithms has failed, with few exceptions, to comply with the 10° rule-of-thumb.

Artificial neural networks seem to offer a compromise between these two methods. After the network is trained, it offers quick solutions to diverse inputs that are presented, and can be set up to assure the physical feasibility of solutions through manipulations of the neuronal activation functions. The main advantage of the ANN approach is that no assumptions are made with respect to functions that the body attempts to minimize or maximize. The network simply determines, based on its training process, the most appropriate output for the sets of inputs presented. The main disadvantage of this approach, however, also lies in the training process. In order to provide useful results, the network has to be exposed to a series of input-output sets that allow it to modify its internal connections and adapt itself to represent the data that are presented. Thus, the training set that is presented to the network has to be carefully chosen. This supervised training approach can also limit the extent to which the network is considered predictive, as its outputs are usually based on some previously obtained empirical information. However, some manipulations have been made in the past to curtail this problem (Nussbaum and Chaffin, 1996). In general, local and/or global rules can be introduced in the network to limit or avoid the need for explicit training data. The training process is also computationally intensive, but, contrary to the inverse kinematics and optimization algorithms, usually occurs only once in the life of the network. While levels of performance of ANNs, especially recurrent ANNs, in motion prediction have seldom been numerically reported, past performance of ANNs in other applications suggests that this tool has considerable potential in the field of motion prediction.

While previous efforts have employed the inverse kinematics and optimization methods in attempts to predict lifting motions, no such effort has been undertaken employing ANNs.

Furthermore, the moderate prediction accuracies obtained using inverse kinematics and optimization in the prediction of joint angles while lifting have limited their implementation in ergonomic design software. These two methods also typically rely on a series of assumptions regarding human behavior. These assumptions, while verifiable in a laboratory environment, may not translate to human behaviors in the real world. Previous performance of ANNs in motion prediction under simpler conditions (i.e. arm reaches) has been satisfactory and does not require the series of behavioral assumptions that inverse kinematics and optimization need. Thus, ANNs are proposed for use in this investigation to predict lifting motions. As an initial step in this process, it is important to examine the importance of variability in the creation of these models. Biomechanical models that fail to properly account for human variability are only of limited use in real world applications, as their results can seldom be generalized.

Chapter 3 LIFT MOTION MODIFIERS

The creation of a motion prediction model that is accurate for a range of lifting situations must be preceded by an effort to understand and quantify the real effects, if any, that various factors have on motion. With some exceptions, the lift motion modifiers that are discussed in this Chapter represent factors that are considered outside the realm of inter- or intra-person variability (as discussed in Chapter 2). In most cases, these factors can be modified without requiring a change in the worker. Their modification, however, usually results in changes in individual behavior (voluntary or involuntary), which is one goal of ergonomic interventions. As a result, the study of these factors is typically made with an intention of evaluating their feasibility as ergonomic interventions, rather than a detailed study of the behavioral changes that result from the interventions.

Thus, many of the studies available focus on dependent measures that are typically thought to be good estimates of injury risk. While posture is considered by many to be a risk factor for musculoskeletal injury, it is not frequently thought of as an estimate of injury risk. Therefore, in most studies of lifting, the focus is not on the posture the participant may assume and the movements they perform, but rather on the effect those postures and movements have on the risk of injury. While this approach is certainly justified, it has limited somewhat the availability of information on the various factors that affect motion, especially psychological and psychophysical factors. The data exist, but haven't been analyzed in this particular context.

Some research on lift motion modifiers exists, however, and is summarized in this chapter. These modifiers have been organized here in biomechanical, psychological, and psychophysical categories. The order in which they are presented also represents in descending order the frequency with which they have been studied.

3.1 Biomechanical Modifiers

Biomechanical modifiers encompass different characteristics of the lift and the load that change the resultant kinematics. These factors are typically based on the job requirements. Examples include the speed of the lift, the weight of the lift, and type of lift. To a certain extent, the worker may select some of these factors (Burgess-Limerick et al., 1995). For example, different workers that are instructed to "lift normally" may differ in their speed selection. Reasons for these differences between individuals should also be identified and quantified in any accurate motion prediction algorithm that is to be useful in a variety of lifting situations.

The majority of studies of lifting biomechanical modifiers focus on the spine and trunk kinematics. The high incidence of low-back pain in industrial settings, especially those where manual materials handling activities are required, has motivated this trend in the literature. Thus, little information exists on the effect of biomechanical modifiers for lifting on arm and leg kinematics.

3.1.1 Lift Style

Lift style has an obvious effect on lifting kinematics, as it directly affects the lifting motion when it is provided as an instruction. The instruction might be of experimental nature in a laboratory setting, or be part of a retraining effort in industry, where it would be provided and enforced by a supervisor. Unless instruction is provided, however, lift style is not a modifier of motion, but rather the result of a particular strategy an individual decides to follow to perform a lift. The context considered in this document, where lift style becomes a modifier, assumes that a form of instruction is being provided to the individual that in turn modifies their approach to the performance of a particular lift.

There are two predominant classifications for lift style, stoop and squat, depending on the initial lifting posture. Stoop lifts begin with a substantial amount of trunk flexion and little or no knee flexion. Squat lifts begin with a substantial amount of knee flexion and little or no trunk flexion. These definitions imply a continuum between these extremes for which quantification attempts have been made (Burgess-Limerick and Abernethy, 1997).

There is no consensus in the literature concerning the best lift style (Burgess-Limerick, 2003; Dieën et al., 1999). Although there is evidence against the use of stoop lifts (Anderson et al., 1987), some studies suggest that there are inherent physiological advantages to it, especially in repetitive lifting (Hagen et al., 1993; Hagen et al., 1994; Wiker, 1992). The adoption of one technique over the other is likely a function of different factors that are discussed in more detail in some of the subsequent sections. Horizontal distance to the load has been identified as one of these factors (Burgess-Limerick and Abernethy, 1998). Frequency of the lift has also been identified as a factor (Chen, 2000a, also see next section), as have whether the load is being lifted or lowered (Burgess-Limerick et al., 2001) and stability requirements (Lee and Lee, 2002). Variability in the lifting kinematics of squat lifts has also been observed to be higher than the corresponding variability in stoop lifts (Hagen et al., 1995), suggesting possible fatigue effects.

Lifting style might also be dictated by physical constraints of the space in which the lift is performed. Research on constrained lifting has pointed to some adaptive postural and movement behaviors. Bobick et al. (1987) simulated several materials-handling tasks performed by low-seam coal miners while kneeling. Kinematic recordings were made of leg, trunk, and arm action, but only the trunk was found to contribute significantly to the overall kinematics. Trunk extension and rotation were the primary actions used in achieving the required task. Similar studies have confirmed these findings (Gallagher and Unger, 1990).

3.1.2 Lift Velocity and Lift Frequency

Lift velocity and frequency are usually related in work environments. When imposed lift frequencies are high, the lift velocities must also be high, because otherwise workers fall behind on their job. When lifting frequencies are low, then self-selection of lifting velocity is typically observed, as the worker is not obligated to lift quickly to perform their job on time. Most studies attempt to consider these two entities separately, however, failing to recognize this relationship.

Hagen et al. (1995) studied changes in lifting kinematics as a function of lift frequency. They recorded only motion ranges for the angular displacements of the thigh and the lower-trunk and forced the participants to employ both stoop and squat lifting techniques. The lift frequency did not influence the motion ranges of the two segments under study in stoop lifting, but for squat lifting the thigh motion range was significantly smaller at a lifting frequency of 20 lifts/min than at a frequency of 10 lifts/min, which were the two frequencies tested. In this study, however, fatigue and frequency effects were confounded. The reduction in the thigh range of motion was gradually observed while the participants performed a particular weight/frequency combination. This led the authors to identify the quadriceps muscle as the limiting factor in the exertion, which was most likely fatigued throughout the experiment. The extent of the fatigue level, however, was not measured.

Mirka and Kelaher (1995) performed a similar study with lower lifting frequencies (3, 6 and 9 lifts/min). Their focus was the low-back area, so only kinematics for the spine were reported. While no report of ranges of motion was provided, they did indicate that non-linear increases in the sagittal acceleration of the lumbar region occurred with greater frequency of lifting.

Chen (2000a) conducted studies to identify the kinematic differences that existed in the psychophysical determination of maximum acceptable weight of lift (MAWL) for various lift

frequencies. Their motion analyses showed that a more stooped technique was used in frequent tasks. Infrequent tasks (with higher MAWLs) required an increase in the vertical acceleration of the load and the subsequent shortening of the load's moment arm during landing. The landing adjustment was accomplished through adjustments in the upper extremities. Fatigue effects should have been minimized by the psychophysical approach used.

Rather than examining lift frequency, Delisle et al. (1996) compared accelerated and normal executions of lifting and lowering tasks. The accelerated condition did not reduce body asymmetry of posture, but did reduce the length of the path traveled by the global center of gravity and the duration of the supporting phase of the box. While the accelerated strategy resulted in smaller production of work, representing an economy of energy, the authors suggest that accelerated strategies be avoided based on their resultant increases in estimated risk of low-back injury. No indication of possible fatigue effects is provided.

The possibility of fatigue being a factor in some of these studies is supported by Dieën (1998), who studied the effects of repetition on the kinematics in lifting. Constant weights (as percentage of body mass) and lift speeds were used across participants. A total of 630 lifts were required in a 40 min period. These researchers observed that over time, trunk extension velocity in the initial 250 ms of the lifting movement decreased, reaching negative (increasing flexion) values in most subjects. In contrast, hip extension velocity increased. The consequence of these changes was an increased phase lag between hip and trunk extension. As time increased, the participants also started the lifting movement with their legs more extended and their trunks further flexed. The conclusions state that while the increase in hip-trunk extension lag could be interpreted as fatigue, the changes in lifting movement were likely the result of adaptations to retard fatigue development. Similar results have also been obtained by Sparto and colleagues (Sparto et al., 1997a; Sparto et al., 1997b), who observed kinematic changes during fatiguing lifting exertions. At the end of the endurance test, these researchers observed less knee and hip range of motion and greater spine peak flexion. Finally, in a study of asymmetrical lifting and lowering tasks, Fraser et al. (2000) also observed slight increases in maximum flexion with increasing levels of fatigue. Fatigue also resulted in differences in the levels of lateral bend and axial twist between lifting and lowering exertions, the latter exhibiting increased levels of lateral bending and axial twist.

3.1.3 Lift Asymmetry

The change of a lifting task from sagittally symmetric to sagittally asymmetric requires significant adjustments in motion. Allread et al. (1996) found, in a study comparing one- and two-handed lifting, that increases in lift asymmetry affected trunk kinematics. As the loads were placed in increasingly asymmetric positions, the values for trunk range of motion, velocity and acceleration also increased. Marras et al. (1999) found that several measures of spinal kinematics differed between symmetric and asymmetric lifts. These measures included trunk sagittal, lateral, and twisting postures; trunk lateral and twisting velocities; hip posture; hip flexion and rotation velocities; and hip rotation acceleration. The extent of these observed changes, however, probably depends more on the change in initial and final lift positions than in the fact that the load start and end points were asymmetric given that task demands will obviously affect the lifting kinematics.

3.1.4 Other Lift Characteristics

Allread et al. (1996) identified trunk kinematic differences between lifts performed using either one hand (with the other hand unsupported) or two hands. Results of this study showed that one-handed lifting exhibited significantly higher ranges of motion in the lateral and transverse planes and greater flexion in the sagittal plane than the two-handed technique. However, the two-handed lift technique produced faster trunk motions in the sagittal plane and equal or larger acceleration and deceleration magnitudes in all planes of motion than the one-handed technique. Marras et al. (1999) compared the spinal kinematics of single lifters and team lifters. Differences between single- and team-lifters were observed for trunk twist, trunk sagittal velocity, and trunk sagittal acceleration.

3.1.5 Use of tools and other devices

Some researchers have attempted to observe changes in lift kinematics based on the use of various tools and devices in lifting exertions. Elford et al. (2000) studied the effect of using patient slings on health care workers performing patient lift tasks. The study focused on spine kinematics. These researchers found that spine angular displacement, velocity, and acceleration were significantly greater in the frontal, sagittal and transverse planes for the no-sling technique compared to techniques using slings. The amount of sagittal flexion and rotation were also affected significantly by the use of slings, but to a smaller practical scale. Marley and Duggasani (1996) observed no changes in sagittal plane lifting kinematics between lifting exertions with

and without a back belt. In contrast, Marras et al. (2000) found that wearing a back support resulted in modest but significant decreases in the maximum sagittal flexion angle and the sagittal trunk extension velocity in free-dynamic symmetric and asymmetric lifting exertions.

3.1.6 Load magnitude

A variety of studies have provided some solid findings relating lifting kinematics to load magnitudes. Allread et al. (1996), in a study of kinematic differences between one- and two-handed lifts, varied the magnitude of loads that participants were exposed to. The results indicated that increasing the load magnitude had small effects on trunk kinematics, which were limited to small increases in sagittal and lateral bending. Burgess-Limerick et al. (1995) performed a study where workers self-selected their lift kinematics. The posture adopted by participants at the start of the lift varied between stoop and squat. Coordination between knee, hip, and lumbar vertebral joints during lifting was observed, and, together with absolute joint angles, was considerably affected by increases in load magnitude. The kinematics of the load itself were also affected as the load's velocity and acceleration were lower for the higher load magnitudes. A follow-up study obtained similar results (Burgess-Limerick and Abernethy, 1997). Davis and Marras (2000) studied a lifting task that involved load carrying. The mass of the box varied between 9.1 kg and 41.7 kg. Increases in box weight resulted in decreases in the sagittal plane velocity and acceleration. Granata and Sanford (2000) found changes in the coordination of lumbar spine and the pelvis as load magnitude was increased. Schipplein et al. (1990) found that increases in weight lifted were associated with increases in the angular velocity of the knee joint while lifting. This tendency served to extend the knees earlier in the lift as larger weights are used. Scholz et al. (1995) studied kinematic changes during a squat-lifting task under increasing loads. They found that the relative phase of movement between joints such as the knee and lumbar spine changed in a quasi-linear fashion with increasing load during lifting but not during lowering. Some researchers, however, have not found differences in lifting kinematics due to load magnitude. Hagen et al. (1995), for example, concluded that load masses from 1 kg to 17 kg had no effect on the kinematics of the trunk or thigh.

Other researchers have looked at the effects of load magnitude uncertainty in lifting kinematics. Burg et al. (2000) evaluated the kinematic effects of lifting an unexpectedly heavy object. The results indicated that, while estimates of low-back injury risk increased, the posture of the lumbar torso, as defined by the maximum lumbar angle, did not increase when compared

to the condition where the participants lifted a box that was as light as they expected. Butler et al. (1993), varied the weight of their load between 0 N and 300 N with and without participant's knowledge. When the load was unknown and had a magnitude of 0 N, a "jerk-like" motion resulted, which was also observed at 150 N (the next weight step in the experiment). At higher load levels, however, this effect disappeared.

3.1.7 Distance to load

Burgess-Limerick and Abernethy (1998) determined the effects of distance to load in initial lift posture. The horizontal distance from the hand to the ankle at the start of the lift was varied between 20, 40, and 60 cm. The initial horizontal distance from the load to the ankle had considerable effects on the starting posture. Ankle and knee flexion were reduced as the ankle-load distance decreased, as was hip flexion. Lumbar flexion, however, remained relatively unchanged. Trunk inclination increased with reductions in distance, indicating the adoption of more stooped postures. While in this case different postures might have indicated anticipatory adjustments to particular moments, further analysis performed by these researchers suggests otherwise, as conditions with different hand-ankle distances but equal moment resulted in the adoption of different postures.

3.1.8 Injury

Gracovetsky et al. (1990), while studying free lifts, determined that particular injuries resulted in measurable changes in several kinematic parameters. Lariviere et al. (2000) observed decreases in lumbar spine flexion and increases in thoracic spine flexion for patients when their kinematic patterns were compared to those of healthy individuals.

3.2 Psychological Factors

Studies on the effect of psychological and psychosocial factors on motion have been severely limited. The main source of this lack of research is the difficulty of manipulating psychological factors reliably in the context of a lifting experiment. Experiments of this nature must, by necessity, be run in real work environments. These environments either preclude the use of postural measurement techniques or change the focus of the experiment to generating risk of injury estimates, which may use posture estimates but not depend solely on it. Therefore, interesting problems such as return to heavy work after injury and the relationship between stress and lifting technique have not been addressed. Among the few psychological factors that have received any degree of attention in motion prediction are training and experience. Some

behavioral studies have also identified psychological aspects of lifting, but the emphasis of these studies has been on determining motion control mechanisms utilized by the central nervous system, rather than relate kinematic changes to specific behavioral observations.

3.2.1 Training and experience

The concept of learning has received considerable attention in the kinematics literature (Rose, 1997), albeit the information that is encoded and the encoding method remain unknown. It is widely accepted that humans adapt their movements with experience. Thus, it is not surprising that considerable differences have been observed between the kinematics of lifts performed by experienced and inexperienced individuals. Brown and Abani (1985) studied the kinematics patterns followed by skilled and unskilled groups of teenage power lifters. The skilled group exhibited more upright postures at lift-off than the skilled group. Furthermore, skilled lifters achieved maximum vertical bar acceleration and maximum trunk angular acceleration near lift-off. Other researchers have indirectly studied experience through the comparison of various general lifting patterns that are typically observed in either experienced or inexperienced individuals. Delisle et al. (1999) studied kinematic differences in workers that interacted with a 12 kg box using what the authors deemed as “expert” and “novice” strategies. The box had to be moved between two unequal height surfaces that were placed at a 90° angle from each other. Expert strategies resulted in either the minimization of the center of gravity’s movement or the minimization of the final posture asymmetry. Novice strategies resulted in higher values for these two parameters. More recently, Milosavljevic et al. (2005) have reported differences in lumbar and hip coordination in a sheep shearing task between experienced and non-experienced individuals.

3.2.2 Behavioral approaches

Kerlirzin et al. (1999) studied the trajectories of the hands and the whole-body center of mass during whole-body lifting tasks. The lifts were performed both with and without kinematics constraints (i.e. to produce a straight hand trajectory while lifting, and to lift without any instructions, respectively). While the different instructions resulted in different hand paths, the path of the center of mass was not altered between conditions. Thus, other kinematic adjustments, not measured in this experiment, must have occurred. Since the involuntary response of the body was to maintain a smooth center of mass trajectory, movement constraints must require adaptive changes to the lifting movement. The ability of individuals to voluntarily

adapt to other types of lifting strategies has also been demonstrated (Hsiang and McGorry, 1997). Other research has focused on predicting posture through the use of observed behaviors (Young, 1995), but these behaviors are themselves simple IF-THEN rules based on observation, rather than the result of changes in any psychological factor in the individual. A similar approach was described by Beck and Chaffin (1992).

3.3 Psychophysical Factors

Psychophysics is defined as the scientific study of the relationship between stimuli and sensation. While many studies exist relating changes in kinematics with changes in psychophysical measures (e.g. the MAWL - Smith et al., 1992), the research base is somewhat limited in determining how discomfort (the typical basis of psychophysics in this realm) affects a selected lifting motion. Cruse and colleagues (Cruse et al., 1993b; Cruse et al., 1990) have addressed this topic in human arm reaching movements. They found a U-shaped function between joint angle and subjective discomfort. As the joint angle deviated from a resting position, typically near the middle of the joint's range of motion, the subjective discomfort increased. Cruse and colleagues suggested this technique as a possible optimization objective function in the prediction of motion. Jung and colleagues successfully utilized this approach (Jung and Choe, 1996; Jung et al., 1994; Jung et al., 1995; Lim et al., 1999) and have attempted to extend it to whole-body lifts (Jung and Park, 1997). Byun (1991) used a maximum perceived stress level objective function in their study, but the function was represented by a ratio of joint torque to joint strength. No verification of the relationship between this measurement and the perceived stress was provided. Finally, the ability of people to describe their own posture has shown some reliability with physical therapists' observations (Lindstrom et al., 1994), suggesting that the human movement control system is at least partially the result of cognitive processes, rather than a fully automatic system.

Sources of human variability also serve to indicate which of these factors, and some of the factors discussed in Chapter 3, are essential in a particular modeling situation. The next section discusses human variability in more detail. The composition and number of the inputs that might be needed for creating an ANN-based motion prediction model depend on those environmental, task, and 'person' factors (i.e. sources of variability) that might have an effect on the sequence of postures adopted by an individual.

3.4 Accounting for human variability in motion prediction models: a prescription for realistic models

Inter-person variability, and to a lesser extent intra-person variability, are often classified in the literature as “individual differences” (Allread et al., 2000; Burgess-Limerick et al., 1999; Lavender et al., 2000; Lin et al., 1999; Nussbaum et al., 1997; Scholz and McMillan, 1995). In an experimental design, this term usually groups together those sources of variation that could not be used, or were not used, as experimental factors. In any human factors experiment, however, the term “individual differences” includes all of the sources of variation, since all of them are the result of differences either between or within a number of individuals.

In the traditional sense, “individual differences” are simply the portion of intra- and inter-person variability that remains unexplained after this variance allocation process. This variability is considered error in subsequent analyses, but in reality is a combination of error (which is unavoidable in any empirical process) and a variety of other factors that vary between- and within-individuals but which were not, or could not be, identified and/or controlled in the experimental procedure. If the experiment was ideally designed and all the “important” factors were considered and/or controlled, then this residual variability will be small when compared to the variability of the experimental factors.

Referring only to this portion of the total variability as individual differences is misleading, however, as most of the variability obtained in a human factors experiment is calculated as the result of individual differences in performance. The factors in a human factors experiment which remain isolated from “individual differences” are simply experimental manipulations that change the performance of the individuals through various mechanisms. By comparing the various levels of performance these individuals exhibit, a statistical conclusion is reached about the effectiveness of the experimental manipulation. However, this conclusion is mostly reached, assuming a negligible effect of instrumentation errors and other sources of bias, based on levels of inter- and intra-individual differences.

In part because of this misuse of the terms, there seems to be no set definition for which aspects of human performance are represented by inter- and intra-person variability. While some studies may choose, or be forced, to consider only a few factors, others might consider a large variety of factors. For example, two gait studies might be conducted in which stride length is a dependent variable. It is well known that stride length is highly correlated to some body

dimensions. In study A, these correlations are not considered. In study B, either a factor is added or the data normalized to account for the correlation. Under otherwise equivalent conditions, study A would yield a high level of individual differences, while study B would yield a low level of individual differences. Thus, the level of individual differences reported in a study does not simply account for differences between- and within-individuals, but also depends on which of these differences have already been factored out. Therefore, no formal definition of what constitutes an inter-person difference or what constitutes an intra-person difference exists.

3.4.1 Inter- and intra-person variability in motion prediction models

Empirical models based on experimental data should initially be based on significant experimental factors, as these factors account for large differences between- and within-individuals due to experimental manipulations. The typical biomechanical model, however, often attempts to operate beyond the constraints that statistical models offer, especially those constraints involving “individual differences”. While, for example, it would be difficult to include muscle moment arms (which vary between-individuals) as a factor in an analysis of variance (ANOVA), this information is often implemented in models that convert surface electromyography (sEMG) signals to joint moments (e.g. McGill, 1992). Thus, the biomechanical modeler is often faced with the selection and model-implementation of human characteristics that have not been, or could not be, statistically tested. While often the characteristics that may cause the variability are readily apparent (e.g. differences in height, weight, body composition), this is not always the case, especially when dealing with psychological issues (e.g. differences in behavior) or in the case of intra-person issues (e.g. fatigue resistance, baseline myoelectric muscle activity) where intra-individual issues would take a considerable role.

The biomechanical modeler is aided in this model-component selection task by a variety of different techniques that can be used to implement components of human variability in human models. The use of a particular technique depends on the type of model used and the type of construct under consideration. While some of the factors explaining variability might be ideally suited for use as model inputs (Cholewicki et al., 1991; Nussbaum and Chaffin, 1997), others might be better used as denominators in an input (or output) normalization process (Pierrynowski and Galea, 2001). In some other cases, the modeler might wish to generate, through a simulation process, a population of ‘pseudo-individuals’, with slightly varying characteristics, which are

then used as inputs to the model (e.g. Byun, 1991). In many other cases, and for a number of reasons (e.g. a low level of model complexity is desired), the factors explaining variability are simply disregarded or a central tendency measure (e.g. mean) is used to represent them in the model, which implies that the variability of the particular factor is not modeled (e.g. anatomy representation in Nussbaum and Chaffin, 1997).

3.4.1.1 Inter-person variability

Inter-person variability is the result of diverse performance-affecting characteristics between different participants of an experiment that are not manipulated by an experimenter. Examples of these characteristics in the realm of lifting research are many, as can be expected. The most important of these characteristics are briefly discussed in this section, together with implications for their modeling for motion prediction.

Maybe the most cited source of inter-person variability, gender, remains an open area of investigation. While many researchers have found differences between genders in lifting technique or capacity, most of these investigations failed to account for underlying anthropometry factors that might differ between genders and which might be responsible for the observed difference (e.g. muscle mass, tissue tolerance, strength). When proper accounting for these differences is made, usually via a normalization process, the differences typically disappear. Weisman, Clark, Haugh, and Pope (1992), for example, observed similar patterns of force while lifting in males and females, after correcting for the maximum force during the lift. In a motion prediction model that used joint forces normalized by individual static strength (Bernard et al., 1999), few statistical differences were found between model prediction errors for males and females. Chaffin et al. (2000) found little effect of gender in reach postures after considering stature in their analysis. Dysart (1994) found no gender effect on the movement predictions of a model that considered anatomical link lengths in its calculations. While Lindbeck and Kjellberg (2001) observed differences between males and females in knee-hip coordination in lifting exertions, some of their “normalization” procedures (e.g. different box weights for males and females) may not be completely appropriate. Reed et al. (2000) determined that differences between males and females in a reach experiment could be explained by variations in body size. Overall, these studies suggest that anatomical differences, and not gender *per se*, are responsible for kinematic differences between males and females.

Several approaches are available to model anatomical differences, as they have been recognized as causal factors of inter-person differences for quite some time. Some of these approaches have made their way into motion prediction models, and provide some guidance into how to consider these factors in future models. The most common approach is to allow the modeler to specify the relevant anthropometry of the person to be modeled, which typically includes only link or segment lengths (Badler et al., 1993; EDS, 2001; Loczi and Dietz, 1999; Reed et al., 1999). This specification can be achieved in several different ways. One common method is to produce “scaled” versions of a standard human that are based on a proportion, typically the ratio of the “real” human’s height to the standard virtual human’s height (Beck and Chaffin, 1992; Dysart, 1994; Faraway, 2000). Another approach is to use a “standard” anatomy that remains the same for all the data modeled (Abdel-Malek et al., submitted; Chang et al., 2001; Chou and Song, 1992; Gundogdu, 2000; Hsiang and McGorry, 1997). This approach is generally acceptable for exploratory modeling, but tends to be inaccurate at modeling empirical data. A less common approach is to randomly or systematically generate a series of “virtual” humans that represent a population and model each of those humans. The output from this process is used to generate a probabilistic distribution of responses (Byun, 1991). Albeit not often used, this approach is excellent at generating performance “envelopes” and guidelines. The last option is to ignore anatomical representation of the individual, an option when models can adapt their structures or assumptions to fit these individual differences. Neural networks (Jung et al., 1994; Koike and Kawato, 2000) and some optimization algorithms (Zhang et al., 1998) are examples of these model types. Regardless of the approach followed, however, accounting for anatomical differences seems essential in movement prediction.

As a subset of anatomical differences, another important inter-person difference is strength capacity on the various joints. This measure has been used somewhat successfully in various motion prediction models that employ optimization (e.g. Dysart, 1994). However, it hasn’t been considered in motion prediction models outside the realm of optimization models. The main drawback in using this factor is that it requires a detailed database of values for the strength capabilities of a certain individual as they assume a sequence of postures, or at least a method of mathematically estimating these capabilities.

Inter-person variability also depends on behavioral factors. These factors include training/experience issues, the existence of previous injuries (or thoughts of predisposition

towards them), and psychological factors. While many of these have been studied extensively with respect to their relationship to musculoskeletal injury, their relationship to the adjustment of kinematics has received less attention. When studies relating training and injury address kinematics, it is usually done in a qualitative manner. Thus, quantification of behavioral factors has not been achieved, and it is highly unlikely it will be, since behavioral factors are difficult to quantify. As a result, the use of factors such as these in modeling is considerably difficult. For example, while the experience of an individual could be numerically identified with respect to time, the characteristics of such experience cannot be. This still remains an open, albeit very challenging, area of investigation which is discussed further in the next chapter.

Finally, inter-person variability is also subject to noise. Empirical measurements such as those that generate data for human models are not error-proof. The variability of the error, however, should be: (1) low enough to be negligible when compared with the variability due to other factors; and (2) random. While a random error generator could be easily implemented in most of the current motion prediction models to consider the presence of noise, results of such a simulation have not been published.

3.4.1.2 Intra-person variability

Intra-person variability is the result of diverse performance-affecting characteristics in the same individual who performs exactly the same task at different times or trials. Comparisons between intra- and inter-subject variability, when possible based on the data obtained, typically show that inter-subject variability is considerably larger than intra-subject variability (Alstermark et al., 1993; Granata et al., 1997; Lindbeck et al., 1997; Reed et al., 2000). Even so, in some cases the magnitude of intra-personal variability might still be considerable (Granata et al., 1999; Mirka and Baker, 1996; Schmitz et al., 1999).

Intra-person variability is often low enough, and additional factors that identify it difficult enough to pinpoint, that it is usually considered an indicator of the overall error of the measurement method used to obtain values of the dependent variable; in essence a reliability measurement. While this interpretation is in some cases appropriate, in most cases the reliability of experimental measurements is confounded with the intra-person variability, and reliability is most likely underestimated, making this a conservative estimate. In addition, small perturbations that are not controlled may induce unaccounted variability. For example, Hatze (1986)

analytically describes how even small stochastic inputs in the neural processes might produce what is likely unavoidable variability in motion trajectories.

Fatigue is one important source of intra-individual variability, having been demonstrated to affect lifting performance in a wide array of experiments. For example, fatigue or weakness of specific muscles has been shown to affect the selection of a particular lifting technique (i.e. stoop vs. squat, Trafimow et al., 1993; Zhang and Buhr, 2002). Sparto and colleagues (Sparto et al., 1997a; Sparto et al., 1997b) also documented fatigue by the observation of a reduction in average lifting force and hip and spine torque generation. Fatigue was associated with decreased knee and hip motion, and increased lumbar flexion. Similar results were found by Bonato and colleagues, who observed significant changes in the angular displacements of the knee, hip, trunk, and elbow, as well as increased in box acceleration, as a function of increased fatigue (Bonato et al., 2002; Bonato et al., 2003). Chow et al. (2004) found decreases in box velocity with increasing fatigue. Dieën (1998) found, with increasing fatigue levels, a reduction in the trunk extension velocity, an increase in the hip extension velocity, and a change in the overall kinematic pattern to more leg extension and more trunk flexion. They also observed an increase in trunk twisting with increasing levels of fatigue. These results were different from earlier results from the same researchers in which there were few differences due to fatigue (Dieën et al., 1996). However, these discrepancies could be due to different fatigue protocols. Chen (2000b), in a study of localized arm fatigue under repetitive lifting, observed that increases in arm fatigue led to the use of increasingly stooped postures at the beginning of the lift and stiffening of the arms at the end of the lift. Changes due to fatigue have also been observed in the activation timing of torso muscles (Gorelick et al., 2003), prompting researchers to consider the minimization of muscle fatigue as an implicit motor control objective function (Prilutsky et al., 1998). These kinematic changes can also lead to modifications in internal forces and moments (e.g., torso bending moment and spinal compression, Dolan and Adams, 1998). Overall, these studies suggest that fatigue plays a large role in lift coordination.

Learning effects can also be an important source of intra-individual variability. When fatigue is not an issue, repetition of an activity by an experienced individual typically results in low performance differences. However, if the individual is not experienced in the task there is the risk that there will be a learning effect (e.g. Gagnon, 1997), albeit it can be relatively slow (Chaffin et al., 1999).

Assigning causes for within-individual performance differences that are not due to fatigue or learning is usually difficult, as apparent reasons are typically scarce (if evident at all). Possible causes for these uncategorized performance differences include an individual's attitude, level of boredom with the task, laboratory equipment errors, experimental procedure inconsistencies, and biochemical changes in the body. The effect of any of these on performance is usually difficult (or even impossible) to quantify using current methods and tools, and in some cases is not even understood. Therefore, modeling of any of these factors is typically not performed, although perhaps these sources of variability should be considered normal and predicted by a good model.

3.4.1.3 Implications of accounting for inter- and intra-person variability

The main implication of including inter- and intra-person variability factors, such as those previously discussed, in any model, is an increase in the model's physiological fidelity. That is, the model includes in its parameters factors that are known (with various degrees of certainty) to affect the modeled human behaviors in the real world. If the model is able to simulate responses to changes in these factors that agree with empirical data, then the model may be considered a more faithful abstraction of reality. Depending on its structure, a "faithful" model could potentially be "reverse-engineered" to generate new hypotheses related to human behavior. In this case, the process could lead to improved understanding of the motor control processes that the human brain employs.

When these factors are not included in a model, the reverse is true. Model fidelity is potentially decreased. However, a simpler and faster model typically results. Depending on the particular modeling situation, the decrease in model fidelity may not be large enough, or the additional information gathered from the model trustworthy enough, to outweigh the replacement of a simpler model by a more complex model. In the realm of motion prediction, these additions to the model will likely prove important in a model's accurate operation, especially those additions that are based on the anatomical information of the individual. However, the effect of omitting these factors will simply be a function of the amount of variability that these factors account for.

If a statistical model accounts for 99% of the variance in a dataset, then any extra modeling would only 'tweak' that remaining 1%. In this case, developing a complex model is very likely a waste of time, since a good (probably simpler) model already exists. Thus,

analyzing the remaining inter- and intra-person variability will not result in any performance gain. The best model is already available, and predictions can be obtained from it.

However, assuming that the statistical model accounts for only 50% of the variance in a dataset, the situation changes considerably. Inter- and intra-individual differences now account for somewhat less than 50% of the remaining variability. If the decision is made not to improve upon the statistical model, then predictions will be made that show considerable error. In essence, the model will predict motions that differ most of the time from the empirically determined ones. This level of performance directly affects any predictions that are made with subsequent models, including, for example, predictions of low-back injury risk. Even if a perfect model for low-back injury risk was available, the prediction performance of that model would depend on the accuracy of its inputs, and consequently be far from acceptable.

Perhaps the main idea suggested by this discussion is that the modeling of central tendency should not be the only goal of a predictive model. While a description of central tendency (e.g. mean) is essential in any model, this construct is not sufficient to characterize the inherent variability in human performance. Predicting ‘normal’ variability within a set of relevant categories (e.g. a performance ‘envelope’ surrounding a central tendency) should therefore be considered essential for a good model. This is especially the case for motion prediction models, given their role in an overall injury prediction modeling sequence.

In ergonomic biomechanical modeling, motion prediction can be considered an early link in a modeling chain. Determining the characteristics of an individual based on a simple set of attributes can be considered a first link. The modeler must also know, or design, the task characteristics that will be modeled. At this point, motion prediction allows for determining how that particular task will be performed. The results of motion prediction are later used in predicting muscle activation patterns, strength requirements, and injury risk, among others. Obtaining the maximum fidelity and accuracy possible from this model is essential in providing appropriate inputs to other models down that chain and is the main goal of this proposed investigation.

3.5 Strategies for inclusion of lift motion modifiers in motion prediction models

Various motion prediction models, particularly those that employ optimization methods, have attempted to simulate the effects of the aforementioned motion modifiers. The ratio of joint torque to joint strength, an alleged estimate of psychophysical discomfort, has been used in the

past as either a constraint or an objective function (Bernard et al., 1999; Byun, 1991; Dysart, 1994; Dysart and Woldstad, 1994, 1996; Lee, 1988; Park, 1973). Other investigations have modeled the constraints imposed by the workstation (Lee, 1988) and the line of sight (Woldstad, 1997). Still others have used observed behaviors to eliminate or reduce the redundancy of the musculoskeletal system, especially when inverse kinematics algorithms are used (Badler et al., 1993; Chang et al., 2001; Verriest et al., 1991; Zhao and Badler, 1994), or to produce complete motion prediction algorithms (Beck and Chaffin, 1992; Young, 1995). The work of Jung and colleagues, described above, has yielded models based on psychophysical factors (Jung and Choe, 1996; Jung et al., 1994; Jung et al., 1995; Jung and Park, 1997; Lim et al., 1999).

During the literature review, instances where these factors were included in neural network motion prediction models could not be found, and it is assumed that the reason for this absence from the literature is that such an inclusion has either been implicit, indirect, or not performed. The changes in posture observed due to many biomechanical factors, for example, can be simply modeled as part of the changes in the initial and end positions of a lift, or as a function of the time required by the lift (if this is not a predicted parameter). Any psychological and psychophysical changes in the data used to train the network are simply absorbed as sources of unexplained variation, and are mixed with the prediction errors of the network.

In reality, there is still much work to be done in determining which of these factors, if any, have real influences in the kinematics of a lift. However, the current research base can assist the motion modeling process by suggesting appropriate (i.e. necessary) inputs. This process is essential in the evolution of lifting motion prediction models that go beyond the typically small set of lifting situations within the sagittal plane.

Chapter 4 RESEARCH OBJECTIVES

As presented in the previous chapter, work has already been performed on the exploration and use of the wealth of existing MMH literature with the purpose of uncovering the different variables that may have an effect on lifting strategy and the interactions between these variables. This investigation uses a lifting kinematics database containing variations of some of these factors in the process of creating and verifying a motion prediction model. The main goal of this investigation is to create a movement prediction model using artificial neural network technology. Two primary areas were explored.

First, several significant motion modifiers (see Chapter 5 for a description of these modifiers) were used to create (i.e. train) and verify the performance of recurrent ANNs for the prediction of human lifting kinematics. Network structures and parameters were varied to improve network performance and to determine the robustness of the network's solutions to small perturbations in the input data and its parameters. Kinematic data, which were used for training the network, are often noisy, and such robustness is a requirement of any appropriate motion prediction algorithm. Best-performing networks were also compared against empirical data using a variety of performance indicators.

Second, the activation patterns of the various network layers were analyzed. While ANNs are an abstraction of reality, they have been demonstrated in the past to perform data processing that is similar to principal components analysis (Ferran and Pflugfelder, 1993; Stitt et al., 1998). ANNs may thus provide a low-dimensionality representation of kinematics data that accurately depicts the high-dimensionality of human kinematics. Abstraction of this low-dimensionality representation might allow for the generation of rules which in turn could be used to hypothesize high level control structures that may be used by the human brain to solve the degrees of freedom problem (Whiting, 1984). Depending on its structure, a 'faithful' model could potentially be 'reverse-engineered' to generate new hypotheses related to human behavior. In this case, the process could lead to improved understanding of the motor control processes that the human brain employs.

In summary, this research intended to answer the following experimental questions:

- Can a subset of previously identified lifting motion modifiers be used to create a model that accurately predicts lifting movements?

- Would a single, all-encompassing, model suffice? Are situation-specific models necessary?
- How can such a model (or set of models) best be evaluated? What tradeoffs are inherently present in this evaluation process?
- Given an accurate motion prediction model, how sensitive is it to changes in its various input parameters?
- From an accurate motion prediction model, can motor control hypothesis be extracted that are sustainable based on past research or which can be the basis of future research?

Chapter 5 MOTION SIMULATION DATABASE

The motions used in the development and evaluation of the motion prediction model were taken from The University of Michigan's HUMOSIM project site (www.humosim.org). This site serves as a repository of motion capture data. These data include standing lift exertions with various object types and weights. Methods for obtaining these data are summarized in this section; the reader is referred to the HUMOSIM website for more detailed descriptions of the various studies that are included within the database.

The standing reach study that produced the data used here was performed in 1999. It was part of a larger study that collected data on one- and two-handed seated and standing lifts and reaches, using various end lift positions, in the presence or absence of barriers constraining the movement, and employing a variety of objects.

A total of 10 men and 10 women volunteers were recruited for the 1999 study. All were healthy and their ages ranged from 21 to 68 years. Forty-one anthropometric, shoulder and back extensor strengths were measured on each subject. They then performed 213 reach trials in two separate 2-3 hour sessions. The trials required four separate motions; 1) beginning from a standardized 'home' position, deliver an object to a shelf, 2) return hands back to 'home' position, 3) go get the object, and 4) bring the object back to the 'home' position. For the purpose of this investigation, only movements 1 and 4, which required a load transfer, were used. These movements will be referred to as 'deliver' and 'bring back', respectively, throughout this document. A total of 16,920 motions were performed (some of which were repetitions of equivalent movements and can be used to estimate the within-subject variability) combining both seated and standing exertions. Lift style and velocity were self-selected, and no repetitive lifts were performed. The various objects used during the movements allowed the simulation of different situations. A tote box allowed for the simulation of MMH situations, whereas cylinders allowed for the simulation of tool use. Initial distance to the load was maintained constant across participants. Participant experience and training in MMH were not controlled. No guidance was provided during the performance of experimental exertions. No data on discomfort experienced from the various lifts are provided.

While participants were performing the various exertions, kinematics data (i.e. marker position and orientation, when applicable) were collected from skin surface markers. Various anatomical locations were derived from these markers when needed. Thus, locations could be

classified based on whether they were obtained optically or derived from optical data (Table 1). ,
These locations could then be used to derive joint positions and angles

Table 1. Available anatomical locations.

Location	Available Data	Landmark Location	Measurement Method
Top Head	(x, y, z) location	Skin Surface	Optical
Left Head	(x, y, z) location	Skin Surface	Optical
Right Head	(x, y, z) location	Skin Surface	Optical
Head origin	(x, y, z) location	Virtual point	Derivational
Nasion	(x, y, z) location	Skin Surface	Derivational
Sight end	(x, y, z) location	Virtual point	Derivational
C7/T1	(x, y, z) location	Joint Center	Derivational
Sternoclavicular Joint	(x, y, z) location	Joint Center	Derivational
Suprasternale	(x, y, z) location	Skin Surface	Electromagnetic
L5/S1	(x, y, z) location	Joint Center	Electromagnetic
PSIS	(x, y, z) location	Joint Center	Electromagnetic
Left Shoulder	(x, y, z) location	Joint Center	Derivational
Left Acromion	(x, y, z) location	Skin Surface	Optical
Left Elbow	(x, y, z) location	Joint Center	Derivational
Left Lateral Epicondyle of Humerus	(x, y, z) location	Skin Surface	Optical
Left Wrist	(x, y, z) location	Joint Center	Derivational
Left Grip Center	(x, y, z) location	Virtual point	Derivational
Left Hand	(x, y, z) location	Skin Surface	Electromagnetic
Right Shoulder	(x, y, z) location	Joint Center	Derivational
Right Acromion	(x, y, z) location	Skin Surface	Optical
Right Elbow	(x, y, z) location	Joint Center	Derivational
Right Lateral Epicondyle of Humerus	(x, y, z) location	Skin Surface	Optical
Right Wrist	(x, y, z) location	Joint Center	Derivational
Right Grip Center	(x, y, z) location	Virtual point	Derivational
Right Hand	(x, y, z) location	Skin Surface	Electromagnetic
Left Hip	(x, y, z) location	Joint Center	Derivational
Left Knee	(x, y, z) location	Joint Center	Derivational
Left Lateral Epicondyle of Femur	(x, y, z) location	Skin Surface	Optical
Left Ankle	(x, y, z) location	Joint Center	Derivational
Left Lateral Malleolus	(x, y, z) location	Skin Surface	Optical
Left Ball of Foot	(x, y, z) location	Virtual point	Derivational
Left Metatarsalphalangeal	(x, y, z) location	Skin Surface	Optical
Right Hip	(x, y, z) location	Joint Center	Derivational
Right Knee	(x, y, z) location	Joint Center	Derivational
Right Lateral Epicondyle of Femur	(x, y, z) location	Skin Surface	Optical
Right Ankle	(x, y, z) location	Joint Center	Derivational
Right Lateral Malleolus	(x, y, z) location	Skin Surface	Optical
Right Ball of Foot	(x, y, z) location	Virtual point	Derivational
Right Metatarsalphalangeal	(x, y, z) location	Skin Surface	Optical

The coordinate system for the data originated at the center of the ball of the left foot, which was not allowed to move. The X-axis is positive to the right, Y is positive in the anterior direction, and Z is positive in the superior direction, all with respect to the participant. For more detailed information on the derived measures, the reader is referred to the HUMOSIM documentation on their web site (www.humosim.org).

5.1 Data Processing

The data from the HUMOSIM files were processed before being used. This processing involved the standardization of trial start and end points and the removal of missing data by interpolation or trial cropping. The first step in this process was to determine the trajectory of the left-right and anterior-posterior centroid for the object transported during the trial by averaging the left and right hand coordinates. The inferior-superior location of this centroid was also determined in this process. This approach assumed symmetry of the object around the hands, which was plausible given the nature of the object (i.e., a box). Once this trajectory was determined, the starting point was defined as the sample where either the left-right axis difference in box centroid position between that sample and a sample at 10/25 sec in the future was more than 4 cm or the corresponding difference in right hand position in the inferior-superior axis was more than 10 cm. These two axes and the limits were selected via a trial-and-error process comparing direct observation by the experimenter against the algorithm's decision for starting point (Figure 4). Movement in the anterior-posterior axis was not considered since it was found, based on the types of movements that were performed, to not be very sensitive to the initiation of a movement. The 10/25 sec limit was also selected via trial and error; note that the number represents 10 successive frames, given the 25 Hz data collection rate. The goal in selecting this number was to minimize the number of frames needed to detect the initiation of a movement.

The stopping point was defined as the sample where any axis difference in box centroid position between that sample and a sample at 10/25 sec in the past was less than 4 cm. As before, these limits were determined based on a trial-and-error process.

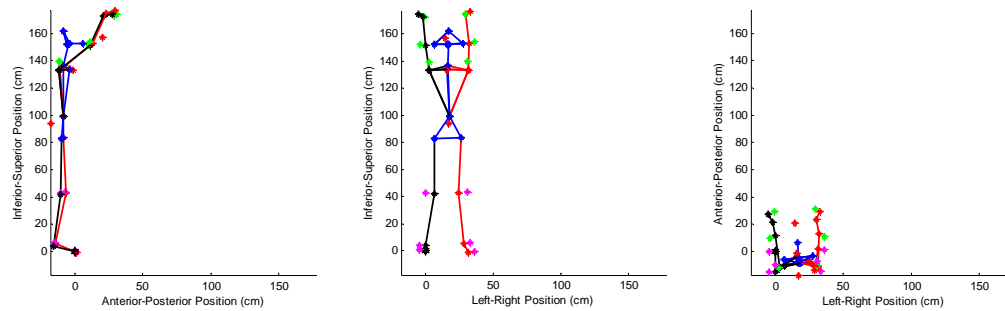


Figure 4. Stick figure representation of a posture. These representations were visually inspected to verify the appropriateness of start and stop points. All distances are in centimeters.

Files with missing data were removed by one of two methods. If the missing data were not at the end of the file (i.e. the file ended with missing data), linear interpolation was performed between the postures available immediately before and after the missing data. Possible errors due to this interpolation process were limited by removing from the sample those files where more than 25 consecutive samples of data (1.00 sec) were unavailable. This length of time represented approximately a third of the total time duration for most movements and was seldom reached for movements that were kept. In most cases where interpolation was needed, the number of missing data points was less than 15, representing less than 0.6 sec of missing data. If the missing data were at the end of the file, the file was removed without further considerations, since no end point was available for interpolation.

Two datasets were created after this initial processing. The first dataset included only sagittally symmetric movements; these data were reduced from three to two dimensions (2-D, see below for a description of this process). The second dataset included all movements; these data were used in their original three-dimensional (3-D) format. This manipulation allowed the separate creation of 2-D prediction models that might provide a design basis for the 3-D prediction models (see next chapter). The 3-D dataset required no further processing other than the variability quantification discussed in the next section. The 2-D dataset was created from the 3-D data by taking only sagittally-symmetric movements and averaging the anterior-posterior and superior-inferior coordinates of those joints with sagittal symmetry (e.g. knee, elbow).

Once these initial pre-processing stages were complete, an additional round of error checking was completed. The initial and final coordinates of similar movements across participants were compared. Coordinate values for individual participant movements that were

more than 15 cm apart from the mean in any of the three axes were studied further. This limit was selected based on judgment of the error that could be possible given the experimental procedure. If a cause could be determined for the difference, and the movement starting and end points changed so that the coordinates were within the 15 cm limit, the movement file for the participant was maintained for further use. Otherwise, the movement file was removed from further consideration. The appropriateness of the 15 cm limit was verified after observation of the data. After these corrections, ‘bring back’ movements had standard deviations for their start- and end-points of less than 12 cm. ‘Deliver’ movements had corresponding standard deviations of less than 7 cm.

For the 2-D database, where the maximum number of movement files in the database would have been 400 (20 participants X 10 locations X 2 actions [‘Deliver’, ‘Bring back’]), 329 files remained after this process. Correspondingly, the maximum number of movements for the 3-D database would have been 1200 (20 participants X 30 locations X 2 actions). The total number of 3-D movements available was 1080.

5.2 Quantification of inter- and intra-subject variability within the HUMOSIM database

5.2.1 Two Dimensions

To implicitly account for differences in anthropometry, this analysis was carried out in terms of joint angles. Standard trigonometric techniques were used to define joint angles based on a horizontal reference (represented by the antero-posterior axis), rather than included angles. Thus, for example, the knee angle represents the angle of the thigh with respect to a horizontal axis with origin at the knee. This approach allowed for an independent angular description of each segment. Continuing with the knee angle example, if a value is provided under the angular scheme employed, it is possible to visualize the orientation of the thigh in space without requiring any knowledge of the orientation of the lower leg. This visualization would not be possible if included angles were used.

The output of inverse trigonometric functions was adjusted as needed to maintain arithmetic continuity between successive joint angle values while maintaining trigonometric equivalency. For example, if a particular joint tended to exhibit values from 270° to 90° (i.e., from 270° to <360° and then from 0° to 90°), the range from 270° to <360° was re-expressed as -90° to <0° by subtracting 360° from angles larger than 180°. Note that the re-expressed values

achieve a cartesian continuity in the values (i.e. from -1° to 0°), as opposed to the ‘jump’ that would be observed between 359° and 0° if the original range of values were maintained. Note also that this approach does not introduce any limits on the range-of-motion of any joint or affect the inputs to any successive trigonometric functions.

Given that different participants completed the motions within different time lengths, movements had to be standardized in their duration to allow meaningful between-subjects comparisons. Thus, movements were time standardized into 20 different time phases, each representing 5% of the total movement time. The point with the closest time-stamp to each percentage was used to select which points to use on each time bin. For example, if the movement duration was 2 sec and the 20% point was being sought, the data point with the time-stamp closest to 0.4 sec (2 sec X 0.20) would be selected as the 20% data point.

Once the joint angles were determined and the movement time standardized, plots were used to observe the general form of the movements for both ‘Deliver’ and ‘Bring back’ motions (see example in Figure 5). These plots were used to observe inter-subject variability within the dataset. Any sudden ‘jumps’ in angle values (e.g., see the clavicle angle in Figure 5) were examined further to determine whether they were admissible within the data. This examination process used stick figure plots such as those already shown (Figure 4), but in this case the progression of successive time samples was manually controlled by the experimenter. The movement was maintained within the database unless an assignable cause for the ‘jump’ could be found.

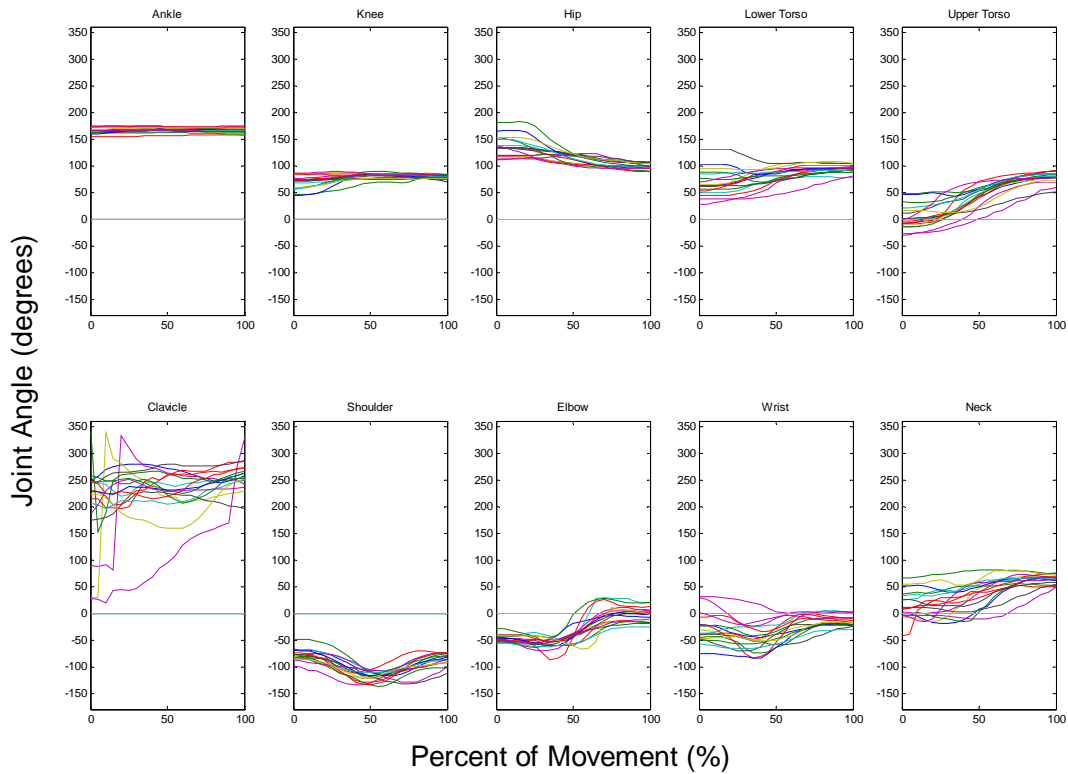


Figure 5. Joint angle time history for a movement that brings back the load from the lower near location. Each line represents a different participant.

These qualitative time histories were also used as another method of error checking. Any patterns that were observed to deviate substantially from the ‘pattern cloud’ prompted an additional observation of the movement to determine any data collection artifacts. No movement exclusions had to be made in this final round of error checks.

Quantitative analysis of the inter-subject variability was also performed to allow for later comparison of error magnitudes. The maximum standard deviations across time samples for each movement and joint combination were calculated (Table 2). For each point in time, the mean across-subject joint angle and corresponding standard deviation were calculated (Figure 6). The maximums reported here represent the maximum standard deviation observed across the time history for the movement. The clavicle angle tended to have larger maximum standard deviation values than any other joint angle. Likewise, lower movement locations seemed to exhibit significantly greater maximum variability than movements at other locations.

Table 2. Maximum standard deviation for each joint angle and movement location, calculated across time samples.

		Maximum Standard Deviation of Joint Angle (degrees)									
Movement Location		Ankle	Knee	Hip	Lower Torso	Upper Torso	Clavicle	Shoulder	Elbow	Wrist	Neck
Bring Back-Near	Lower	5.1	12.9	19.3	25.7	22.8	82.3	14.8	22.7	28.7	27.0
	Middle Lower	4.6	11.4	11.5	13.9	13.1	24.0	16.9	25.2	31.6	18.8
	Middle	3.1	2.8	4.1	9.5	5.2	10.4	12.8	14.5	9.0	8.8
	Middle Upper	5.2	3.6	4.6	9.1	5.0	21.9	27.9	22.3	22.7	8.9
	Upper	6.5	4.3	4.8	10.1	8.7	25.6	34.4	25.4	35.5	12.6
Bring Back-Far	Lower	8.9	12.8	26.0	26.5	28.0	88.7	17.4	28.9	36.4	38.6
	Middle Lower	11.6	19.8	22.4	13.7	15.5	28.0	22.2	30.9	27.9	19.2
	Middle	6.5	4.2	5.3	9.4	8.4	17.8	12.3	14.1	19.2	11.4
	Middle Upper	4.2	3.5	6.0	9.5	6.3	25.6	18.0	20.4	25.5	10.7
	Upper	8.3	3.8	5.4	10.6	6.5	25.6	22.0	17.7	21.1	13.8
Deliver-Near	Lower	4.6	13.9	16.3	22.2	22.0	68.7	19.5	28.9	29.5	24.8
	Middle Lower	5.3	8.4	10.5	13.3	14.2	33.8	12.7	11.4	25.4	17.8
	Middle	3.4	3.8	2.5	9.5	8.4	18.0	19.8	13.3	20.2	8.0
	Middle Upper	5.3	3.5	4.9	9.7	5.7	22.8	18.7	19.0	29.8	8.6
	Upper	9.0	4.5	5.5	9.5	7.5	31.8	36.4	25.2	22.4	10.6
Deliver-Far	Lower	10.4	13.9	22.6	26.0	26.4	68.7	18.1	27.6	30.2	33.8
	Middle Lower	12.0	22.1	24.1	13.7	16.0	25.1	18.2	31.3	27.9	16.4
	Middle	6.3	4.8	5.6	7.4	4.5	19.0	9.6	8.0	15.6	8.5
	Middle Upper	4.3	3.4	5.7	9.6	5.3	33.2	20.7	16.9	35.8	8.2
	Upper	12.0	3.6	6.7	12.3	6.4	72.4	32.3	27.9	33.5	12.7

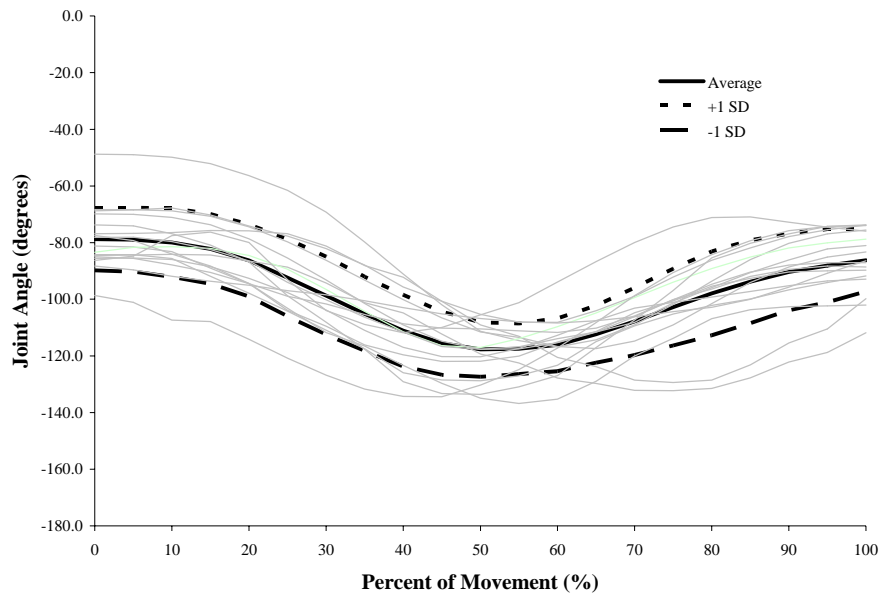


Figure 6. Joint angle time history for the shoulder joint during a movement that brings back the load from the lower near location. The gray lines show individual traces for each subject.

Intra-subject variability was determined by comparing those movements for which a replication had been performed. These included a total of 41 ‘Bring back’ motions and 39 ‘Deliver’ motions across all participants and trials. Maximum standard deviations for intra-

subject movements were in many instances lower than those representing inter-subject movements (Table 3), but this was not true for 42.4% of all cases. Given the smaller sample available, sufficient data for some of the ‘Middle’ movement locations were not available. Also, given that between-subjects and within-subject means did not use the same samples in their computation, they tended to differ qualitatively while their associated standard deviations were relatively close (Figure 7).

Table 3. Maximum within-subject standard deviation for each joint angle, calculated across time samples. Italicized cells indicate smaller within-subject variability than between-subjects variability (as shown in Table 2).

		Maximum Standard Deviation of Joint Angle (degrees)									
Movement Location		Ankle	Knee	Hip	Lower Torso	Upper Torso	Clavicle	Shoulder	Elbow	Wrist	Neck
Bring Back-Near	Lower	5.7	22.1	28.8	<i>13.5</i>	<i>10.1</i>	146.0	23.6	<i>17.3</i>	34.7	34.1
	Middle Lower	5.9	22.0	19.0	<i>11.0</i>	<i>12.7</i>	45.9	<i>14.6</i>	35.0	32.8	25.4
	Middle						N/A				
	Middle Upper	<i>1.3</i>	<i>1.9</i>	<i>1.5</i>	<i>3.1</i>	<i>3.9</i>	9.8	<i>19.3</i>	8.3	<i>14.7</i>	10.1
	Upper	3.2	2.7	2.3	3.3	4.5	33.1	<i>15.6</i>	<i>15.8</i>	36.8	6.9
Bring Back-Far	Lower	12.7	24.7	43.2	33.2	43.5	210.7	38.6	41.8	<i>29.4</i>	51.1
	Middle Lower	14.6	8.7	<i>17.3</i>	<i>10.5</i>	24.6	28.4	22.9	<i>21.8</i>	<i>24.6</i>	32.0
	Middle	2.3	<i>3.1</i>	<i>2.4</i>	<i>4.3</i>	<i>4.2</i>	2.8	4.7	2.8	3.7	4.5
	Middle Upper	2.2	2.3	2.9	3.0	3.4	<i>11.4</i>	<i>9.4</i>	8.2	<i>24.0</i>	7.9
	Upper	<i>7.1</i>	3.3	2.7	<i>3.4</i>	<i>3.9</i>	<i>9.1</i>	<i>15.2</i>	<i>10.7</i>	<i>13.9</i>	<i>11.7</i>
Deliver-Near	Lower	7.2	14.5	22.0	<i>12.7</i>	29.0	178.1	32.8	56.1	38.3	<i>14.1</i>
	Middle Lower	6.4	6.8	15.7	<i>13.1</i>	<i>14.1</i>	50.5	31.1	44.3	39.0	28.3
	Middle						N/A				
	Middle Upper	<i>0.6</i>	2.2	<i>1.8</i>	2.9	5.9	9.8	<i>13.5</i>	36.1	37.7	<i>7.0</i>
	Upper	4.2	5.5	4.8	2.3	3.6	30.3	42.4	38.1	48.3	7.8
Deliver-Far	Lower	15.9	21.8	66.5	36.4	36.7	117.8	56.2	30.7	43.4	41.3
	Middle Lower	17.0	5.0	4.9	8.8	6.4	34.5	<i>13.1</i>	<i>13.8</i>	<i>18.8</i>	<i>15.8</i>
	Middle						N/A				
	Middle Upper	<i>2.1</i>	<i>1.9</i>	3.7	2.8	2.8	<i>12.2</i>	56.6	33.5	38.1	12.6
	Upper	8.6	5.5	8.0	5.3	3.9	<i>34.7</i>	<i>55.2</i>	49.3	<i>33.0</i>	<i>12.3</i>

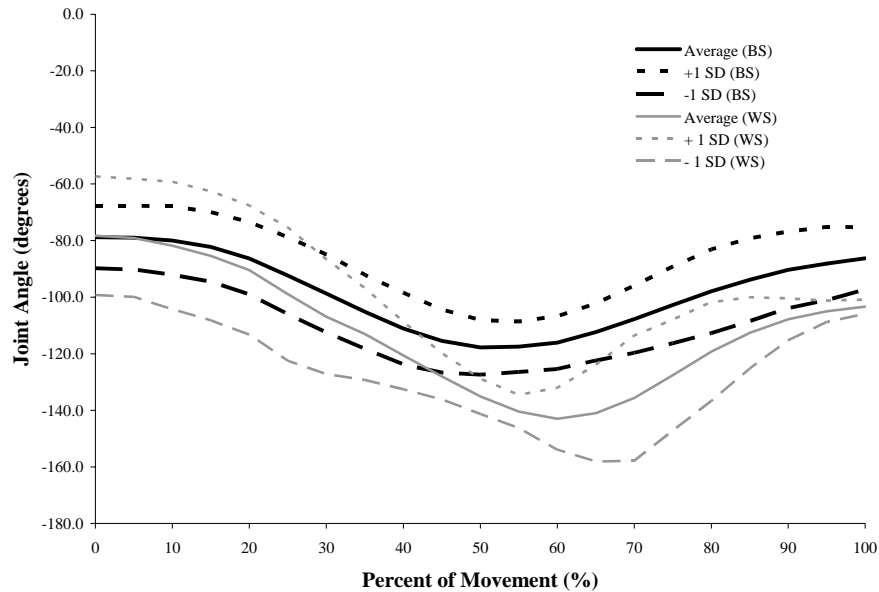


Figure 7. Joint angle time history for the shoulder joint during a movement that brings back the load from the lower near location. Black lines show the average and standard deviation between-subjects; gray lines show the average and standard deviation within-subject.

Statistical analysis was carried out to determine significant differences in maximum across-time samples standard deviation due to Source of Variability (Between-subjects vs. Within-subject), Joint (10 joints under consideration), Type of Movement (Deliver-Near, Deliver-Far, Bring Back-Near, Bring Back-Far), and Location (Lower, Middle Lower, Middle, Middle Upper, Upper). Between-subjects ANOVA was used to determine significant effects for these main factors and their two-way interactions only. The calculation of higher order interactions consumed too many degrees of freedom to maintain a stable test sensitivity. *Post hoc* tests were used to determine significant levels within each of the main factors, and used the Tukey-Kramer correction. A maximum Type I error of 1% was allowed.

The statistical results confirmed the qualitative observations based on the data in Table 2 and Table 3. Joint and Location were the two significant main effects ($F(9,261)=46.58$, $p<0.0001$; and $F(4,261)=71.06$, $p<0.0001$, respectively). For joint, the clavicle had significantly higher maximum standard deviation than all other joints (44.0° for the clavicle). The elbow, shoulder, and wrist had the second largest levels of maximum standard deviation (22.6° - 26.7°). The lower location had significantly higher levels of maximum standard deviation than all other locations (35.5°). The interactions of Source of Variability, Joint, and Type of Movement with

the Location factor were also significant ($F(4,261)=71.06, p<0.0001$; $F(4,261)=11.96, p<0.0001$; and $F(36,261)=11.86, p<0.0001$, respectively).

5.2.2 *Three Dimensions*

The three dimensional analysis of variability was also performed in terms of joint angles, allowing for a representation of each joint that was independent of participant anthropometry. Standard trigonometric techniques were used to define a rotation matrix for each joint, which was then converted into a set of Z-Y-X Euler joint angles. This sequence implies three rotations described by three different angles. The first rotation occurred around the inferior-superior axis and was quantified by α . The second rotation then occurred around the rotated anterior-posterior axis and was quantified by β . The third and last rotation occurred around the rotated left-right axis and was quantified by γ . Given that the joint coordinates available did not allow for the measurement of axial rotation for each body segment, the first two Euler angles (α and β) were sufficient to completely represent each of the joints (i.e., $\gamma=0$ for all conditions). The coordinate system used was identical to the coordinate system in which the motions were described, where the X-axis is positive to the right, Y is positive in the anterior direction, and Z is positive in the superior direction, all with respect to the participant and with an origin on the center of the ball of the left foot. As in the 2-D cases, the output of trigonometric functions was adjusted as needed to maintain arithmetic continuity between successive joint angle values.

As for the 2-D analysis, given that different participants completed the motions within different time lengths, movements had to be standardized in their duration to allow meaningful between-subjects comparisons. Thus, movements were time standardized into 20 different time phases, each representing 5% of the total movement time. The point with the closest time-stamp to each percentage was used to select which points to use on each time bin.

Once these angles were determined and the movement time standardized, plots were used to observe the general form of the movements for both ‘Deliver’ and ‘Bring back’ motions (see example in Figure 8). These plots were used to qualitatively observe inter-subject variability within the dataset. As for the 2-D case, any sudden ‘jumps’ in angle values were visually examined further to determine whether they were admissible within the data. These tended to be very common for the β angles.

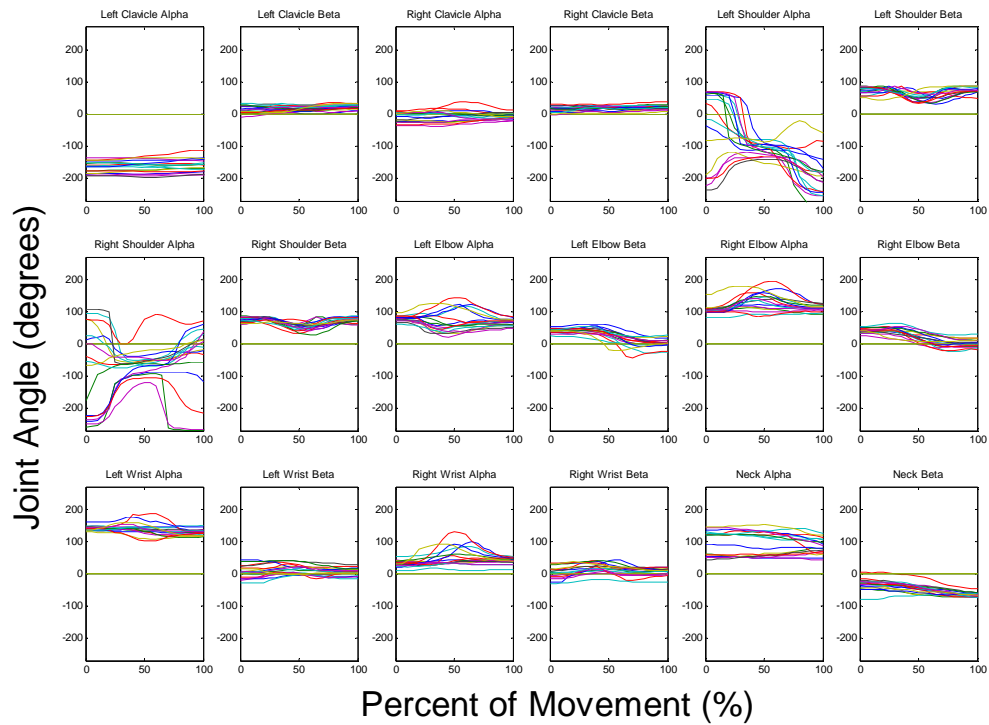
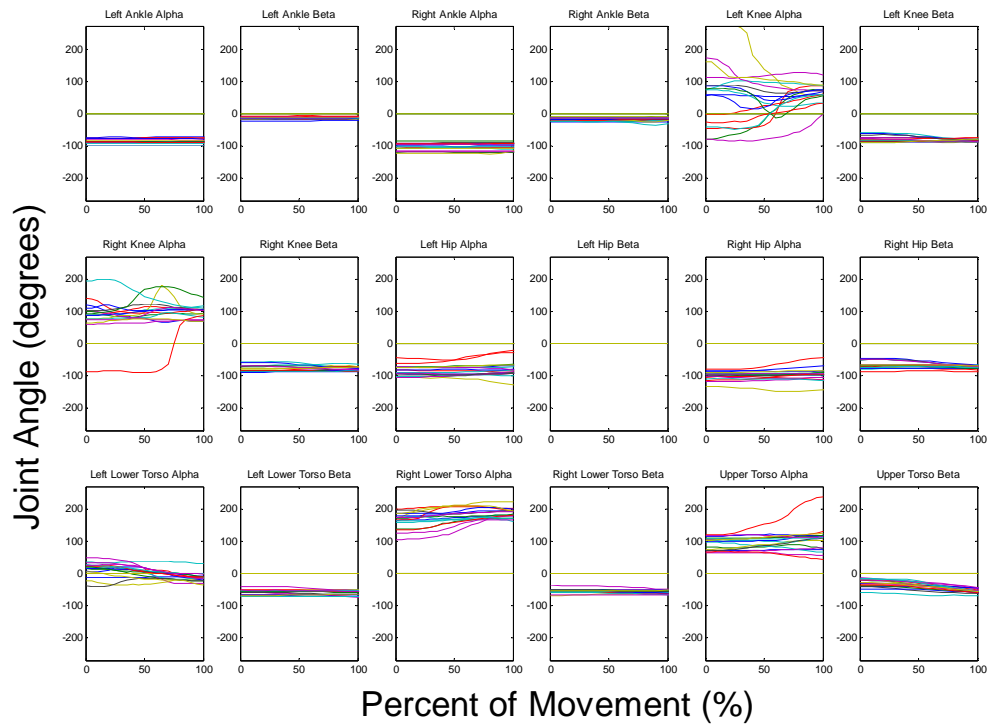


Figure 8. Joint angle time history for a movement that brings back the load from the lower near location. Alpha and Beta represent the two Euler angles used to describe the posture of each joint.

As in the 2-D case, these qualitative time histories were also used as another method of error checking. Any patterns that were observed to deviate substantially from the ‘pattern cloud’ prompted an additional observation of the movement to determine any data collection artifacts. No movement exclusions had to be made in this final round of error checks.

Quantitative analysis of the inter-subject variability was also performed. The maximum standard deviations for each movement and joint combination were calculated (Table 4). The left shoulder α angle exhibited the largest variability. Other angles with high variability included the upper torso α , right shoulder α , left hip α , right hip α , and the right knee α . These angles exhibited standard deviations in the 70° to 150° range. No discernible pattern in variability could be observed due to movement type, location, or required level of rotation.

Table 4. Maximum between-subjects standard deviation for each joint angle, calculated across time samples.

		Maximum Standard Deviation of Joint Angle (degrees)																																						
		Left														Right																								
		Ankle							Knee							Hip							Torso							Shoulder							Wrist		Neck	
		Alpha	Beta	Alpha	Beta	Alpha	Beta	Alpha	Beta	Alpha	Beta	Alpha	Beta	Alpha	Beta	Alpha	Beta	Alpha	Beta	Alpha	Beta	Alpha	Beta	Alpha	Beta	Alpha	Beta	Alpha	Beta	Alpha	Beta	Alpha	Beta							
No Rotation	Bring Back- Near	Lower	8.9	5.2	15.2	10.2	102.6	16.0	38.6	14.7	52.7	30.4	53.0	17.3	39.9	38.7	43.8	40.2	50.6	21.6	39.7	108.0	32.7	119.2	139.0	24.5	119.7	25.1	45.2	21.4	42.6	51.7	28.1	29.9	35.9	45.8	24.5			
		Middle Lower	7.3	3.9	11.5	7.0	95.7	9.3	55.9	10.7	29.5	11.3	22.8	11.9	22.6	7.7	26.7	7.1	37.9	12.8	21.4	11.9	18.0	8.7	122.3	14.9	137.8	13.4	36.1	19.2	29.4	15.5	19.3	20.2	29.6	20.2	38.8	17.7		
No Rotation	Bring Back- Far	Middle	7.7	4.9	9.3	5.6	14.0	2.7	19.2	3.0	88.3	3.8	90.4	3.1	14.6	5.7	16.2	5.7	112.5	3.6	6.5	6.8	4.2	153.2	8.3	84.5	8.9	6.8	14.5	4.9	14.4	10.1	9.0	9.7	8.6	13.7	7.2			
		Upper	7.7	4.8	5.3	4.8	16.9	3.8	25.6	3.8	74.4	3.3	108.1	3.6	15.0	5.8	15.8	5.2	147.7	2.6	8.3	3.9	10.3	4.3	180.2	23.8	44.2	25.0	14.1	19.3	4.0	20.7	17.0	15.5	16.2	22.8	23.1	8.4		
		Middle Upper	7.8	4.7	10.2	9.3	21.1	4.3	30.6	5.5	72.0	4.0	94.1	4.4	17.0	7.2	17.0	6.4	167.1	5.8	12.1	6.5	10.3	5.9	170.9	26.5	44.9	28.3	24.4	21.7	29.4	21.2	41.2	27.2	48.6	25.8	88.8	11.6		
		Upper	14.1	9.5	20.2	13.2	43.3	15.7	77.3	15.4	23.8	166.2	29.0	26.4	32.9	13.4	40.9	13.0	37.8	26.8	38.7	15.9	34.4	22.3	146.8	14.7	166.7	15.7	44.7	19.1	49.0	22.5	34.4	29.4	39.6	22.1	50.1	30.4	18.5	
	Deliver-Near	Middle Lower	7.7	6.1	42.5	16.4	83.0	12.5	72.8	27.4	38.3	72.1	24.0	18.6	21.7	9.2	27.9	8.8	24.5	15.1	18.4	13.7	15.8	7.5	136.6	23.2	120.9	22.8	66.0	26.5	31.5	23.1	31.7	26.7	37.5	21.1	25.8	18.5		
		Middle	11.7	4.7	9.0	6.4	20.5	4.6	29.0	5.1	82.1	3.6	91.6	6.8	12.8	6.2	15.3	5.3	39.7	8.0	7.9	4.8	7.9	4.9	124.9	9.2	40.6	9.7	7.8	14.3	9.0	14.5	13.0	15.2	13.1	13.0	14.5	10.3	10.5	
		Middle Upper	6.7	3.2	7.2	5.3	16.0	3.4	21.3	4.3	103.4	3.6	103.1	4.5	15.1	6.5	16.9	5.9	96.5	5.2	9.4	4.6	8.3	4.6	179.9	16.2	41.6	16.0	9.0	18.6	7.8	18.7	19.7	17.7	18.9	17.8	73.5	10.2		
		Upper	9.2	4.2	10.3	6.3	18.0	4.0	36.1	4.1	145.8	4.0	123.7	3.8	16.2	6.4	18.3	5.7	115.5	4.3	9.0	5.0	10.2	4.5	161.3	18.5	30.9	19.5	11.1	16.1	11.3	15.8	22.1	16.5	20.8	19.6	94.2	10.2		
	Deliver-Far	Lower	7.3	4.7	21.6	13.7	80.4	11.1	34.5	18.3	78.3	74.8	70.0	14.7	39.8	13.5	37.0	12.9	85.3	20.1	33.2	19.5	28.9	16.3	137.2	12.6	129.3	12.1	32.3	25.0	37.1	23.8	25.3	24.6	33.6	24.4	46.4	21.4		
		Middle Lower	7.5	4.9	13.8	6.7	103.9	7.7	50.9	8.9	95.2	10.0	89.5	11.0	23.1	8.1	28.5	6.5	98.9	13.9	25.9	14.5	26.0	9.6	161.4	12.6	113.6	14.8	31.4	21.0	30.3	23.4	24.5	17.7	30.4	19.2	38.6	17.3		
		Middle	6.5	2.7	8.8	5.0	17.2	2.9	14.4	3.7	84.1	3.7	65.6	2.8	16.7	6.5	14.2	6.1	106.1	4.5	7.2	5.5	7.7	3.6	161.9	14.9	47.6	15.4	12.9	20.8	7.5	20.9	26.2	20.1	23.1	21.6	13.6	7.2		
		Upper	7.7	4.5	9.8	4.9	19.0	3.7	21.8	4.8	108.9	3.8	109.8	3.4	15.9	6.1	16.2	5.3	137.0	3.3	8.9	3.9	10.3	7.7	3.7	187.9	17.1	84.0	14.7	26.1	20.5	10.9	17.6	19.6	27.1	23.3	27.4	90.9	7.1	
Medium Rotation	Bring Back- Near	Lower	13.3	9.9	46.9	17.6	82.0	13.2	35.7	21.3	55.6	169.4	53.8	24.5	34.2	13.1	42.0	14.5	56.0	24.7	31.7	19.5	31.7	23.1	136.5	11.8	160.3	14.7	41.0	20.5	45.1	22.0	36.1	24.4	34.5	21.8	49.0	27.9		
		Middle Lower	8.1	10.1	43.7	18.4	57.4	15.3	65.9	29.0	105.9	101.1	82.5	20.8	21.4	8.8	27.7	7.8	83.0	15.2	22.4	15.9	21.8	9.5	126.3	18.9	157.8	16.7	33.8	21.9	33.7	25.0	39.1	25.5	29.7	23.9	26.8	15.7		
		Middle	11.4	4.5	15.3	7.4	47.2	4.9	54.7	5.9	101.3	4.2	118.7	6.7	15.3	5.8	14.1	5.8	14.2	10.5	8.5	5.6	9.0	4.8	167.5	13.5	84.5	13.5	10.8	16.2	7.4	14.4	24.4	24.1	29.1	25.9	18.0	8.9		
		Upper	6.9	2.7	7.3	4.5	17.9	3.0	22.5	3.9	103.5	3.9	85.1	5.2	15.6	6.3	16.5	5.9	106.9	4.7	10.0	4.6	9.3	4.1	153.9	17.7	84.1	16.6	14.3	15.9	8.5	16.3	21.0	29.8	29.7	32.0	96.7	6.3		
	Deliver-Near	Lower	8.8	6.1	10.1	6.3	20.6	4.2	25.8	4.2	137.9	3.4	122.6	8.5	19.1	6.8	19.6	5.5	97.1	5.9	12.6	6.3	12.2	5.8	173.2	26.8	41.2	26.0	14.6	24.2	13.9	24.3	28.3	23.9	26.1	21.9	103.3	8.0		
		Middle Lower	8.2	4.4	19.4	5.1	27.6	6.5	115.8	5.4	44.0	8.3	26.9	9.5	15.1	7.5	22.9	6.9	35.1	10.2	17.0	12.1	15.0	12.9	136.5	12.8	121.1	15.3	16.3	16.5	22.0	18.6	29.8	27.9	17.8	24.0	31.5	19.1		
		Middle	6.6	4.6	11.0	4.3	17.7	4.1	31.6	4.6	111.7	3.1	69.8	4.1	12.7	5.4	17.7	5.3	94.1	6.3	10.1	4.6	10.6	5.9	145.3	10.0	68.6	13.6	12.9	16.9	10.3	16.7	14.9	17.3	13.1	18.3	30.3	10.7		
		Upper	6.8	3.9	18.0	4.6	17.5	4.3	38.4	4.2	74.4	3.1	90.8	5.6	17.0	6.7	21.1	6.4	134.7	3.6	11.9	4.0	14.2	4.8	165.2	16.8	68.9	22.9	19.7	17.2	12.4	20.2	16.0	16.3	24.0	19.5	81.9	9.6		
	Deliver-Far	Lower	11.2	14.6	14.4	5.4	15.9	5.8	29.0	4.7	82.6	3.9	87.0	6.9	13.0	6.4	20.5	6.2	162.6	3.0	9.9	6.6	12.7	5.4	173.4	30.9	38.6	28.2	26.0	18.3	23.3	19.2	29.3	19.6	31.3	23.2	119.0	9.7		
		Middle Lower	11.9	10.0	16.6	7.6	28.4	13.5	114.9	12.0	35.8	21.9	15.4	20.5	27.0	9.8	35.2	9.8	25.0	19.5	21.1	17.4	16.9	10.7	95.3	18.3	108.8	16.5	36.4	23.2	67.0	17.6	35.9	22.1	28.3	22.4	22.9	18.6		
		Middle	9.7	7.3	14.7	7.3	21.4	5.9	98.3	5.1	69.1	5.8	23.1	7.6	13.6	8.6	20.3	7.7	27.1	11.6	15.0	12.1	12.8	8.0	142.2	14.4	68.5	12.1	15.3	19.1	24.2	15.4	27.7	22.6	16.1	17.9	19.2	15.8		
		Upper	10.2	11.7	13.6	6.3	23.2	6.8	97.5	4.7	81.6	5.7	35.4	7.5	14.0	6.0	18.3	7.2	62.2	8.8	11.0	5.8	9.0	7.2	157.7	11.1	64.0	11.4	14.1	16.8	15.8	15.4	15.1	14.4	12.9	12.8	57.0	12.5		
High Rotation	Bring Back- Near	Lower	10.7	12.4	14.0	6.0	16.4	7.0	88.6	4.6	63.6	6.0	45.5	6.5	11.0	6.5	18.6	7.4	96.2	6.5	10.5	5.9	11.9	6.3	158.3	13.1	49.8	15.6	15.6	18.7	17.0	19.6	18.9	16.2	18.6	17.6	88.8	11.2		
		Middle Lower	27.2	16.1	13.8	7.1	15.1	7.0	74.9	5.7	81.3	6.5	61.0	8.5	13.9	6.5	21.1	8.5	140.1	6.3	13.7	7.7	13.3	6.4	169.1	22.8	31.5	20.5	23.1	16.1	24.1	20.5	26.8	20.0	26.0	18.9	98.1	8.4		
		Middle	8.7	5.3	22.0	12.5	37.9	12.1	73.5	17.2	93.4	79.5	64.2	18.4	20.9	10.0	26.2	9.5	84.5	17.3	22.0	12.5	20.8	11.8	165.5	14.6	102.8	13.4	19.1	18.1	27.6	20.3	26.1	27.0	24.8	25.5	27.6	21.6		
		Upper	7.6	4.6	19.1	5.4	29.9	5.1	99.1	5.8	114.0	7.8	72.3	7.3	15.1	8.3	23.1	7.4	102.0	12.7	16.5	12.6	15.4	12.4	171.1	10.6	115.7	12.0	22.3	17.3	15.9	21.6	22.7	27.5	28.4	28.9	31.6	15.1		
	Deliver-Near	Lower	8.2	4.8	15.3	4.8	15.4	4.4	42.9	5.2	99.6	3.5	109.5	5.8	13.1	5.7	16.3	5.4	104.0	6.2	11.6	4.8	8.1	4.0	184.6	10.1	94.2	12.3	16.8	15.8	10.1	15.8	20.2	23.2	28.0	28.7	20.3	8.7		
		Middle Lower	7.2	4.2	17.9	6.4	17.1	4.1	82.0	4.4	95.1	3.2	107.7	4.7	15.7	6.2	18.4	6.1	122.6	3.5	14.4	4.3	11.1	4.7	167.6	20.8	84.5	21.3	21.9	23.4	13.3	23.0	22.7	23.4	27.2	25.9	59.9	7.5		
		Middle	9.9	10.2	15.3	5.6	17.2	4.7	67.2	4.9	109.2	3.6	116.3	6.9	13.3	7.3	19.6	6.7	157.7	3.1	12.9	7.5	10.2	6.2	185.1	30.6	66.7	27.9	35.2	25.6	24.2	25.9	24.7	21.1	25.6	23.6	102.0	9.5		
		Upper	17.6	10.3	14.2	8.8	23.7	14.5	124.8	17.5	64.9	75.4	50.2	21.1	28.0	10.9	34.5	11.6	84.1	18.4	16.7	15.6	16.9	11.8	162.0	11.6	96.5	13.3	21.4	17.6	19.2	14.8	22.6	20.0	24.8	15.5	34.0	23.3		
	Deliver-Far	Lower	10.9	7.2	15.0	7.4	26.3	6.5	111.6	4.7	108.1	6.9	67.3	9.5	18.1	7.7	19.6	7.2	88.0	12.4	11.6	10.2	14.0	9.3	175.8	11.7	97.5	11.3	18.0	19.7	16.7	17.0	21.0	28.9	29.7	27.9	19.6	16.6		
		Middle Lower	12.7	14.8	14.7	6.7	15.5	7.2	98.1	4.9	118.4	5.8	60.8	8.3	14.2	6.1	17.4																							

Intra-subject variability was observed by comparing those movements for which a replication had been performed. These included a total of 232 ‘Bring back’ motions and 232 ‘Deliver’ motions across all participants and trials. Maximum standard deviations for intra-subject movements were in many instances lower than those representing inter-subject movements (Table 5), but this was not true for 42.5% of all cases. Given the smaller sample available, sufficient data for some of the ‘Middle’ movement locations were not available.

As in the 2-D case, statistical analysis was carried out to determine significant differences in maximum across-time samples standard deviation due to Source of Variability (Between-subjects vs. Within-subject), Joint (10 joints under consideration), Type of Movement (Deliver-Near, Deliver-Far, Bring Back-Near, Bring Back-Far), and Location (Lower, Middle Lower, Middle, Middle Upper, Upper). An additional factor, Rotation (No Rotation, Medium Rotation, High Rotation), was added in consideration of those movements that were not sagittally symmetric. Between-subjects ANOVA was used to determine significant effects for these main factors and their two-way interactions only. The calculation of higher order interactions consumed too many degrees of freedom to maintain a stable test sensitivity. *Post hoc* tests were used to determine significant levels within each of the main factors, and used the Tukey-Kramer correction. A maximum Type I error of 1% was allowed.

The statistical results (Table 6) confirmed the qualitative observations based on the data in Table 4 and Table 5. All main effects were significant. Within-subject variability was significantly smaller than between-subjects variability (Within-subject: 31.3°, Between-subjects: 35.6°). *Post hoc* analysis of the significant Source of Variability interactions with Joint and Rotation confirmed the results from the Source of Variability main effect, that is, when there was a significant difference in the interactions, within-subject variability was higher than between-subjects variability. The interaction of Source of Variability with Location, however, showed a reverse effect for the Middle location.

For the Joint factor, the left shoulder α angle had significantly higher variability associated with it than any other joint (Left shoulder α : 171.3°, Closest joint: 110.7°). This finding held across the significant interactions of Joint with Source of Variability, Type of Movement, and Rotation. However, it was not consistently observed across levels of Location, where the right shoulder α angle was equivalent in magnitude to the left shoulder α angle for the Lower and Middle Lower locations. *Post hoc* tests also showed a second group of joints (right shoulder α , the upper torso α , the left and right hip α , the left and right knee α , the neck α , and the right elbow α) with significantly smaller variability than the left shoulder α but larger variability than any of the remaining joint angles. With the exception of the left knee α , this group was consistently observed independent of Source of Variability and Type of Movement. However, the grouping was not consistently observed across levels of Location (specifically the lower, middle lower, and middle locations) and Rotation (specifically the no rotation conditions).

Deliver movements (both near and far) had significantly higher variability than Bring Back movements (Deliver: 35.6°-36.3°, Bring Back: 32.5°-32.8°). However, *post hoc* tests of the significant Joint X Type of Movement interaction showed that this difference did not exist across all joints. In terms of Location, all the different locations were significantly different from each other. The lower movement location had the highest variability (42.3°) followed by the upper location (39.5°), middle lower location (35.6°), middle upper location (28.9°), and middle location (22.4°). Finally, the conditions that required rotation around the inferior-superior axis exhibited higher variability than the conditions where no rotation was required (High rotation: 36.8°, Medium rotation: 34.8°, No rotation: 31.5°). These findings were also observed across the significant Location X Rotation interaction.

Table 6. Statistical results for comparisons of maximum standard deviation across time samples for the 3-D case. Italicized p-values indicate significant effects.

Factor	F-value	p-value
Source of Variability	F(1,3695)	<0.0001
Joint	F(33,3695)	<0.0001
Source of Variability X Joint	F(33,3695)	<0.0001
Type of Movement	F(3,3695)	0.0003
Source of Variability X Type of Movement	F(3,3695)	0.3625
Joint X Type of Movement	F(99,3695)	<0.0001
Location	F(4,3695)	<0.0001
Source of Variability X Location	F(4,3695)	<0.0001
Joint X Location	F(132,3695)	<0.0001
Type of Movement X Location	F(12,3695)	0.5981
Rotation	F(2,3695)	<0.0001
Source of Variability X Rotation	F(2,3695)	0.0010
Joint X Rotation	F(66,3695)	<0.0001
Type of Movement X Rotation	F(6,3695)	0.6081
Location X Rotation	F(8,3695)	<0.0001

5.3 Synthesis of database processing

The steps described above allowed for the calculation of estimates of database reliability through the determination of inherent measures of variability within the dataset. These estimates will become useful as modeling of the database is attempted, as they establish a useful bound for any model predictions. Between-subjects estimates of variability represent an appropriate comparison point for models that do not attempt to account for inter-subject variability. In those situations, the mean joint trajectory across participants is the prediction goal, and predictions within the variability envelope suggested by between-subject variability are plausible.

When models attempt to account for inter-subject variability, within-subject estimates of variability represent the appropriate comparison points. In these cases, a perfect model that received the appropriate inputs would be able to correctly account for differences between participants. Model predictions within the variability envelope suggested by within-subject variability would thus be considered plausible, as the model would have no information that allows it to differentiate between movement repetitions for each particular participant. In these cases, the mean joint trajectory within a participant is the prediction goal.

Statistical results allowed for some interesting observations to be gleaned from the data. In both the 2-D and 3-D cases, differences in variability were observed across the joint of interest and the location to which the movement was performed. The shoulder and clavicle joints tended to exhibit higher levels of variability than other joints, which is not surprising given the number of degrees of freedom available at the shoulder. Other than this commonality, however, the 2-D and 3-D cases differed on the joints with the largest variability. The 2-D case showed that upper limb joints had larger variability, whereas the 3-D case included some lower limb joints (e.g. knee and hip). This suggests that the variability observed in the 3-D case for the lower limb joints occurs in planes other than the sagittal plane.

For both 2-D and 3-D situations, the lower locations had significantly higher variability than other locations. In the 3-D case, lower locations were clearly followed by the upper locations and the middle upper and lower locations. These results support the intuitive conclusion that the further a movement departs from its point of origin, the larger the room for changes in movement performance and thus, increases in the variability of the selected motion path. This might in turn support theories of motor control that do not posit the existence of rigid motor programs. If these programs are rigid, then it would be expected that variability would not be a function of the location to which a movement is performed. Alternatively, it could also support that these motor programs are scaled such that the variability is modified as a function of one or more mobility representation parameters (e.g. range-of-motion).

Finally, the variability observed in this analysis is not atypical. Chang, et al. (2001), for example, graphically describe elbow, shoulder, hip, knee, and ankle trajectories during a sagittally symmetric lifting task. The range of trajectory values, extrapolated from the graphs, differed between-subjects as much as 29°, albeit typical values are closer to the 10° range. Similar observations can be gathered from the data presented graphically in Lee (1988) and Lin

et al. (1999). Of the joints studied here, the shoulder exhibited the highest levels of variability. It is possible that, in addition to the inherent variability that can be accounted for given the large number of degrees-of-freedom for this joint, the angle representation selected was not stable in representing the joint (although it accurately allowed the reconstruction of joint position). If this was the case, then some of the large variability found could perhaps be reduced if an alternate angle representation were used.

With the processing of the data complete and quantitative knowledge of the reliability of the dataset, the next chapters describe the process of modeling the HUMOSIM database using artificial neural networks.

Chapter 6 SIMULATING MOVEMENTS FOR AN INDIVIDUAL

The approach in this investigation was to initially develop simple models that could be increased in complexity, as needed, in order to model more complex situations. This chapter describes the results obtained for these initial efforts. Given the relatively large levels of between- and within-subject variability observed in the previous chapter, initial models were developed to predict motion for only a single participant without considering movement repetition. Thus, the models discussed in this chapter have the goal of using artificial neural networks to predict mean motion paths for one specific individual. The expectation was that the network structure developed from this effort could be expanded to assimilate the increased variability introduced by modeling across humans.

The chapter is divided into two main sections, which separate the models created based on their applicability to two or three dimensions. Two-dimensional models were created initially since the number of inputs and the associated model complexity were smaller. These models are described first. Three-dimensional models were then developed that employed structures found effective for the two-dimensional cases.

Within each of these two sections, two modeling approaches are described. The first approach used ANNs to predict joint positions. The second approach, which proved more successful, predicted joint angles using the same ANN technology with a different model structure. Each of these approaches, prediction of joint positions and prediction of joint angles, is described with respect to different training sets of increasing size. The networks were initially trained using a small subset of movements, the size of which was increased as needed to improve prediction accuracy and to examine the ability of the network to adapt its inner parameters to fit increasing amounts of data.

The final result of this process is a particular network structure that models the data with acceptable levels of error, and which is ready for expansion to accept and adapt to data from diverse humans. In addition, a series of lessons learned are also discussed in terms of particular structures and/or assumptions with varying degrees of effectiveness.

During the process of developing the network structures that are reported, a series of smaller-scale iterations were necessary in many instances. For example, a sufficient number of hidden units had to be determined for each network structure, a process for which no analytical solution exists as of this writing (Touretzky and Pomerleau, 1989). These steps are considered

secondary to the process of defining an appropriate structure, and are thus not documented in detail. While, for example, the number of hidden units in the networks is documented in this writing for replication, no detailed discussion is provided on the iterations needed to determine the appropriateness of that number.

6.1 Predicting joint positions

6.1.1 Two-dimensions

Two-dimensional movement modeling is substantially simpler than three-dimensional modeling, as the number of degrees of freedom in the model is reduced. This results in simpler models that train quicker than comparable three-dimensional models. For these reasons, two-dimensional modeling was used initially to test different network structures and establish their usefulness.

6.1.1.1 Determining the inputs of the ANNs

Based on previous discussions of inter- and intra-person variability (Chapter 2) and lift posture modifiers (Chapter 3), a variety of inputs were deemed useful in the development of an effective ANN posture prediction model. Important inter-personal variability factors appeared to be gender, anatomical differences, strength capabilities, and behavioral factors. Gender, however, seemed to be better modeled as a covariate of anatomical differences, and will be treated as such in this investigation. The influence of behavioral factors has not been properly quantified and appropriate descriptors were not available within the HUMOSIM database used in this investigation. As a result, in addition to accounting for task-dependent factors, the motion prediction techniques in this investigation accounted only for anatomical differences and strength capabilities.

The method for including these factors depends in large part on the assumed control structure synthesized by the network. For example, either joint angles or joint positions could be considered as the predicted entity. Generally, joint angles are used as the predicted entity, as they allow for a reduction in the variability that must be modeled, given that different person-to-person anthropometries determine different joint positions, even when the individuals assume similar postures. Joint angles have also been shown to exhibit a certain level of invariance with respect to the kinematic environment (Adamovich et al., 2001). However, their prediction requires the use of a scheme to translate joint angles into end-effector positions, which increases model complexity slightly and perhaps unnecessarily. Thus, given the exploratory nature of this

effort, the initial networks created predicted joint positions. As the reader shall surmise, it became necessary to shift efforts towards the prediction of joint angles, based on results obtained for the prediction of joint positions.

Given that the models described in this chapter consider only the motions performed by a particular participant, more detailed discussions on including inter-personal factors in model development are reserved for future chapters. The reader should note, however, that the possibility of future inclusion of these factors indirectly shaped the network structures considered within the context of a single individual.

6.1.1.2 Creating the ANNs

The Matlab (Mathworks, Natick, MA) Neural Network Toolbox was used to create and evaluate the various neural networks. This toolbox is capable of creating a variety of networks and training them using a variety of approaches. These networks include basic perceptron units, linear and adaptive filters, backpropagation networks, control system networks, radial basis networks, self-organizing and learning vector quantization networks, and recurrent networks. The last type, recurrent networks, will serve as the basis for the motion prediction networks developed as part of this section.

Among the various types of recurrent networks, two specific structures stand out. These structures are Jordan-Elman networks and Hopfield networks. Jordan-Elman networks are backpropagation networks with an additional feedback connection from the output of the hidden layer (Elman network) or from the output of the network (Jordan network) to its input. This feedback path, which is delayed by at least one time step (i.e. the inputs at time i provide an output at time i , but this output is not fed back to the network until time $i+1$), allows Jordan-Elman networks to learn to recognize and generate temporal patterns in addition to spatial patterns (Elman, 1990; Jordan, 1986). Hopfield networks are used to store one or more stable target vectors. These stable vectors are then used as ‘memories’ that the network recalls when provided with similar vectors that cue the network memory (Li et al., 1989). Jordan-Elman networks were the structural basis for the networks created as part of this section since their structure provided the feedback loops envisioned as necessary for this application. While useful in many situations, Hopfield networks are better suited to classification or categorization tasks, which are not a direct goal of the current effort. Although it has been hypothesized that motor programs, which might be better modeled via Hopfield networks, play a role in movement

coordination (e.g., Biguer et al., 1982; Corradini et al., 1992), the goal of this investigation was not to define what these programs might be (as use of a Hopfield network might allow) but rather to examine the kinematics behind the execution of the motion.

The initial neural network topology (Figure 9) was based on the work of Bellan et al. (1999), and is a modified version of the Jordan-Elman network previously discussed. These researchers showed that this network structure can synthesize arm reaching movements with relatively low levels of error. Given these encouraging results, the initial approach was to modify their model structure to fit the lifting exertion, which can be more difficult to model than an arm reach given the additional degrees of freedom available. The Bellan et al. (1999) network topology uses two feedback loops originating from the output layer.

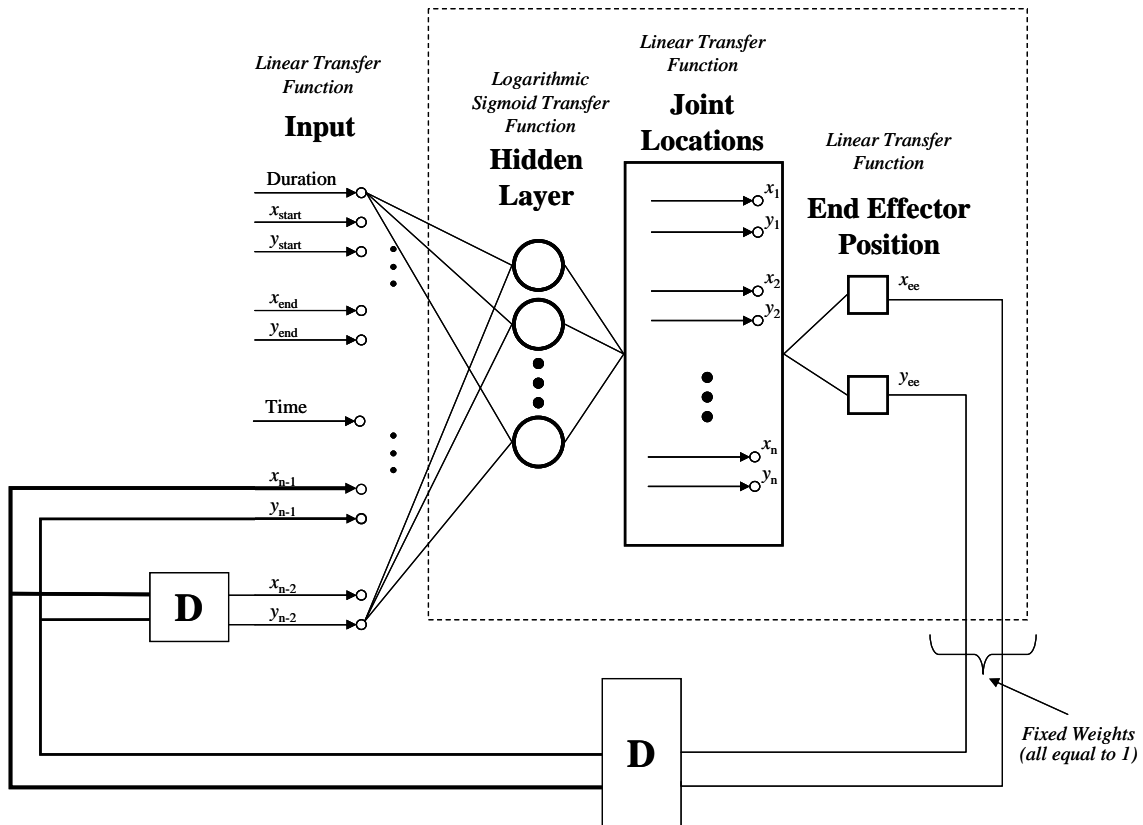


Figure 9. Initial two-dimensional network structure, based on a Jordan-Elman network. Although all layers are fully interconnected, some connections are omitted for clarity. A detailed diagram of the connections within the dashed-line box is presented in Figure 10. Boxes with 'D' represent a single time delay.

There are 10 inputs to the network, four of these with associated delays. The duration and time inputs were expected to combine to provide the network with an indication of the speed

of the lift, so that the movement sequence was properly timed. The start and end x and y coordinates indicate initial and final object center-of-mass locations. The last set of inputs represented delayed states of end-effector position, and provided the network with historical information on the movement. One set of outputs providing information for these inputs was delayed by one cycle while the remaining set of outputs was delayed by two cycles. Bellan, et al. (1999) hypothesize that these single and double delays provide the network with information on movement speed and acceleration, respectively.

The coordinates input to the model require a coordinate-system origin located at the ball of the left foot, as provided by HUMOSIM data. Information from other lifting kinematics databases could be used within the models described in this section after a suitable transformation of their coordinate systems is made.

The input layer was fully interconnected with the first hidden layer, which had no implicit physiological meaning. Pilot testing suggested the use of a hidden layer with 100 nodes for the prediction of 12 different joint positions (with two-dimensions each) and the x and y positions for the end effector. The pilot tests compared the speed of training and minimum error achieved by networks with different hidden layer sizes. Layers of size 25, 50, 100, and 200 were tested. The network with the 100 units in the hidden layer achieved similar error rates to those for the 200 unit network, but trained faster due to the reduced number of weights that had to be determined.

The hidden layer fully interconnected with the joint location layer. These joint location nodes indicated the position of each joint selected for inclusion in the model. In turn, these joint location nodes were fully interconnected with the end-effector location layer to produce the end-effector position prediction (Figure 10). At this point, no assumptions were made, or constraints placed, on the kinematic chain and/or link lengths.

All weights were modifiable by training except for those connections between the end-effector location layer and the delayed inputs, as it was desired for these delayed inputs to remain equal to end-effector position. Only the hidden layer bias was trained. Biases for the joint location and end-effector location layers were set equal to the initial posture, and were not changed during the learning process. Initial pilot tests allowed for these biases to be trained, and it was found that the network was unable to converge to a small enough error, which, in contrast, occurred when biases were pre-set.

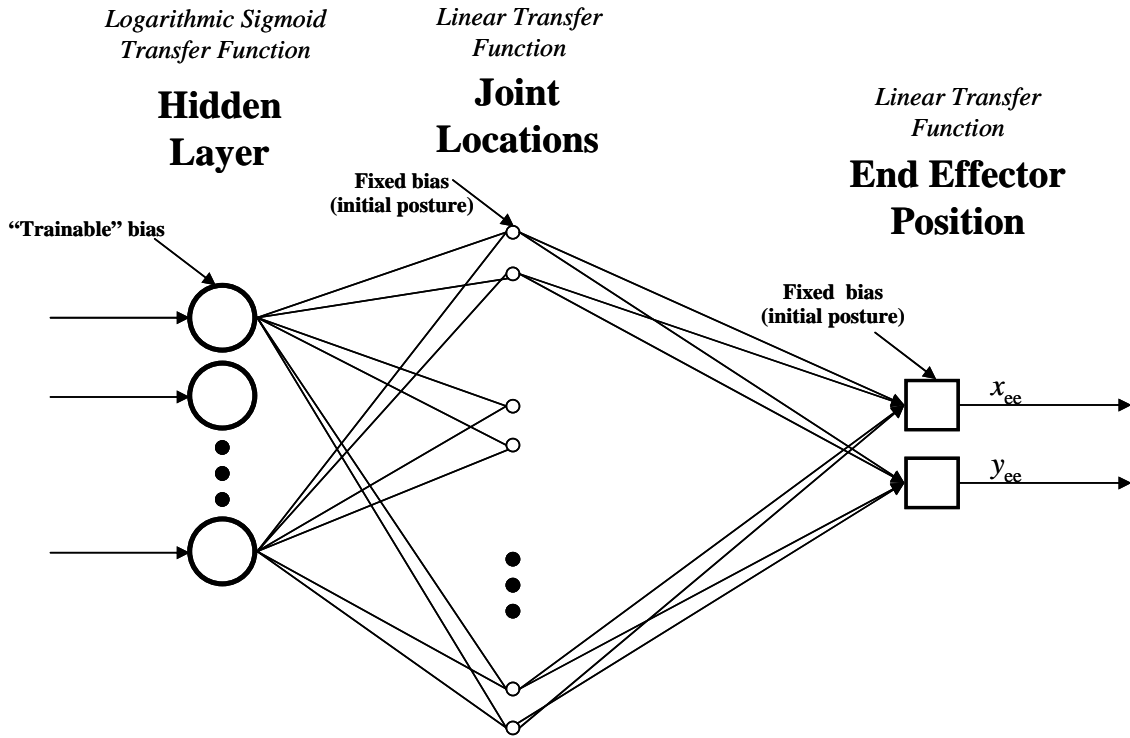


Figure 10. Detail of connections for the joint locations layer. Note that this diagram represents a detail of Figure 9.

Initial activation functions of the hidden layer used a sigmoid function (Equation 1). This function requires knowledge of a net input to the neuron (Equation 2) and a value for the bias (i.e., a baseline input level). The sigmoid function constrains the activation of a neuron between 0 and 1, which is desirable in normalizing inputs to subsequent layers.

$$a_i = \frac{1}{1 + e^{-(net_i + bias_i)}} \quad (1)$$

where,

- i identifies the node
- $bias_i$ variable term applied to unit i
- net_i net activation input (see equation 2)
- a_i resultant activation for node i

A unit's net input (net_i) is determined using the following formula.

$$net_i = \sum_j a_j * w_{i \leftarrow j} \quad (2)$$

where,

j	indexes all units that connect to unit i
a_j	activation level of unit j
$w_{i \leftarrow j}$	weight of connection from j to i

Activation functions for the joint location and end-effector position layers were linear with an intercept of 0 and slope of 1. Thus, the activation of each of these nodes was equal to their net input.

The training dataset contained time-stamped input and output vectors with values for, respectively, each of the input nodes and empirical coordinates for each of the joints under consideration and the end-effector. Errors were backpropagated from the end-effector nodes and the joint location nodes. Batch training was used, thus, network parameters were updated based on overall errors of the network for the global training set, rather than sequentially as each training observation was presented. Sequential training was tested in pilot runs, but resulted in errors that were at least an order of magnitude higher than those obtained from batch training. A training function with adaptive learning rates and momentums was used to speed network convergence to an acceptable error rate (Hagan et al., 1996), while reducing the chance for local minima (in prediction error) to be reached instead of the more desirable global minima. To further reduce this chance, for the initial networks more than one training process was conducted which employed differentially initialized networks. If similar levels of performance were obtained from these independent networks, then the chance that local minima were being identified was reduced. Throughout these tests, similar performance levels were observed between differentially initialized networks, and it was assumed for the rest of the investigation that the training function used was indeed effective in avoiding stopping the training process at local minima.

The maximum number of epochs was set at 500,000; however, this number was never reached. The training was either manually stopped as the errors stabilized or a maximum error threshold was reached. Manual stopping of the network was performed when errors had not improved by more than 10% within 20,000 epochs. Network performance was measured through the mean square error (mse) when the joint location and end-effector position outputs

were compared to the known movement. The mse training threshold was set at 0.001 cm^2 . The initial learning rate was set at 0.2, and the initial momentum constant was set at 0.1. These settings were selected based on researcher experience with the training function used. The reader should note that these rates were adaptable, which reduces the influence of the initial values selection at the cost of increased training times. Tests with different values for the learning rate and momentum constant in close proximity with those used (i.e. < 1.0) did not seem to affect network training performance in pilot tests.

Data were converted to two dimensions on the sagittal plane by collapsing the movement on the left-right axis. This collapsing process involved the averaging of coordinates for the same axis of left and right joints. For example, to obtain the 2-D coordinates for the shoulder, the averages for the anterior-posterior and superior-inferior coordinates were calculated. To reduce the possibility for asymmetry on the left-right axis, only movements that were expected to be sagittally symmetric were included.

One movement was simulated from the HUMOSIM database (Figure 11). This movement required the delivery of the box to an approximately shoulder-height location directly in front of the participant. The movement and participant were selected at random from those movements and participants available, since this initial effort was meant to serve as a proof of concept.

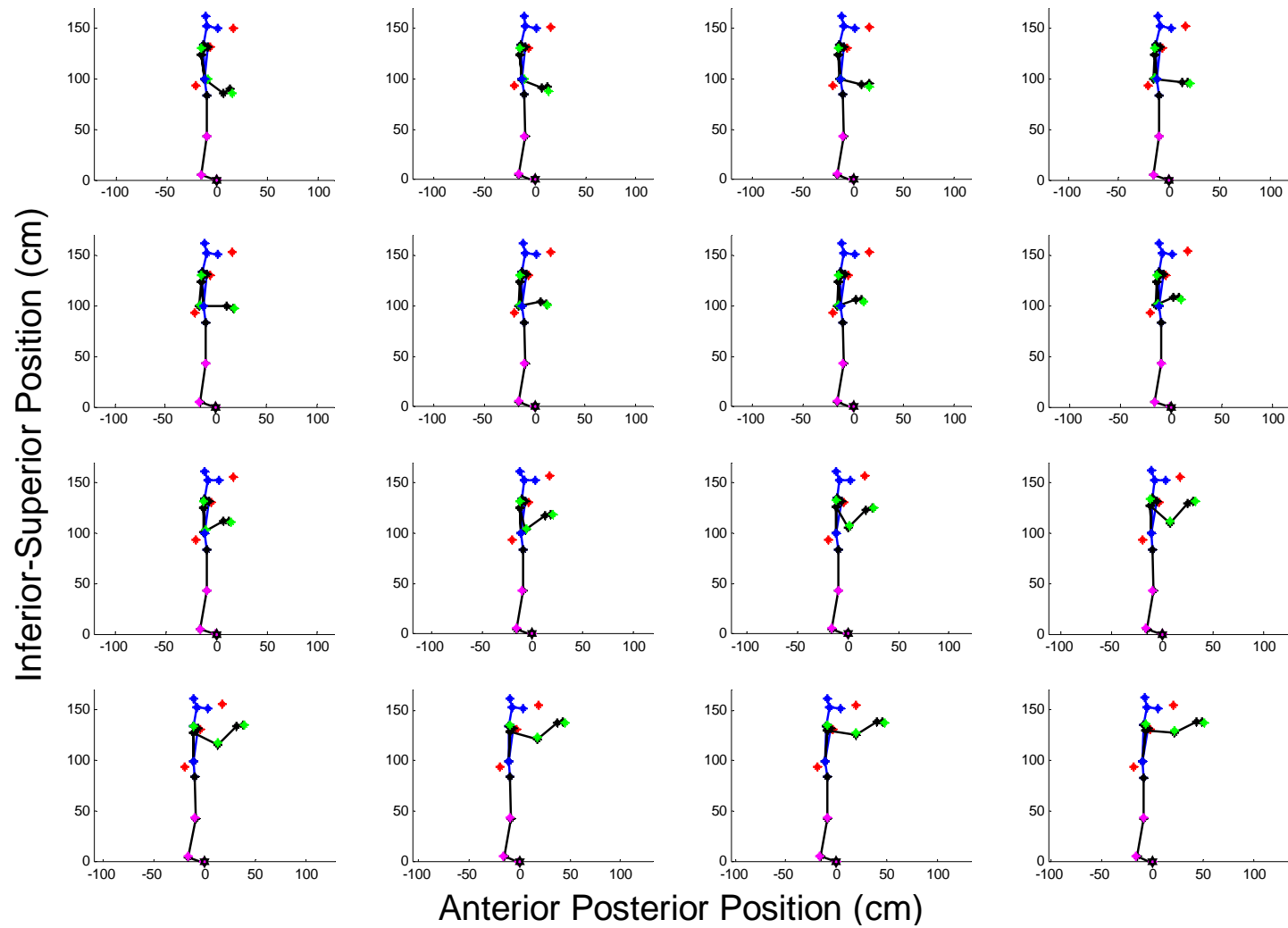


Figure 11. Time sequence for the first simulated movement. The sequence proceeds from left to right and top to bottom. Markers indicate the different joints and/or surface marker positions.

Other motions for the same participant were also input to the network once it was trained. Apart from changing the inputs to the network for different movements, joint and end-effector biases were updated to represent the initial posture for the movement being tested. Testing other movements allowed for the examination of the network's capacity to generalize its learning to novel motions. Given that the network was trained using a single movement, however, it was not expected to predict these novel motions satisfactorily.

6.1.1.3 Results

Although the mse training threshold was set at 0.001 cm^2 (equivalent root-mse: 0.03 cm), the network would not produce errors smaller than $\sim 11 \text{ cm}^2$ before training was manually stopped due to stabilization in error levels. This mse level, however, would result in root mean square errors (rmse) of only 3.3 cm. The exact average taken across time samples of the across-joints rmse obtained for the training movement was 3.38 cm (range across time samples: 1.54-5.54 cm). There was a slight temporal pattern in the errors (Figure 12).

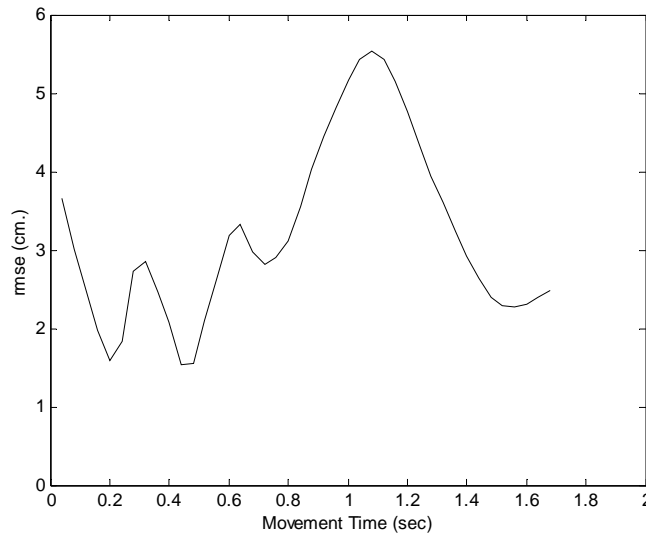


Figure 12. Error temporal pattern for the simulated movement.

Errors were also dependent on the joint and direction of movement (Figure 13). For the first network, errors were largest for the hand, wrist, and elbow joints and the box position. They were smallest for the lower limb joints. The errors observed were proportional to the distance traveled for some directions of movement, but not all of them (Figure 14). Even when a

normalization for distance traveled is made, the upper limb joints exhibit some of the largest errors. In terms of axis, the anterior-posterior direction of movement exhibited the largest errors.

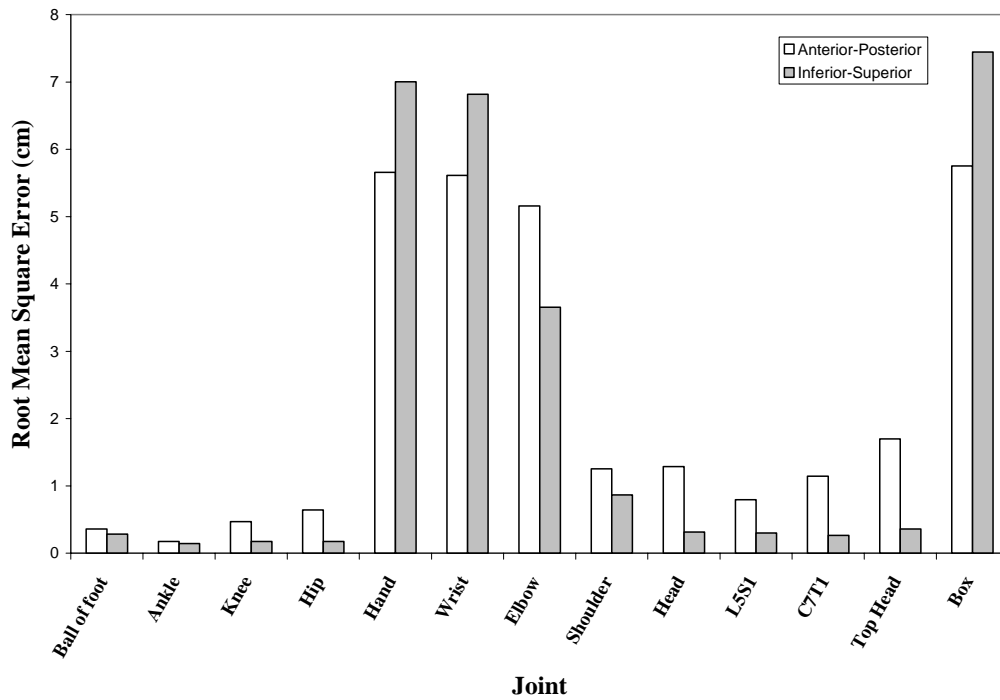


Figure 13. Root mean square error by joint and direction of movement.

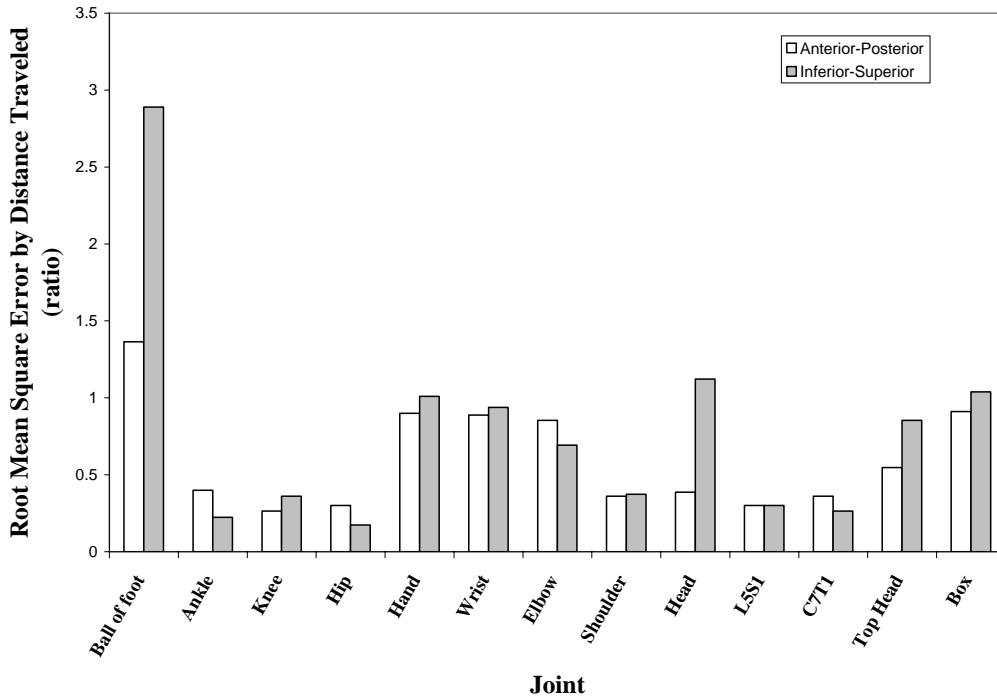


Figure 14. Root mean square error normalized for joint travel distance by joint and direction of movement.

Network performance for other movements was not satisfactory. The best rmse (calculated across joints and time samples) for other sagittally symmetric movements from the same participant was 8.20 cm (range across movements: 8.20-33.86 cm). Furthermore, this low error was obtained for a movement that was qualitatively similar to the training movement, with the only difference being a lower required lifting height. The tendency of the network was to model the original movement, even when the network inputs required a vastly different end location (Figure 15), which resulted in increased errors as the end locations of the various movements tested deviated further from the original movement's end location.

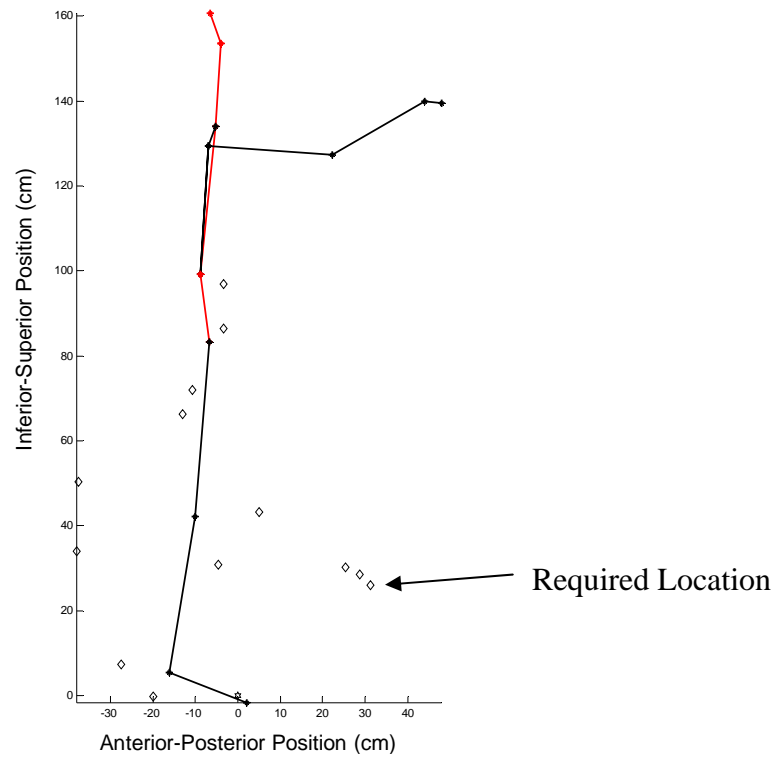


Figure 15. Comparison of the predicted (stick figure) and input (hollow diamonds) end posture. Note that the network still simulates the training movement, even when the inputs to the network indicate a lower end location.

6.1.1.4 Training with more than one movement

While the results are not included here for the sake of brevity, training patterns including more than one motion were also tested using this network structure. It was expected that this might aid in allowing the network to generalize to other motions. However, including more than one motion on the training pattern resulted in non-convergence through the training process. Errors did not reach any goals nor stabilize over the limit of 500,000 epochs.

6.1.2 Three-dimensions

The network architecture presented in the previous section was extended to three dimensions (Figure 16 and Figure 17). The same inputs, internal structure, and outputs were maintained, with the exception of additional nodes that accounted for the additional axis of movement. Pilot tests similar to those described for the 2-D case showed that 100 hidden units were also sufficient to assimilate the training data provided to the network. The networks were created and trained using the same procedure described in the previous section. While the results obtained for the two-dimensional representation using this network architecture were

discouraging, it was desirable to determine the effects of additional degrees of freedom on the network performance.

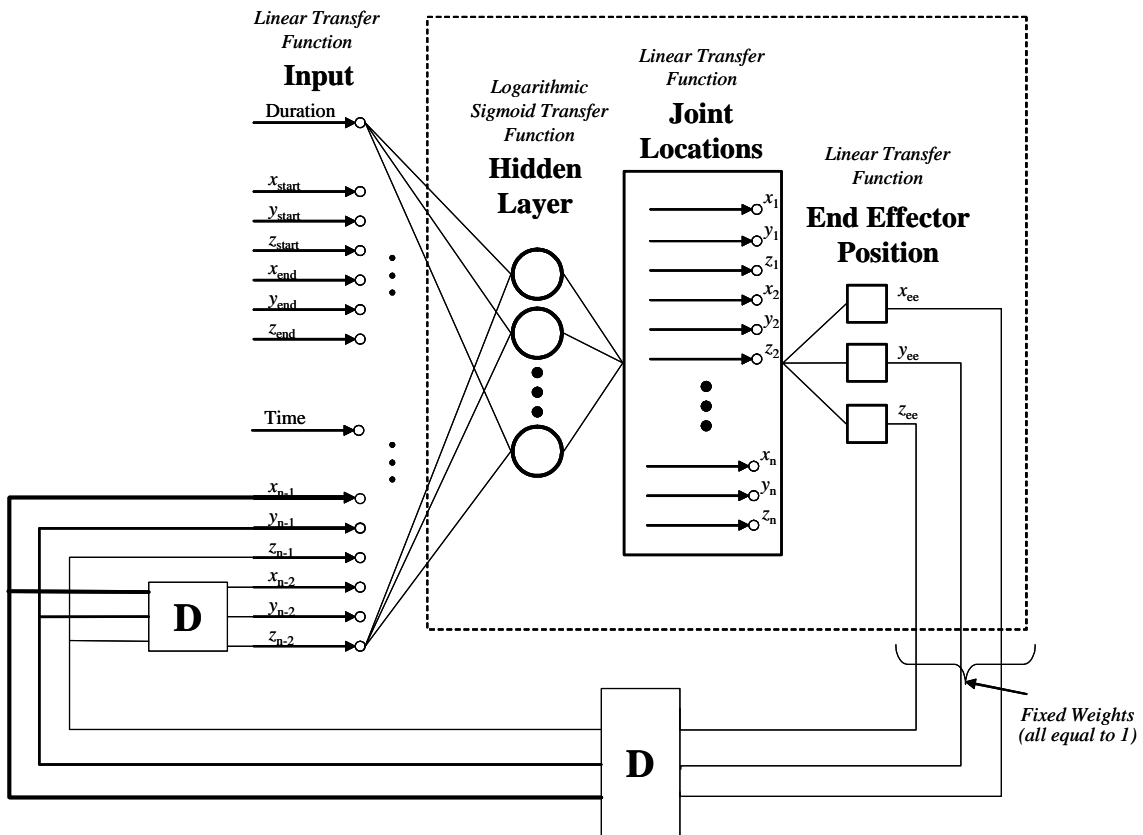


Figure 16. Initial three-dimensional network structure, based on a Jordan-Elman network. Although all layers are fully interconnected, some connections are omitted for clarity. A detailed diagram of the connections within the dashed-line box is presented in Figure 17.

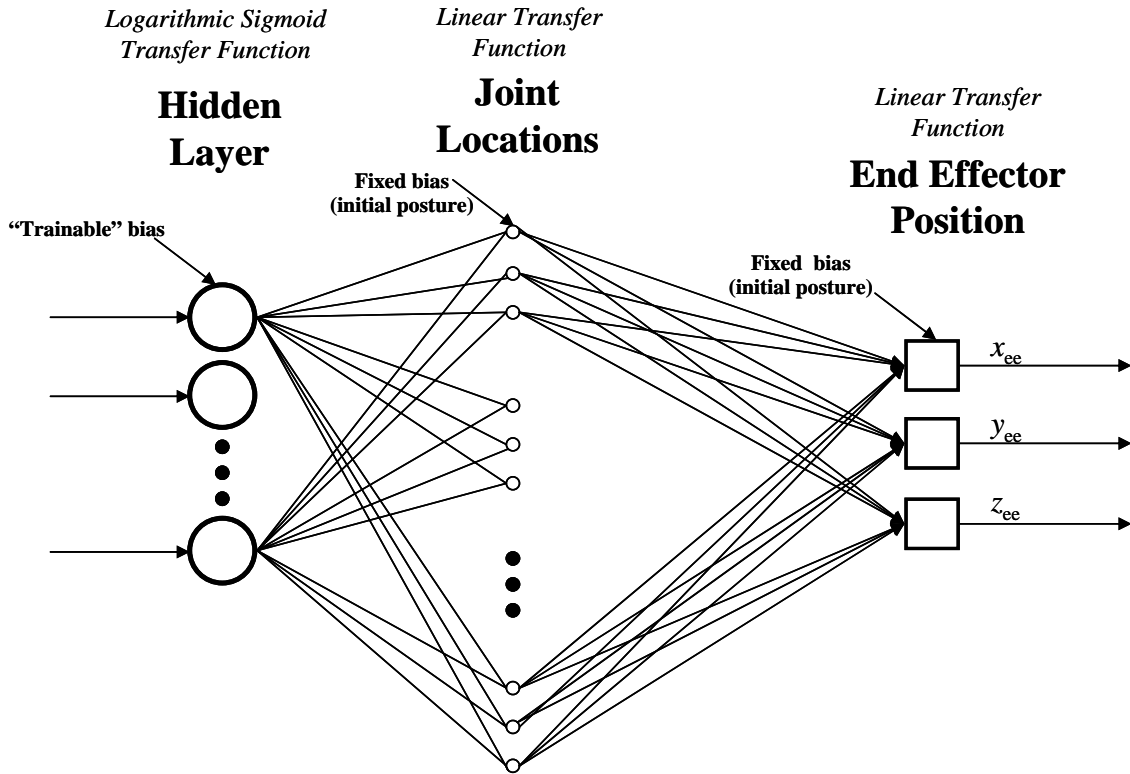


Figure 17. Detail of connections for the joint locations layer. Note that this diagram represents a detail of Figure 16.

To expand on the training performed in two dimensions and consider the possibility that a network trained on a different movement might be more likely to generalize to other movements, two different movements were simulated from the HUMOSIM database (Figure 18 and Figure 19). Modeling these two motions required the creation of two separate networks, one for each of the movements. Although both movements consisted of picking up a box and delivering it to a location, the delivery points differed between movements. The first movement (Figure 18) required the delivery of the box to an overhead location directly in front of the participant. The second movement (Figure 19) required delivery of the box to a lateral location at elbow height. To avoid introducing between-subject variability, the movements were selected randomly from those available for a randomly chosen participant.

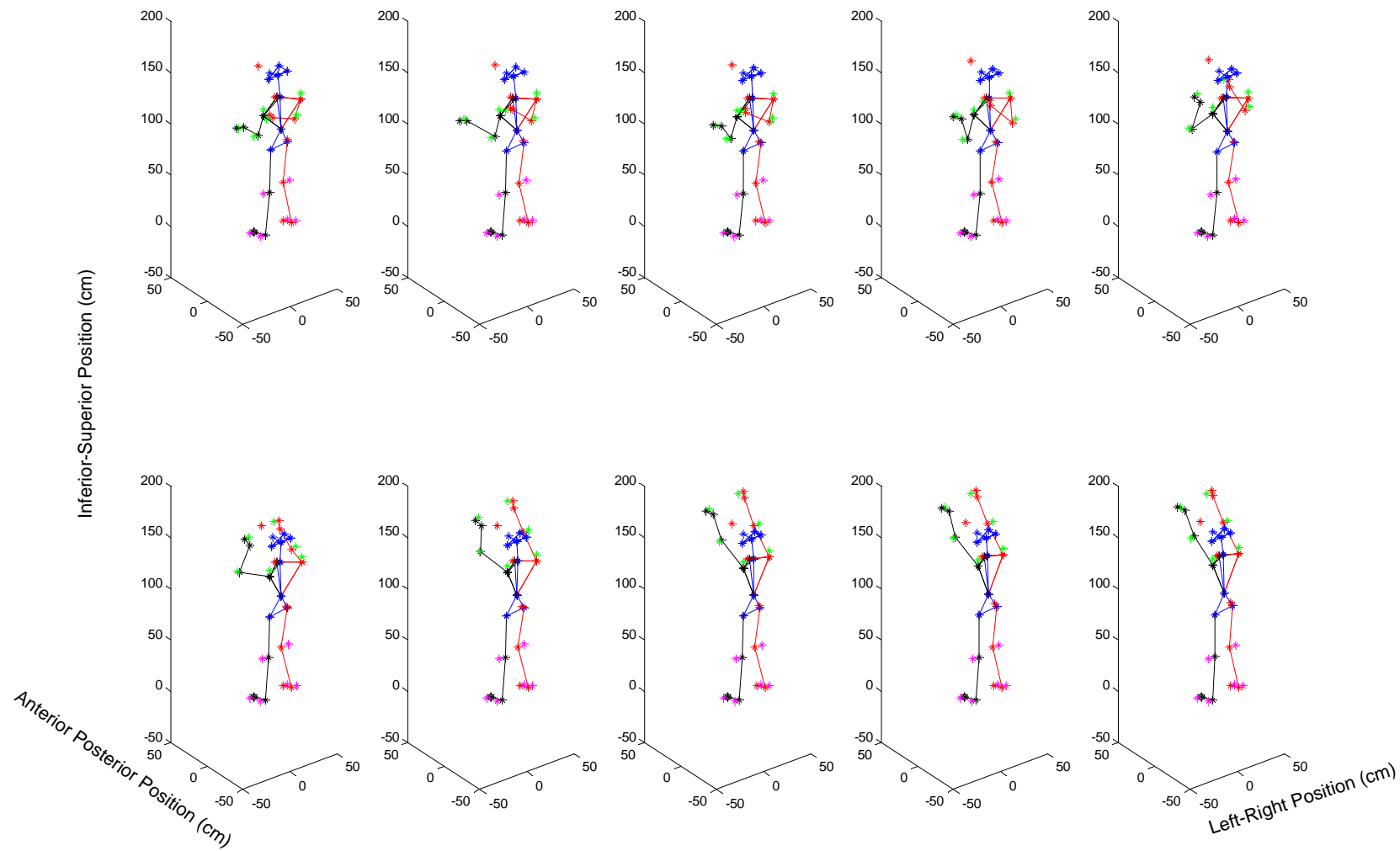


Figure 18. Time sequence for the first movement, which required overhead lifting. Markers indicate the different joints and/or surface marker positions.

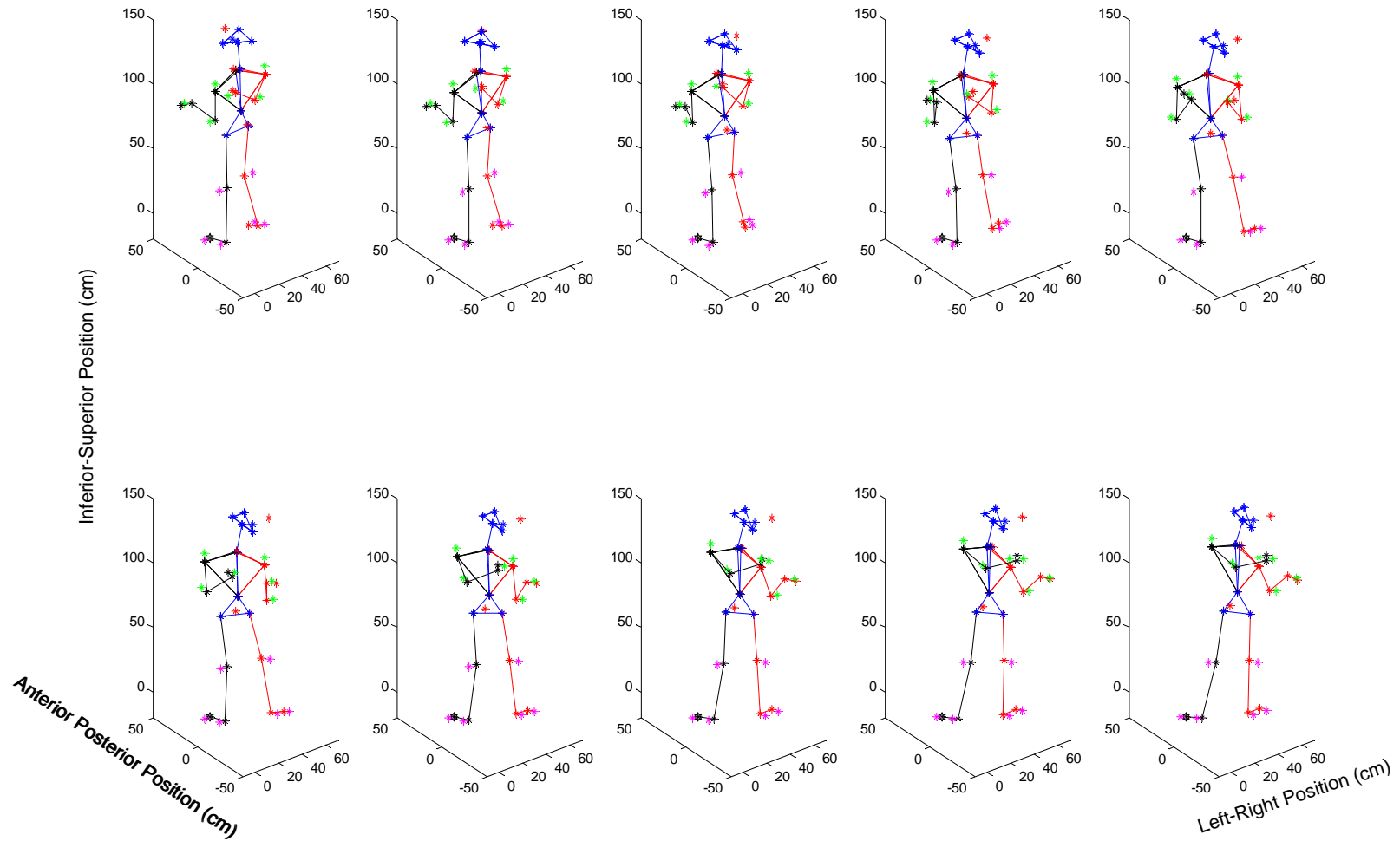


Figure 19. Time sequence for the second movement, which required a lateral transfer. Markers indicate the different joints and/or surface marker positions.

As for the network created for two dimensions, other motions for the same participant were also input to these two networks once they were trained. Apart from changing the inputs to the network for different movements, joint and end effector biases were updated to represent the initial posture for the movement being tested.

6.1.2.1 Results

Although the mse training threshold was set at 0.001 cm^2 (equivalent root-mse: 0.03 cm), the networks would not produce errors smaller than $\sim 5 \text{ cm}^2$ within less than 500,000 training epochs. This mse level is equivalent to relatively small root mean square errors, in the order of $\sim 2.2 \text{ cm}$. Specifically, the average taken across time samples of the across-joints rmse obtained for the first training movement was 2.26 cm (range across time samples: 0.79-3.48 cm). The corresponding average for the second training movement was 2.56 cm (range across time samples: 0.88-4.30 cm). Note that these errors refer to tests of each of the movements only within the network that the movement trained. There was a slight temporal pattern in the errors (Figure 20), albeit not consistent for the two different motions and their associated networks. In general, however, the networks appeared to reduce error around the 25% and 75% portions of the movement and produce larger errors at the halfway point and the begin and end points.

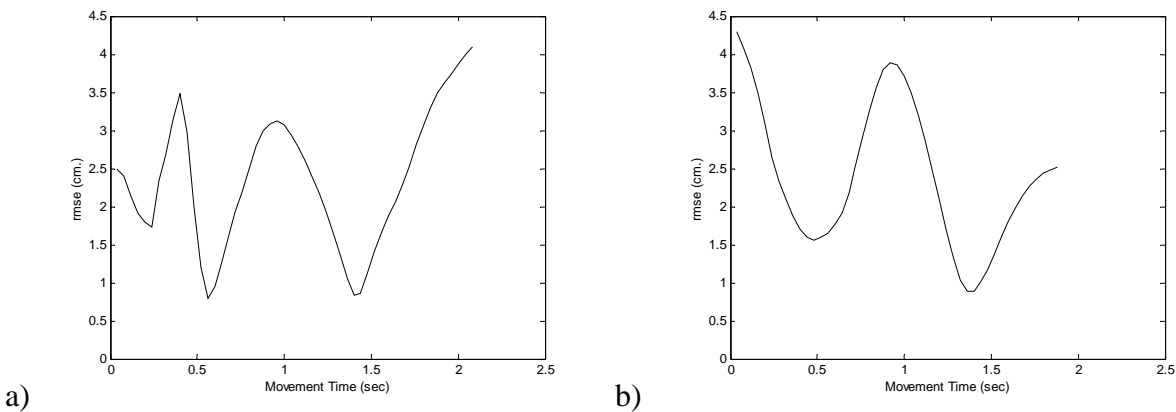


Figure 20. Error temporal pattern for movement 1 (a) and movement 2 (b).

Errors were also dependent on the joint and direction of movement (Figure 21). For the first network, errors were largest for the hand, wrist, and elbow joints and the box position. They were smallest for the joints on the lower limbs. The errors observed were proportional to the distance traveled for some directions of movement, but not all of them (Figure 22). Even when a correction for distance traveled is made, the upper limb joints exhibit some of the largest errors.

In terms of axis, the anterior-posterior direction of movement exhibited the largest errors. These patterns were also observed for the second network (Figure 23 and Figure 24).

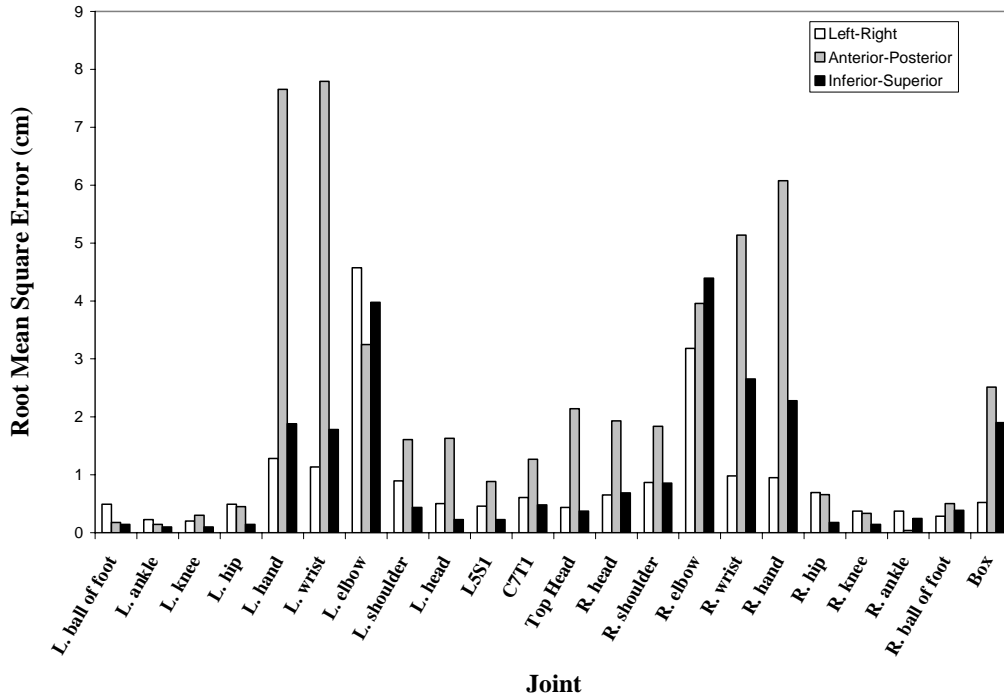


Figure 21. Root mean square error by joint and direction of movement. These data correspond to the first network.

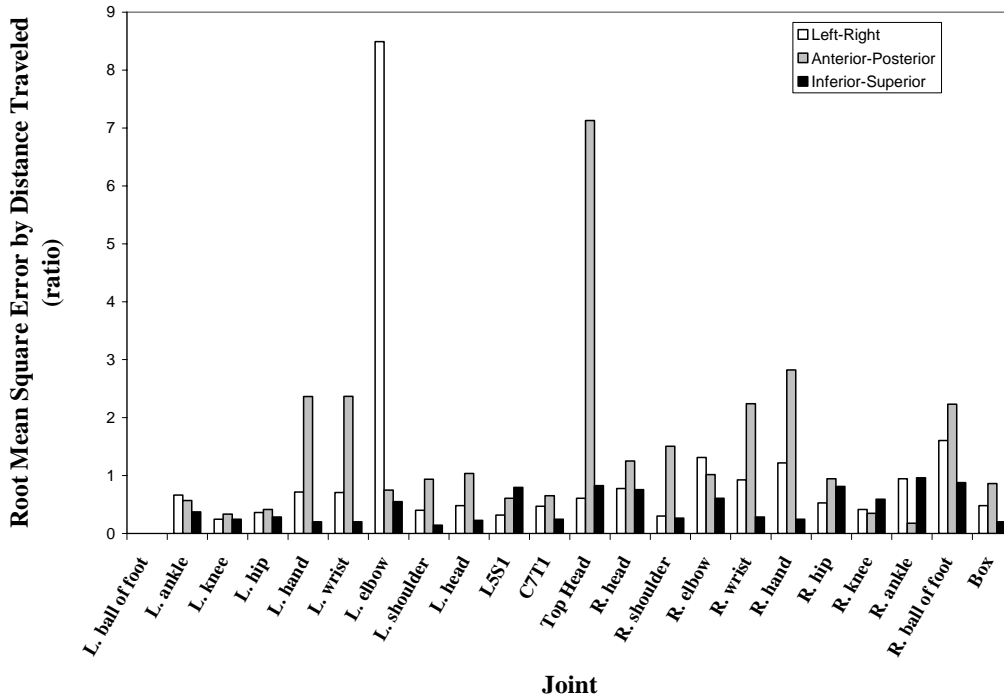


Figure 22. Root mean square error corrected for joint travel distance by joint and direction of movement. These data correspond to the first network. Values for the left ball of foot are not presented as this joint was fixed in space throughout the trial.

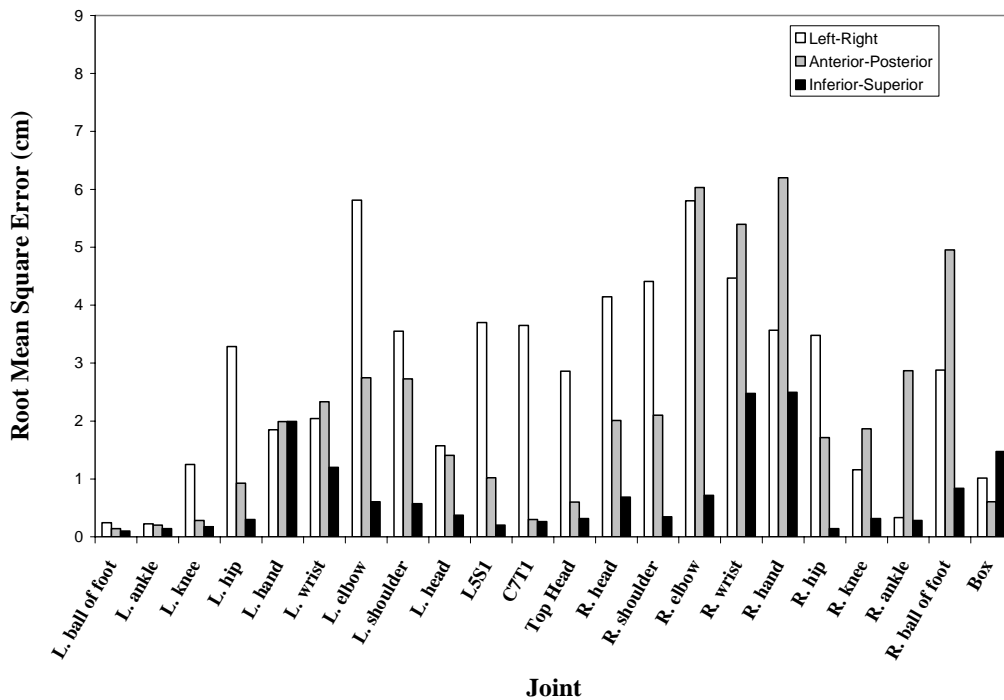


Figure 23. Root mean square error by joint and direction of movement. These data correspond to the second network.

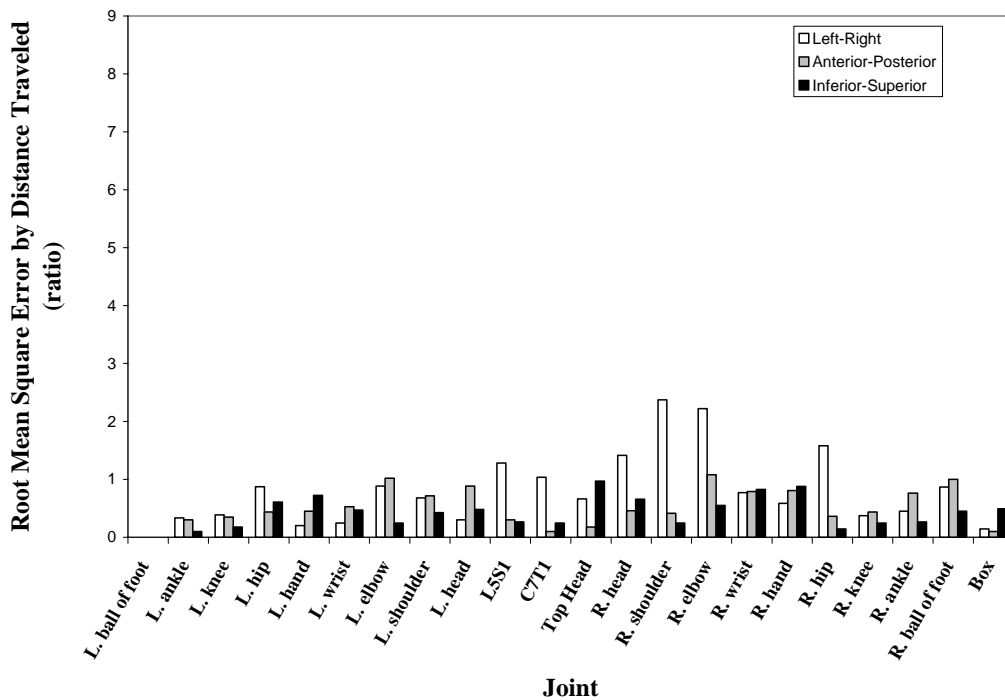


Figure 24. Root mean square error corrected for joint travel distance by joint and direction of movement. These data correspond to the second network. Values for the left ball of foot are not presented as this joint was fixed in space throughout the trial.

Network performance for other movements performed by the same subject from whom the training movements were obtained was not satisfactory. The lowest rmse (calculated across joints and time samples) for other movements tested under the first network (i.e. trained with the first movement) was 8.20 cm (range across movements: 8.20-42.10 cm). Furthermore, this lowest error was obtained for a movement that was qualitatively similar to the training movement, with the only difference being a lower required lifting height. The tendency of the network was to model the original movement, even when the network inputs required a vastly different end location (Figure 25), which resulted in increased errors as the end locations of the various movements tested deviated further from the original movement's end location. These results were also observed when performing similar testing for the second network (i.e. trained with the second movement). The lowest rmse (calculated across joints and time samples) for other movements tested under the second network was 7.49 cm (range across movements: 7.49-31.04 cm).

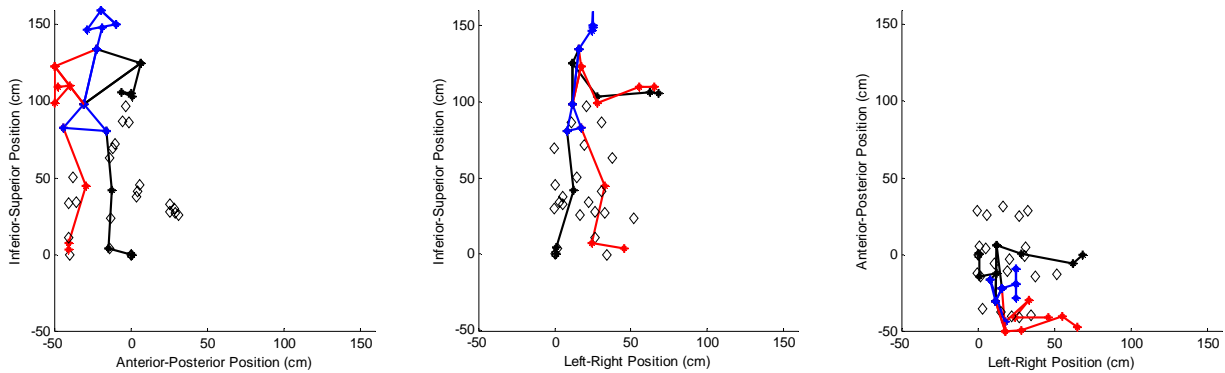


Figure 25. Comparison of the predicted (stick figure) and input (hollow diamonds) end postures for the first network. Note that the network still simulates the training movement, even when the inputs to the network indicate a lower end location.

6.1.2.2 Training with more than one movement

While the results are not included here for the sake of brevity, training patterns including more than one motion were also tested using this network structure. It was expected that this might aid in allowing the network to generalize to other motions. However, as was also observed for the 2-D case, including more than one motion on the training pattern resulted in non-convergence through the training process. This effect was observed for both of the networks discussed in this section. Errors did not reach any pre-established thresholds nor stabilized over the limit of 500,000 epochs.

6.1.3 Implications of Results for an Unconstrained Network Structure

The main goal of the effort described in the previous section was to design, build, train, and test a neural network to predict particular movements for an individual. This process was intended to serve as a ‘proof-of-concept’ that demonstrated the ability of the ANN-based approach to converge to an acceptable solution. This goal was to be achieved with the smallest possible number of assumptions about expected behavior and/or interactions between joints and end-effector position.

Recurrent networks of certain characteristics were shown to converge to low-error solutions for particular movements provided enough training. Some of these errors, however, seemed temporal and joint-specific. It is likely that this temporality in error patterns is due to the network trying to ‘catch-up’ with the actual movement. If this occurred, errors would oscillate

from stable states where the network is ‘caught-up’ to trying to follow a quick change of movement direction. In some instances, overcompensation was also observed.

In joint-specific terms, the upper limb position predictions exhibited the largest errors. Joints with limited involvement in the motion exhibited lower errors, which increased as more involvement from the specific joint was required by the movement. Normalizing errors by the distance traveled by the joint failed to aid in uncovering any particular error-prone joints through the motion.

The network structure employed was able to model each training movement very closely, but could not generalize to other movements. The tendency of each network was to continue simulating the training movement, even when the inputs for the beginning and end points of the box were changed drastically. This suggests overtraining of the network, which was somewhat unavoidable here, as only a single training trial was used. However, efforts to simulate a wider variety of motions using the same network structure were unfruitful, as the network structure was unable to suitably adapt to more than one training movement.

Overall, the results of this section suggest that further constraints on the structure of the network are needed. Theories abound on the control structures used in movement generation, and many, if not all, of these theories can be synthesized mathematically. However, it is not the purpose of this investigation to test the applicability of these theories, but, rather, to develop a tool that might implicitly embody them, without doing so in explicit terms. Thus, the constraints that will be added to the network will be of a kinematic nature (e.g. predicting joint angles rather than joint positions). The next section describes this process in more detail.

6.2 Predicting Joint Angles

The results from the attempted prediction of joint positions suggested that the networks being created were too unconstrained in structure to synthesize movement control mechanisms that allowed generalization to novel movements. Prediction of joint angles rather than joint positions was hypothesized to address some of these drawbacks, as it provided integrated additional knowledge within the network without requiring any assumptions on a particular motor control scheme. Thus, network structures and inputs were modified as needed to test this hypothesis.

6.2.1 *Two dimensions*

The network structure for the prediction of angles is similar to that of the networks previously discussed. The type of inputs and outputs, however, were substantially different (Figure 26). Ten joint angles were used as the predicted entities. Initial and final values for each of these joint angles were used as inputs, together with inputs corresponding to the time duration and current time within the movement. Outputs were the time-stamped progression of these same joint angles. The conversion process from these joint angles to the coordinates that represented the end effector position is trivial if link lengths are known, and was not coded within the network to make the training process more efficient. While these parameters could have been added without affecting the training results, the training algorithm would have had to compute these additional connections at every model recalculation, which would have taken computing resources from the more important training task.

Data were converted to two dimensions on the sagittal plane by collapsing the movement on the left-right axis. This collapsing process involved the averaging of coordinates for the same axis of left and right joints. For example, to obtain the 2-D coordinates for the shoulder, the averages for the anterior-posterior and superior-inferior coordinates were calculated. To reduce the possibility for asymmetry on the left-right axis, only movements that were expected to be sagittally symmetric were included. The segmental link lengths were obtained by calculating Euclidean distances between successive joints. Measurement error was reduced by calculating and using average link lengths across all time samples. While these values were not used directly in the network while it was trained, they were needed to convert the ANN-predicted joint angles to joint positions, which allowed for errors to be directly comparable with those obtained for the network predicting joint positions. These link lengths and the resulting joint positions are shown in Figure 26 within a dashed box.

Obtaining joint coordinates once the network had made a prediction simply required following a kinematic chain originating at the anchor point (ball of foot). Sines and cosines of the joint angles were then multiplied by the respective link length and the resulting distance added to the previous joints coordinates. This process was iteratively followed until the kinematic chain reached the end effector. From the ten joint angles predicted, the neck angle did not have any effect on the position of the end effector, but was calculated nonetheless to allow for the prediction of head position.

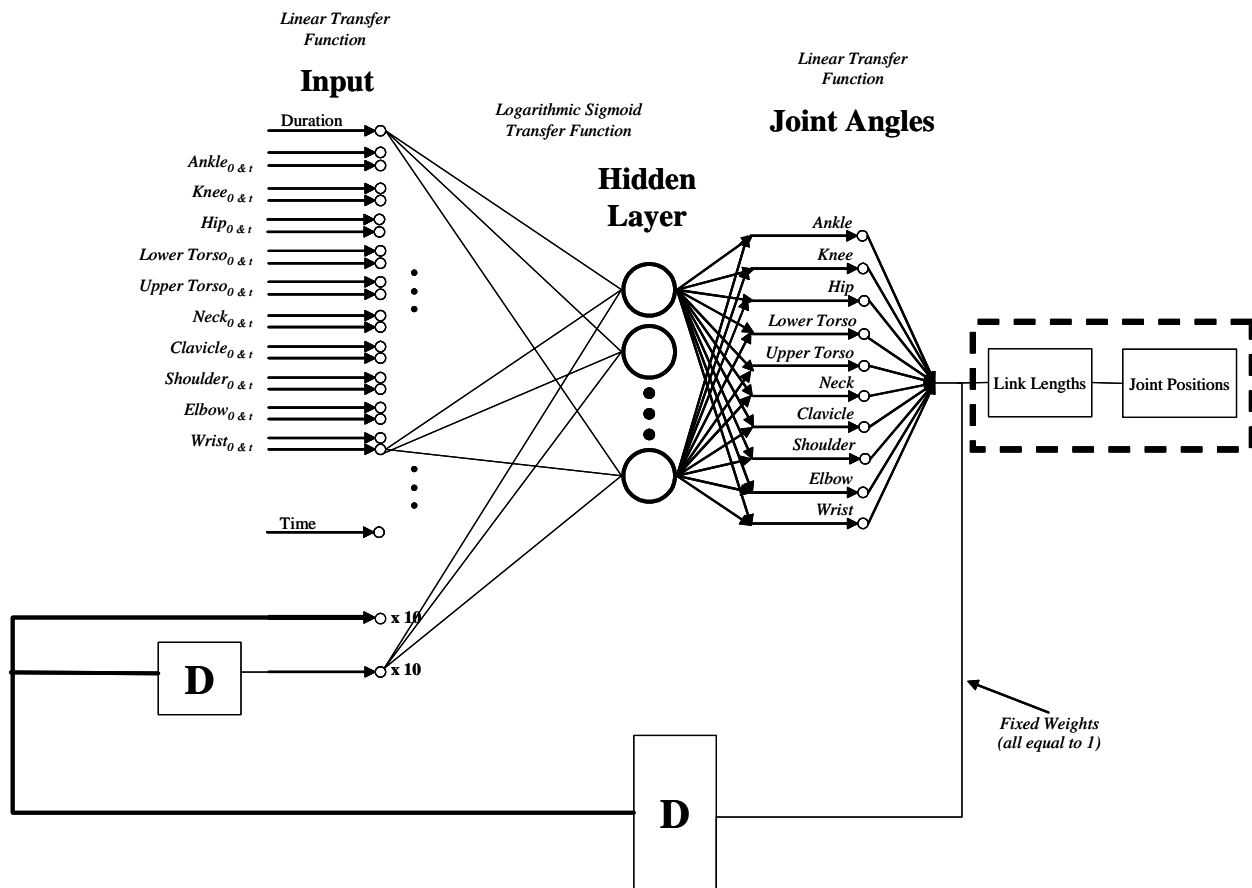
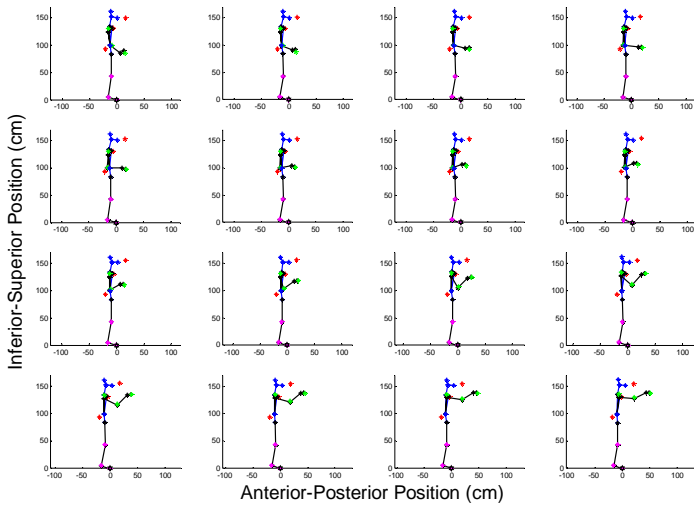
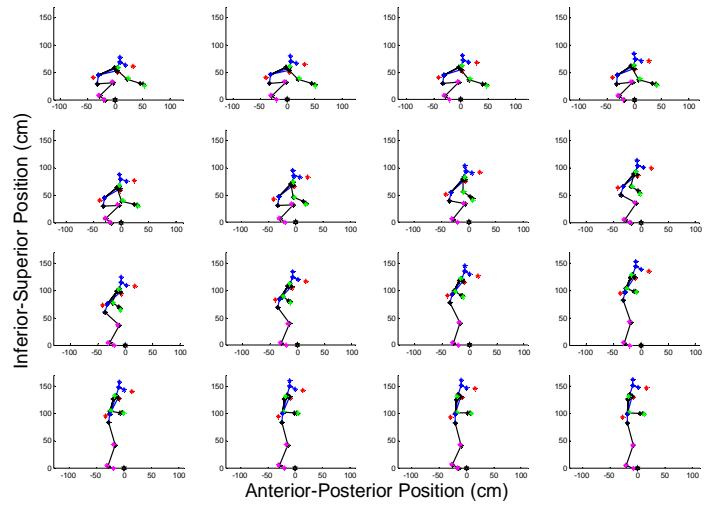


Figure 26. Two-dimensional network structure using joint angles as the input and prediction basis. Although all layers are fully interconnected, some connections are omitted for clarity. Boxes with 'D' represent a single time delay. The 'x 10' next to two of the inputs indicates that each of these nodes represents ten different inputs (each corresponding to one of the outputs). The dashed box indicates components of a conversion process that was not coded within the network (see text for details).

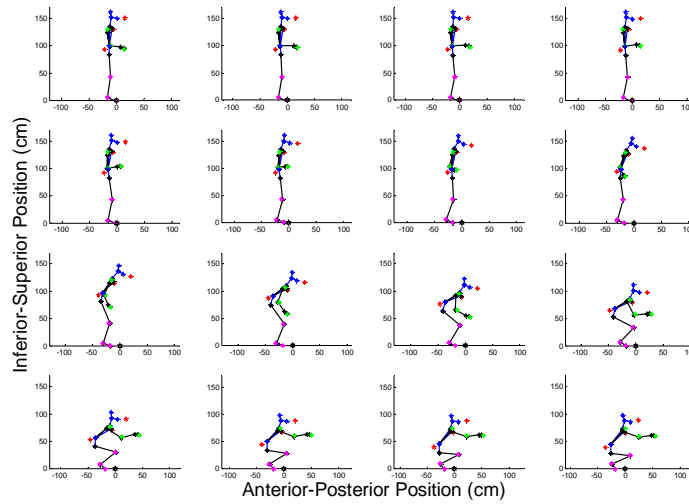
Given the results obtained for the joint position prediction networks, it was expected that a neural network would be able to acceptably predict joint angles when trained using a single movement. Thus, instead of initially training the network with a single movement, three motions were used in the training process (Figure 27). These motions were randomly selected from the nineteen motions available for a particular, randomly selected, participant. This random selection process yielded two 'Deliver' motions (*a* and *c* in Figure 27) and one "Bring back" motion (*b* in Figure 27).



a)



b)



c)

Figure 27. Time sequences for the three movements used in network training. Note that the movements are qualitatively different in their requirements. Markers indicate the different joints and/or surface marker positions.

6.2.1.1 Results

The mse threshold for this network structure was set at 0.001 rad^2 , and training was manually stopped when the mse approximated 0.003 rad^2 , as the error had stabilized. The corresponding rmse was 0.05 rad (3.1°). However, to allow for direct comparison with models described in previous sections, these errors were translated to errors in the prediction of joint positions. While knowledge of the errors in joint angle predictions is also valuable, consideration of these is reserved until future chapters, when absolute characterizations of model

performance (as opposed to the relative comparisons to other models that are of interest here) are needed and inputs to the models include data from multiple participants.

Across time samples, the across-joints average rmse for the first training movement was 0.86 cm (range: 0-1.57 cm). Comparative values for the second and third training movements were, respectively: 1.58 cm (range: 0-2.42 cm) and 1.07 cm (range: 0-1.80 cm). In comparison, the rmse for the joint position prediction network structure was 3.38 cm. The networks seemed to predict slightly better a little after the start of the motion, with a relatively stable error afterwards (Figure 28). Error spikes tended to be present at the start of the motion.

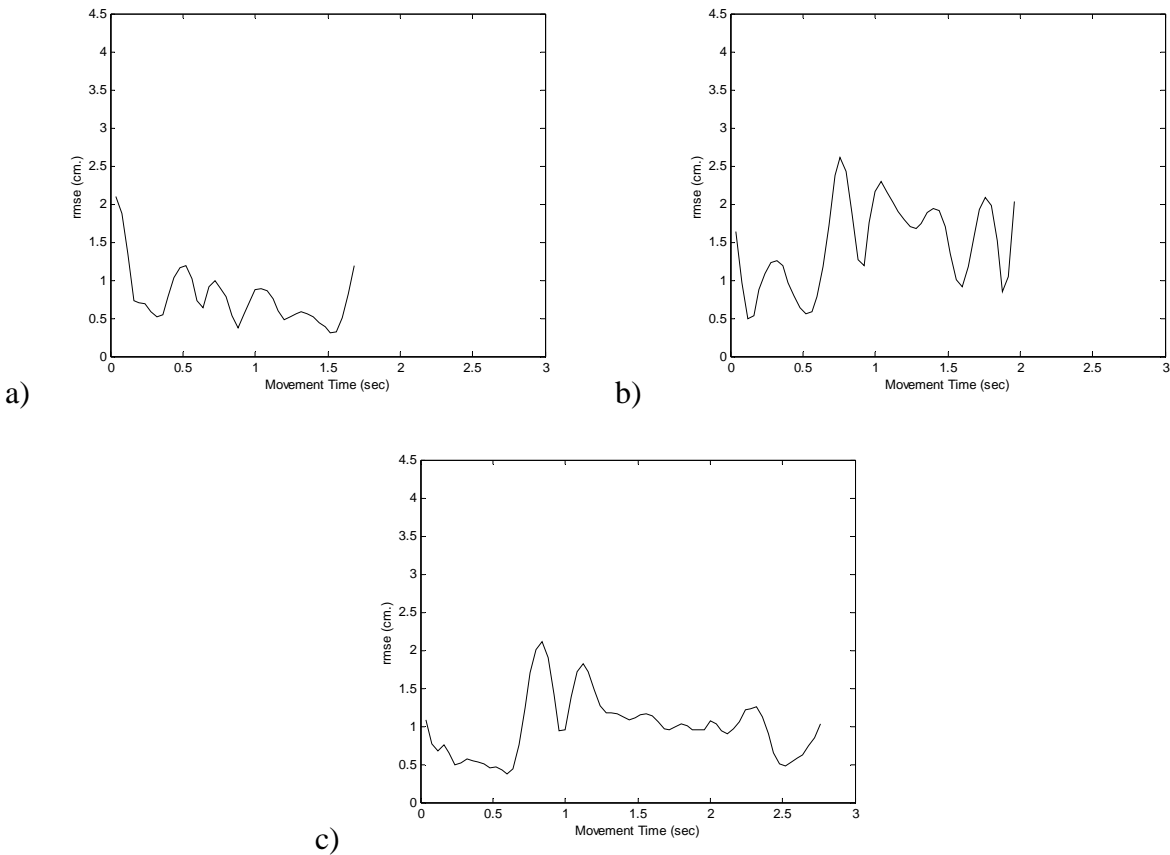


Figure 28. Error temporal pattern for movement 1 (a), movement 2 (b) and movement 3 (c).

Errors were also dependent on the joint and direction of movement (Figure 29, Figure 30, and Figure 31). As in joint position prediction networks, the anterior-posterior axis exhibited slightly larger errors. In general, errors were also larger for the upper limb, likely due to their cumulative nature. The kinematic chain started in the feet, thus, any errors in joint position

could be additive to joints that were located further along the chain (e.g. elbow and hand). No discernible pattern was observed in the joint prediction errors across the movements.

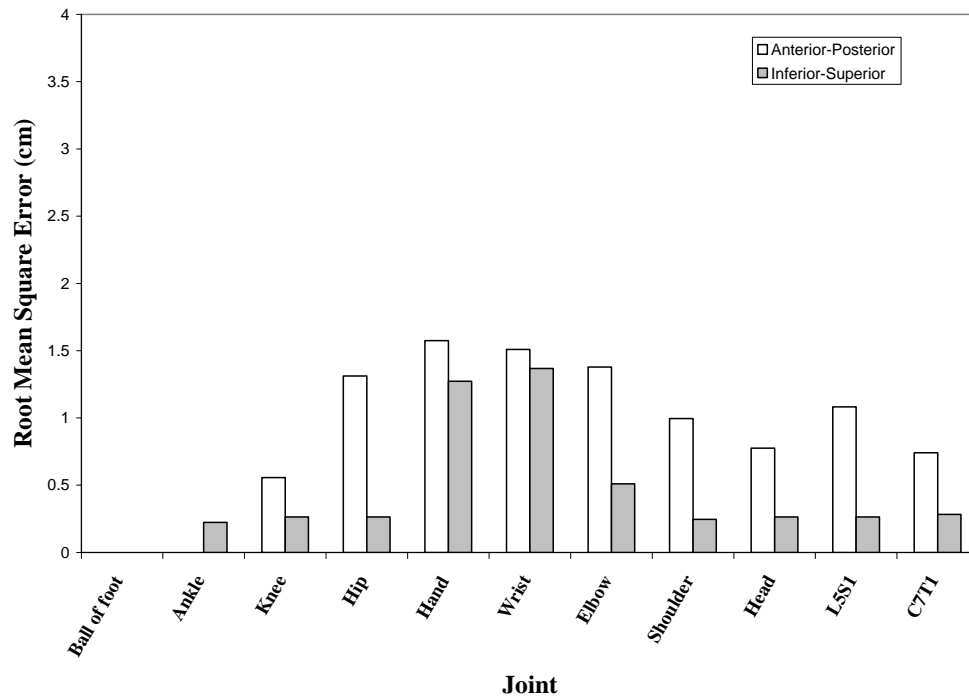


Figure 29. Root mean square error by joint and direction of movement. These data correspond to the first training movement.

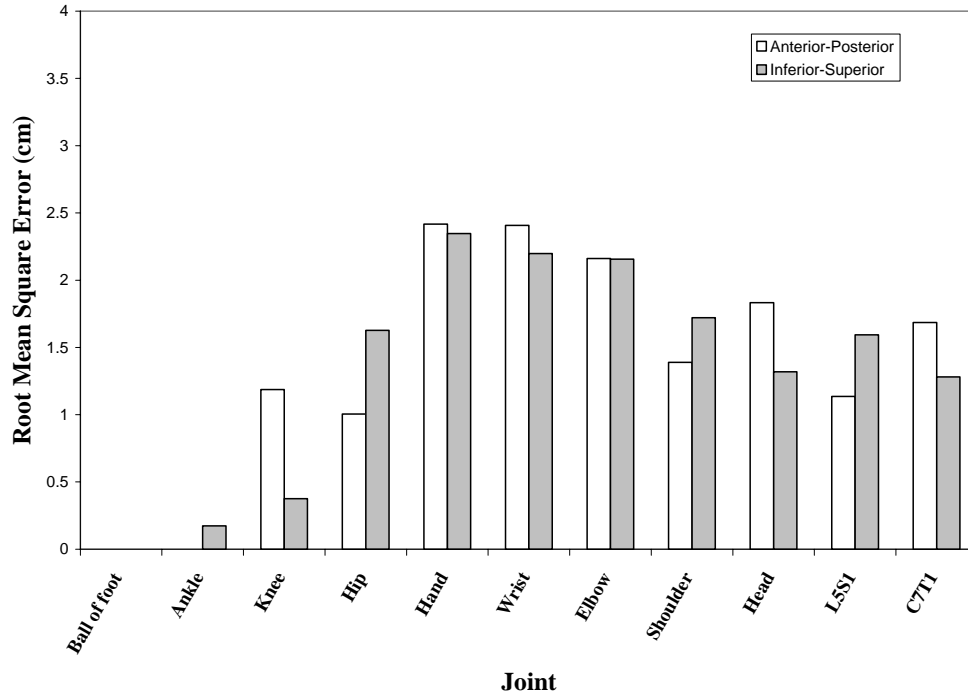


Figure 30. Root mean square error by joint and direction of movement. These data correspond to the second training movement.

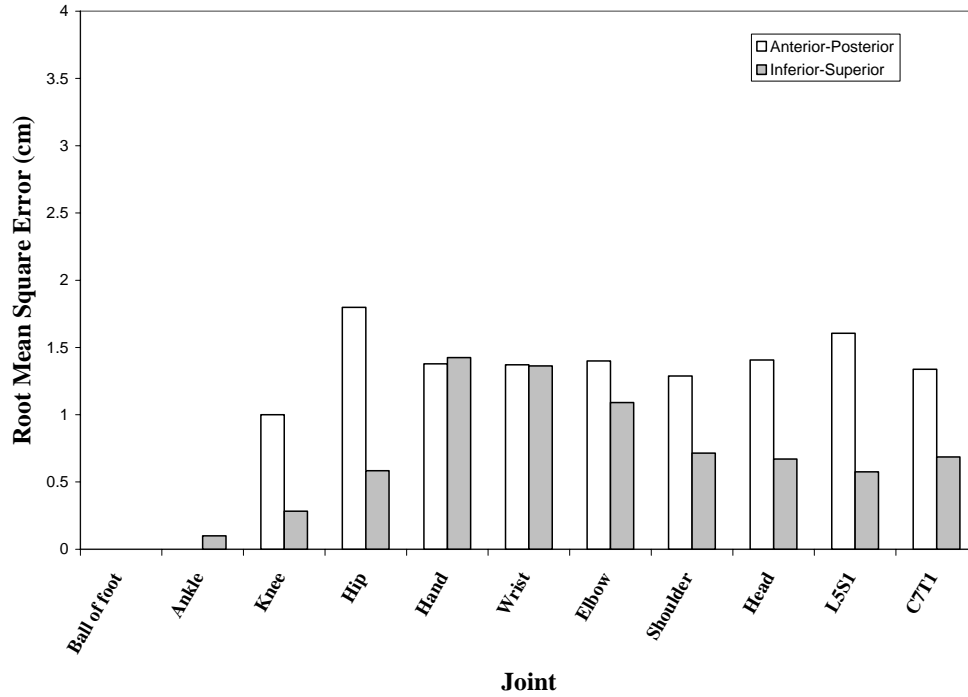
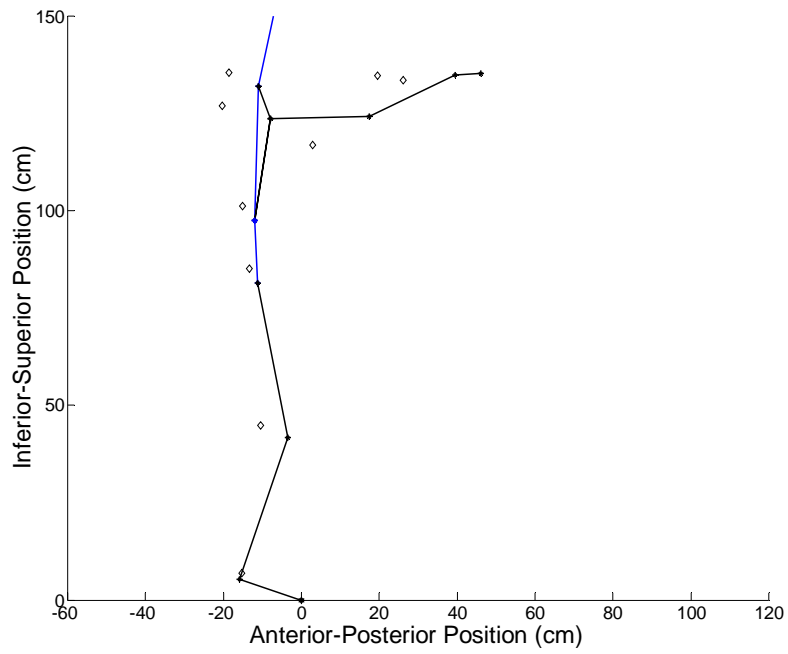
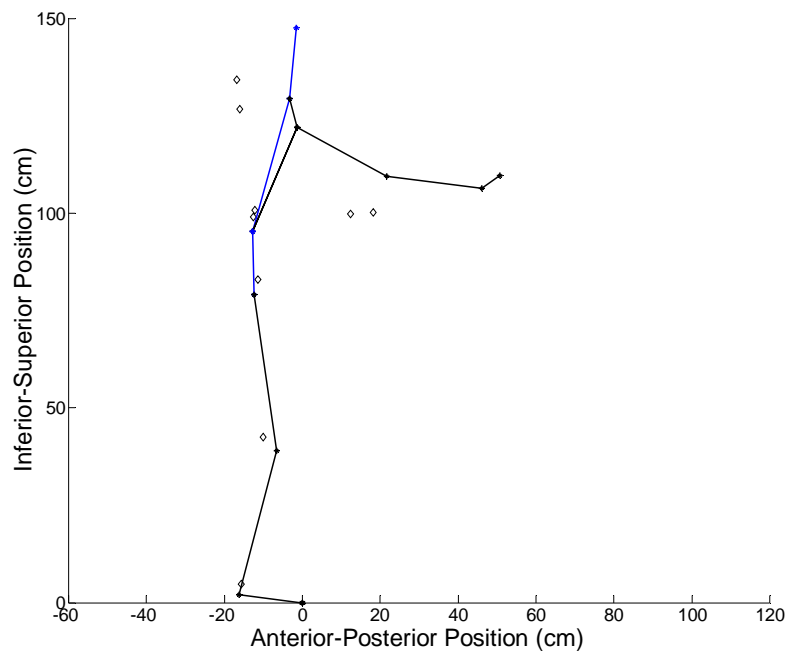


Figure 31. Root mean square error by joint and direction of movement. These data correspond to the third training movement.

Testing with other movements from the same participant that were not included in the training patterns resulted in unsatisfactory prediction levels. The lowest rmse (calculated across joints and time samples) for these novel movements was 6.38 cm (range across movements: 6.38-30.6 cm). The movements that resulted in the lower prediction errors tended to be closer in destination to those that had been used in the training process (Figure 32). None of the additional movements had a lower rmse than the training movements.



a)



b)

Figure 32. Comparison of the predicted (stick figure) and input (hollow diamonds) end postures for the best (a) and worst (b) predicted novel movements.

6.2.1.2 Implications of results

While the results obtained from this type of network were not acceptable from a performance standpoint, they were considerably better than results obtained from the initial networks that directly predicted joint positions. Furthermore, errors were comparatively small for some movements that were not used during training but differed only slightly from the training movements. These observations prompted the use of a larger training dataset that included the complete set of sagittally-symmetric movements performed by a single individual in the dataset. Using a larger training set also allowed for a similar representation of movements that required lifts from the origin to a destination and vice versa. The goal of the effort was to determine if the network was able to assimilate a much larger variety of movements. If the network was able to converge to an acceptable amount of error, it would have been able to integrate within its structure implicit knowledge about all of the movements. If this was not the case, then either the network was not complex enough to assimilate the amount of information being provided or, more unlikely, there was no discernible pattern in the data. The results of these efforts are summarized in the next section.

6.2.1.3 Results for an extended training dataset

An extended dataset, employing all of the sagittally symmetric movements available for the same participant used in previous network iterations, was used to train a network with the same structure as those previously used in this section (Figure 26). Given the larger number of training patterns available, the maximum number of epochs allowed was increased to 1,000,000. The network error converged to an mse of slightly less than 0.003 rad^2 within $\sim 300,000$ epochs. The corresponding rmse was 0.05 rad (3.1°). As before, these errors were translated into joint position prediction errors.

Across movements, the average rmse (calculated across joints and time samples) ranged from 0.66 to 2.58 cm. No discernible pattern could be observed in the error distribution across the different motions. Furthermore, errors seemed to be randomly distributed across movement stages for each of the movements (Figure 33). Errors were also dependent on the joint and direction of movement; disparities in prediction were highest for the upper extremity joints and antero-posterior movement (Figure 34).

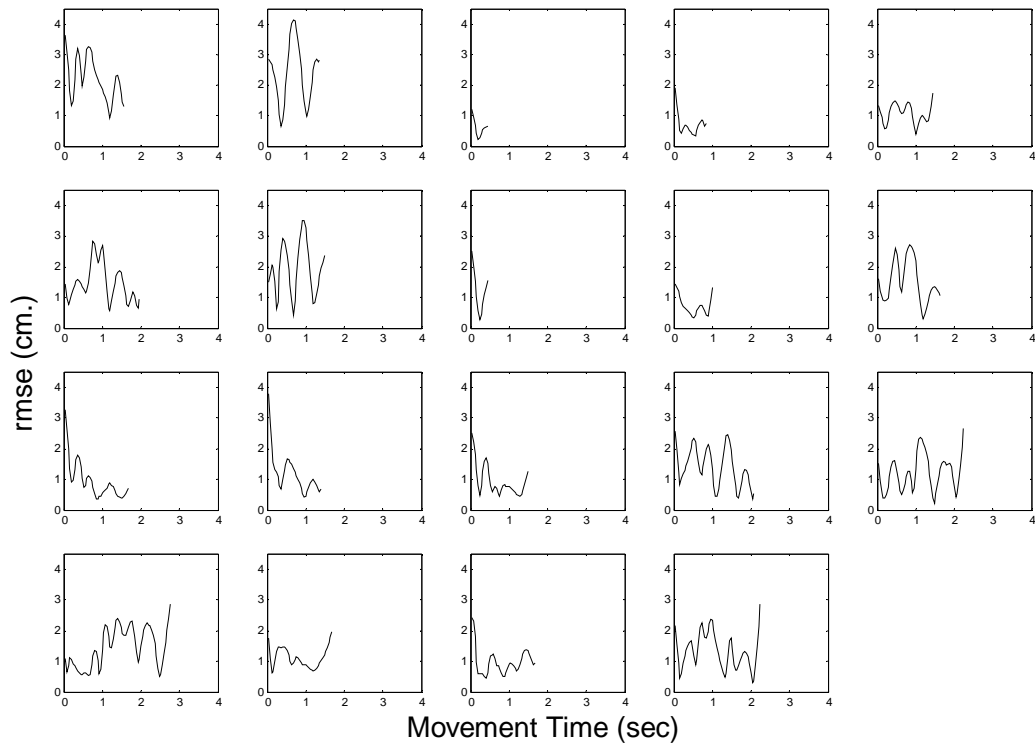


Figure 33. Error temporal pattern for the 19 movements from the same participant that were used for training.

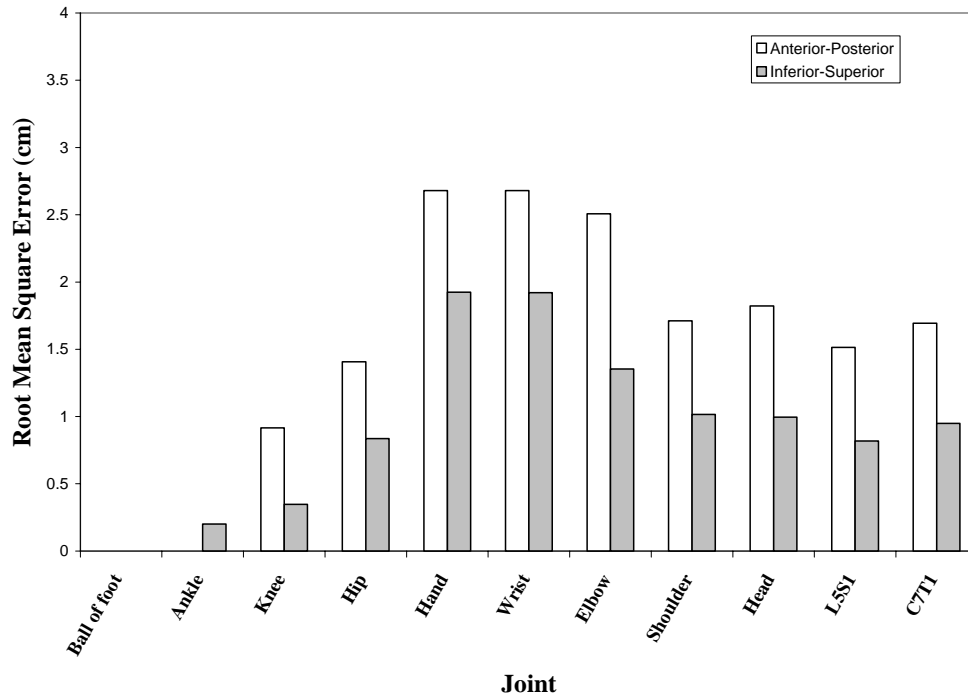


Figure 34. Root mean square error by joint and direction of movement for the 19 movements.

Network generalization capabilities were tested by providing the network with movements from an additional individual. This person was anthropometrically dissimilar from the participant that provided the training movements. The training movements were obtained from a 21 year-old female with body mass of 67.1 kg and a height of 163.1 cm. The verification movements were obtained from a 35 year-old male with body mass of 81.0 kg and a height of 186.1 cm. Network performance was unsatisfactory; across the different motions for the dissimilar individual, the lowest rmse (calculated across joints and time samples) observed was 4.07 cm (range across movements: 4.07-12.74 cm). Given the substantial difference in anthropometries, another test was run with a person of more similar height and weight. For this second comparison, data were used from a 48 year-old female with body mass and height of 67.3 kg and 163.9 cm, respectively. Prediction errors for this individual were in some instances higher than for the anthropometrically dissimilar person, with a minimum rmse (calculated across joints and time samples) across the different movements for this similar individual of 3.61 cm (range across movements: 3.61-16.79 cm). Thus, the network had trouble generalizing to other individuals. This was expected, as the network had been trained with no information on between-subjects variability. As discussed in the previous chapter, this type of variability is

substantial in movement simulation and will be addressed by networks in a subsequent chapter. Even though the two participants were anthropometrically similar, their movement patterns were slightly different (Figure 35). However, it is troublesome that the network could not adapt to these slight changes, and might suggest that the network’s ability to generalize might have been compromised during training. This possibility was considered in more detail when networks were trained with movements from different individuals, as reported in a subsequent chapter.

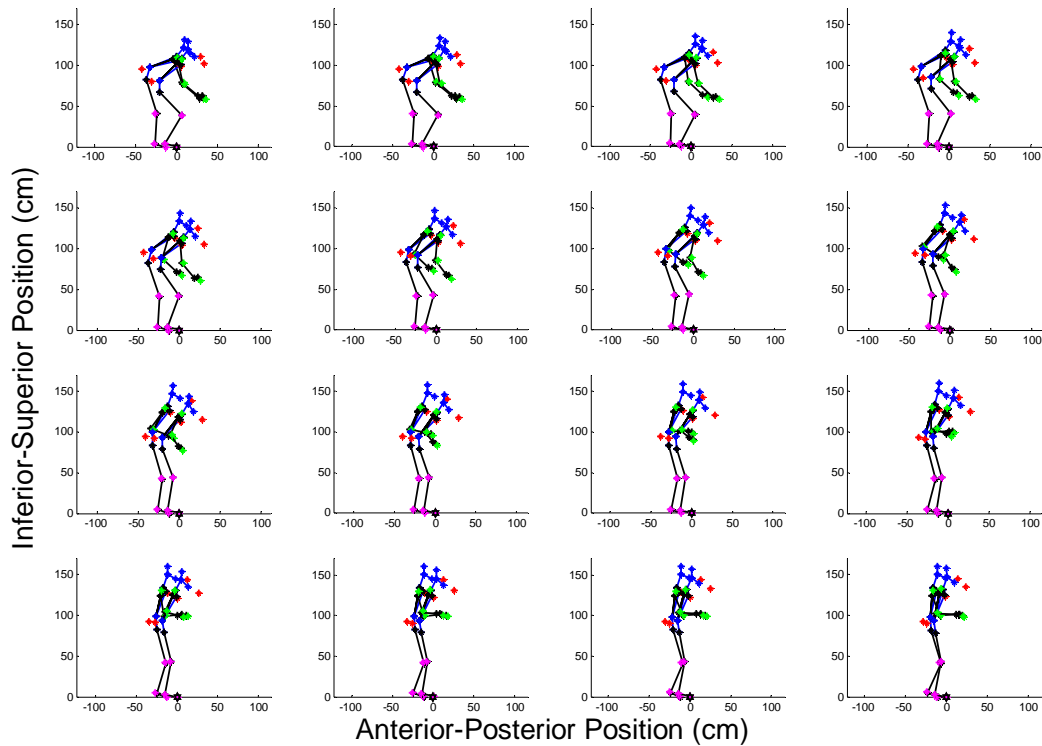


Figure 35. Time sequence for the same movement performed by two anthropometrically similar participants. Markers indicate the different joints and/or surface marker positions.

6.2.1.4 Implications of results – Training with an extended dataset

The process described in the previous section suggests that a network of this structure and size can reproduce a relatively wide set of movements with acceptable levels of errors. However, it is worrisome that the network’s generalization capabilities are low. It thus seems necessary to explore the network’s behavior when between-subject variability is introduced into its training dataset and inputs, as will be accomplished in a subsequent chapter. A secondary

issue is that the network inputs require start and end joint angles. While this is available within a dataset of actual movements, such as the one used here, it cannot necessarily be expected to be available for simulated movements. In those situations, start and end positions of a particular object would be available, and the network would be expected to use those positions to generate initial and end postures. In the current paradigm, this initial generation of postures would best be achieved by a separate network. The generation of this network is also discussed in a subsequent chapter.

Given the promising results observed for two dimensions, the network structure employing joint angles was expanded to predict motions in three dimensions. This transformation is not trivial, as it requires the assumption of a particular representation of joint angles (e.g. Euler, Cardan) for each joint. It also increases the complexity of the network; whereas for two dimensions the movement set was limited to those that were sagittally symmetric, this is not the case in three dimensions. Thus, joints must be treated independently between sides of the body. For example, while a ‘shoulder’ joint sufficed in the 2-D case, left and right shoulder joints must be defined and predicted in three dimensions. The results of this process are described in Chapter 8, in the context of movement prediction for various individuals within the same model. While the same training sequence described in this chapter was completed for three dimensions, the results are not detailed here for brevity, since they closely follow the patterns and performance observed for two dimensions. Note that at this point, there is still the implicit assumption that initial and final joint angles will be available. Methods to generate these values based on the data likely to be available in an applied setting are discussed, for both two and three dimensions, in the next chapter.

An additional important observation arose from the results that have been described in this chapter. It was noticed that joints in the upper limb exhibited consistently higher positioning errors than joints in the lower limbs. This result was hardly unexpected, as a bottom-up kinematic chain was employed to determine joint positions. Thus, any error in the prediction of a lower limb joint is carried upwards to the upper limbs. Various attempts were made to address this problem by modifying different ANNs’ structure, but no improvements were observed in the network predictions. Minimization of this particular artifact will be achieved while discussing future network iterations by incorporating joint angle errors in the discussion. If the assumption

that these errors are due to the particular order in which the kinematic chain is calculated is true, then consideration of joint angles in isolation should yield no discernible error pattern.

Chapter 7 PREDICTING INITIAL AND FINAL POSTURES

7.1 Introduction

The final models presented in the previous chapter used joint angles as their inputs and produced joint angles as their outputs. While this approach seemed promising, it has an important drawback: joint angles are typically not available as inputs in the real world. What are usually available as inputs are the start and end locations of interest that, arguably, pre-characterize the movement that will be used to perform an object transfer.

Thus, it became necessary to create a model that bridges that gap between start or end location and the joint angles (or posture) used to start and end the movement. This chapter discusses the development of an ANN-based model to achieve this goal.

The approach requires the separation of a movement into two distinct components, the initial and final postures and the actual motion performed to transform the initial posture into the final posture, while moving the object of interest. The former element is discussed in this chapter, the latter was discussed in the prior chapter and will be the subject of more attention in the next chapter.

7.2 Methods

Contrary to the networks discussed in the last chapter, consideration will be provided to between-subjects variability in developing an appropriate network structure and training the networks. The three most important factors, based on the literature review for this investigation, were anthropometry, biomechanical factors, and behavioral and psychophysical factors. Potential strategies for, and the feasibility of, the inclusion of these factors are briefly considered.

7.2.1 Lift Modifier Factors

7.2.1.1 Anthropometry

A possibility for implementing anatomical information into a neural network developed for posture prediction is to place it as a transformation function between the layer that generates the joint angles, if this is the level of control desired, and the final layer that presents end-effector position. This transformation function would be time-invariant and unique for different individuals. Given proper training and provided enough degrees of freedom, the neural network should modify its angle predictions to produce proper end-effector positions. The main drawback of this approach is that a unique network would have to be created and trained for each individual. An alternative approach would be to provide the network with a “standard”

transformation function and provide as an input a “scaling” parameter based on a ratio of, for example, individual height over standard height. This alternative would be more efficient, but its ability to converge to a desired result is most likely worse than for the fully adaptive alternative presented earlier.

An alternative approach, which is employed in the networks discussed in this chapter, standardizes anthropometric measures for the different participants and uses these as inputs to the network. This approach avoids having to individually standardize every anthropometric input while still providing the network with individual-specific information. The principal components approach used for standardization, which is discussed later in this section, provided a small number of inputs that condensed a substantial percentage of the information contained within the anthropometric data available.

7.2.1.2 Biomechanical factors

The analysis of lift modifiers previously discussed identified strength as one of the principal biomechanical factors. Any relationship between strength and end-effector position cannot be modeled simply by a weight layer between joint angles and end-effector position, as strength is likely to have an effect on the joint angles rather than be influenced by them. Thus, any effects in kinematics due to strength will be reflected on the joint angles. This reasoning suggested the use of strength as one of the inputs to the model using the same principal components approach used for anthropometry.

Other biomechanical factors were not directly available within the HUMOSIM dataset and were thus not modeled directly. These possible inputs included fatigue, lift frequency, lift asymmetry, one- and two-handed lifts, use of tools, distance to load, and injury. Each of these factors could be considered as an input to networks for motion prediction, but are not considered in this investigation. Some other factors are considered implicitly. For example, load magnitude, which can be a very important factor in self-selected lifting kinematics, was standardized within the HUMOSIM dataset employed and thus not explicitly used in the models. Lift velocity was implicitly considered via inputs indicating the current time for each movement sample and the overall duration for the movement. Another biomechanical factor, lift style, could be derived from the data using classification approaches (Park et al., 2005), but this approach would reduce the predictive ability of the network, as these data would not typically be available for a novel motion. The goal of the current approach is to model the kinematics of the

motion that an individual is likely to use, based on the assumption that these kinematics and the lift style in which they result are in some way related to known individual characteristics (e.g., anthropometry). Including the lift style as an input when no particular lifting instructions are given (which is the case with the current dataset) would instead model the kinematics of the motion provided an assumed lift style.

7.2.1.3 Behavioral and psychophysical factors

Implementation of behavioral and psychophysical factors (e.g., experience and training, guidance, and discomfort) was not considered due to their absence in the HUMOSIM database. As was discussed before, quantification of these factors is still an evolving area of research. Without appropriate quantification, these factors cannot be considered in this type of biomechanical model and were not considered for the models discussed in this chapter.

7.2.2 Two Dimensions

A typical feed-forward neural network trained via error back-propagation was used to predict initial and final postures (Figure 36). The network had seven inputs, ten outputs, and a single hidden layer with 50 nodes. The quantity of hidden layer nodes was determined based on initial pilot runs where patterns of training error for models employing different hidden layer sizes were observed. Sizes of 10, 25, 50, and 100 nodes were considered. The model with 50 nodes represented a reasonable tradeoff between error minimization and time. Biases in the hidden and output layers were trained. A sigmoid transfer function was used in the hidden layer, while a linear transfer function was used for the output units.

Inputs consisted of the position of the end-effector and five separate coefficients. One of these coefficients corresponded to strength of the individual, the remaining four accounted for the anthropometric characteristics of the person. These coefficients were derived using principal components regression (Johnson, 1998) on the available anthropometric characteristics of the participants, which can be obtained from the HUMOSIM website (www.humosim.com).

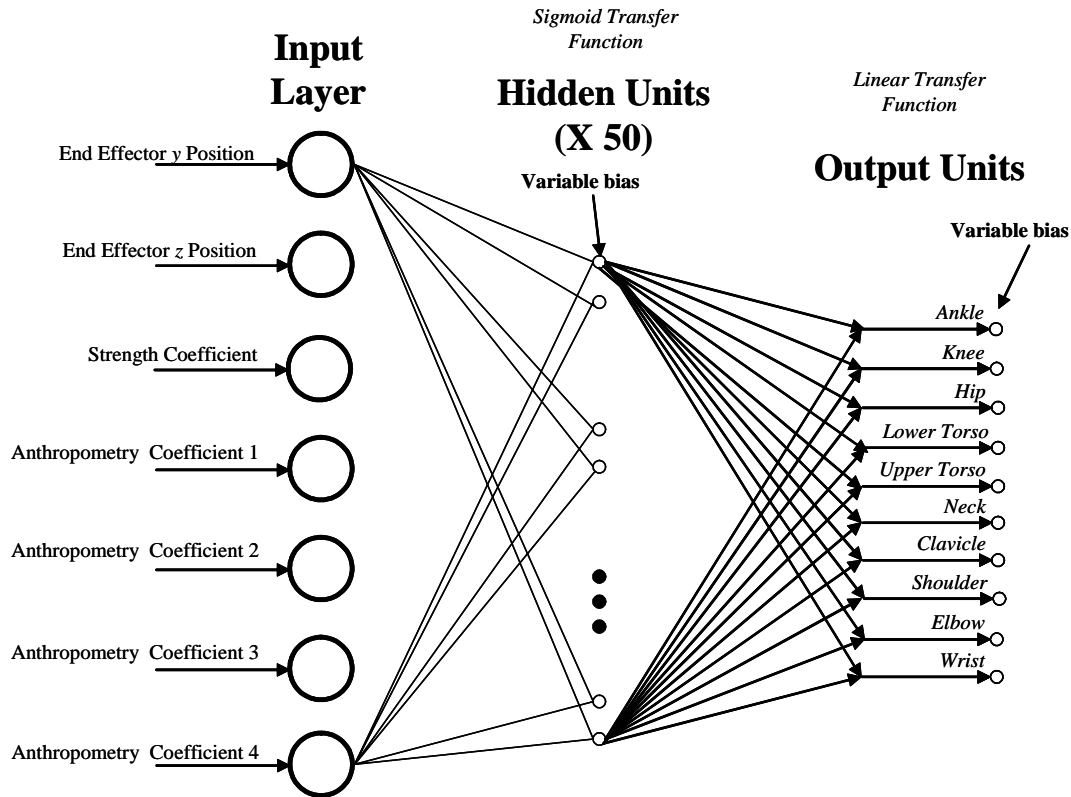


Figure 36. Network structure used for initial and final 2-D posture predictions.

The strength coefficient used five different variables (Table 7). A single linear combination of these variables (the first principal component) predicted 89.9% of the variability in the data, and was thus selected to be used within the network. The coefficients (eigenvector) for this linear combination and the means and standard deviations for the variables of interest are also shown in Table 7. Based on the eigenvector, all values had similar levels of influence on the principal component score, and consequently on the strength coefficient used as an input to the network.

Table 7. Strength coefficient parameters.

Variable	Eigenvector	Mean	Standard Deviation
Weight Used Box (N)	0.462	26.8	12.5
Avg. Shoulder Flexion Strength (N)	0.463	57.2	26.8
Avg. Shoulder Abduction Strength (N)	0.462	54.0	25.1
Avg. Shoulder 45 Degree Abduction Strength (N)	0.453	57.5	25.3
Avg. Torso Extension Strength (N)	0.391	410.6	116.1

The four anthropometry coefficients resulted from the combination of 45 different variables (Table 8). For this principal components regression, four components predicted 67.9% of the overall variability in the data. While this percentage is lower than the corresponding

number for strength, the addition of further components only added less than 5% each to the predicted variability and, when weighted against the increased complexity of the resulting neural network, did not warrant inclusion. The coefficients (eigenvectors) for this linear combination and the means and standard deviations for the variables of interest are also shown in Table 8. While most of the variables had an influence on the first eigenvector, the second through fourth eigenvectors were influenced by a reduced number of variables. However, values for all variables, even those with reduced influence on an eigenvector, were used in calculating each of the four anthropometry coefficients.

Once the input vectors had been calculated, a training set was built. Eighty percent of the participants were used in the training process, with the remaining 20% used to determine the generalization potential for the trained network. These conservative proportions were selected based on experimenter judgment, with the goal of providing enough training data to the network while saving sufficient data for verification. While the results will show that the data were sufficient for the network to model the verification set reasonably well, the question remains whether a smaller training dataset would have been sufficient. This form of sensitivity analysis was not a goal of the current investigation and is not addressed here.

The split of the participants was performed randomly, via a permutation process employing a random number generator. The training process used a limit of 500,000 epochs, with a maximum error limit of 0.003 rad².

ANOVAs were performed to detect significant differences between the ANN predictions and the empirical data. Significant differences within significant main effects were determined using Student-Newman-Keuls (SNK) tests. A Type I error of 1% was used for all statistical tests.

Table 8. Anthropometry coefficient parameters.

Variable	Eigenvector 1	Eigenvector 2	Eigenvector 3	Eigenvector 4	Mean	Standard Deviation
Weight (kg)	0.141	0.073	0.264	0.247	69.9	13.60
Stature w/o Shoes (cm)	0.216	0.034	-0.035	0.038	167.6	11.47
Stature with Shoes (cm)	0.216	0.009	-0.049	-0.047	170.2	11.70
C7 Height (cm)	0.217	0.006	-0.052	-0.050	145.2	10.35
EM Height at Suprasternale (cm)	0.217	0.022	-0.045	0.016	137.6	9.77
L5 Height (cm)	0.200	0.049	-0.078	-0.060	101.7	6.97
Greater Trochanter Ht. (cm)	0.182	0.033	-0.157	-0.091	90.7	5.91
Knee Ht. (cm)	0.162	0.057	0.070	0.020	49.3	6.45
Malleolus Ht. (cm)	0.042	0.088	-0.283	-0.195	9.2	1.29
Seated Ht. (cm)	0.201	0.029	-0.049	-0.038	155.9	5.22
Seated Eye Ht. (cm)	0.192	0.053	-0.007	0.052	145.2	5.22
Seated C7 Height (cm)	0.202	0.074	0.016	0.034	132.5	4.37
Seated Ankle Horizontal Distance (cm)	0.109	-0.182	-0.096	0.129	37.6	4.47
Seated Ankle Vertical Distance (cm)	-0.148	-0.178	-0.082	0.169	30.6	4.13
Head Width (cm)	0.065	0.257	0.147	0.086	14.9	0.72
Head Depth (cm)	0.188	0.016	0.043	0.183	19.4	0.89
Nasion Ht. (cm)	0.215	0.008	-0.065	-0.114	158.9	10.72
Nasion to Top of Head (cm)	0.120	-0.068	-0.168	-0.040	9.5	2.21
C1 to C7 (cm)	0.045	0.069	0.063	-0.266	6.7	1.49
C7 to L5 (cm)	0.180	-0.066	0.011	-0.457	43.5	4.62
Horz. Distance from C7 to Suprasternal Notch (cm)	0.123	-0.0235	0.321	0.195	11.3	1.62
Vert. Distance from C7 to Suprasternal Notch (cm)	0.023	-0.115	-0.044	0.147	7.5	2.18
Suprasternal Notch to Left AP (cm)	0.167	-0.011	-0.032	0.305	18.6	1.85
Suprasternal Notch to Right AP (cm)	0.172	0.054	-0.067	-0.159	18.6	2.41
Inter-AP (cm)	0.192	-0.037	-0.023	-0.054	37.4	2.91
Upper Arm Length (cm)	0.149	-0.087	0.049	-0.005	32.0	3.28
Elbow Width (cm)	0.087	0.287	-0.071	0.049	7.1	1.17
Forearm Length (cm)	0.190	-0.075	-0.100	0.094	24.8	2.50
Hand Length (cm)	0.196	0.042	0.042	-0.066	18.9	1.81
Hand Width (cm)	0.159	-0.029	0.148	-0.191	8.1	0.73
Wrist to 1st Knuckle (cm)	0.078	-0.351	0.056	-0.146	9.0	2.17
Wrist Depth (cm)	0.099	0.142	0.318	0.008	4.2	0.58
Wrist Width (cm)	0.153	-0.115	0.146	0.151	5.6	0.74
ASIS Horizontal to Greater Trochanter (cm)	-0.088	-0.190	0.332	0.032	7.7	2.52
Femoral Epicondyle Width (cm)	-0.015	0.418	0.014	0.117	10.4	1.02
Lateral Malleolus Horizontal to 1st Metatarsalphalangeal (cm)	0.142	-0.191	-0.033	-0.086	15.7	2.80
Malleolus Width (cm)	0.165	0.065	0.251	0.038	7.0	0.52
Cylinder L1 (cm)	0.097	0.034	0.114	-0.059	3.6	0.71
Cylinder L2 (cm)	0.116	0.001	-0.264	0.132	3.8	1.33
Cylinder L3 (cm)	-0.052	0.353	0.170	-0.189	6.2	1.52
Cylinder L4 (cm)	0.115	-0.179	-0.184	0.265	6.7	1.47
Tote L1 (cm)	0.077	-0.180	0.279	-0.110	4.1	0.76
Tote L2 (cm)	0.121	-0.068	-0.057	0.034	5.0	1.59
Tote L3 (cm)	-0.083	0.190	-0.162	-0.088	2.9	1.67
Tote L4 (cm)	0.068	0.263	-0.150	0.220	4.0	1.17

7.2.3 *Three Dimensions*

The approach used for three dimensions followed the same steps as the two-dimensional approach. However, the number of network outputs was increased from the ten angles predicted for two dimensions to the 36 that are necessary for three dimensions (the process for obtaining these angles is detailed within Chapter 8). This increase in network outputs required an increase in the number of hidden units employed within the network, based on similar pilot runs to those described for the 2-D case. In this case, networks of 50, 75, 100, and 150 hidden nodes were tested. The network with 100 hidden nodes exhibited the best tradeoff between training efficiency and error minimization. An additional input was introduced to account for the end-effector position in the left-right axis. The anthropometry and strength inputs remained unchanged (Figure 37).

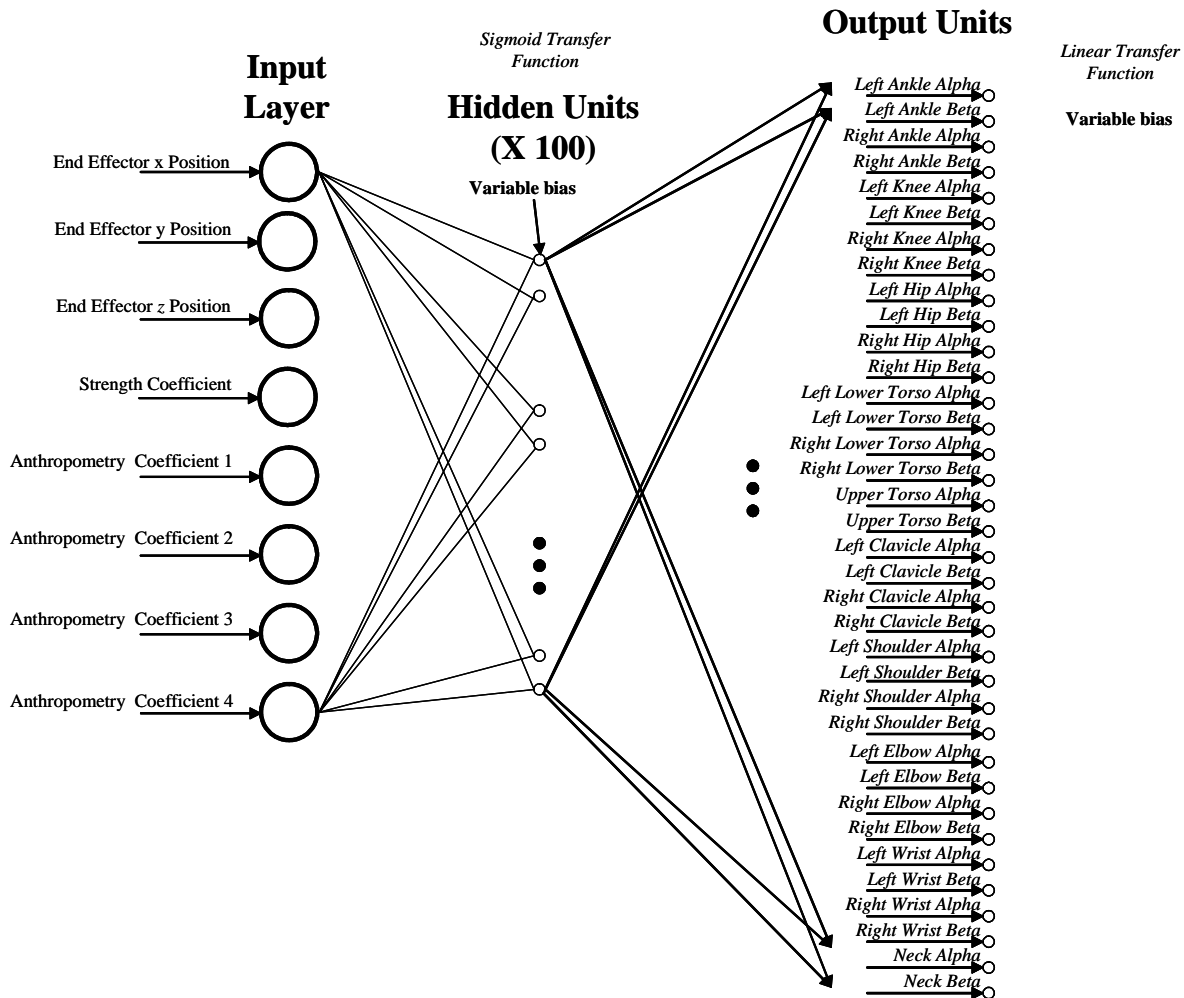


Figure 37. Network structure used for initial and final 3-D posture predictions.

Once the input vectors had been calculated, a training set was built. The training set used for the three-dimensional case was slightly different than for the two-dimensional case, in order to explore the ability of the network to produce accurate predictions for completely novel conditions. When this training set was built, results from the 2-D case were available, and indicated that the network was able to reproduce the training data when initial and final postures from all movements performed by the included participants were available for training. Recall that the motions performed by all participants were standardized in terms of start and end point. Thus, in the 2-D case, no novel start and end points necessarily existed within the generalization dataset. The training process used for the 3-D situation intended to change this, with the underlying goal of examining the capacity of the network to predict, rather than reproduce, posture. If the network was available to predict postures for novel movements, then it could be considered a prediction model, as opposed to a model that simply reproduced pre-observed patterns. The opposite finding, that the network was unable to predict acceptable postures for novel movements, would support the opinion that the network serves as a reproduction tool; it is able to accurately reproduce movement patterns that it has been exposed to, but is not able to translate this 'knowledge' to novel conditions.

As for the 2-D case and, again, based on experimenter judgment, 80% of the participants were used in the training process, with the remaining 20% used to determine the generalization potential for the trained network. The split of the participants was performed randomly, via a permutation process employing a random number generator. However, distinctly from the 2-D case, not all movements performed by each of the sixteen included participants were included in the training. All movements to the Middle Lower and Middle Upper locations were excluded and used in network performance verification. This approach resulted in three verification datasets. The first allowed the performance of the network to be determined for novel movements performed by familiar participants. The second dataset allowed performance verification for conditions in which the participant was novel but the movement was familiar. Finally, the third dataset examined network performance for conditions in which both the participant and the movement were novel. The training process used a limit of 500,000 epochs, with a maximum error limit of 0.003 rad^2 .

ANOVAs were performed to detect significant differences between the ANN predictions and the empirical data. Significant differences within significant main effects were determined

using Student-Newman-Keuls (SNK) tests. A Type I error of 1% was used across all statistical tests.

The three dimensional model predictions were compared against the predictions of The University of Michigan's 3D Static Strength Prediction Program (3DSSPP™). Given the available 3DSSPP™ outputs, joint angle predictions for the ankle (due to no toe or ball of foot information), wrist (due to no finger location prediction), and neck (due to no head location prediction) could not be obtained and were thus not used in the comparison. The program was provided with anthropometric information for each participant, including height and weight, and with the participant's gender. All motions were used in this comparison given the similarity observed in artificial neural network performance for the training and generalization datasets. Given this similarity, this decision was not expected to substantially favor the network (which had been created using a portion of the data) in this comparison.

Similarly, the Jack™ simulation environment (UGS, Plano, Texas) was also used to obtain comparisons to the ANN's performance. The humanoid in the software was scaled according to the gender, height, and weight of each participant and manipulated to acquire control of a virtual object that represented the box employed by the 'real' participants. The inverse kinematics algorithm in Jack™, which is augmented with a series of constraints and behaviors, was then tasked to provide a candidate posture. This posture was taken as the software's prediction. This process was repeated for the initial and final movement locations across all participants and tasks. As for the 3DSSPP™ comparisons, all available data were used.

These two software packages, 3DSSPP™ and Jack™, provided as output a set of predicted joint locations. To avoid any differences in coordinate systems to affect the comparisons, these joint locations were obtained and transformed into the angle definitions used in this investigation based on the process described in Chapter 5. The analysis was performed only in 3-D, as that is the operational mode of both of these simulation environments.

7.3 Results

7.3.1 Two Dimensions

The maximum error limit (0.003 rad²) was not reached within the 500,000 epoch limit. The training process was stopped once the mse stabilized (i.e. did not change by more than 10%

within 20,000 epochs). The mse after training was 0.05 rad^2 , equivalent to an rmse of 0.22 rad (12.8°).

No significant differences in rmse were found between the training dataset and the generalization dataset. Overall rmse values calculated by joint across participants and postures were highly dependent on the joint of interest (Table 9) when simulating training and generalization postures. Rmse levels across the training and generalization datasets differed significantly across joints ($F(9,190)=39.27, p<0.0001$), movement locations ($F(9,166)=15.38, p<0.0001$), and the interaction between these factors ($F(81,1304)=5.46, p<0.0001$). *Post hoc* tests showed that the clavicle angles exhibited the largest amount of error, followed by the wrist angles. The remaining angles could be clustered in terms of their error levels, with the ankle exhibiting the lowest overall error. These results were expected, as the clavicle and wrist joints exhibited large amounts of variability in the dataset, especially the clavicle angle. However, their effect on final position is likely slight, as the link lengths associated with the angles are small. Thus, the effect of these errors on overall posture is minimal.

Table 9. Root mean square errors for the posture prediction network using the training and generalization postures.

Joint	Rmse (Training, degrees)	Rmse (Generalization, degrees)
Ankle	6.55	6.31
Knee	8.70	8.22
Hip	11.68	12.89
Lower Torso	12.56	10.41
Upper Torso	11.93	15.04
Clavicle	33.67	36.33
Shoulder	13.20	13.11
Elbow	13.77	14.50
Wrist	24.35	23.31
Neck	14.87	16.12

No patterns on the rmse values were observable qualitatively when errors were separated by participant and joint (Table 10). The clavicle and wrist continued to exhibit the highest levels of error. The generalization and training datasets could not be differentiated qualitatively in terms of this error. Table 10 also indicates rmse levels that are outside a confidence interval of two standard deviations around the mean. No assignable cause could be found to indicate that these were special cases, and they were maintained in the database.

Few differences could be qualitatively observed in terms of movement location (Table 11). However, the statistical analysis detected significant differences in the sample based on movement location. *Post hoc* Student-Newman-Keuls tests showed that the near and far lower locations had significantly larger errors associated with them than other higher locations. Other locations could not be distinguished statistically. Also, note that the near middle location was not represented in the generalization data, since data for it were not available for any of the participants within the generalization dataset.

Altogether, these errors at times represented substantial deviations from actual postures (Figure 38). This can result in problems when the postures are introduced on a movement prediction network, as the inputs might not be sufficiently accurate.

Table 10. Prediction root mean square errors by participant and joint. *Italicized values are separated from the mean rmse for each joint by more than two standard deviations.*

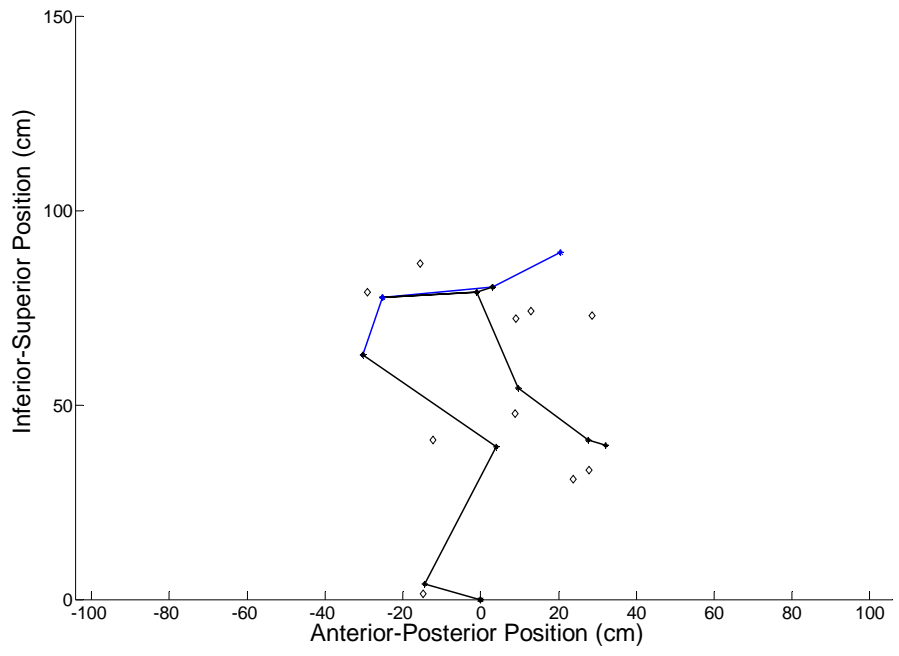
Joint	Training															
	Subject 2	Subject 3	Subject 4	Subject 5	Subject 6	Subject 7	Subject 8	Subject 9	Subject 10	Subject 11	Subject 12	Subject 14	Subject 15	Subject 16	Subject 19	Subject 20
Ankle	4.08	7.58	8.56	8.65	6.38	8.24	1.36	2.73	8.13	3.08	8.17	7.95	8.79	4.85	4.17	5.29
Knee	12.14	8.62	5.57	7.48	7.9	6.13	4.01	7.17	9.69	8.24	10.29	8.4	8.28	7.5	<i>14.97</i>	7.89
Hip	16.84	13.1	11.15	13.24	8.78	10.89	6.02	9.45	11	13.09	10.56	14.33	11.78	10.56	6.17	11.94
Lower Torso	8.44	10.6	18.96	13.41	9.86	10.87	7.41	16.99	9.15	7.11	17.68	19.92	10.62	8.5	4.3	14.45
Upper Torso	13.87	11.39	9.17	13.58	11.06	11.49	8.69	10.03	8.97	13.76	16.83	9.27	12.43	14.86	9.73	12.59
Clavicle	21.35	38.99	25.98	41.07	54.04	32.81	21.53	41.52	21.64	29.66	<i>62.13</i>	34.94	16	33.04	18.11	27.73
Shoulder	<i>18.42</i>	12.09	13.1	12.99	7.87	13.16	14.2	12.17	13.54	10.71	<i>18.49</i>	10.5	11.96	13.64	12.81	12.8
Elbow	15.24	11.14	14.23	11.43	9.71	11.8	16.64	18.17	14.76	10.63	12.09	15.08	14.43	15.07	13.37	12.43
Wrist	15.45	22.52	13.67	23.41	10.79	23.45	32.01	27.25	30.96	<i>43.95</i>	30.87	19.72	27.51	14.52	18	16.32
Neck	17.25	18.41	11.47	10.47	14.22	12.47	11.81	12.06	18.82	16.82	12.57	11.66	11.86	14.85	17.32	19.56

Joint	Generalization			
	Subject 1	Subject 13	Subject 17	Subject 18
Ankle	7.82	3.37	7.81	3.82
Knee	7.26	4.83	9.56	9.4
Hip	15.31	8.98	14.66	10
Lower Torso	11.82	7.2	8.67	12.03
Upper Torso	15.76	11.04	16.25	15.24
Clavicle	34.22	23.08	54.45	18.49
Shoulder	14.73	14.03	11.15	12.46
Elbow	11.88	15.51	11.46	18.51
Wrist	31.6	12.44	18.26	22.85
Neck	14.14	23.79	11.68	15.76

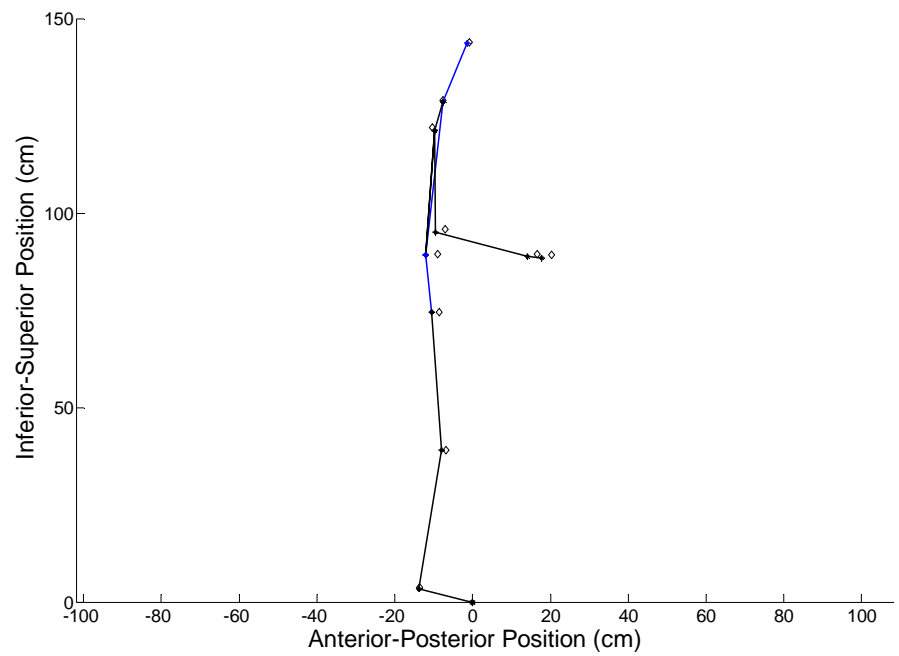
Table 11. Prediction root mean square errors by movement location and joint. *Italicized values are separated from the mean error for each joint by more than two standard deviations. LL-Lower Location, MLL-Middle Lower Location, ML-Middle Location, MUL-Middle Upper Location, UL-Upper Location. Locations combine errors for both Deliver and Bring Back movements, since only static postures were considered.*

Training										
Joint	LL Near	MLL Near	ML Near	MUL Near	UL Near	LL Far	MLL Far	ML Far	MUL Far	UL Far
Ankle	5.1	4.74	3.21	4.74	6.63	7.27	<i>10.17</i>	6.9	4.08	8.33
Knee	10.71	10.74	3.88	3.17	3.86	12.37	16.04	4.48	3.36	3.22
Hip	15.17	12.08	4.22	5.36	4.84	19.4	19.38	6.29	6.04	5.42
Lower Torso	18.24	11.35	9.11	9.17	9.68	<i>19.36</i>	11.74	10.34	9.41	10.68
Upper Torso	16.95	12.24	7.07	7.13	8.2	19.7	13.19	10.89	6.9	7.3
Clavicle	59.52	29.33	15.47	18.9	21.4	48.44	22.18	24.93	26.45	34.95
Shoulder	13.18	11.57	12.55	9.16	10.79	12.43	18.43	19.41	11.65	8.92
Elbow	12.99	11.94	13.75	17	10.06	13.4	<i>18.58</i>	13.02	12.99	11.87
Wrist	26.56	24.55	17.95	21.01	27.56	27	24.83	20.81	24.17	23.96
Neck	20.19	16.24	8.32	9.82	12.69	24.72	15.39	8.37	8.83	12.07

Generalization										
Joint	LL Near	MLL Near	ML Near	MUL Near	UL Near	LL Far	MLL Far	ML Far	MUL Far	UL Far
Ankle	5.44	6.04		6.54	4.82	7.67	6.33	7	3.18	8.03
Knee	9.12	14.41		3.63	2.74	12.25	11.19	3.35	2.46	2.76
Hip	10.03	13.96		4.19	4.91	29.22	12.07	5.25	4.52	3.65
Lower Torso	10.28	8.26		6.96	5.93	<i>19.25</i>	10.8	11.45	5.97	6.51
Upper Torso	14.91	15.14		7.76	9.56	25.69	21.58	11.69	7.98	6.25
Clavicle	28.56	13.32		27.25	39.26	42.98	29.87	22.67	30.48	<i>61.32</i>
Shoulder	10.06	8.9		6.31	9.68	13.32	16.36	<i>24.53</i>	13.84	9.76
Elbow	11.85	13.09		16.1	13.24	13.91	15.73	10.71	15.38	16.77
Wrist	24.36	24.29		18.1	19.45	26.29	23.24	21.98	28.3	21.08
Neck	13.17	11.41		9.66	9.11	<i>31.27</i>	16.8	14.93	12.62	10.18



a)



b)

Figure 38. Comparison of predicted posture (stick figure) and actual posture (joint positions are represented by hollow diamonds) for training cases where maximum (a) and minimum (b) rmse levels were observed.

Analysis of rmse levels by subject showed relatively close clustering (Table 12). However, subject 12 appeared to exhibit higher rmse than any other subject, including those in the generalization dataset.

Table 12. Root mean square error (in degrees) by subject, split in training and generalization groups.

	Subject Number	Rmse (degrees)
Training	2	15.08
	3	17.84
	4	14.28
	5	18.2
	6	19.48
	7	16.03
	8	15.14
	9	19.05
	10	16.21
	11	19.52
	12	25.18
	14	17.05
	15	14.34
	16	15.56
Generalization	1	18.2
	13	12.99
	17	12.83
	18	15.67

7.3.2 *Three Dimensions*

The maximum error limit (0.003 rad^2) was not reached within the 500,000 epoch limit. The mse after manually stopping training, once the mse had stabilized, was 0.52 rad^2 , equivalent to an rmse of 0.72 rad (41.5°).

Significant differences in rmse levels were observed as a function of the training/generalization dataset used ($F(3,40)=4.78, p=0.0061$). However, a *post hoc* test showed that the training dataset did not differ significantly from any of the other generalization groups. The significant effect was due to a difference between the generalization groups with novel participants, which had significantly higher rmse levels than the generalization group with novel

movements performed by familiar participants. This last generalization group had, in fact, the lowest overall levels of average error (10.33°), even lower than the errors for the training set (14.66°). Average errors for the remaining generalization datasets were both between 21° and 22° .

Qualitatively, overall rmse levels seemed to be highly dependent on the joint of interest when simulating the training postures (Table 13). As in the 2D case, significant effects in rmse levels were observed across joints, movement locations, and the interaction between these factors ($F(35,684)=12.75, p<0.0001$; $F(29,534)=9.82, p<0.0001$; $F(1015,18006)=13.84, p<0.0001$, respectively). Three different joints, the right knee α , left hip α , and left shoulder α , exhibited significantly higher errors than the remaining joints, which could not be differentiated statistically. The right knee α had the largest average error (58.07°) while the right ankle β had the lowest (4.64°). Qualitatively, the shoulder and hip angles generally tended to exhibit the largest amount of error, the ankles tended to exhibit the smallest. Overall, the observed qualitative errors were considerably larger than those obtained for the 2-D case. Recall that the first generalization dataset (Generalization 1) included novel movements performed by familiar participants. The second generalization dataset (Generalization 2) included conditions in which the participant was novel but the movement was familiar. The third generalization dataset (Generalization 3) included conditions in which both the participant and the movement were novel.

Table 13. Prediction root mean square errors for the posture prediction network using the training and three generalization datasets.

Joint	Rmse (Training, degrees)	Rmse (Generalization 1, degrees)	Rmse (Generalization 2, degrees)	Rmse (Generalization 3, degrees)
Left Ankle Alpha	10.94	7.75	9.97	9.68
Left Ankle Beta	9.20	6.46	6.90	5.70
Right Ankle Alpha	24.23	19.59	25.48	13.47
Right Ankle Beta	7.13	6.20	6.10	5.90
Left Knee Alpha	25.73	33.21	22.01	29.58
Left Knee Beta	8.19	8.34	6.96	7.10
Right Knee Alpha	55.24	63.44	48.63	74.55
Right Knee Beta	8.62	8.57	6.32	6.18
Left Hip Alpha	80.65	82.13	69.56	75.91
Left Hip Beta	39.89	18.46	39.70	12.40
Right Hip Alpha	77.30	73.28	66.48	62.33
Right Hip Beta	11.31	13.82	10.97	11.10
Left Lower Torso Alpha	20.62	18.56	13.89	13.96
Left Lower Torso Beta	7.99	9.02	6.10	6.47
Right Lower Torso Alpha	23.90	26.05	21.10	21.29
Right Lower Torso Beta	7.88	7.36	5.95	5.40
Upper Torso Alpha	85.29	84.64	88.96	95.21
Upper Torso Beta	14.31	20.72	14.48	19.69
Left Clavicle Alpha	18.12	19.12	18.02	18.31
Left Clavicle Beta	8.95	9.32	9.63	9.40
Right Clavicle Alpha	17.53	17.35	17.18	16.99
Right Clavicle Beta	8.40	7.47	7.89	6.97
Left Shoulder Alpha	151.23	155.01	138.13	144.46
Left Shoulder Beta	32.10	26.10	29.81	21.68
Right Shoulder Alpha	71.87	80.27	85.92	103.16
Right Shoulder Beta	33.60	26.28	31.82	21.40
Left Elbow Alpha	16.63	17.27	16.67	16.17
Left Elbow Beta	26.03	24.02	24.49	22.48
Right Elbow Alpha	47.74	48.12	41.45	48.40
Right Elbow Beta	27.79	25.95	25.84	24.36
Left Wrist Alpha	22.34	20.62	19.99	19.92
Left Wrist Beta	20.26	19.75	17.99	18.02
Right Wrist Alpha	27.48	26.40	23.31	23.34
Right Wrist Beta	19.41	19.57	16.12	19.03
Neck Alpha	61.09	47.95	53.76	40.00
Neck Beta	14.77	17.08	15.59	17.17

No patterns were observable within the rmse levels when errors were separated by participant and joint (Table 14). Generalization and training participants could not be qualitatively differentiated in terms of this error. Table 14 also indicates errors that are outside a confidence interval of two standard deviations around the mean. No assignable cause could be found to indicate that these were special cases, and they were maintained in the database.

In terms of significant effects due to Movement Location, the far lower movement location with no rotation exhibited the largest average error (50.10°). The near lower movement location with no rotation exhibited the second largest average error (30.86°). Remaining movement locations could not be statistically distinguished. Qualitative observation (Table 15) showed that the near and far upper locations within the training dataset contained a cluster of large errors within the upper limb joint angles, but this pattern was not observed across the generalization samples.

Table 14. Prediction root mean square errors by participant and joint. *Italicized values are separated from the mean error for each joint by more than two standard deviations. The table is continued on the next three pages.*

Joint	Training															
	Subject 2	Subject 3	Subject 4	Subject 5	Subject 6	Subject 7	Subject 8	Subject 9	Subject 10	Subject 11	Subject 12	Subject 14	Subject 15	Subject 16	Subject 19	Subject 20
Left Ankle Alpha	6.4	15.9	16.2	7.8	3.7	6.2	2.5	7.0	22.7	5.2	13.2	4.0	18.5	8.1	8.1	4.2
Left Ankle Beta	7.6	5.5	16.0	10.1	2.5	4.6	4.2	4.5	18.0	10.1	10.4	8.1	10.6	8.2	4.2	7.2
Right Ankle Alpha	67.0	11.5	20.3	18.5	21.9	11.6	18.1	14.5	14.8	17.8	21.6	17.3	10.9	18.7	26.4	13.8
Right Ankle Beta	11.2	4.6	7.9	3.9	4.8	4.5	4.1	4.5	10.0	12.9	4.9	8.3	3.8	5.2	6.5	6.9
Left Knee Alpha	31.9	19.0	23.9	33.7	27.7	18.5	13.8	29.5	32.5	16.5	39.9	19.7	20.7	19.7	32.9	19.0
Left Knee Beta	7.8	7.7	7.7	9.9	8.7	6.3	5.3	6.1	10.2	10.9	7.4	6.2	11.8	6.8	7.2	7.9
Right Knee Alpha	46.2	60.3	86.0	67.2	64.6	20.5	34.1	62.7	29.5	69.3	68.1	37.2	33.8	69.8	32.5	50.1
Right Knee Beta	14.2	6.2	5.2	7.0	5.8	7.2	4.4	7.3	8.9	14.1	9.1	10.8	8.1	5.5	9.9	5.7
Left Hip Alpha	109.2	83.6	28.5	103.8	110.6	54.9	53.4	54.3	38.6	107.5	37.5	81.1	59.6	102.8	115.2	37.6
Left Hip Beta	96.7	41.2	16.9	20.8	15.5	26.0	21.2	10.1	18.0	56.9	12.7	52.7	33.9	36.3	22.9	40.9
Right Hip Alpha	43.2	142.2	13.0	126.7	48.8	33.9	57.5	55.6	30.7	147.6	26.4	104.5	20.3	87.2	26.8	39.2
Right Hip Beta	14.7	13.2	10.1	12.2	7.6	10.4	9.2	10.3	10.3	11.4	11.0	10.6	14.9	9.9	10.0	12.3
Left Lower Torso Alpha	15.7	16.9	30.5	20.9	10.8	13.3	22.3	23.4	15.1	22.7	26.4	26.1	20.2	14.7	15.2	24.7
Left Lower Torso Beta	6.7	6.8	8.1	13.9	5.4	9.0	5.4	5.6	5.5	13.8	9.5	6.6	5.9	4.3	3.7	9.3
Right Lower Torso Alpha	26.5	24.8	29.0	20.3	36.6	20.0	15.0	18.6	21.1	18.6	22.7	32.7	24.0	15.2	15.1	27.8
Right Lower Torso Beta	6.2	10.2	10.6	8.9	6.3	8.1	5.6	6.4	8.3	6.6	11.9	7.0	4.9	6.7	7.4	8.1
Upper Torso Alpha	106.9	132.8	69.7	91.2	77.0	20.9	73.9	59.4	121.1	126.3	47.5	31.6	62.7	72.2	102.2	58.0
Upper Torso Beta	17.7	21.8	16.2	12.3	13.2	14.5	11.5	6.7	14.0	11.1	13.0	12.9	16.1	14.6	10.7	15.1
Left Clavicle Alpha	14.2	18.0	19.5	18.3	19.1	20.1	18.8	15.1	18.6	19.8	19.3	15.2	15.2	17.5	20.4	19.2
Left Clavicle Beta	9.1	6.1	11.7	8.8	7.7	6.7	8.2	7.7	8.9	12.3	12.4	7.4	7.4	10.8	6.7	8.0
Right Clavicle Alpha	19.2	19.1	19.7	17.4	16.7	16.5	15.1	16.8	20.8	16.2	15.5	16.7	15.0	17.0	19.7	17.1
Right Clavicle Beta	6.7	7.0	7.1	7.2	6.5	8.2	8.0	9.3	9.6	12.5	10.0	8.3	6.4	9.5	8.1	8.0
Left Shoulder Alpha	154.6	141.3	149.9	141.1	166.4	131.8	150.3	158.9	158.1	156.0	149.5	163.6	145.9	129.0	168.7	147.7
Left Shoulder Beta	34.2	27.2	34.1	27.8	23.3	19.7	28.4	28.5	40.3	56.5	28.5	25.5	30.2	38.0	28.1	22.3
Right Shoulder Alpha	108.2	90.1	58.2	83.0	42.7	94.4	55.5	76.1	54.2	81.1	50.4	49.5	76.4	90.5	51.1	41.2
Right Shoulder Beta	36.6	27.7	35.7	29.6	23.0	20.3	32.0	31.2	42.7	57.5	29.9	26.2	32.0	39.4	28.4	25.0
Left Elbow Alpha	18.8	16.2	18.8	14.7	13.9	17.9	16.9	18.6	15.9	14.5	15.5	18.1	18.1	15.2	13.4	18.3
Left Elbow Beta	24.6	25.6	29.4	19.5	19.4	24.3	28.1	30.2	32.7	34.2	21.5	19.3	26.7	32.5	20.0	20.8
Right Elbow Alpha	26.1	23.9	63.1	24.1	20.7	19.1	85.3	104.0	26.3	66.3	27.7	30.0	67.7	28.3	21.9	24.0
Right Elbow Beta	24.8	27.2	30.5	22.7	22.7	25.9	29.7	29.2	35.8	36.8	24.0	22.2	27.6	33.2	22.7	23.4
Left Wrist Alpha	16.9	19.0	21.5	19.0	17.7	22.9	22.0	20.2	41.9	25.2	18.2	18.6	22.3	20.9	19.0	21.9
Left Wrist Beta	14.1	25.4	13.0	16.2	10.5	23.4	27.0	22.2	30.9	25.6	25.9	16.3	18.8	17.1	15.3	12.3
Right Wrist Alpha	22.2	21.4	29.6	26.0	19.7	20.5	40.2	28.4	42.4	36.4	19.7	23.2	27.1	25.3	22.1	22.4
Right Wrist Beta	13.8	19.5	12.6	15.6	16.4	19.3	30.0	23.1	28.0	22.6	21.3	15.1	20.8	16.4	16.3	13.2
Neck Alpha	38.0	22.5	61.7	54.0	66.4	30.6	79.8	54.2	64.8	94.0	64.5	46.7	47.7	60.9	78.3	67.4
Neck Beta	18.1	21.3	16.4	13.5	12.7	14.5	12.4	9.0	14.1	16.2	11.0	13.9	14.6	16.9	12.6	12.8

Table 14 (continued)

Joint	Generalization Dataset 1															
	Subject 2	Subject 3	Subject 4	Subject 5	Subject 6	Subject 7	Subject 8	Subject 9	Subject 10	Subject 11	Subject 12	Subject 14	Subject 15	Subject 16	Subject 19	Subject 20
Left Ankle Alpha	3.9	16.1	8.1	9.4	3.4	6.7	1.9	5.6	9.2	5.0	11.9	4.2	11.5	4.1	5.3	3.5
Left Ankle Beta	4.4	4.5	10.3	6.3	2.7	4.4	3.4	5.3	13.3	5.7	10.7	7.8	3.2	5.7	2.7	4.2
Right Ankle Alpha	28.0	10.2	22.5	17.2	19.8	14.8	18.8	18.3	12.8	15.2	18.7	17.4	11.5	21.0	36.4	9.3
Right Ankle Beta	11.6	4.9	8.6	3.6	4.9	3.3	3.3	5.6	7.5	3.3	4.9	4.6	2.8	4.7	9.3	6.8
Left Knee Alpha	45.2	27.8	25.1	56.7	47.3	22.2	9.8	23.6	33.0	19.2	37.6	20.0	18.0	29.9	46.6	24.9
Left Knee Beta	7.8	9.1	7.7	9.2	8.8	6.1	6.3	8.7	9.7	8.3	10.9	8.6	6.9	6.9	9.4	8.2
Right Knee Alpha	49.3	57.1	101.3	79.0	85.2	22.6	37.1	69.7	36.3	83.7	56.2	34.6	56.1	62.0	28.8	77.5
Right Knee Beta	11.8	6.4	6.2	7.2	6.2	9.5	6.0	7.9	9.4	4.8	6.8	6.9	6.6	7.2	17.6	7.2
Left Hip Alpha	126.2	90.8	28.3	113.5	78.6	46.5	32.8	74.0	37.5	116.0	29.3	81.5	40.8	111.6	103.0	42.6
Left Hip Beta	47.4	7.1	10.4	9.4	7.3	12.8	15.2	16.2	20.4	14.9	6.1	20.9	12.1	13.8	21.9	8.9
Right Hip Alpha	53.4	144.1	12.4	112.1	49.4	38.4	43.3	54.9	33.0	125.3	16.5	85.9	15.9	93.8	28.1	32.2
Right Hip Beta	13.0	16.5	14.3	14.4	12.1	13.9	13.7	13.0	13.5	13.7	12.6	14.7	14.8	12.8	12.6	14.5
Left Lower Torso Alpha	15.9	16.5	27.6	22.0	11.6	12.6	22.9	24.6	10.0	22.2	23.4	18.1	10.9	15.8	13.4	19.7
Left Lower Torso Beta	6.0	6.6	8.4	15.6	6.9	9.7	5.7	6.7	8.5	16.0	7.9	7.9	6.9	4.5	5.2	11.2
Right Lower Torso Alpha	27.9	26.8	34.8	26.7	34.7	19.8	18.7	25.5	24.4	20.3	28.9	28.8	20.9	14.3	26.2	28.1
Right Lower Torso Beta	4.7	9.8	9.5	6.6	8.5	9.6	6.6	6.4	7.1	4.5	8.0	7.1	4.5	6.8	8.8	7.4
Upper Torso Alpha	102.3	134.6	60.0	120.0	31.7	16.4	67.4	62.1	109.4	131.2	25.1	29.2	48.3	65.8	116.3	38.5
Upper Torso Beta	23.0	21.6	20.8	24.1	21.7	16.9	18.7	20.3	20.2	22.1	19.0	17.8	20.5	18.8	22.1	20.4
Left Clavicle Alpha	18.9	19.6	19.5	21.2	17.6	18.4	20.1	19.8	20.7	19.0	12.6	18.6	17.2	17.0	23.4	18.5
Left Clavicle Beta	9.3	7.4	9.4	11.0	7.9	6.2	7.8	10.6	12.5	11.3	10.8	8.8	6.5	8.5	10.5	8.1
Right Clavicle Alpha	17.9	22.0	18.5	19.6	13.0	14.3	15.3	16.1	21.0	15.9	13.5	18.6	13.8	16.0	20.3	16.1
Right Clavicle Beta	4.6	5.6	4.8	7.7	7.9	11.5	5.8	6.2	7.5	11.6	7.9	4.4	7.9	8.0	9.6	4.8
Left Shoulder Alpha	157.9	135.1	160.2	178.8	167.4	135.0	147.5	176.0	167.6	154.6	149.6	168.5	142.6	120.2	164.5	137.0
Left Shoulder Beta	28.2	19.3	28.4	25.0	20.8	18.5	20.3	24.2	29.0	50.0	15.9	20.2	20.2	29.8	20.4	21.7
Right Shoulder Alpha	128.9	87.4	48.2	80.0	35.9	114.3	51.5	80.5	70.4	64.1	79.2	62.7	86.0	110.0	73.6	57.2
Right Shoulder Beta	29.1	16.8	29.2	24.5	20.4	18.6	21.2	26.7	29.8	48.8	13.3	20.0	21.1	31.1	19.4	23.6
Left Elbow Alpha	19.0	20.1	17.9	21.1	12.6	16.1	15.8	18.8	16.3	16.4	16.1	19.3	18.0	15.3	14.6	15.8
Left Elbow Beta	27.5	17.2	26.3	20.3	14.9	22.2	25.5	28.2	29.1	30.0	22.4	21.5	19.1	28.9	21.1	24.3
Right Elbow Alpha	26.7	27.6	49.9	22.7	22.6	25.9	56.5	113.6	52.6	53.4	27.1	31.1	80.9	28.3	21.0	28.5
Right Elbow Beta	28.2	21.2	25.7	21.5	18.9	24.6	26.4	27.1	31.6	34.8	25.1	21.4	23.6	31.5	21.8	26.4
Left Wrist Alpha	18.4	20.9	20.8	24.1	17.4	18.9	24.5	16.7	18.3	23.6	20.0	19.9	23.8	22.6	18.8	17.6
Left Wrist Beta	18.1	26.1	12.4	19.4	8.5	18.7	26.4	19.6	22.3	26.6	23.5	16.7	22.0	16.4	16.9	15.0
Right Wrist Alpha	25.3	21.2	29.0	30.9	20.2	19.0	35.5	29.6	23.2	36.3	19.5	27.3	25.4	22.3	23.8	22.8
Right Wrist Beta	18.1	18.8	11.6	14.1	15.0	23.1	32.1	21.5	21.3	25.6	18.5	18.6	21.4	15.2	14.0	18.0
Neck Alpha	23.8	24.8	68.2	41.5	35.9	23.3	79.7	32.3	51.1	70.6	32.1	45.1	33.7	54.3	50.9	45.8
Neck Beta	17.4	23.3	16.7	16.8	15.5	14.3	13.2	16.4	19.6	16.9	15.7	17.3	13.6	18.6	18.3	15.1

Table 14 (continued)

Generalization Dataset 2				
Joint	Subject 1	Subject 13	Subject 17	Subject 18
Left Ankle Alpha	11.1	9.4	7.0	8.1
Left Ankle Beta	7.2	5.5	4.9	11.1
Right Ankle Alpha	16.4	54.9	15.6	15.1
Right Ankle Beta	9.6	7.6	4.2	4.7
Left Knee Alpha	35.5	18.0	19.7	18.2
Left Knee Beta	7.1	7.6	6.9	8.0
Right Knee Alpha	29.8	30.1	60.3	76.4
Right Knee Beta	5.7	6.7	6.4	7.0
Left Hip Alpha	33.3	48.9	61.2	121.1
Left Hip Beta	46.6	20.7	40.9	39.6
Right Hip Alpha	16.8	22.2	77.1	120.3
Right Hip Beta	14.3	9.0	9.4	12.3
Left Lower Torso Alpha	15.0	12.4	12.3	15.5
Left Lower Torso Beta	6.3	7.0	6.8	4.5
Right Lower Torso Alpha	23.6	21.5	18.2	19.4
Right Lower Torso Beta	4.1	4.2	5.6	7.2
Upper Torso Alpha	58.0	56.9	103.7	128.6
Upper Torso Beta	16.8	14.8	10.6	13.3
Left Clavicle Alpha	17.3	20.7	15.2	21.1
Left Clavicle Beta	11.9	8.3	7.6	11.3
Right Clavicle Alpha	18.5	16.4	18.6	17.0
Right Clavicle Beta	8.0	5.5	8.2	10.7
Left Shoulder Alpha	119.1	114.8	149.2	153.5
Left Shoulder Beta	35.4	29.0	29.7	33.6
Right Shoulder Alpha	127.0	95.1	72.0	73.7
Right Shoulder Beta	36.9	31.7	31.4	36.6
Left Elbow Alpha	15.4	18.3	15.6	17.1
Left Elbow Beta	24.0	22.2	23.8	26.1
Right Elbow Alpha	24.9	31.7	26.0	76.8
Right Elbow Beta	22.4	22.8	27.3	27.4
Left Wrist Alpha	22.5	19.7	20.5	14.1
Left Wrist Beta	18.3	21.8	15.8	15.0
Right Wrist Alpha	20.8	33.0	26.0	19.4
Right Wrist Beta	20.7	21.2	13.9	12.8
Neck Alpha	47.3	36.5	47.7	71.3
Neck Beta	14.7	20.1	16.7	11.5

Table 14 (continued)

Joint	Generalization Dataset 3			
	Subject 1	Subject 13	Subject 17	Subject 18
Left Ankle Alpha	10.9	7.7	7.8	11.4
Left Ankle Beta	6.3	4.5	7.6	3.1
Right Ankle Alpha	13.8	15.0	14.9	9.9
Right Ankle Beta	9.5	2.7	5.2	2.8
Left Knee Alpha	25.1	26.4	34.1	31.1
Left Knee Beta	6.2	8.2	7.6	6.5
Right Knee Alpha	71.1	90.3	86.8	46.2
Right Knee Beta	7.2	7.0	6.1	4.0
Left Hip Alpha	32.8	47.1	126.2	54.3
Left Hip Beta	8.0	21.1	12.3	5.1
Right Hip Alpha	16.7	16.8	112.9	36.5
Right Hip Beta	11.8	9.2	12.7	10.0
Left Lower Torso Alpha	11.5	10.6	18.2	13.6
Left Lower Torso Beta	6.6	7.4	5.9	6.1
Right Lower Torso Alpha	19.6	18.6	26.5	18.8
Right Lower Torso Beta	2.8	4.9	5.3	7.4
Upper Torso Alpha	61.5	52.7	156.9	59.4
Upper Torso Beta	20.2	17.3	18.5	21.9
Left Clavicle Alpha	19.4	14.2	23.1	14.2
Left Clavicle Beta	9.2	6.8	13.3	5.8
Right Clavicle Alpha	15.8	15.8	22.2	12.3
Right Clavicle Beta	6.3	5.6	9.2	5.8
Left Shoulder Alpha	117.3	157.0	166.4	135.4
Left Shoulder Beta	22.8	19.7	24.7	18.5
Right Shoulder Alpha	152.7	71.9	105.9	38.7
Right Shoulder Beta	24.1	16.9	24.7	17.7
Left Elbow Alpha	15.1	15.4	17.3	16.6
Left Elbow Beta	20.4	21.8	23.9	23.5
Right Elbow Alpha	29.9	28.9	80.3	28.8
Right Elbow Beta	20.4	25.7	24.0	27.2
Left Wrist Alpha	22.8	21.4	18.0	17.4
Left Wrist Beta	22.3	14.5	14.1	19.0
Right Wrist Alpha	25.5	29.2	20.5	18.1
Right Wrist Beta	25.2	15.6	17.3	15.6
Neck Alpha	32.3	26.2	58.0	32.8
Neck Beta	15.8	22.9	14.5	15.8

Table 15. Prediction root mean square errors by movement location and joint. *Italicized values are separated from the mean error for each joint by more than two standard deviations. LL-Lower Location, MLL-Middle Lower Location, ML-Middle Location, MUL-Middle Upper Location, UL-Upper Location. Locations combine errors for both Deliver and Bring Back movements, since only static postures are considered. The table is continued on the next three pages.*

Joint	Training Dataset																	
	No Rotation						Medium Rotation						High Rotation					
	LL Near	ML Near	UL Near	LL Far	ML Far	UL Far	LL Near	ML Near	UL Near	LL Far	ML Far	UL Far	LL Near	ML Near	UL Near	LL Far	ML Far	UL Far
Left Ankle Alpha	6.51	5.94	7.16	12.95	11.13	8.82	7.69	6.66	8.9	12.56	12.18	27.06	7.58	7.54	6.48	7.98	6.95	11.92
Left Ankle Beta	4.55	3.71	5.47	7.88	4.35	4.07	5.18	4.01	10.79	9.02	<i>13.51</i>	<i>21.75</i>	5.1	4.98	6.56	8.11	6.57	<i>14.72</i>
Right Ankle Alpha	14.94	8.95	10.49	29.36	13.25	9.79	19.5	11.62	12.98	15.04	13.99	13.08	63.22	20.16	22.75	44.26	22.41	21.44
Right Ankle Beta	9.17	5.07	7.8	<i>12.91</i>	5.99	5.19	<i>11.58</i>	3.9	4.06	7.21	5.19	5.73	<i>11.22</i>	4.3	5.6	6.02	5.23	4.93
Left Knee Alpha	47.46	15.17	19.74	27.11	28.56	17.23	26.93	18.29	18.35	28.92	23.27	24.89	36.77	19.59	18.53	27.86	20.13	22.21
Left Knee Beta	9.99	3.52	4.2	11.35	5.46	4.77	9.24	4.79	6.01	11.23	8.81	10.17	12.48	5.11	5.52	11.31	7.96	6.46
Right Knee Alpha	19.22	16.92	19.31	22.67	38.54	20.67	48.87	35.5	31.68	72.4	71.02	58.84	67.36	69.87	67.61	91.96	70.9	64.21
Right Knee Beta	14.21	3.52	5.97	<i>15.6</i>	5.48	4.08	<i>15.21</i>	4.82	4.59	11.43	4.56	4.74	14.36	3.54	4.67	9.33	6.16	4.58
Left Hip Alpha	52.34	89.83	75	34.01	95.26	<i>122.42</i>	61.08	99.33	90.97	46.26	93.39	111.38	70.48	75.96	71.35	59.18	70.94	77.45
Left Hip Beta	62.08	5.08	4.21	<i>115.18</i>	5.41	4.75	<i>80.38</i>	4.62	5.09	42.78	5.92	7.35	44.77	3.9	4.95	52.67	5.77	5.24
Right Hip Alpha	47.24	80.31	92.6	33.41	110.31	<i>133.26</i>	42.34	95.94	94.56	34.94	44.26	57.62	58.28	84.89	73.85	58.17	88.15	74.61
Right Hip Beta	19.27	5.02	4.22	17.37	6.53	4.9	15.5	5.17	5.32	17.42	7.18	5.5	15.76	5.57	5.41	14.58	17.12	5.03
Left Lower Torso Alpha	38.2	16.27	17.19	26.33	18.35	17.3	21.6	14.82	16	23.76	13.68	13.42	25.01	19.32	18.16	20.66	19.92	17.36
Left Lower Torso Beta	11.14	6.24	7.2	9.8	6.33	6.59	9.62	5.79	6.68	8.51	6.07	6.11	10.12	6.89	6.03	9.62	10.62	6.64
Right Lower Torso Alpha	27.7	18.62	18.79	30.01	15.29	19.93	22.15	22.1	25.08	28.12	26.54	25.12	27.34	17.66	19.98	20.33	33.9	22.13
Right Lower Torso Beta	<i>10.86</i>	5.91	6.14	<i>10.49</i>	5.93	5.93	8.74	5.47	5.91	8.55	6.11	7.03	9.97	6.41	7.49	<i>11.01</i>	7.43	8.41
Upper Torso Alpha	58.75	112.3	121.81	32.69	52.8	78.33	53.98	74.56	118.09	48.56	55.27	79.16	54.57	81.46	138.44	53.29	76.57	132.18
Upper Torso Beta	30.87	7.39	5.88	18	9.92	6.57	15.11	6.69	7.36	14.64	13.02	6.59	15.87	6.91	6.72	12.51	28.46	6.41
Left Clavicle Alpha	27.96	10.69	11.57	17.14	14.61	11.98	17.41	24.39	20.97	13.96	24.2	20.8	22.03	15.07	13.38	17.78	14.7	14.96
Left Clavicle Beta	13.87	6.23	6.45	11.36	6.4	6.24	10.3	5.06	8.76	10.51	7.66	11.26	11.06	6.06	8.11	10.46	6.38	8.92
Right Clavicle Alpha	21.56	17.08	13.95	14.95	12.91	12.61	17.14	19.81	24.48	11.33	21.63	23.36	20.54	10.17	17.17	17.8	13.04	16.5
Right Clavicle Beta	12.57	5.25	6.33	<i>16.79</i>	6.96	6.07	10.27	4.68	6.72	9.41	5.68	7.49	9.32	5.04	7.27	9.57	7.76	5.91
Left Shoulder Alpha	138.57	170.88	181.89	121.06	145.33	156.22	145.62	150.96	163.72	131.77	150.96	150.51	116.5	168.62	165.94	110.09	164.88	164.06
Left Shoulder Beta	18	23.39	32.88	22.12	23.94	20.96	25.64	18.53	<i>61.7</i>	17.87	18.63	<i>60.5</i>	23.34	25.51	45.04	19.12	17.96	41.71
Right Shoulder Alpha	105.7	66.1	44.12	125.4	61.64	38.24	90.42	62.92	39.79	72.84	50.93	45.27	99.44	57.7	47.05	93.87	76.53	47.65
Right Shoulder Beta	17.2	23.98	33.88	22.43	25.02	20.55	27.05	17.53	<i>63.36</i>	17.78	18.03	<i>61.99</i>	21.06	30.09	50.87	18.79	19.48	46.8
Left Elbow Alpha	14.4	13.83	16.73	11.7	14.66	12.64	12.64	21.79	25.68	9.89	19.23	22.22	16.82	13.46	18.27	14.44	12.48	18.02
Left Elbow Beta	21.8	19.99	26.04	18.96	22.38	18.25	22.17	15.42	<i>46.34</i>	15.73	15.93	<i>43.73</i>	22.31	23.16	36.59	14.81	18.96	32.29
Right Elbow Alpha	12.2	12.58	14.67	12.81	14.3	13.1	12.3	29.32	27.98	12.8	28.7	24	47.07	68.36	83.65	87.51	62.55	<i>97.21</i>
Right Elbow Beta	25.5	19.3	26.12	18.54	21.1	17.81	23.38	15.33	<i>48.7</i>	17.13	16.63	<i>47.42</i>	25.23	23.1	40.1	19.29	19.38	37
Left Wrist Alpha	17.53	21	26.92	15.87	20.38	19.63	13.84	22.22	<i>31.01</i>	15.93	20.47	24.66	23.53	17.04	26.74	15.31	18.23	<i>36.09</i>
Left Wrist Beta	20.79	13.77	20.44	22.61	17.33	19.87	22.75	18.85	23.82	16.72	16.98	22.78	21.43	17.03	20.32	19.35	20.81	24.86
Right Wrist Alpha	19.69	16.89	26.64	22.19	21.7	25.4	19.84	36.65	<i>40.98</i>	16.07	34.06	38.22	22.79	20.66	36.28	19.9	25.21	29.45
Right Wrist Beta	19.49	14.53	20.68	20.25	16.55	19.54	21.2	20.41	<i>25.05</i>	16.22	16.61	20.43	21.24	16.4	20.71	17.54	15.79	23.14
Neck Alpha	40.86	32.11	70.36	42.75	40.54	63.66	45.22	27.49	<i>115.2</i>	26.84	28.39	<i>109.36</i>	35.36	29.39	92.61	31.34	24.9	94.32
Neck Beta	26.91	8.25	9.64	20.84	9.22	9.48	20.42	9.02	11.74	17.14	10.92	11.44	19.27	9.33	11.11	14.13	18.61	11.57

Table 15 (continued)

Joint	Generalization Dataset 1											
	No Rotation				Medium Rotation				High Rotation			
	MLL Near	MUL Near	MLL Far	MUL Far	MLL Near	MUL Near	MLL Far	MUL Far	MLL Near	MUL Near	MLL Far	MUL Far
Left Ankle Alpha	5.43	6.85	7.5	5.83	6.81	6.33	10.12	13.78	7.13	6.51	6.87	6.29
Left Ankle Beta	4.18	4.11	7.08	2.6	4.29	3.71	6.78	14.8	5.38	4.31	6.11	5.79
Right Ankle Alpha	11.3	9.91	36.57	10.78	16.34	14	15.11	14.85	24.23	21.2	21.62	21.84
Right Ankle Beta	5.05	4.19	13.77	4.6	3.73	3.81	5.5	5.37	4.75	5.13	6.59	5.34
Left Knee Alpha	71.32	16.46	30.3	15.65	26.48	16.73	30.01	23.07	53.33	18.27	28.47	20.65
Left Knee Beta	7.57	5	11.85	4.18	5.9	4.53	8.04	8.85	13.67	4.98	11.9	5.7
Right Knee Alpha	20.56	23.18	42.01	20.44	71.36	30.03	65.95	69.05	92.8	67.74	105.89	67.68
Right Knee Beta	8.65	3.95	22.94	4.43	5.43	4.88	6.23	4.4	6.69	3.68	7.39	4.95
Left Hip Alpha	43.87	89.11	69.91	102.97	72.4	85.29	91.75	89.74	74.06	91.39	82.94	76.69
Left Hip Beta	13.18	5.59	59.87	5.01	9.88	5.29	6.92	5.81	6.37	4.39	5.67	4.86
Right Hip Alpha	50.78	100.74	51	99.15	53.6	109.32	45.92	53.69	53.71	81.4	62.01	78.74
Right Hip Beta	12.98	5.56	23.05	5.5	12.03	5.33	16.4	6.08	22.33	5.47	21.48	4.67
Left Lower Torso Alpha	28.17	16.23	22.57	16.84	12.61	19.9	15.65	13.76	20.61	17.66	16.86	17
Left Lower Torso Beta	7.14	6.33	8.95	6.79	7.63	6.62	8.7	6.54	15.36	6.56	13.91	6.98
Right Lower Torso Alpha	23.36	19.07	22.21	17.97	38.57	22.25	32.04	23.94	36.26	15.41	29.69	18.55
Right Lower Torso Beta	6.8	5.65	8.75	6.08	6.45	6.18	8.2	6.77	9.47	6.75	8.24	7.61
Upper Torso Alpha	58.79	116.27	50.8	76.42	60.53	127.51	54.7	65.51	45.67	124.21	59.11	112.45
Upper Torso Beta	36.4	6.82	26.74	6.04	34.87	7.58	25.75	6.4	24.36	7.22	19.4	7.05
Left Clavicle Alpha	19.59	10.46	17.55	13.71	23.89	25.17	17.5	27.17	20.5	14.25	15.6	17.09
Left Clavicle Beta	11.65	5.89	12.95	5.42	12.22	5.52	9.79	7.21	12.32	6.95	10.08	6.65
Right Clavicle Alpha	19.6	14.47	15.77	14.57	25.88	19.09	17.28	18.91	20	10.59	15.53	11.17
Right Clavicle Beta	9.16	6.07	8.87	6.08	11.37	5.12	9.09	4.8	7.22	6.04	6.77	6.26
Left Shoulder Alpha	153.62	181.6	149.19	161.85	130.46	160.01	149.72	158.47	133.27	167.92	138.82	169.68
Left Shoulder Beta	23.17	30.46	26.18	30.1	14.86	36.95	15.25	38.55	21.4	23.36	18.38	23.34
Right Shoulder Alpha	123.42	58.12	121.43	52.52	95.09	45.08	57.71	52.68	98.58	53.48	89.86	59.13
Right Shoulder Beta	23.3	31.25	24.81	31.16	14.67	36.31	15.99	39.99	20.82	23.74	17.21	24.15
Left Elbow Alpha	17.48	12.91	21.33	14.63	18.32	24.24	17.87	19.68	15.63	15.48	14.6	10.97
Left Elbow Beta	28.55	30.16	27.32	23.16	26.67	27.99	19.47	26.02	18.11	23.76	14.59	18.51
Right Elbow Alpha	13.81	14.6	20.01	12.01	26.41	28.53	22.96	32.94	89.64	55.06	87.25	64.12
Right Elbow Beta	29.24	30.23	24.55	22.88	27.56	32.21	20.47	30.78	23.27	28.34	17.63	21.19
Left Wrist Alpha	23.17	16.03	21.87	17.67	18.75	28.52	16.05	24.76	18.86	21.61	18.49	18.26
Left Wrist Beta	17.14	19.25	22.84	19.91	22	17.38	22.95	17.93	21.45	16.99	21.22	15.95
Right Wrist Alpha	15.26	24.99	23.07	22.9	36.89	32.7	31.16	32.94	25.69	20.87	24.43	16.67
Right Wrist Beta	16.24	19.81	21.44	19.53	21.7	17.85	22.25	13.86	22.27	17.8	21.85	17.57
Neck Alpha	51.12	84.17	39.12	60.87	30.13	46.68	27.76	50.54	36.18	44.44	33.29	47.42
Neck Beta	32.17	9.64	22.85	9.84	23.46	10.98	16.71	12.01	16.3	8.59	15.91	9.94

Table 15 (continued)

Joint	Generalization Dataset 2																	
	No Rotation						Medium Rotation						High Rotation					
	LL Near	ML Near	UL Near	LL Far	ML Far	UL Far	LL Near	ML Near	UL Near	LL Far	ML Far	UL Far	LL Near	ML Near	UL Near	LL Far	ML Far	UL Far
Left Ankle Alpha	11.13	11.51	10.36	9.68	10.36	8.54	8.9	7.89	8.51	10.08	9.44	11.05	12.86	10.44	9.98	11.19	9.61	9.84
Left Ankle Beta	5.58	5.82	4.99	6.8	5.4	6.4	4.16	4.66	6.32	4.6	8.74	15.14	7.74	6.53	6.26	4.8	3.72	6.28
Right Ankle Alpha	14.61	12.94	10.61	15.72	16.25	14.92	14.73	9.92	7.85	10.55	10.62	15.15	102.47	16.15	15.18	23.76	23.77	20.06
Right Ankle Beta	8.05	5.56	5.58	7.25	5.43	5.71	6.41	5.7	6.06	5.86	5.94	5.15	7.21	5.96	6.68	5.93	5.53	5.45
Left Knee Alpha	16.01	8.73	8.43	21.14	8.96	8.67	14.73	17.91	10.34	16.58	26.25	22.43	75.75	9.55	14.52	19.7	17.94	12.9
Left Knee Beta	10.46	2.71	3.37	13.3	4.89	3.72	8.3	4.24	4.25	5.94	5.88	7.11	14.8	3.46	3.56	4.53	5.99	4.23
Right Knee Alpha	11.54	12.38	13.28	14.81	16.53	26.51	26.16	39.36	30.17	37.95	63.17	49.91	78.83	78.65	66.66	44.66	94.24	49.46
Right Knee Beta	13.57	1.91	3.47	10.05	4.97	4.69	4.79	5.02	4.56	8.41	4.92	3.59	9.73	2.63	3.18	7.12	6.02	3.21
Left Hip Alpha	41.11	65.87	76.68	36.72	75.77	94.08	62.55	63.84	68.01	34.71	66.46	99.57	100.4	60.6	91.27	23.62	75.97	51.84
Left Hip Beta	51.25	5.86	5.25	145.92	3.92	4.12	19.69	3.24	3.65	15.15	4.33	5.04	19.21	4.98	4.06	12.74	5.48	4.45
Right Hip Alpha	59.27	105.22	109.75	41.51	111.11	66.55	41.19	30.74	73.75	26.22	20.41	35.65	51.18	117.98	56.15	27.76	48.33	87.03
Right Hip Beta	21.45	5.37	5.09	26.61	5.71	4.78	10.75	4.7	6.09	8.21	6.15	6.14	7.2	4.66	5.25	7.35	17.1	3.81
Left Lower Torso Alpha	10.7	9.6	6.35	22.76	13.59	10.44	17.76	15.65	14.31	14.72	8.01	9.48	13.61	14.89	13.07	10.37	15.89	14.12
Left Lower Torso Beta	9.32	2.67	3.48	10.07	3.18	3.28	6.41	3.08	3.83	4.98	4.51	5.76	9.54	3.75	3.16	7.45	10.09	5.05
Right Lower Torso Alpha	28.44	13	12.59	30.82	13.77	14.16	24.42	21.98	18.3	18.14	34.77	27.63	19.27	13.09	10.25	10.23	19.68	13.68
Right Lower Torso Beta	7.18	3.99	4.41	9.18	3.06	3.56	8.01	3.02	4.69	6.08	5.93	8.18	7.77	4.56	5.54	5.38	4.28	6.28
Upper Torso Alpha	44.03	89.05	134.27	53.28	32.03	72.42	56.5	95.28	142.87	52.01	72.95	82.54	58.34	106.4	146.23	24.2	68.7	133.01
Upper Torso Beta	32.09	7.57	7.53	23.09	7.51	6.35	10.2	6.53	8.58	9.55	15.77	6.44	7.57	6.52	6.67	7.89	31.49	7.48
Left Clavicle Alpha	15.37	8.15	8.64	10.91	11.41	9.14	20.52	26.49	23.99	17.47	26.39	19.59	24.7	14.23	15.01	17.32	14.82	17.24
Left Clavicle Beta	10.2	3.88	6.59	16.53	2.31	7.46	9.78	3.48	9.36	15.66	9.99	10.37	12.67	5.49	6.66	12.16	6.94	6.91
Right Clavicle Alpha	17.14	14.77	16.94	11.27	16.94	14.8	21.93	18.3	21.12	13.8	22.84	19.44	24.95	9.84	14.87	16.25	10.3	14.39
Right Clavicle Beta	14.47	2.13	9.13	13.31	4.01	7.86	11.57	4.23	4.65	5.2	8.36	6.85	6.04	5.25	5.12	4	8.5	5.58
Left Shoulder Alpha	113.67	164.32	158.65	130.76	110.71	163	149.01	133.78	152.01	101.03	129.07	138.77	93.44	143.35	170.83	82.78	132.33	170.36
Left Shoulder Beta	14.35	17.39	51.18	17.73	15.29	31.57	12.34	13.88	56.98	15.89	17.29	56.35	15.21	23.32	35.31	13.08	11.14	32.93
Right Shoulder Alpha	153.9	113.92	75.43	171.42	102.26	45.05	81.37	61.94	37.12	70.64	78.25	44.9	51.41	113.88	46.65	54.1	46.93	61.72
Right Shoulder Beta	10.42	15.2	51.44	15.79	13.6	31.4	16.94	13.25	59.62	15.1	16.94	59.34	13.28	31.18	43.41	14.9	18.1	39.14
Left Elbow Alpha	8.83	11.39	17.24	10.44	14.24	16.88	13.7	22.53	27.18	11.36	19.5	22	18.8	11.3	15.2	13.45	12.39	15.33
Left Elbow Beta	25.3	15.42	42.49	18.15	12.41	23.83	11.14	17.44	39.55	13.4	17	38.2	10.99	24.63	31.38	12.4	19.58	27.16
Right Elbow Alpha	8.6	5.61	8.86	11.52	12.69	12.22	12.07	30.86	25.9	17.39	31	29.19	96.55	92.52	88.81	30.78	46.34	38.5
Right Elbow Beta	22.56	15.01	41.08	16.55	11.36	24.6	15.41	14.65	43.05	17.83	15.25	41.67	20.71	24.15	33.39	18.94	18.28	32.12
Left Wrist Alpha	18.29	22.85	16.42	15	19.56	20.67	17.39	23.04	27.42	15.5	19.84	23.35	24.96	15.74	15.86	22.79	17.1	19.99
Left Wrist Beta	21.12	12.19	15.07	21.63	12.98	11.59	17.68	15.07	18.07	15.95	14.97	23.89	16.31	25.91	18.36	16.68	18.64	19.37
Right Wrist Alpha	16.77	14.19	18.67	20.47	14.86	21.57	12.59	33.47	32.27	25.27	36.6	34.07	19.04	20.71	16.3	17.19	16.38	11.36
Right Wrist Beta	19.58	4.47	15.48	16.35	17.19	16.63	13.56	16.07	18.57	17.81	12.96	18.99	12.36	15.86	14.45	12.88	16.81	18.21
Neck Alpha	32.99	21.53	57.45	39.18	14.35	75.42	40.31	29.1	81.25	31.49	33.94	106.85	33.92	17.87	72.53	22.68	25	78.39
Neck Beta	24.4	7.03	11.98	28.71	12.75	10.76	16.26	9.82	13.67	15.13	13.26	12.98	8.49	3.4	11.1	15.41	24.24	10.87

Table 15 (continued)

Joint	Generalization Dataset 3											
	No Rotation				Medium Rotation				High Rotation			
	MLL Near	MUL Near	MLL Far	MUL Far	MLL Near	MUL Near	MLL Far	MUL Far	MLL Near	MUL Near	MLL Far	MUL Far
Left Ankle Alpha	10.82	8.77	8.38	8.84	9.15	7.88	9.61	8.9	11.79	10.28	12.23	9.54
Left Ankle Beta	6.15	6.28	3.48	2.98	4.05	4.24	4.74	10.53	7.23	6.39	5.27	3.42
Right Ankle Alpha	9.51	11.83	10.58	8.57	9.63	12.37	9.13	5.56	21.37	15.04	21.1	18.15
Right Ankle Beta	5.59	5.12	6.37	4.67	5.44	7.63	6.16	5.72	6.01	6.13	5.66	5.77
Left Knee Alpha	62.56	7.28	62.43	8.09	19.13	11.67	26.71	29.25	17.07	8.16	20.15	12.06
Left Knee Beta	8.04	5.72	10.63	4.48	4.8	4.23	7.98	5.96	10.58	3.4	10.31	3.77
Right Knee Alpha	82.8	11.98	66.16	14.13	77.76	84.3	98.23	68.04	108.58	65.97	90.27	70.49
Right Knee Beta	5.9	3.92	12.68	2.86	6.36	5.67	7.94	3.2	5.86	2.58	5.6	3.3
Left Hip Alpha	82.26	71.88	53.44	85.56	51.38	71.85	62.23	116.73	92.75	89.45	54.32	60.83
Left Hip Beta	7.28	4.83	38.02	4.76	7.09	3.4	5.01	4.2	5.05	4.2	6.71	4.05
Right Hip Alpha	50.42	126.67	23.59	50	39.85	34.04	18.79	23.36	44.61	119.81	32.66	75.71
Right Hip Beta	6.69	4.91	14.44	6.37	10.12	5.52	14.64	4.03	19.94	4.14	19.61	4.62
Left Lower Torso Alpha	20.68	9.25	22.56	9.84	10.98	15.84	10.78	9.12	10.66	14.17	10.52	16.24
Left Lower Torso Beta	6.09	2.96	6.15	2.67	5.8	3.74	6.49	3.82	12.14	3.07	12.1	4.66
Right Lower Torso Alpha	25.9	9.83	16.17	7.76	44.28	14.08	26.13	22.98	22.37	10.29	16.11	9.71
Right Lower Torso Beta	5.03	2.94	4.85	4.5	3.96	4.77	5.5	6.88	7.65	4.99	7.08	5.35
Upper Torso Alpha	60.01	112.74	67.13	111.34	72.94	122.22	42.27	102.43	73.92	129.9	45.34	135.35
Upper Torso Beta	35.97	8.5	30.5	8.4	30.43	8.53	17.69	8.28	23.38	7.25	21.11	6.63
Left Clavicle Alpha	13.75	9.5	19.98	8	25.63	24.72	14.4	27.99	17.51	12.73	11.97	18
Left Clavicle Beta	8.52	4.14	18.48	5.4	7.94	5.05	6.58	8.42	14.61	6.77	11.16	5.51
Right Clavicle Alpha	13.46	20.06	15.02	18.16	26.22	15.87	16.37	16.75	20.37	10.75	12.28	10.84
Right Clavicle Beta	9.48	4.05	9.89	5.88	8.71	3.92	7.72	8.19	4.09	7.52	4.88	5.86
Left Shoulder Alpha	94.87	170.04	160.67	155.63	169.69	134.68	123.16	138.44	80.89	159.4	136.59	158.72
Left Shoulder Beta	16.58	20.59	13.57	33.94	12.19	30.19	13.65	35.41	16.87	16.5	14.15	14.23
Right Shoulder Alpha	168.73	90.86	130.88	98.86	122.15	104.05	101.62	68.14	118.73	38.88	77.32	69.39
Right Shoulder Beta	11.03	18.19	10.96	35.58	12.91	25.57	14.88	37.62	15.16	17.2	15.4	15.95
Left Elbow Alpha	15.91	11.86	13.33	16.88	22.48	23.01	16.45	20.19	11.81	13.52	8.23	11.16
Left Elbow Beta	27.87	32.05	23.82	20.2	30.22	26.01	17.76	18.8	13.14	21.96	12.83	13.54
Right Elbow Alpha	7.62	12.77	21.51	11.96	28.53	29	20.59	33.45	124.1	47.71	81.78	49.01
Right Elbow Beta	25.58	33.02	21.73	21.26	29.94	31.85	18.37	23.02	20.48	24.99	16.22	18.67
Left Wrist Alpha	22.94	13.97	13.08	21.47	18.8	28.77	19.32	24.12	15.07	19.75	15.07	20.45
Left Wrist Beta	16.92	12.5	21.67	18.72	25.99	13.48	17.78	15.56	17.19	17.43	18.86	15.5
Right Wrist Alpha	16.04	23.39	20.07	19.57	36.99	29.77	24.92	30.65	16.98	10.59	15.53	15.63
Right Wrist Beta	18.01	15.05	25.23	22.26	24.62	17.36	19.29	15.68	14.51	17.37	16.26	17.34
Neck Alpha	35.86	16.37	22.88	69.59	35.95	54.46	25.7	63.76	22.31	24.44	21.2	33.83
Neck Beta	28.12	10.18	22.55	15.13	24.87	13.77	21.99	15.11	11.75	6.89	12.04	8.93

Altogether, these errors could sometimes represent substantial deviations from actual postures (Figure 39), presenting possible problems when the postures are introduced on a movement prediction network. Analysis of rmse levels by subject showed relatively close clustering (Table 16). No particular subject appeared to exhibit higher rmse than their peers, including those in the generalization dataset.

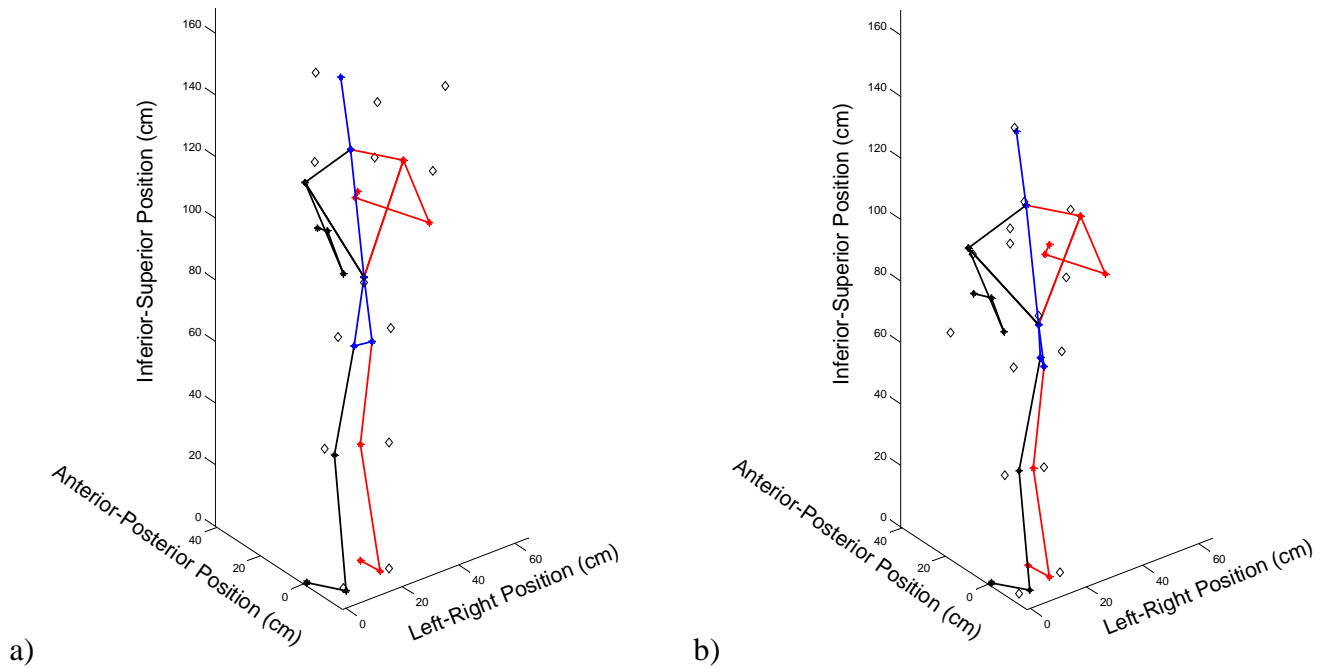


Figure 39. Comparison of predicted posture (stick figure) and actual posture (joint positions are represented by hollow diamonds) for training cases where maximum (a) and minimum (b) rmse levels were observed.

Table 16. Root mean square error (in degrees) by subject, split in training and generalization groups.

	Subject Number	Rmse (degrees)
Training	2	49.21
	3	48.5
	4	45.12
	5	44.06
	6	43.32
	7	39.66
	8	41.52
	9	41.92
	10	40.07
	11	50.89
	12	39.16
	14	43.18
	15	40.23
Generalization	16	47.57
	19	47.09
	20	37.36
	1	48.97
Generalization	13	47.65
	17	48.32
	18	42.58

The 3DSSPP™ predictions had significantly larger error levels than the ANN predictions ($F(1,38)=70.01, p<0.0001$). Across all movement locations and joints, the rmse obtained for the ANN was 25.2°, whereas the rmse for 3DSSPP™ was 37.7°. Significant differences were also detected as a function of the Joint X Model (i.e. ANN or Jack™) and Movement Location X Model interactions ($F(25,456)=83.34, p<0.0001$; $F(29,496)=96.65, p<0.0001$, respectively). While unbalanced data precluded the completion of *post hoc* tests for these interactions, qualitative observations indicate that certain 3DSSPP™ joint predictions, especially for joints in the lower extremities, exhibited disproportionately larger errors (Table 17). The 3DSSPP™ environment was unable to predict a posture for 1.3% of the input box positions, which represented 29 trials. It was not apparent whether these predictions were not calculated due to violation of balance constraints or due to anthropometry assumptions that made the location unreachable by the humanoid.

Table 17. Prediction root mean square errors for the posture prediction network and the 3DSSPP™ simulation environment.

Joint	Rmse (ANN, degrees)	Rmse (3DSSPP™, degrees)
Left Knee Alpha	18.76	71.04
Left Knee Beta	5.65	16.77
Right Knee Alpha	37.07	99.45
Right Knee Beta	5.18	15.22
Left Hip Alpha	57.92	58.58
Left Hip Beta	11.29	37.59
Right Hip Alpha	46.00	62.81
Right Hip Beta	7.93	18.84
Left Lower Torso Alpha	14.21	23.78
Left Lower Torso Beta	5.88	15.24
Right Lower Torso Alpha	18.19	28.39
Right Lower Torso Beta	5.88	14.30
Upper Torso Alpha	59.23	72.56
Upper Torso Beta	11.04	12.80
Left Clavicle Alpha	14.02	25.76
Left Clavicle Beta	6.92	20.32
Right Clavicle Alpha	14.25	21.57
Right Clavicle Beta	5.82	24.17
Left Shoulder Alpha	134.68	169.68
Left Shoulder Beta	20.11	23.67
Right Shoulder Alpha	56.78	51.65
Right Shoulder Beta	20.29	17.32
Left Elbow Alpha	13.32	16.11
Left Elbow Beta	19.06	13.47
Right Elbow Alpha	24.81	35.74
Right Elbow Beta	20.53	13.17

Jack™ rmse levels were also higher than those obtained by the ANN model ($F(1,38)=207.60, p<0.0001$). Across all movement locations and joints, the rmse obtained for the ANN was 22.2°, whereas the rmse for Jack™ was 38.3°. ANOVA also indicated significant differences as a function of the Joint X Model (i.e. ANN or Jack™) and Movement Location X Model interactions ($F(35,646)=299.12, p<0.0001$; $F(29,496)=301.42, p<0.0001$, respectively). While unbalanced data precluded the completion of *post hoc* tests for these interactions, qualitative observations indicate that certain Jack™ joint predictions, especially for joints in the lower extremities and the wrist, exhibited disproportionately larger errors (Table 18).

Table 18. Prediction root mean square errors for the posture prediction network and the JackTM simulation environment.

Joint	Rmse (ANN, degrees)	Rmse (Jack TM , degrees)
Left Ankle Alpha	6.80	8.00
Left Ankle Beta	4.76	10.62
Right Ankle Alpha	13.89	18.91
Right Ankle Beta	4.64	9.91
Left Knee Alpha	18.84	48.06
Left Knee Beta	5.68	8.43
Right Knee Alpha	37.17	60.28
Right Knee Beta	5.21	7.49
Left Hip Alpha	58.07	71.17
Left Hip Beta	11.24	11.39
Right Hip Alpha	45.76	51.11
Right Hip Beta	7.95	9.98
Left Lower Torso Alpha	14.17	20.79
Left Lower Torso Beta	5.87	13.45
Right Lower Torso Alpha	18.28	28.42
Right Lower Torso Beta	5.90	12.95
Upper Torso Alpha	59.01	67.25
Upper Torso Beta	11.04	20.04
Left Clavicle Alpha	14.25	18.42
Left Clavicle Beta	6.95	12.17
Right Clavicle Alpha	14.33	23.67
Right Clavicle Beta	5.83	12.91
Left Shoulder Alpha	135.02	154.11
Left Shoulder Beta	20.48	19.86
Right Shoulder Alpha	56.50	75.41
Right Shoulder Beta	20.68	18.52
Left Elbow Alpha	13.45	27.29
Left Elbow Beta	19.20	33.95
Right Elbow Alpha	24.91	60.04
Right Elbow Beta	20.76	31.24
Left Wrist Alpha	16.73	149.08
Left Wrist Beta	15.24	23.48
Right Wrist Alpha	19.61	138.39
Right Wrist Beta	14.66	18.51
Neck Alpha	36.14	45.10
Neck Beta	11.44	38.56

7.4 Model characterization

Results were encouraging in that training and generalization datasets appeared to be predicted with similar levels of error and with similar distribution of those errors across joints and target locations. These results suggest that the network developed an ability to generalize, with no noticeable increase in error, to novel participants and movements. This supports the use of these networks as posture prediction tools rather than posture reproduction tools, which indicates that certain posture rules were encoded within the networks. These rules do not

necessarily reflect the motor control mechanisms on which humans act, but rather, take information from all the inputs available to the network. The fact that between-subjects information is being provided, for example, might be allowing the network to adapt to reflect a high-probability posture based on the anthropometric characteristics for the individual. To define the network structure in more detail, plots were created that reflect the sensitivity of the network's output as a function of changes in the network inputs, that is, a representation of the network's transformation function. Before introducing these plots, however, it is important to note that their interpretation should be performed with caution since prediction errors were substantial in many cases. These errors are discussed in more detail later in this section.

Recall that, for two dimensions, seven inputs were provided to the network: two for the location of the end-effector, one for a participant-dependent strength coefficient, and four that represented participant-dependent anthropometry coefficients. Plots can then be created that represent the network's transformation function based on each of these parameters. Note that the vertical axis on these plots is not consistently scaled across the different joint angles. This manipulation is taken to purposefully amplify differences that, although present, would not be visible if all graphs were presented on the same vertical scale. Thus, the reader should be careful in making relative comparisons between different joints. In addition, the plots are based on the complete dataset, rather than on training or generalization subsets of the dataset. This approach was selected to make the plots as representative of overall network performance as possible by including as much data as were available. This action was justified based on the similarity between the levels of prediction error attained for both training and generalization datasets.

For the first plot, only the box location in both axes is manipulated, the remaining inputs are zeroed (Figure 40). Neck angle was not included in the plots since it had no effect on the kinematic chain. The plot shows that the network provided a large importance to the inferior-superior box position, as its change controls the shape of the surface. Some joints show effects on the anterior-posterior box position (e.g. the lower torso), but these are much smaller than those observed for the inferior-superior box position. All of this makes intuitive sense, since the distance over which the anterior-posterior box position was varied in the dataset was relatively small (<0.6 m) and probably required only slight postural adjustments from participants.

Similar surfaces can be drawn as other inputs are modified. For example, observation of the strength input value across the 20 participants indicated that this parameter varied from -4 to

4 (the numbers are unit-less). When the strength input is varied between these limits (-4: Figure 41, 4: Figure 42), and the results are compared with those presented in Figure 40, a trend of increased knee, hip, and torso usage with increased strength becomes apparent. This trend is easier to detect in Figure 43, where a slice of the surfaces has been taken at an anterior-posterior position of 40 cm, the mid-point of the interval.

Similar manipulations can be made to examine the contributions of each of the four anthropometry inputs (Figure 44-Figure 47). Increases in the first anthropometry input increase joint utilization for all joints except the ankle. The second anthropometry input increases joint utilization for the lower limbs and torso, but its effects on the upper limbs are less marked than those observed for the first anthropometry input. The third anthropometry input had only slight effects on joint utilization, while the fourth showed slightly higher joint utilization as it increased, mainly for the upper limb joints.

Considered in conjunction, these plots suggest that the 2-D network utilized the inferior-superior box position as its main input, with the strength and first anthropometry inputs generating joint angle adjustments based on the particular individual being modeled. The anterior-posterior box position slightly affected some angles, but not at the same magnitude of these other factors. The remaining anthropometry inputs seemed dedicated to modulating inter-individual differences in particular segments (e.g. upper limbs) and their influences were smaller than those for the first anthropometry input.

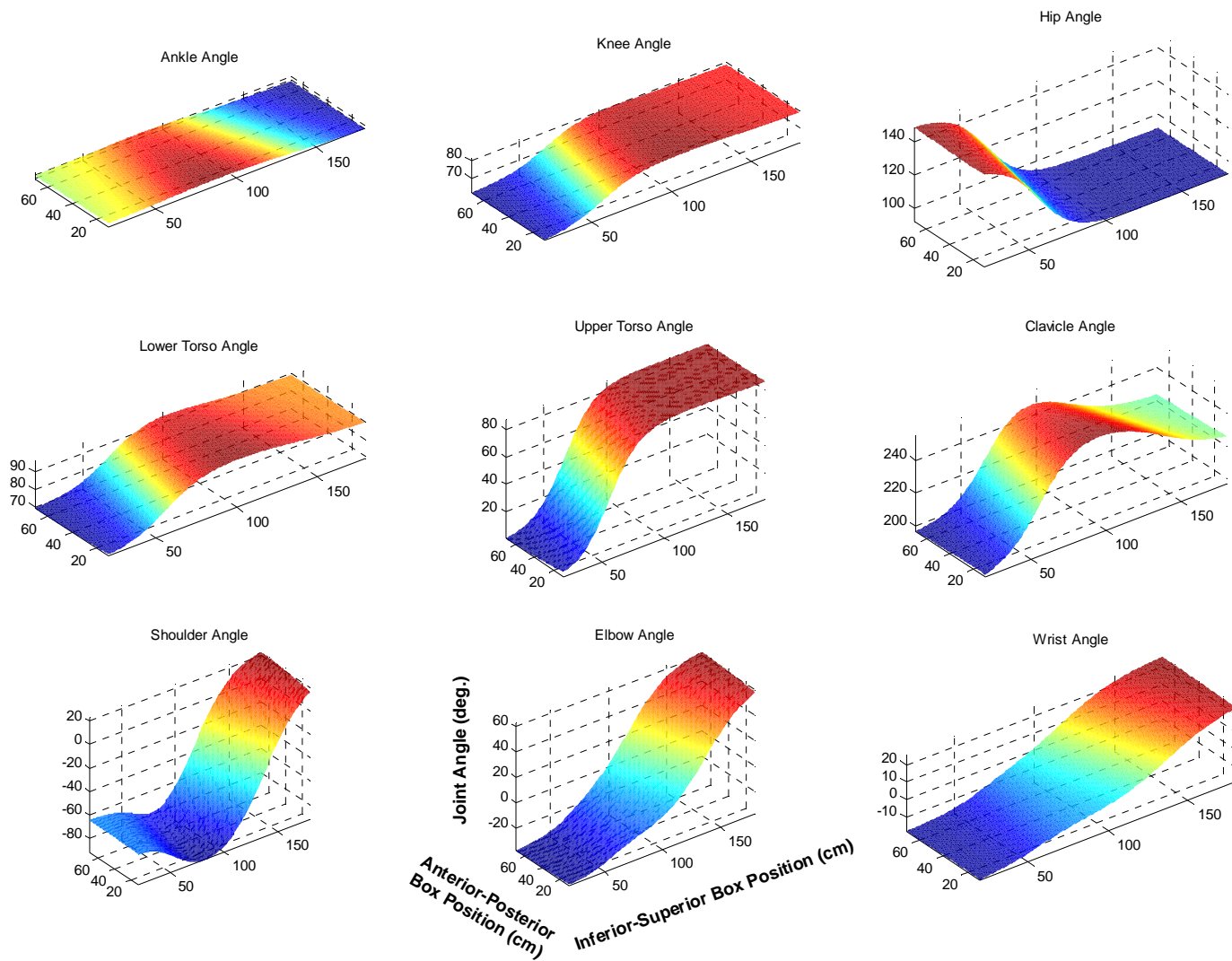


Figure 40. Joint angle predictions as a function of box position.

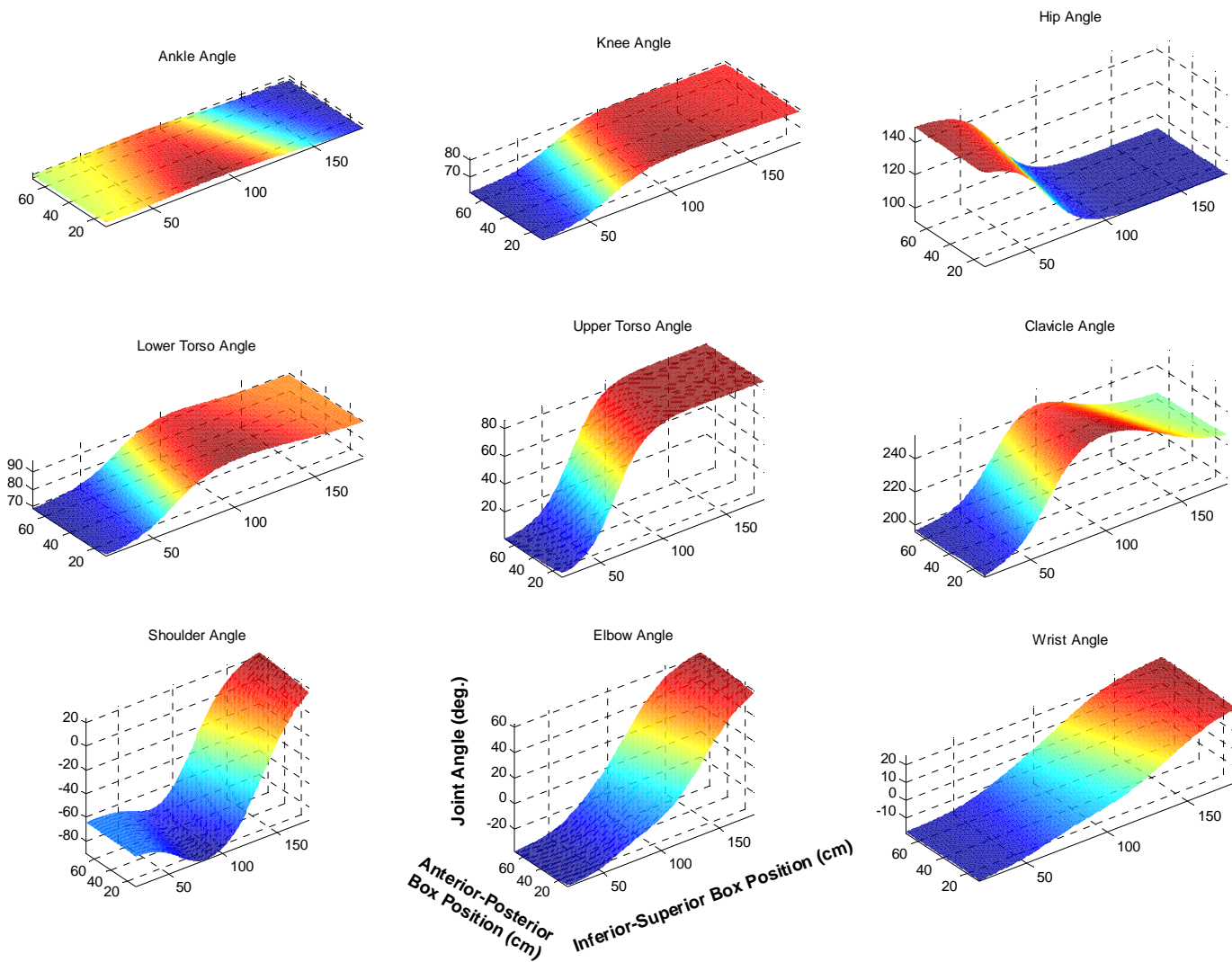


Figure 41. Joint angle predictions as a function of box position with a low strength input.

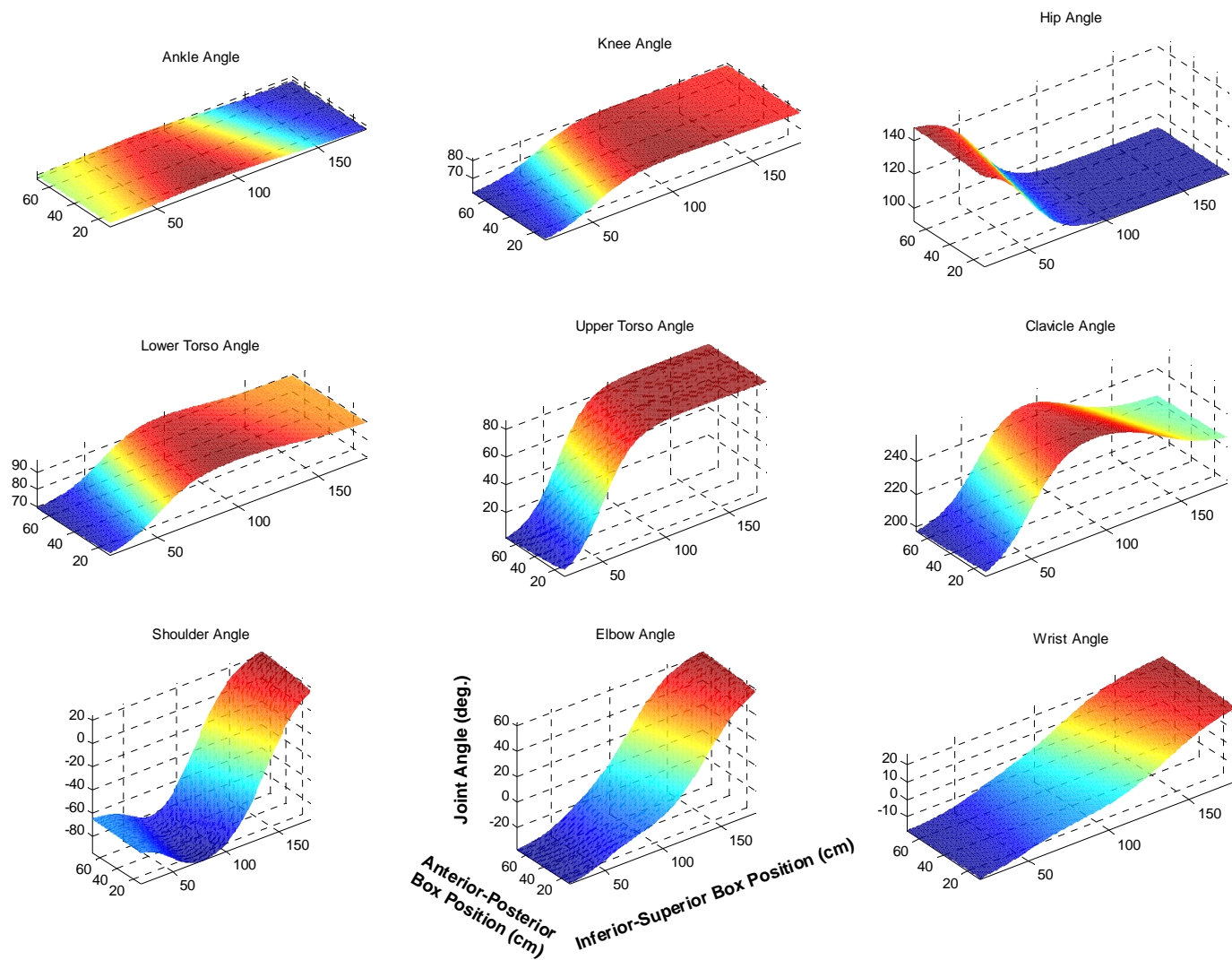


Figure 42. Joint angle predictions as a function of box position with a high strength input.

Joint Angle (deg.)

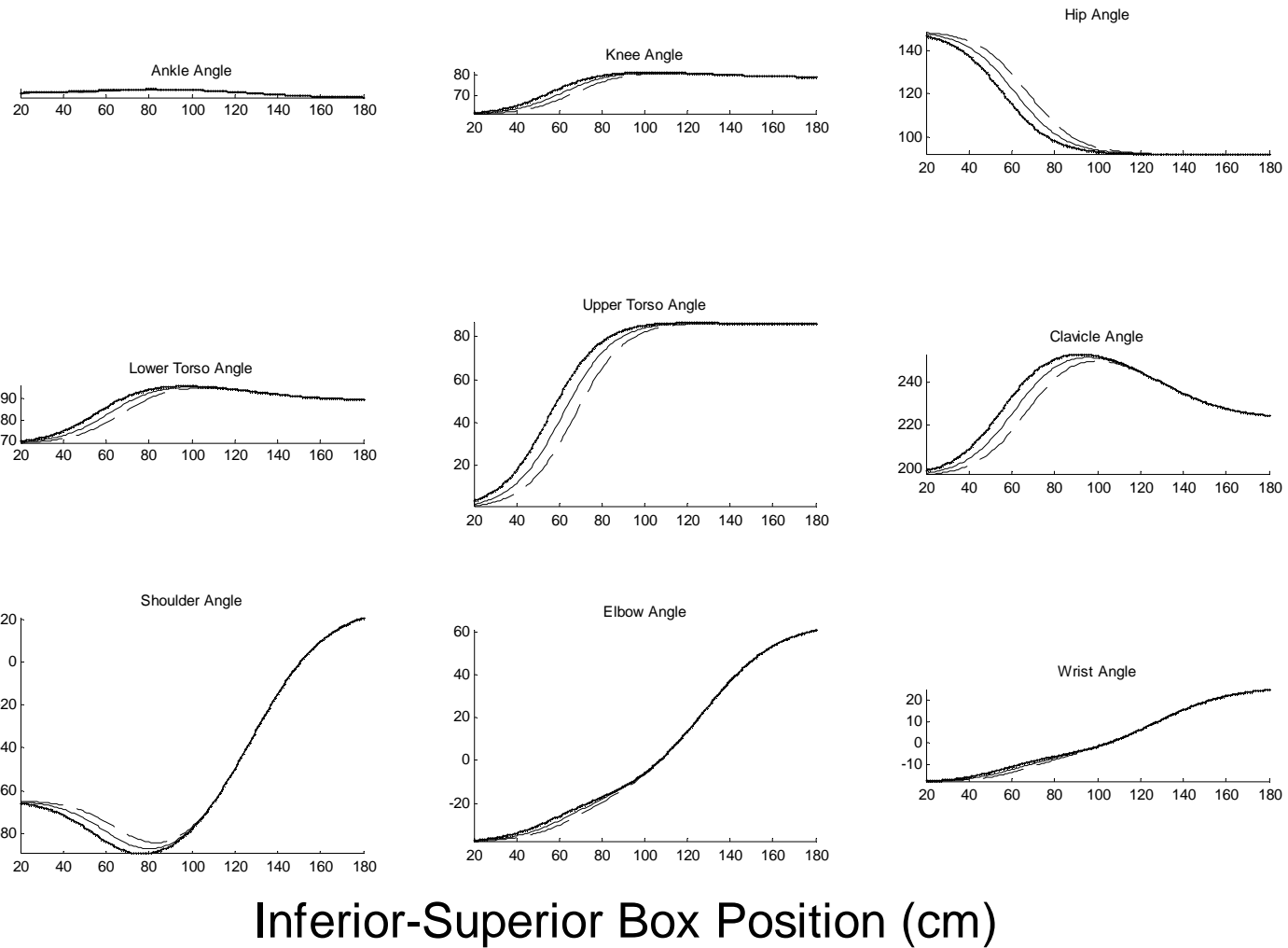


Figure 43. Joint angle predictions as a function of inferior-superior box position. The dashed line represents a low strength input (-4), the solid thin line a neutral strength input (0), and the solid wide line a high strength input (+4).

Joint Angle (deg.)

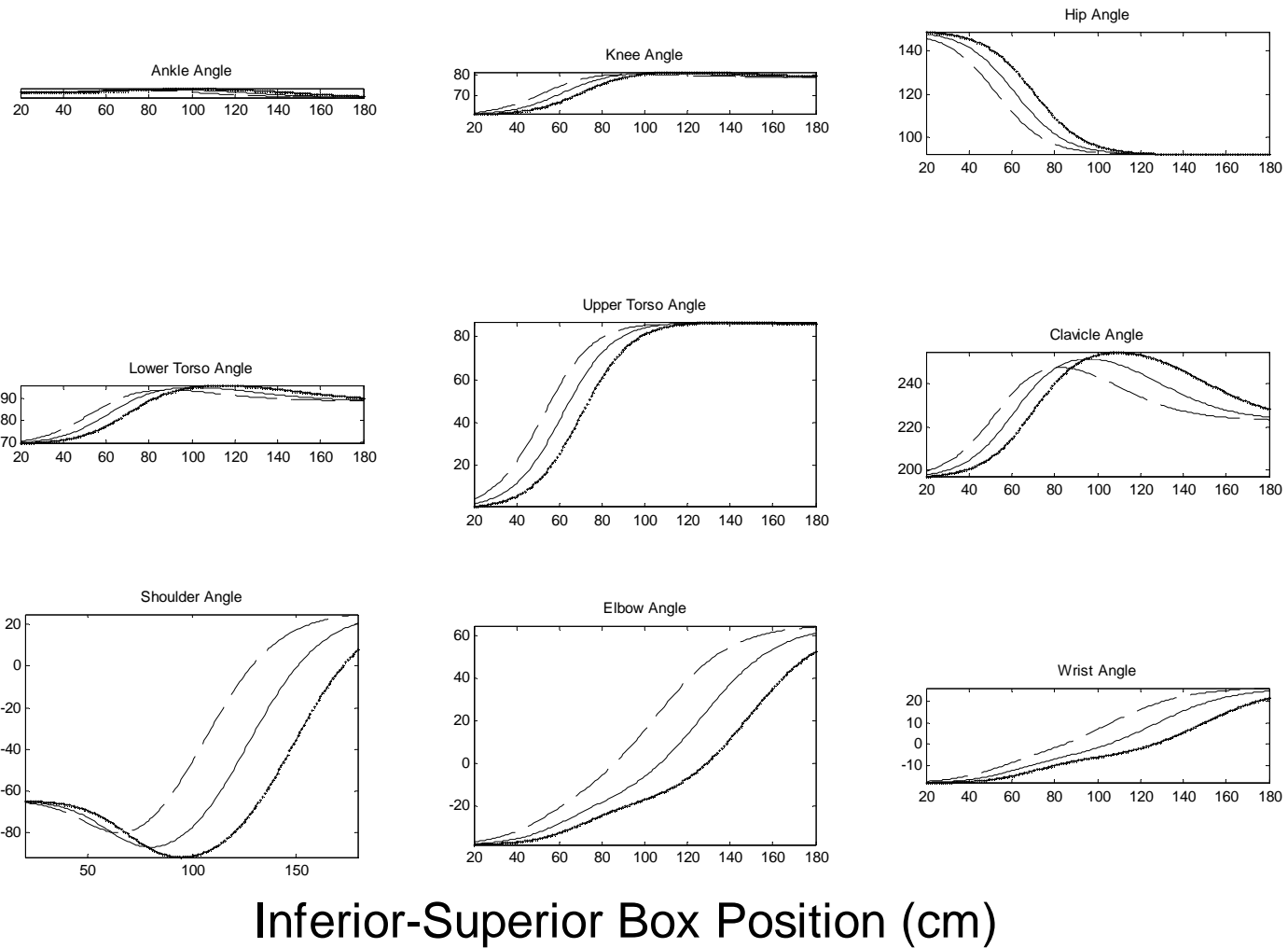


Figure 44. Joint angle predictions as a function of inferior-superior box position. The dashed line represents a low first anthropometry input (-8), the solid thin line a neutral one (0), and the solid wide line a high one (+8).

Joint Angle (deg.)

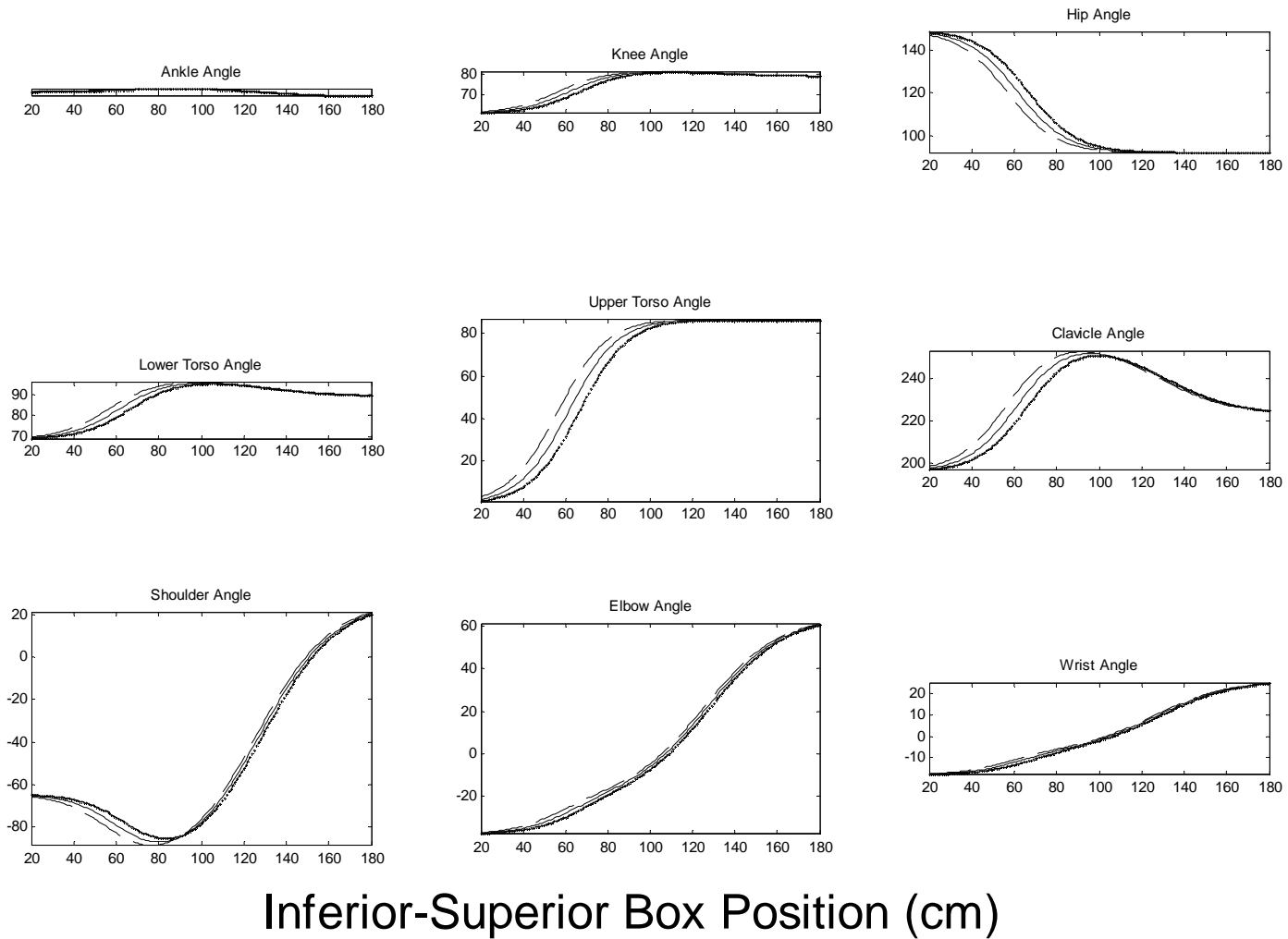


Figure 45. Joint angle predictions as a function of inferior-superior box position. The dashed line represents a low second anthropometry input (-4), the solid thin line a neutral one (0), and the solid wide line a high one (+4).

Joint Angle (deg.)

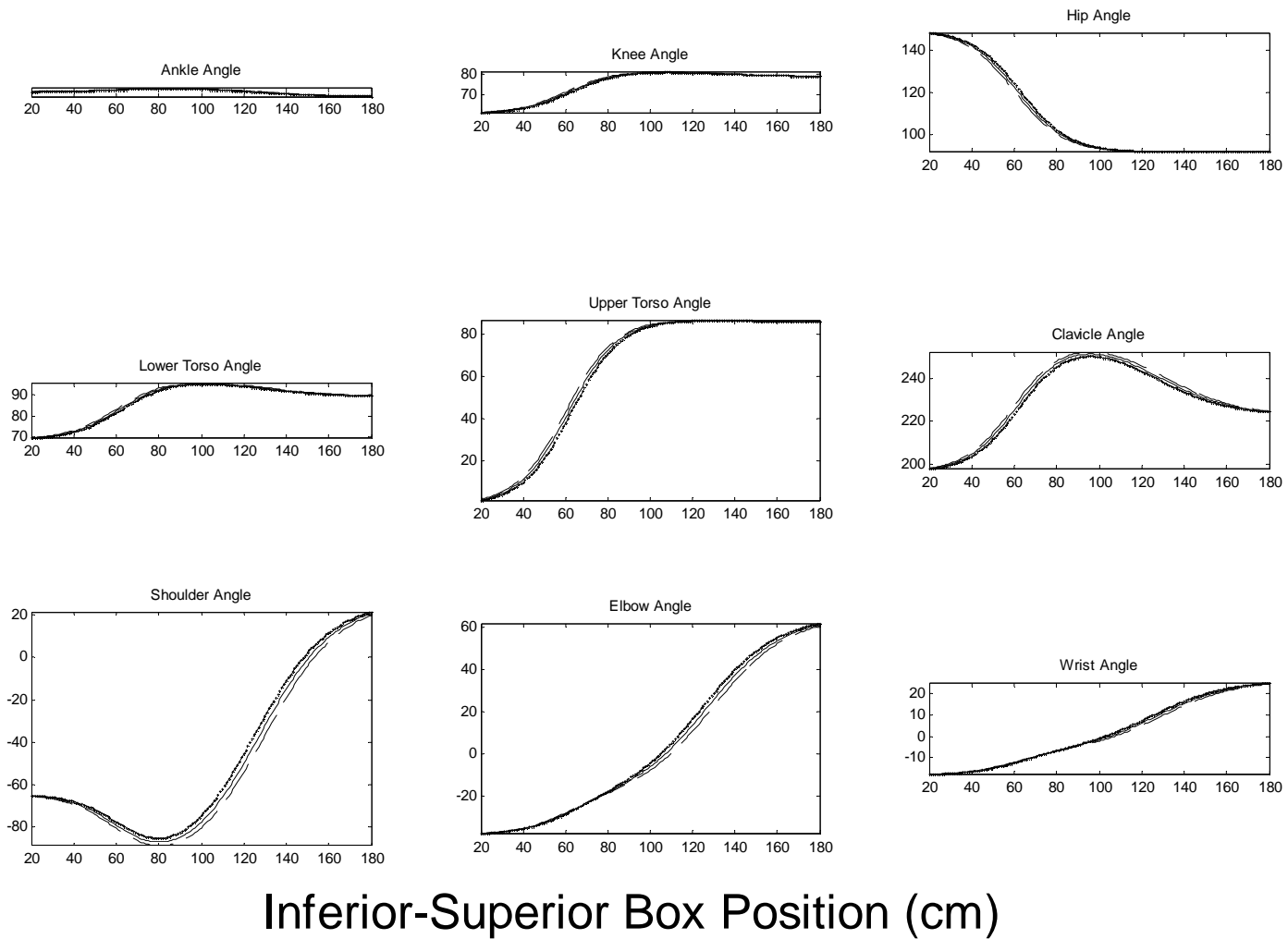


Figure 46. Joint angle predictions as a function of inferior-superior box position. The dashed line represents a low third anthropometry input (-4), the solid thin line a neutral one (0), and the solid wide line a high one (+4).

Joint Angle (deg.)

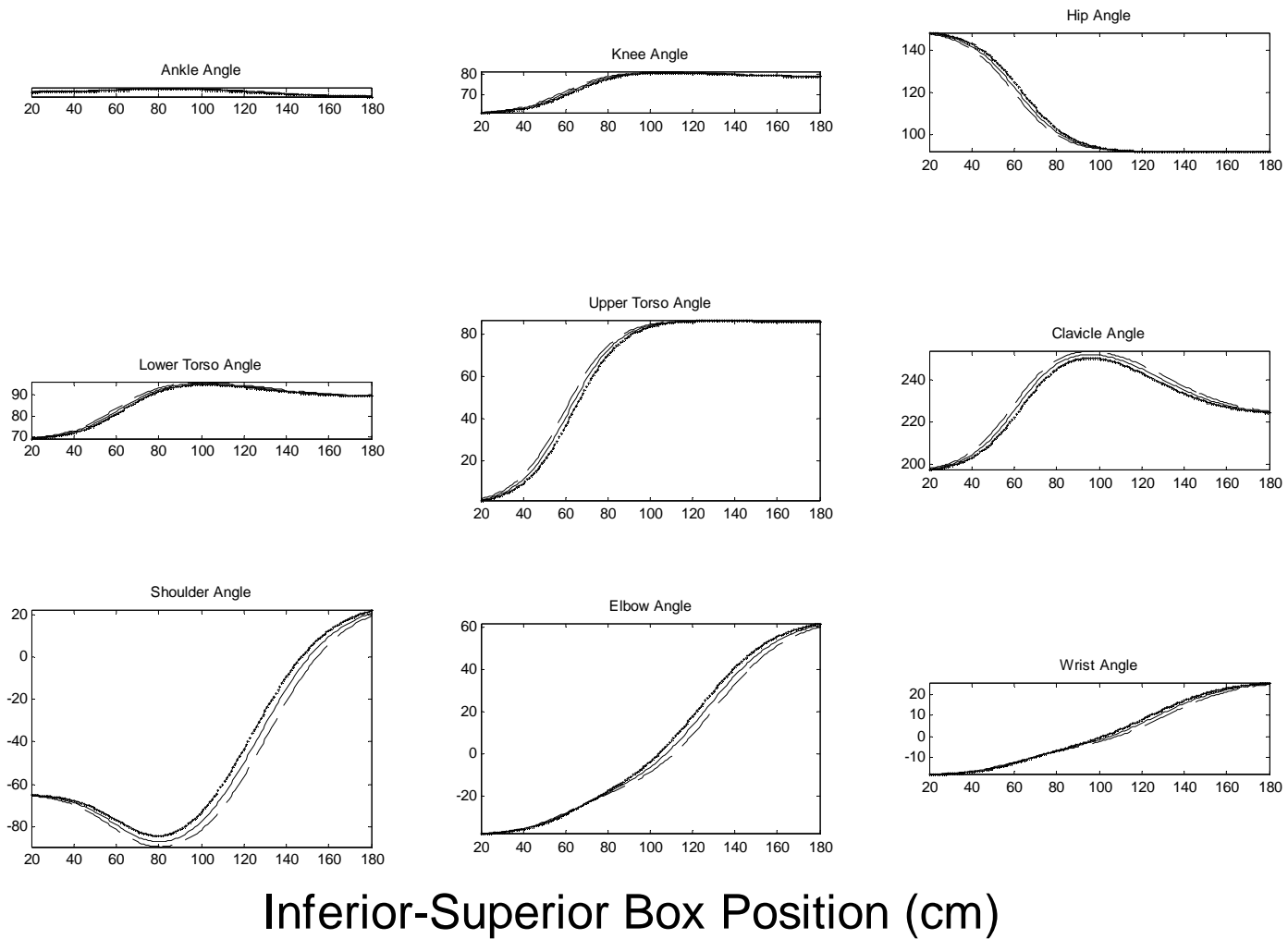


Figure 47. Joint angle predictions as a function of inferior-superior box position. The dashed line represents a low fourth anthropometry input (-4), the solid thin line a neutral one (0), and the solid wide line a high one (+4).

While describing these ‘transformations’ allows some high-level understanding of the network’s inner workings, it is incomplete without comparing the errors observed for the networks against the variability observed and quantified within the dataset. When this process is performed, it shows that the network’s prediction errors are in most cases slightly larger than the within-subject standard deviation around the mean motion path (Table 19). In one case, the network prediction was slightly smaller than the within-subject standard deviation. This is important because it indicates that the network can predict a posture that is in most cases within the envelope of postures that would be expected from an individual that performs these tasks multiple times but in an infrequent basis. Note that within-subject variability for initial and final postures is comparable to the corresponding between-subjects variability, and is in many cases higher. Also note that the ‘Network’ row of values in the table represents the average across all available data, including in it both the training and generalization data subsets. As previously explained, this was justified based on the similarity between prediction errors for both of these datasets.

Table 19. Network rmse (calculated across joint, tasks, and subjects) in comparison to observed average between- and within-subject variability. Maximum values are italicized. All quantities are in degrees.

	Ankle	Knee	Hip	Lower Torso	Upper Torso	Clavicle	Shoulder	Elbow	Wrist	Neck
Network	6.4	8.5	<i>12.3</i>	<i>11.5</i>	<i>13.5</i>	<i>35.0</i>	<i>13.2</i>	<i>14.1</i>	23.8	<i>15.5</i>
Between Subjects	5.3	5.7	7.8	11.1	8.9	25.5	12.7	12.9	<i>24.1</i>	12.7
Within Subjects	4.7	6.6	8.2	5.9	5.9	22.5	10.7	13.1	21.0	13.3

This analysis can be supplemented by graphical comparisons of the between-subject variability present in the data and the variability predicted by the model (through changes in the participant-dependent strength and anthropometry inputs). Again, no distinction between training or generalization datasets was made in creating these plots; all available data were used. The resultant plot shows that the predicted variability tended to be smaller than the variability already present within the data (Figure 48). However, for many angles the shape of both regions was quite similar. These results should be clearly distinguished from those presented in Table 19. While the results in the table show network prediction error, the plot concentrates on showing how well the network performed in assimilating the variability introduced by considering different participants. The plot also shows, to a limited degree, prediction error; the more that bisecting lines for each of the shaded regions overlap, the smaller the error in the mean

joint angle across participants, which is indicative of the overall degree of prediction error. Both results need to be considered together in determining overall predictive performance.

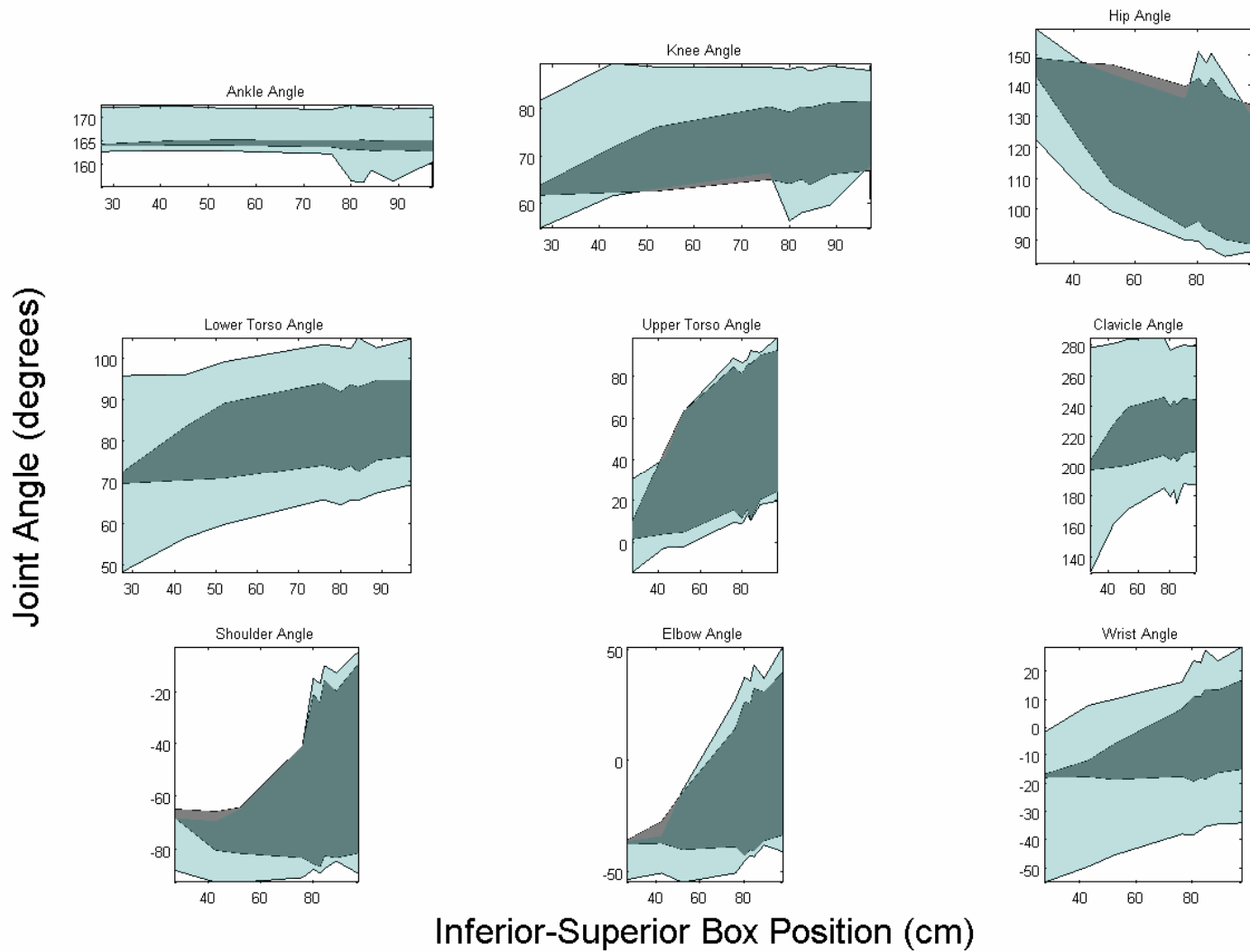


Figure 48. Comparison between target (light gray) and predicted (dark grey) between-subject variability. The shaded regions correspond to a ± 1 standard deviation region around the between-subjects mean for each group.

Taken together, the results suggest that the 2D network performed marginally well in assimilating the available data. The hip, upper torso, shoulder, and elbow angle variability was modeled quite well, and the errors for these joints were within the margins set by inter-human variability. However, the remaining angles, albeit not necessarily being subject to larger prediction error (in fact, these were smaller than those for the hip, upper torso, shoulder, and elbow in many cases), were not modeled within the full extent allowed by the observed variability. In general, the model predicted relatively well the mean joint angles that different individuals would utilize to perform lifting tasks similar to those described in this work, but failed to accurately represent the variability introduced by those individuals. Even when that variability was well modeled (e.g. the upper torso angle), prediction errors were still relatively large, which suggests that the reason the variability was predicted well was simply that the errors were not systematic. Thus, no particular prediction is necessarily made with insubstantial error, but the envelope of erroneous predictions is similar to the envelope established by the empirical data.

Similar analysis can be performed for the 3D model. Recall that the 3D model had an additional input relative to the 2D model: a value that indicated the end-effector position in the left-right axis. Also recall that for the 2D case, the end-effector position in the anterior-posterior axis had little effect on the joint angles. For the 3D case, and in contrast with this finding, the end-effector position in all three axes influenced substantially the different predicted angles. Substantial strength and anthropometry effects could also be seen for many of the angles. The plots on which these conclusions were reached are not included here since the conclusions that were gathered from them are not surprising and simply indicate that the network made use of all the inputs that it was provided.

The more important test of the network's effectiveness in the 3D case lies in its ability to predict postures with relatively low amounts of error. In contrast with the 2D case, however, network errors for the training and generalization datasets were in most cases smaller than the observed within-subject variability, indicating that the predictions are within the bounds set by the same individual performing the same task non-repetitively in multiple occasions.

Table 20. Network rmse (calculated across joint, tasks, and subjects) in comparison to observed average between- and within-subject variability. Maximum values are italicized. All quantities are in degrees.

	Left Ankle Alpha	Left Ankle Beta	Right Ankle Alpha	Right Ankle Beta	Left Knee Alpha	Left Knee Beta	Right Knee Alpha	Right Knee Beta	Left Hip Alpha	Left Hip Beta	Right Hip Alpha	Right Hip Beta	Left Lower Torso Alpha	Left Lower Torso Beta	Right Lower Torso Alpha	Right Lower Torso Beta	Upper Torso Alpha	Upper Torso Beta
Training Set	6.1	5.1	14.4	4.8	13.4	4.7	26.1	5.1	21.9	12.4	17.7	6.1	8.5	5.4	10.4	5.5	28.5	7.4
Novel Movements, Familiar Subjects	6.7	5.4	13.5	5.9	26.7	5.7	45.8	6.9	32.5	15.2	27.9	7.5	11.7	6.6	14.1	6.1	40.6	9.8
Novel Subjects, Familiar Movements	<i>11.7</i>	7.8	22.5	8.0	28.4	6.9	48.8	7.0	39.5	29.3	38.6	9.4	13.4	7.4	16.5	<i>8.0</i>	53.8	11.2
Novel Subjects and Movements	10.9	6.2	14.2	7.4	22.2	6.1	43.4	7.3	40.3	9.7	39.8	9.2	14.3	8.9	16.3	7.5	53.9	11.3
Between Subjects	4.0	1.9	6.0	2.7	10.2	1.9	12.1	2.7	49.1	2.2	42.6	2.5	8.1	3.1	6.4	3.4	49.9	2.4
Within Subjects	8.0	<i>8.0</i>	<i>28.7</i>	<i>8.4</i>	<i>48.0</i>	<i>8.1</i>	<i>92.2</i>	<i>11.2</i>	<i>77.6</i>	<i>39.4</i>	<i>77.3</i>	<i>9.7</i>	<i>14.8</i>	6.2	<i>17.2</i>	6.4	<i>103.3</i>	<i>11.9</i>

	Left Clavicle Alpha	Left Clavicle Beta	Right Clavicle Alpha	Right Clavicle Beta	Left Shoulder Alpha	Left Shoulder Beta	Right Shoulder Alpha	Right Shoulder Beta	Left Elbow Alpha	Left Elbow Beta	Right Elbow Alpha	Right Elbow Beta	Left Wrist Alpha	Left Wrist Beta	Right Wrist Alpha	Right Wrist Beta	Neck Alpha	Neck Beta
Training Set	9.1	5.8	9.2	5.7	34.6	10.2	32.0	10.5	13.2	10.5	24.6	10.5	12.4	10.1	14.0	10.0	29.8	8.4
Novel Movements, Familiar Subjects	12.2	7.3	12.6	6.6	66.5	13.2	53.6	13.1	18.6	14.7	<i>28.4</i>	15.4	18.3	13.1	18.5	13.4	41.3	11.1
Novel Subjects, Familiar Movements	<i>14.1</i>	8.4	<i>14.3</i>	7.7	70.2	18.0	54.8	18.0	20.5	16.8	28.1	17.8	<i>24.8</i>	15.0	21.6	14.3	<i>51.2</i>	13.5
Novel Subjects and Movements	14.0	8.0	14.0	7.8	76.2	17.4	55.3	17.5	20.5	15.9	23.5	15.9	23.0	14.1	21.5	14.5	41.9	13.7
Between Subjects	4.8	4.2	5.1	3.9	71.2	3.8	41.1	3.6	6.0	8.2	4.3	8.1	10.2	12.0	12.6	12.5	14.5	4.5
Within Subjects	11.9	<i>16.8</i>	9.9	<i>16.6</i>	11.7	<i>172.3</i>	21.5	<i>137.5</i>	<i>23.3</i>	<i>27.4</i>	21.5	<i>61.9</i>	21.2	<i>30.8</i>	<i>24.3</i>	26.7	25.5	<i>84.0</i>

As for the 2D case, knowledge on the error amounts in the 3D model can be supplemented by observation of the network's ability to predict the variability inherent in the dataset. To reduce the number of plots, the movements that are considered within each plot are only those where the influence of the axis is greatest and movement in the remaining axes is limited. As previously explained for the 2D case, these plots consider data from both the generalization and training datasets, given their similarity in error magnitudes and the intention of representing network performance for as much data as possible. Thus, the plots presenting the effects of inferior-superior box position only include sagittally symmetric movements in the near location (Figure 49). This plot shows substantial overlap in the empirical and predicted variability for a few angles (e.g. left shoulder β , right shoulder β , right knee β , right hip β), but low overlap for others (e.g. left knee α , upper torso α). However, the predicted variability tended to be included within the envelope provided by the between-subjects variability.

Similar results were observed for plots depicting the effects of anterior-posterior box position (Figure 50), which was calculated comparing the near and far reaches at all the available middle locations (including those with rotation). Finally, plots depicting the effects of left-right box position also showed similar patterns (Figure 51). These plots were developed considering the same movement locations used for the anterior-posterior axis plots.

Combined with the average errors observed for the predictions, these plots show that the network predictions modeled the data relatively well. Improvements are needed in expanding the variability that is predicted by the network, however, in some specific joints. While the errors were modeled within the limits set by the within-subject variability, the network failed to produce a sufficiently large spread of the predictions for a substantial number of joints.

Another consideration that surfaces from the variability plots is whether the angle description used was appropriate. Euler angles were selected here given their relative ease of interpretation. However, as the data show, they also depicted substantial variability within the relatively small performance envelope under study. This might have been due to a combination of two possibilities. First, it is possible that the variability observed is not an artifact of the angle representation method used, but rather to the reality that movement generation is subject to the effects of factors that were not considered within this investigation, perhaps even including elements of randomness. Second, it is also possible that the variability was due to mathematical artifacts in the particular representation approach selected, and that a different representation

would reduce the variability observed, and in turn make for a more easily modeled dataset. The true answer likely lies somewhere between these two extremes, and future research should consider these questions in more detail.

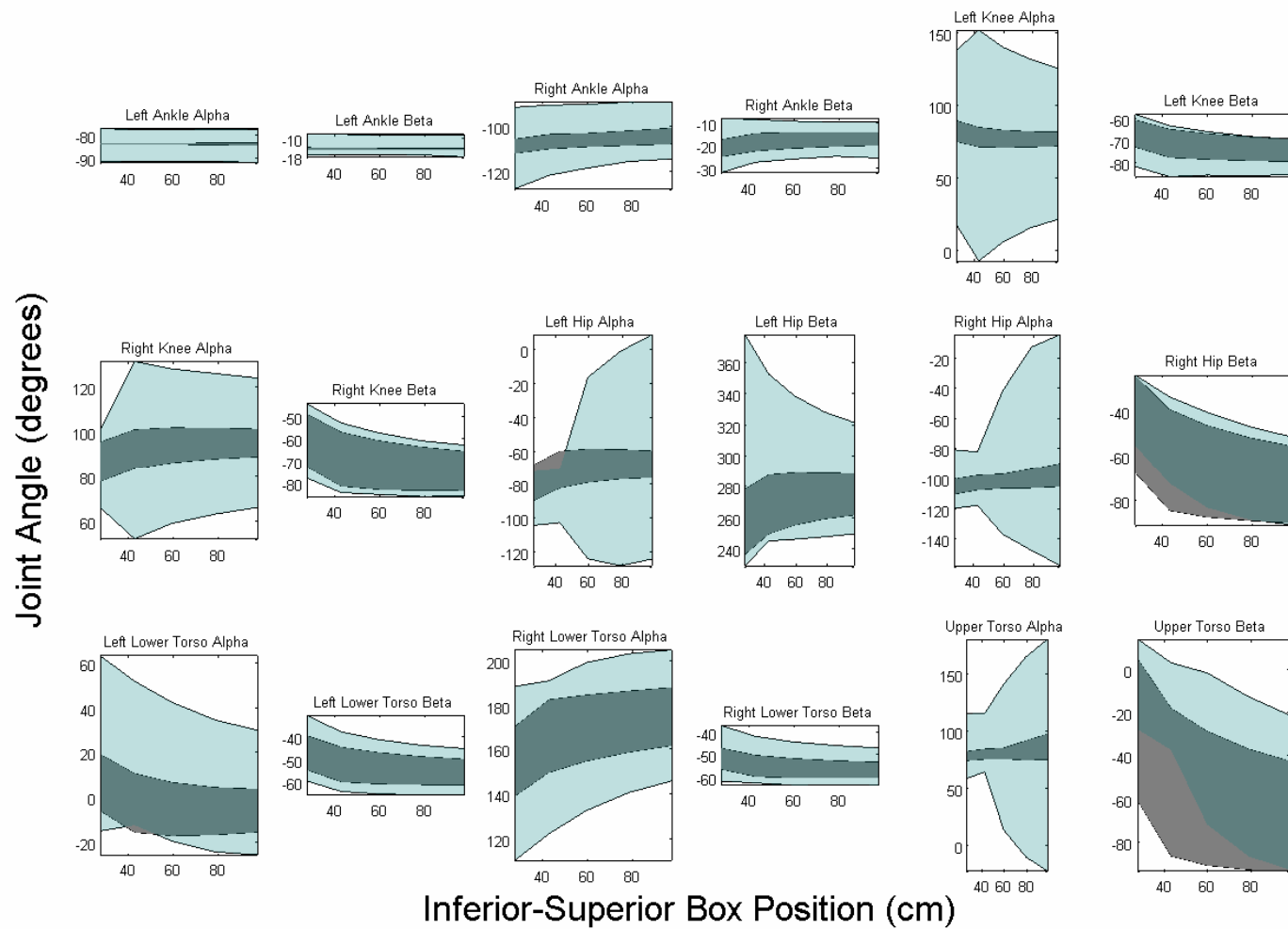


Figure 49. Comparison between target (light gray) and predicted (dark grey) between-subject variability. The shaded regions correspond to a ± 1 standard deviation region around the between-subjects mean for each group. The figure continues on the next page.

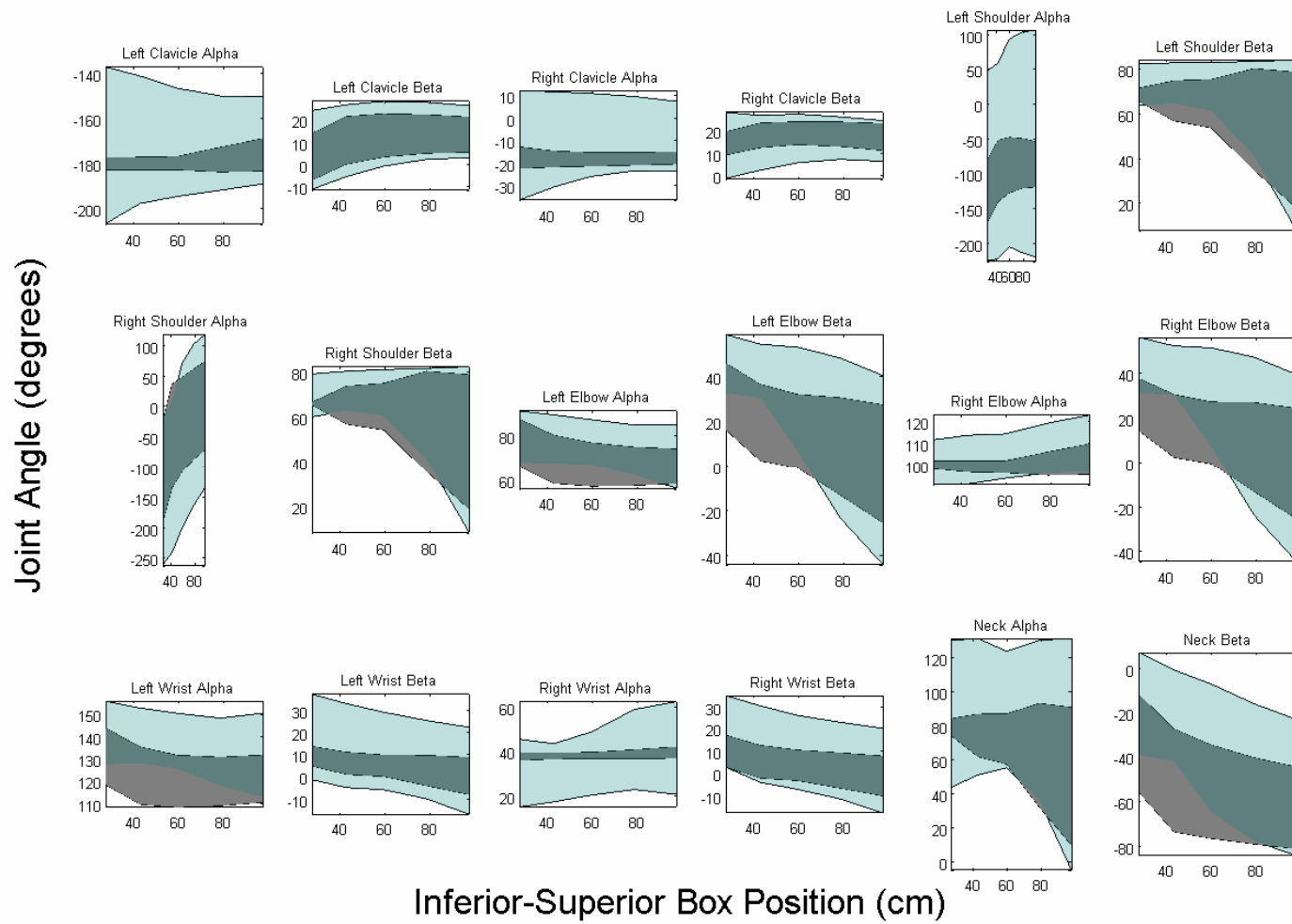


Figure 49 continued.

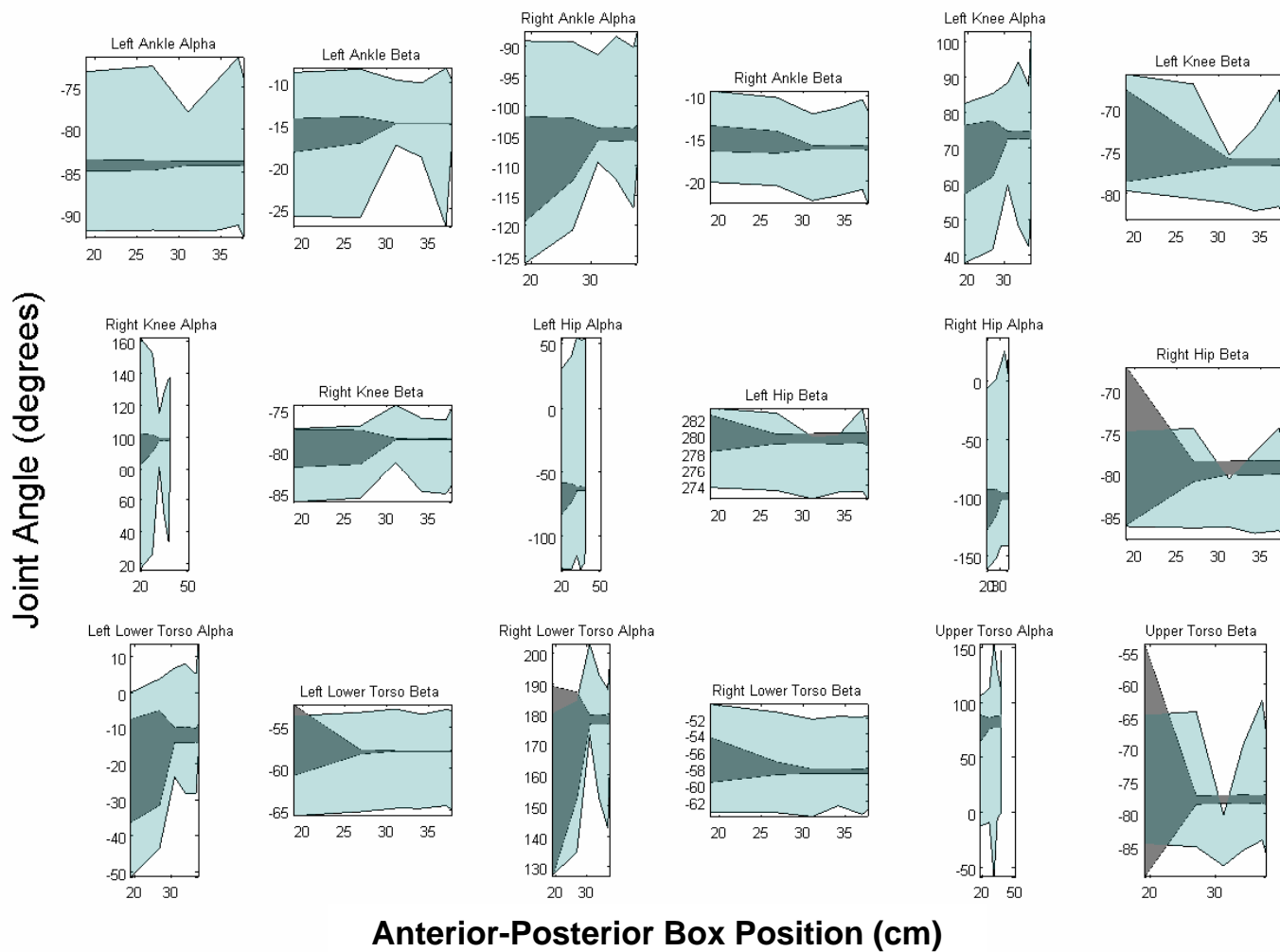


Figure 50. Comparison between target (light gray) and predicted (dark grey) between-subject variability. The shaded regions correspond to a ± 1 standard deviation region around the between-subjects mean for each group. The figure continues on the next page.

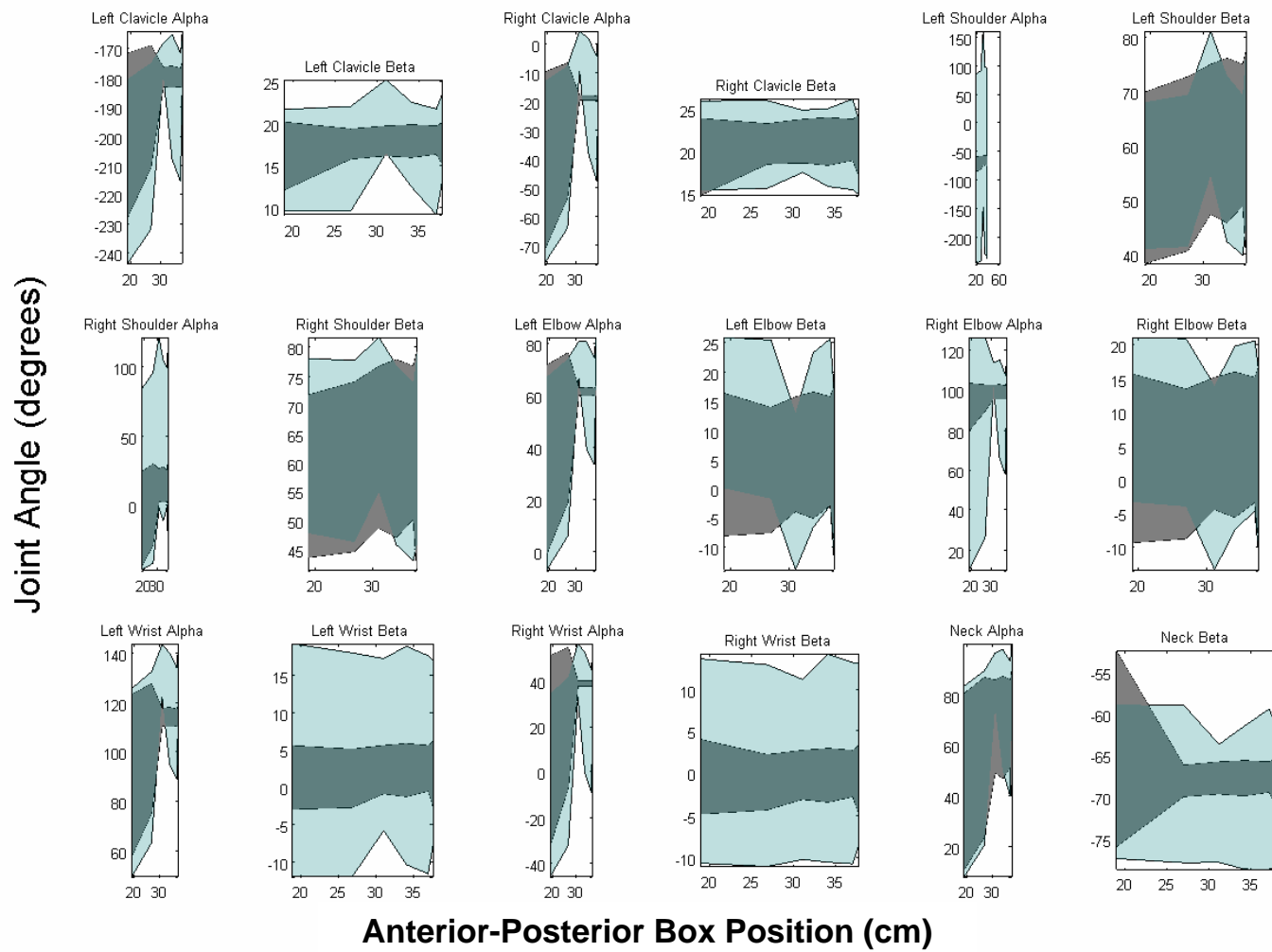


Figure 50 continued.

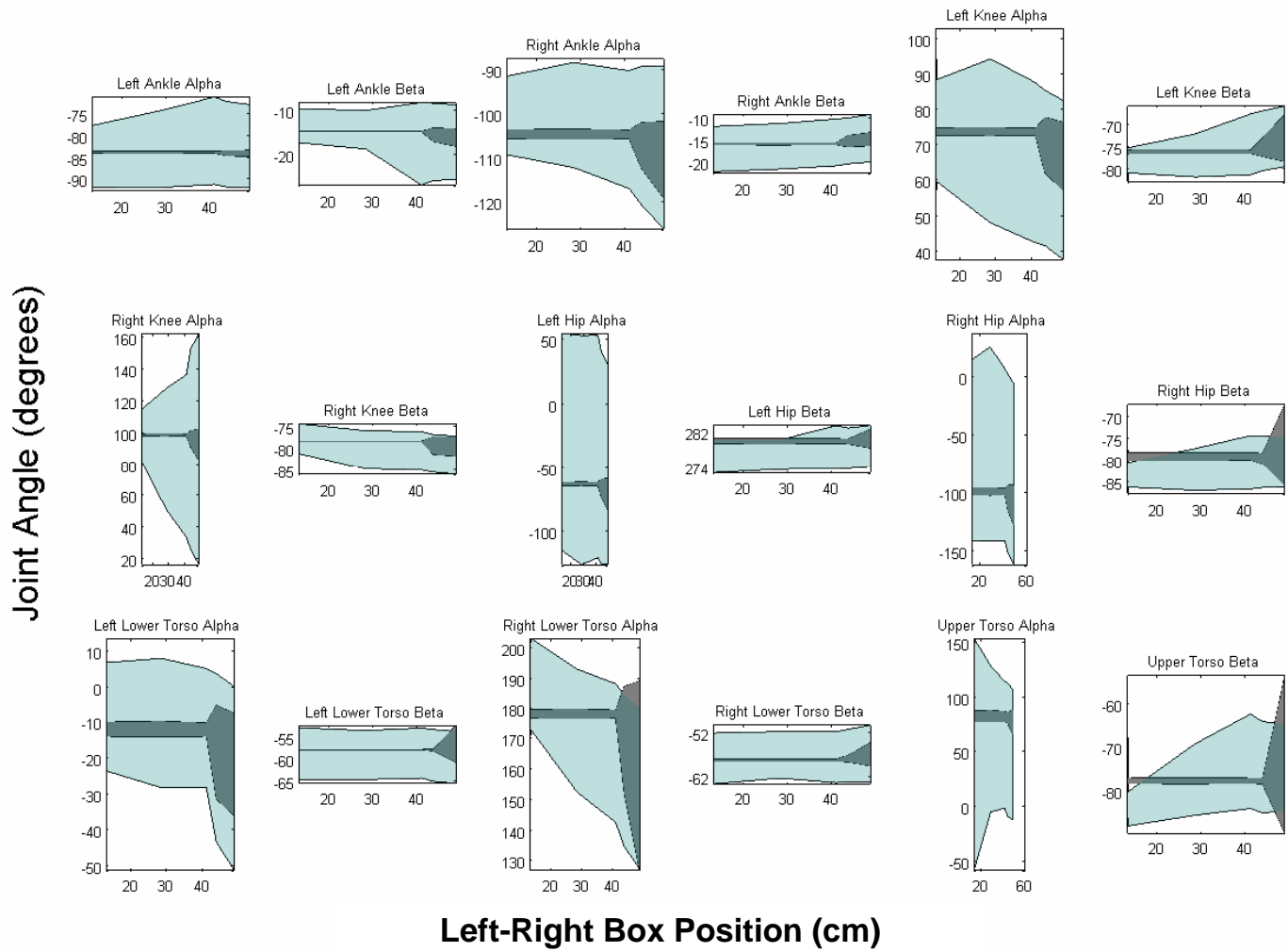


Figure 51. Comparison between target (light gray) and predicted (dark grey) between-subject variability. The shaded regions correspond to a ± 1 standard deviation region around the between-subjects mean for each group. The figure continues on the next page.

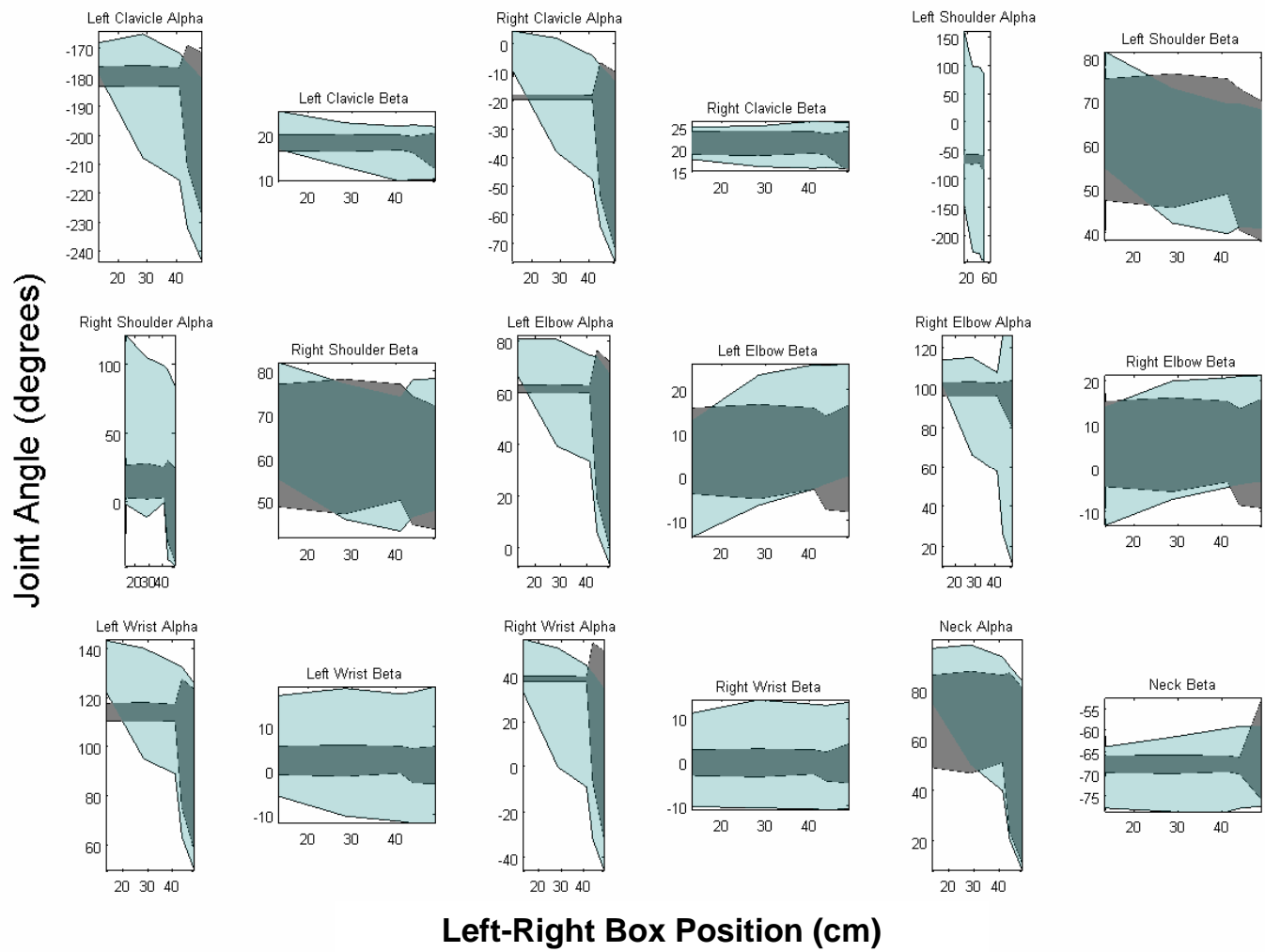


Figure 51 continued.

Another important aspect in determining performance for both 2D and 3D models lies in how the model predictions compare to those of other models that are available. While the network predictions are only marginally acceptable so far, they might represent a substantial improvement over existing methods. Beck and Chaffin (1992), for example, described errors observed when posture was predicted for sagittally symmetric movements using an inverse kinematics approach. They indicated that for postures assumed when participants lifted items at 75% of their strength (which would make their loads higher than those used here), mean errors for leg angle predictions were 13.6° (SD: 6.1°). Respective errors for trunk angle predictions, arm angle predictions, and overall predictions were 5.9 (SD: 3.9°), 9.5 (SD: 4.5°), and 10.4 (SD: 3.3°). These means are comparable to those obtained for the current investigation, albeit the current errors tend to be slightly higher. Note, however, that Beck and Chaffin report mean absolute errors, which in general tend to be slightly smaller than the root mean square errors reported here. In any case, the current model can be considered similar in performance to this inverse kinematics based approach.

The Beck and Chaffin (1992) model has been greatly modified and improved in its current use within 3DSSPP™, but comparisons of this program's predictions against the ANN predictions showed that the ANN predictions were significantly more accurate. Reasons for the higher error in the 3DSSPP™ predictions were not apparent. However, note that the 3DSSPP™ program does not advertise its posture prediction function as an accurate prediction, but rather as a feasible posture that should be modified by the user to represent the posture in which they are interested. Thus, the purpose of their function has likely never explicitly been to maximize accuracy.

Similar results were observed for the Jack™ simulation environment. For this program, these differences in errors, which demonstrate a better performance of the ANN, were likely due to three main factors. First, the Jack™ simulation environment is not designed to predict the most likely posture, but rather a feasible posture that achieves to the fullest extent possible the constraints placed on the humanoid at a particular point in time. Second, in its standard form, Jack™ has no 'behavior' associated with the knee joints, which in turn means that these joints will not shift their angles substantially during the motion. This resulted in some larger prediction errors for the lower extremity angles. Third, control of the hands is not automated (i.e. Jack™ will not attempt to grasp an object unless it is told to do so by a series of commands and manual

adjustment). Thus, high errors were also observed at the wrist joints. It is also important to note that the JackTM humanoid could not achieve in many occasions the posture required by the box position, especially for movements in the lower locations. In those situations, Jack'sTM hands were not attached to the box, but rather directed towards it. This was a function of the limited knee range of motion allowed by the software's motion prediction algorithm.

Note that both 3DSSPPTM and JackTM both had access to the same information that was available to the ANN-based model. This information included the hand location and anthropometric information for each participant. In some cases, further information could have been provided to the programs that might have improved their performance. For example, the 3DSSPPTM model could have used information as to whether the lower extremities were used in attaining a particular posture (e.g. for a squat lift). This information was not provided to the comparison models to avoid providing them with any unfair advantage.

Comparisons against other published models yielded similar results to the ANN-prediction comparisons against 3DSSPPTM and JackTM predictions. For example, the ANN model also outperformed a cost-based optimization model proposed by Jung and Park (1997), who report average mean absolute errors (not rms errors) on the order of 20° to 40°. These researchers performed their optimization process with relatively few constraints, which might explain the low performance levels but which also makes it more comparable to the current model, which included no constraints.

Dysart and colleagues (Dysart, 1994; Dysart and Woldstad, 1994, 1996) report errors in terms of a parameter the authors describe as Euclidean distance, which considers in the calculation the squared prediction errors for the hip location and the forearm orientation. Qualitatively, however, Dysart's investigation (which employed optimization with a number of different objective functions) shows errors larger to the ones observed here for two dimensions in most lifting situations. Further developments of these models, reported in Woldstad (1997), still indicate large errors employing this approach, on the order of 15° or more, although one of the objective functions showed mean absolute errors across joints between 5° and 20°.

Overall, the results showed that the networks were able to model the posture data to a certain extent. Comparisons with past studies of similar situations show that, at the very least, the ANNs were able to match their performance levels. In more than one case, the ANN outperformed the past models. However, prediction errors were still considerable in many

instances, and could benefit from improvement. This improvement could arise from changes to the network structure, introduction of additional inputs that help account for some of the variability in the dataset, and the addition of physiological constraints to the network's outputs, among others. However, the large levels of within-subject variability observed, which in some cases were larger than the network's prediction errors, are troublesome. Further improvements in prediction accuracy will depend in part in controlling or effectively explaining this variability.

Chapter 8 SIMULATING MOVEMENTS ACROSS INDIVIDUALS

8.1 Introduction

The results presented in Chapter 6 suggest that ANNs can attain acceptable predictive values when they are trained and tested with the data from a single individual. However, the output of such a network is not applicable to other individuals. This section describes networks that have been adapted to tailor their output to different individuals.

Given that an important aspect of ANN development is the training set, networks using diverse training sets were compared. This approach has direct bearing on whether the network is considered a movement reproduction tool or a movement prediction tool. A movement reproduction tool would not be expected to perform well in movements for which it has not been trained but which fall within the performance envelope encompassed by other movements that are included in the training set. A movement prediction tool would be expected to perform well across all movements. The distinction is important from a research perspective. If the network is a prediction tool, then it is logical to look into its structure to examine its organization in hopes of finding plausible motor control schemes. This exercise has lower relevance if the network acts as a reproduction tool.

8.2 Methods and Results

8.2.1 Two dimensions

The network structure used in this section is similar to that presented in Section 6.2 for the 2-D case (Figure 52). The main difference is the addition of two other input types, a strength modifier and a set of anthropometry modifiers. These inputs are the same as those already discussed on Chapter 7 for the prediction of initial and final posture. These anthropometry and strength inputs provide the network with synthesized (through principal components analysis) information, reducing the overall number of inputs required needed. The reader is referred to Section 6.2 of this document for further details on the structure of this network.

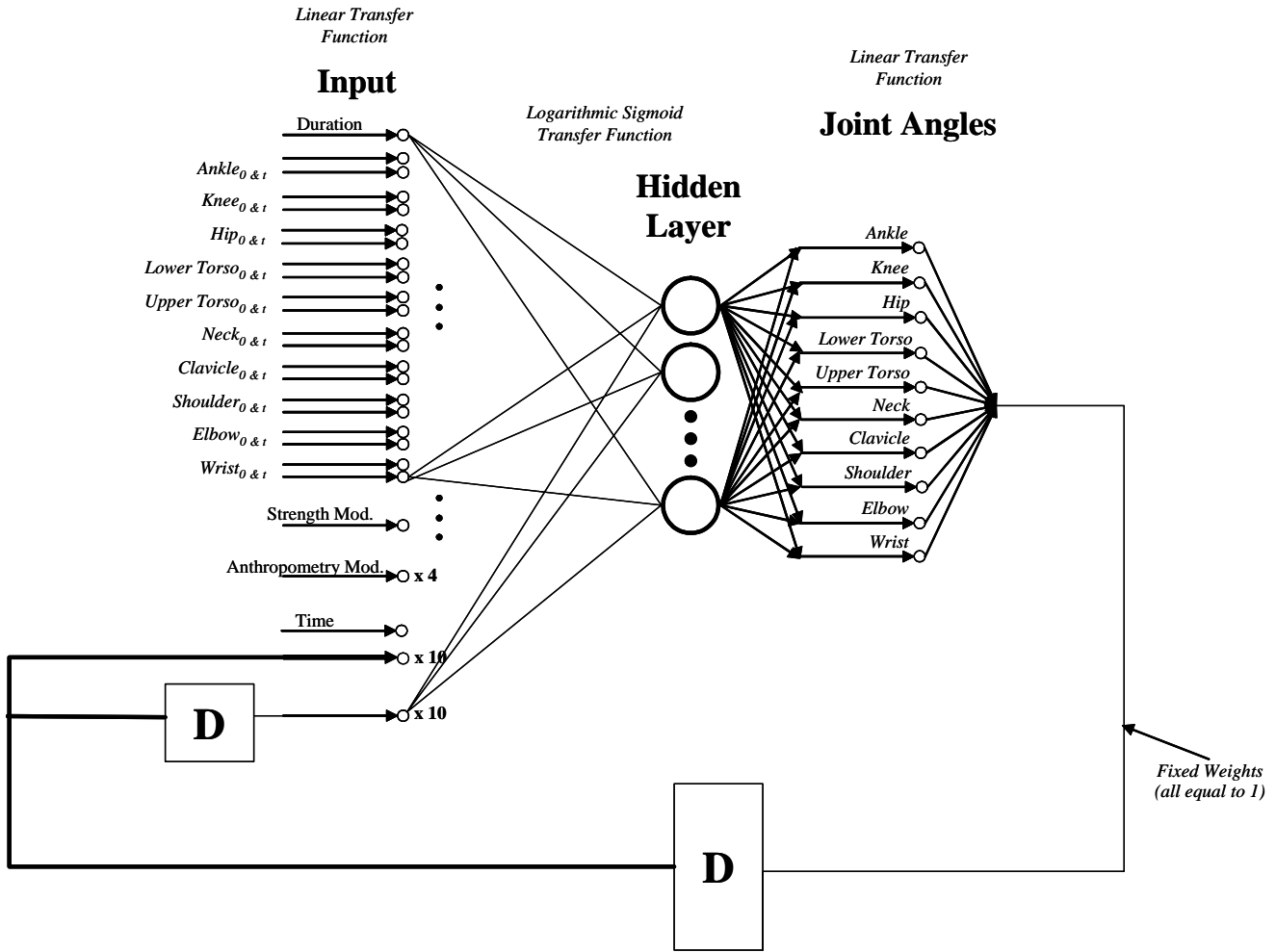


Figure 52. Two-dimensional network structure using joint angles as the input and prediction basis. Although all layers are fully interconnected, some connections are omitted for clarity. Boxes with 'D' represent a single time delay. The 'x 10' next to two of the inputs indicates that each of these nodes represents ten different inputs (each corresponding to one of the outputs). The 'x 4' next to the anthropometry modifier input indicates that there are four of those inputs in the network.

Two training sets were used in training the network. The first training set consisted of all the sagittally symmetric movements for 16 out of the 20 participants (80%), which were randomly selected. Data from the remaining four participants were used for verification of the generalization abilities of the network. As for the posture prediction model discussed in the previous chapter, the large proportion of movements contained within the training set was selected based on experimenter judgment, with the goal of providing enough training data to the network while saving sufficient data for verification. Past results (documented in Chapter 6) had shown that the networks had the ability to learn all of the motions for a single participant if these

data were provided during the training process. However, training the network with a subset of the data for a single participant was not sufficient to achieve acceptable error levels. The goal of training with a large proportion of the data was to assure, to the degree possible, that observations of poor network performance were not due to insufficient training dataset size.

This first training approach provided a ‘best case’ network that has been exposed to all movement types and locations within the dataset (albeit not to all participants). This network would be more likely to function as a movement reproduction tool. The second training set used data from the same 16 participants, but in this case the ‘Deliver’ and ‘Bring back’ movements to the near and far Middle Lower and Middle Upper locations from all participants were excluded. These locations were used within the verification dataset. Their exclusion was due to their location as intermediate points between other locations. The middle lower location was between the lower and middle locations. The middle upper location was between the middle and upper locations. Thus, if the network was properly acquiring knowledge about the lift, it should be able to interpolate within its training set ‘extremes’ to predict motions for these novel locations.

This second training approach generated a network that would have to predict motions that were novel to it, supporting (if performance was adequate) its use as a movement prediction tool. The split in the data allowed three distinct verification sets to coexist. The first verification set would allow for observation of the network’s predictive ability for novel movements performed by individuals whose data had been used in the training process (i.e. 16 out of 20 participants). The second verification set allowed for observation of the network’s predictive ability for novel movements performed by individuals whose data had not been used in the training process. The third verification set allowed for observation of the network’s predictive ability for familiar movements performed by individuals whose data had not been used in the training process.

ANOVA was performed to determine significant differences in prediction error as a function of task characteristics and training or verification dataset. Significant differences within significant main effects were determined using Student-Newman-Keuls (SNK) tests. A Type I error of 1% was used across all statistical tests.

8.2.1.1 Results

First Training Set

The mse threshold for the training set with all data for 16 of the 20 participants was set at 0.001 rad^2 . Training was manually stopped when the mse approximated 0.023 rad^2 (calculated across participants, joints, and time samples), as the error stabilized at this point. Approximately 100,000 training epochs had elapsed when training was manually stopped. This 0.023 rad^2 error represented an rmse of 0.15 rad (8.6°). To compare directly across past models, however, these errors were translated to errors in the prediction of joint positions. The joint position rmse for the training set was 3.79 cm (range: $1.34\text{-}9.61 \text{ cm}$).

Errors in the training set were dependent on the joint and direction of movement (Figure 53). Error in the antero-posterior axis was higher than error in the inferior-superior axis (except for the ankle joint). Errors also increased down the ankle-to-hand kinematic chain. Statistical analysis of error across Movement Type ('Bring back', 'Deliver') and Location showed significant differences as a function of Location ($F(9,114), p < 0.0001$). *Post hoc* tests of the Location factor indicated that the Lower Far Location had significantly higher rmse levels than any other location. The Lower Near Location and Middle Lower Far Location had the second highest levels of rmse. The remaining locations were statistically indistinguishable. In general, movements to higher locations tended to exhibit lower rmse levels than movements to lower locations (Table 21).

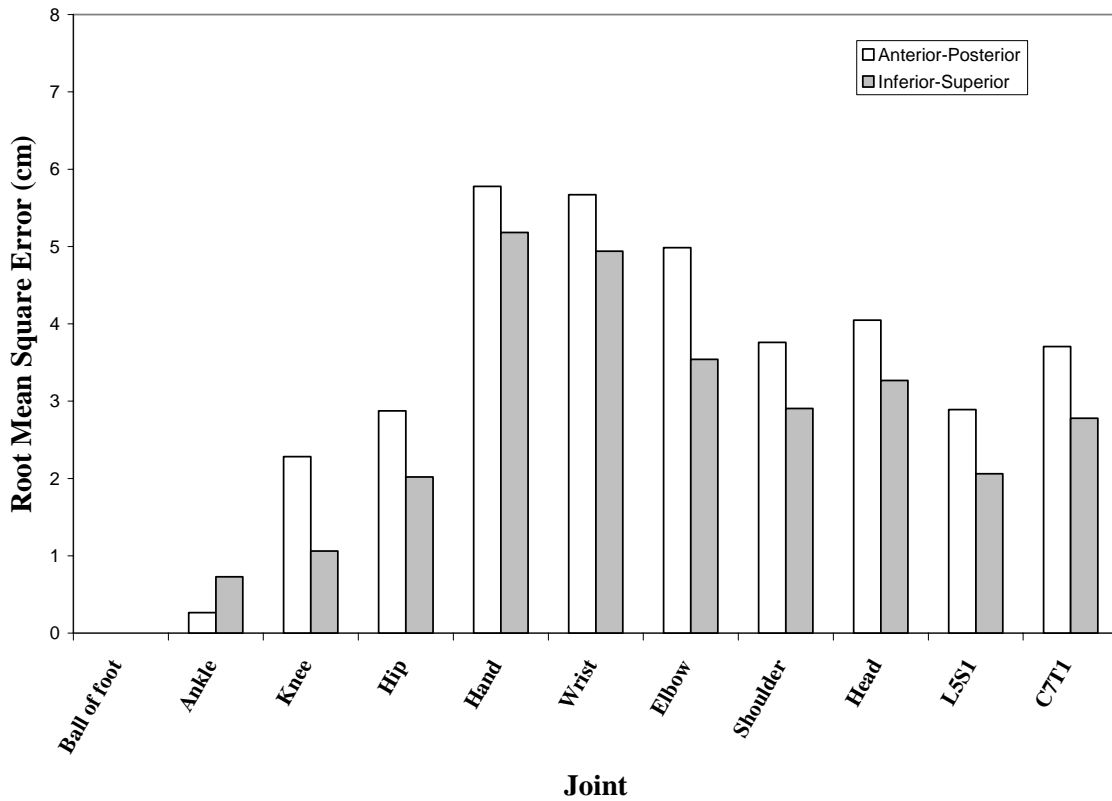


Figure 53. Root mean square error by joint and direction of movement. Training dataset.

Table 21. Rmse levels across Movement Location. Training dataset.

Location	rmse (cm)	SNK Letter Rating
Lower Far	4.85	A
Lower Near	4.26	B
Middle Lower Far	4.26	B
Upper Far	3.42	C
Middle Lower Near	3.29	C
Upper Near	2.81	C
Middle Far	2.55	C
Middle Upper Far	2.38	C
Middle Upper Near	2.32	C
Middle Near	2.23	C

Errors in the verification set were also dependent on the joint and direction of movement (Figure 54). Error in the antero-posterior axis was in most instances higher than error in the

inferior-superior axis. Errors also increased along the ankle-to-hand kinematic chain. Statistical analysis of error across Movement Type ('Bring back', 'Deliver') and Location showed significant differences as a function of Location ($F(9,24)$, $p=0.0006$). *Post hoc* tests of the Location factor indicated that the Lower Far Location had significantly higher rmse levels than the Middle Near Location. The remaining locations were statistically indistinguishable (Table 22).

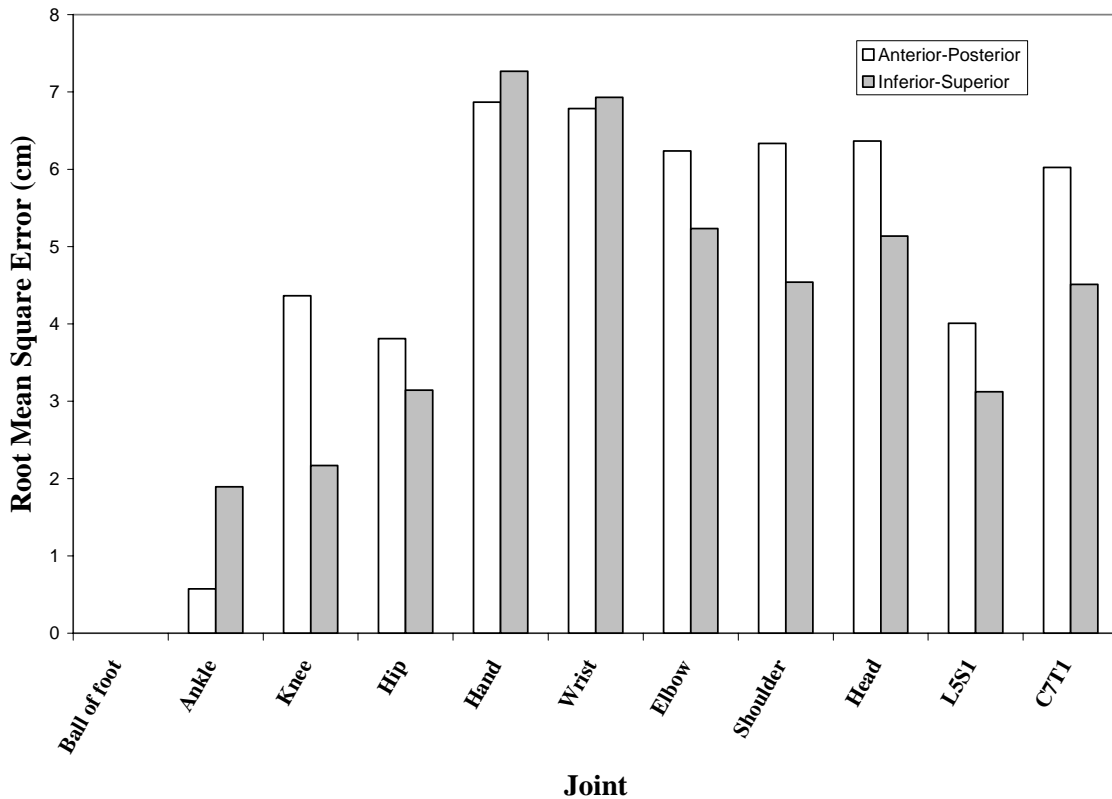


Figure 54. Root mean square error by joint and direction of movement. Verification dataset.

Table 22. Rmse levels across Movement Location. Verification dataset.

Location	rmse (cm)	SNK Letter Rating
Lower Far	4.85	A
Lower Near	4.26	B
Middle Lower Far	4.26	B
Upper Far	3.42	C
Middle Lower Near	3.29	C
Upper Near	2.81	C
Middle Far	2.55	C
Middle Upper Far	2.38	C
Middle Upper Near	2.32	C
Middle Near	2.23	C

The generalization abilities of the network were tested statistically by comparing rmse levels across the training and verification datasets. An ANOVA considering the different datasets showed a significant difference ($F(1,18)=50.75, p<0.0001$) between the training and verification datasets. The mean rmse for the training dataset was 3.42 cm, while the corresponding mean for the verification dataset was 4.87 cm.

Analysis of rmse levels by subject showed relatively close clustering (Table 23). However, subject 3 appeared to exhibit higher rmse than any other subject, including the other subjects included within the generalization dataset.

Table 23. Root mean square error (in degrees) by subject, split in training and generalization groups.

	Subject Number	Rmse (degrees)
Training	2	10.35
	4	9.32
	5	11.56
	6	9.9
	7	8.74
	8	9.77
	9	9.24
	10	9.35
	12	11.69
	13	8.03
	14	9.61
	15	8.09
	17	12.27
Generalization	18	7.25
	19	8.72
	20	10.07
	1	10.39
	3	17.69
	11	11.02
	16	12.41

Second Training Set

Recall that the second training set contained movements to the Lower, Middle, and Upper locations (near and far), performed by 16 out of the 20 participants. As for the first training set, the mse threshold was set at 0.001 rad^2 . Training was manually stopped when the mse (calculated across participants, joints, and time sample) approximated 0.037 rad^2 , as error had stabilized. Approximately 100,000 training epochs had been completed when training was stopped. This error represented an rmse of 0.19 rad (11.02°), slightly higher than the average rmse for the first training set. To compare directly across past models, these errors were translated to errors in the prediction of joint positions. The joint position rmse for the training set was 3.73 cm (range: $0.94\text{-}7.44 \text{ cm}$). These numbers represent slight improvements over the first training set.

Errors in the training set were dependent on the joint and direction of movement (Figure 55). Error in the antero-posterior axis was higher than error in the inferior-superior axis (except

for the ankle joint). Errors also increased down the ankle-to-hand kinematic chain. Statistical analysis of error across Movement Type ('Bring back', 'Deliver') and Location showed significant differences as a function of Location ($F(5,60)=16.64, p<0.0001$). *Post hoc* tests of the Location factor indicated that the Lower Far Location and the Lower Near Location had significantly higher rmse levels than any other location. The Upper Far Location and Upper Near Location had the second highest error rates. The Middle Far and Middle Near Locations had the lowest rmse levels (Table 24).

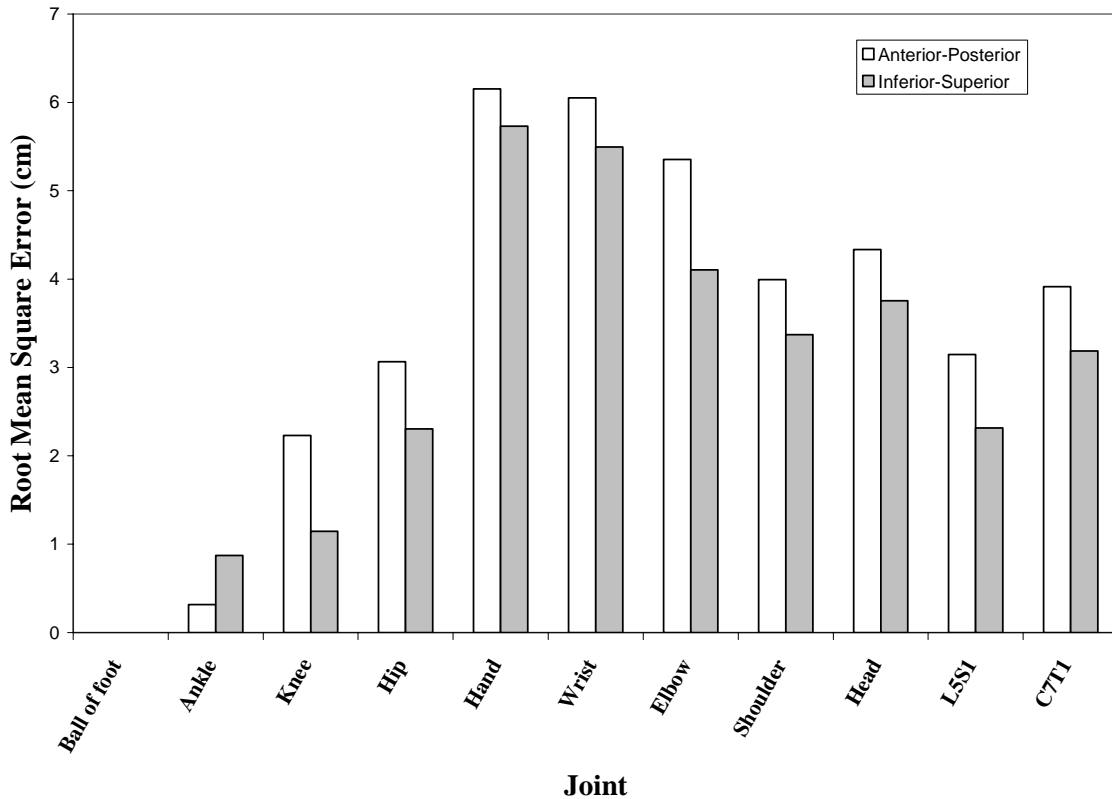


Figure 55. Root mean square error by joint and direction of movement. Training dataset.

Table 24. Rmse levels across Movement Location. Training dataset.

Location	rmse (cm)	SNK Letter Rating
Lower Far	4.72	A
Lower Near	4.38	A
Upper Far	3.52	B
Upper Near	3.39	B
Middle Far	2.67	C
Middle Near	2.28	C

Errors in the verification set consisting of additional movements performed by the participants in the training set were also dependent on the joint and direction of movement (Figure 56). Error in the antero-posterior axis again exceeded error in the inferior-superior axis in all cases except the ankle joint. Errors also increased along the ankle-to-hand kinematic chain. Statistical analysis of error across Movement Type ('Bring back', 'Deliver') and Location showed significant differences as a function of Location ($F(3,39)=31.86, p<0.0001$). *Post hoc* tests of the Location factor indicated that the Middle Lower Far Location had significantly higher rmse levels than the Lower Near Location, which in turn had higher rmse levels than the Middle Upper Far and Middle Upper Near Locations (Table 25).

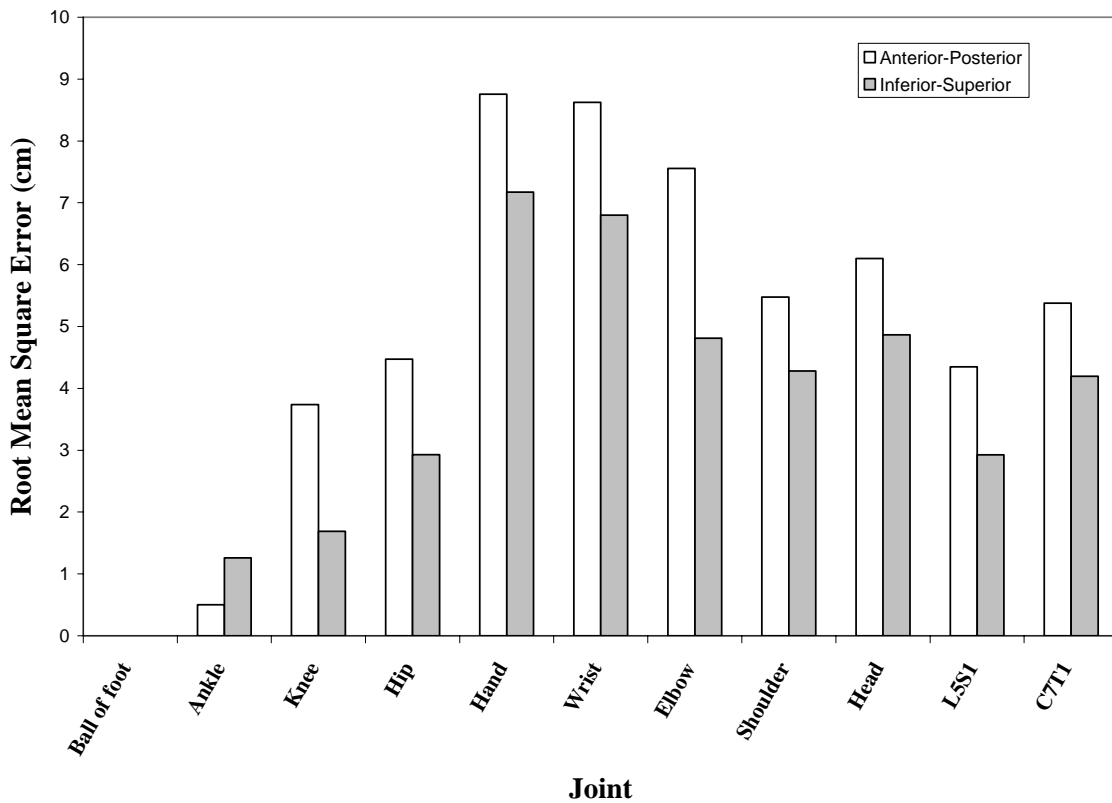


Figure 56. Root mean square error by joint and direction of movement. Verification dataset.

Table 25. Rmse levels across Movement Location. Verification dataset.

Location	rmse (cm)	SNK Letter Rating
Middle Lower Far	7.09	A
Middle Lower Near	5.50	B
Middle Upper Near	3.27	C
Middle Upper Far	3.25	C

Errors in the verification set consisting of movements in which the network was trained but were performed by a different set of participants showed joint- and direction of movement-dependent errors that were similar to those observed for the training set (Figure 57). For the ankle, hand, and wrist joints, however, error in inferior-superior axis was higher than error in the anterior-posterior axis. As before, errors also increased along the ankle-to-hand kinematic chain. Statistical analysis of error across Movement Type ('Bring back', 'Deliver') and Location showed no significant differences.

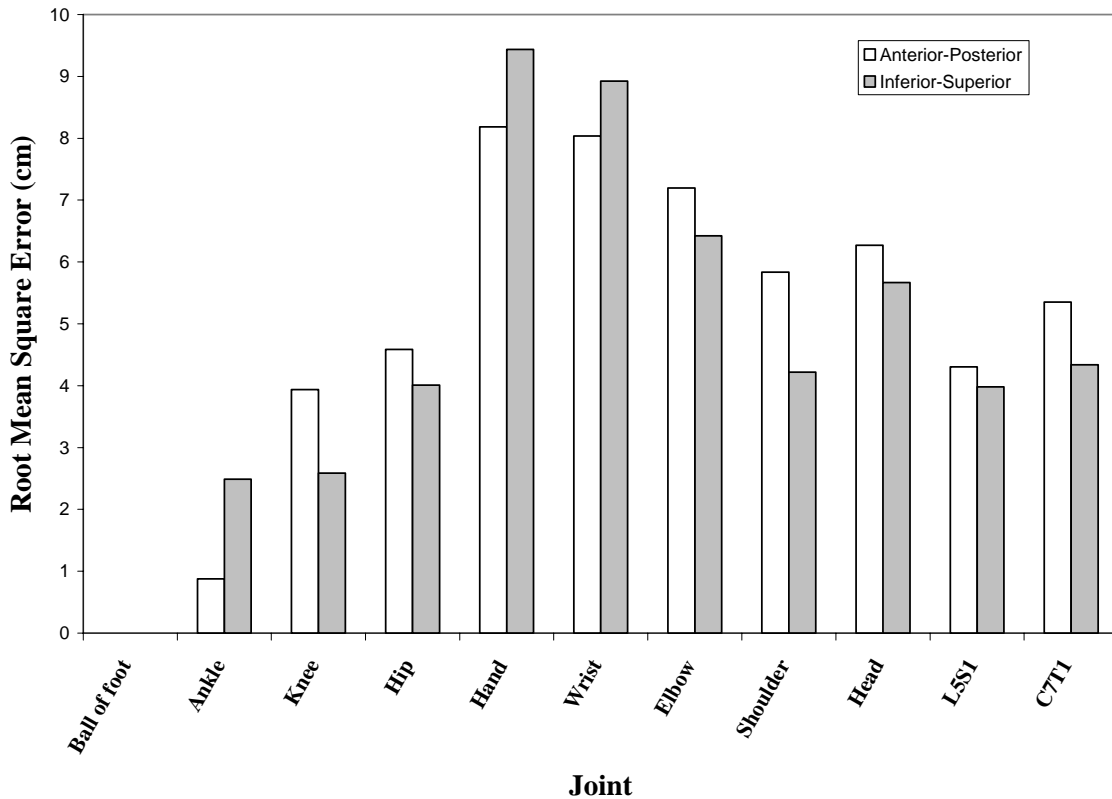


Figure 57. Root mean square error by joint and direction of movement. Verification dataset.

Errors in the verification set consisting of novel participants and movements were also dependent on the joint and direction of movement (Figure 58). For the ankle, hand, and wrist joints, error in inferior-superior axis was higher than error in the anterior-posterior axis. As observed in all previous training and verification datasets, errors also increased down the ankle-to-hand kinematic chain. Statistical analysis of error across Movement Type ('Bring back', 'Deliver') and Location showed significant differences as a function of Location ($F(3,9)=17.04$, $p=0.0005$). *Post hoc* tests of the Location factor indicated that the Middle Lower Far and Middle Lower Near Locations had significantly higher mse levels than the Middle Upper Far and Middle Upper Near Locations (Table 26).

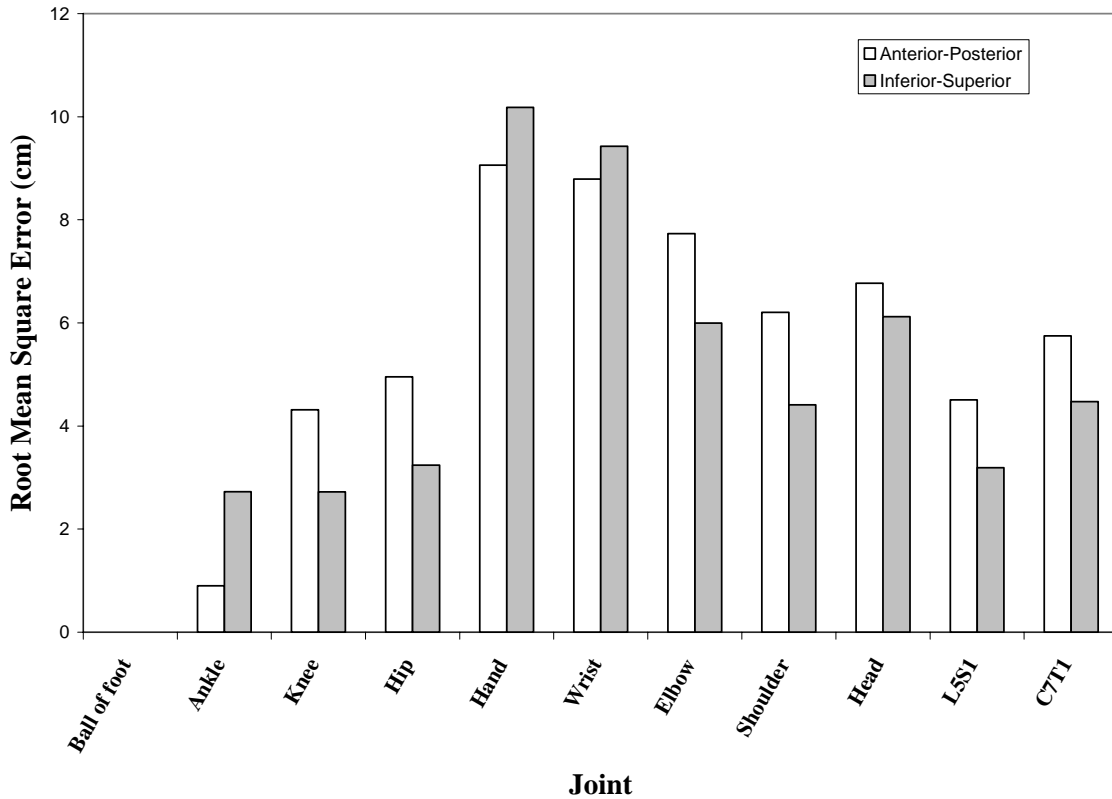


Figure 58. Root mean square error by joint and direction of movement. Verification dataset.

Table 26. Rmse levels across Movement Location. Verification dataset.

Location	rmse (cm)	SNK Letter Rating
Middle Lower Far	7.36	A
Middle Lower Near	6.47	A
Middle Upper Near	4.47	B
Middle Upper Far	4.35	B

The generalization abilities of the network were tested statistically by comparing rmse levels across the training and verification datasets. An ANOVA considering the different datasets showed a significant difference in rmse ($F(3,36)=17.41, p<0.0001$) between datasets. The training dataset had the lowest rmse level (3.73 cm) while other datasets were indistinguishable from each other based on their rmse level (range: 5.04 cm – 5.81 cm).

8.2.1.2 Implications of training dataset

Results showed that network training did not fully transfer to novel data, as was the case when the networks were used to predict postures. The resultant errors, however, do not necessarily justify the dismissal of the ANN-based modeling approach. When errors in the first training and verification datasets are specified in terms of angles, they are shown to be smaller than the standard deviations for the between- and within-subject mean movement trajectories (Table 27, training and generalization errors apply to the first training set used). This suggests that the errors in network predictions are not beyond the variability that can be expected in a movement path as an individual repeats a motion, and strengthens the argument that the network is capable of synthesizing the dataset.

Table 27. Network root mean square error (first training set) in comparison to observed average between- and within-subject variability. All numbers are expressed in degrees. Maximum values are italicized.

	Ankle	Knee	Hip	Lower Torso	Upper Torso	Clavicle	Shoulder	Elbow	Wrist	Neck
Training Set	3.0	3.6	4.3	3.7	5.0	15.8	9.4	10.9	9.2	6.4
Verification Set	6.8	6.2	6.3	5.2	9.6	16.7	12.7	12.2	11.9	7.9
Between Subjects	6.8	8.0	10.7	<i>13.6</i>	11.8	37.2	20.2	21.6	26.4	16.0
Within Subjects	<i>6.9</i>	<i>9.0</i>	<i>14.6</i>	10.0	<i>12.6</i>	<i>56.8</i>	<i>27.3</i>	<i>27.3</i>	<i>30.1</i>	<i>19.0</i>

Perhaps more importantly, however, even though significant differences exist in training and generalization dataset errors (with generalization dataset errors being higher), these errors are also smaller than the standard deviations for the between- and within-subject mean movement trajectories. Thus, even these predictions could be useful.

The network also seemed able to track the variability within the dataset reasonably well as the movement progressed (Figure 59). The figure shows the near lower movement location for a ‘Bring back’ movement. This movement was selected as it was consistently the source of relatively large errors. Thus, differences observed in the plot will likely be lower for the remaining movement locations. Note that the network tracked the time history of all angles. The shoulder angle was slightly under-predicted for this particular movement. Network-predicted variability also tended to stay within the bounds set by the between-subject variability.

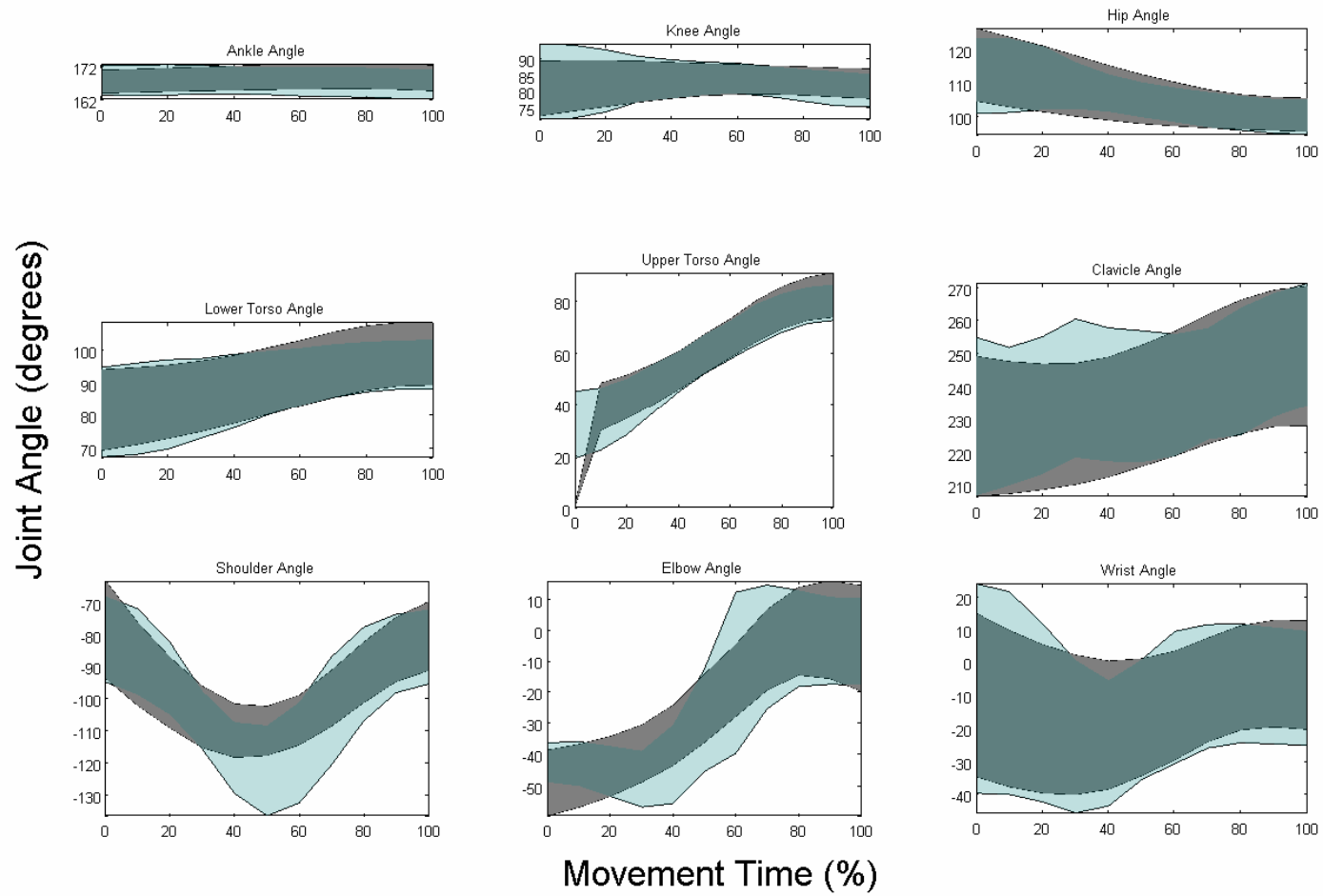


Figure 59. Comparison between target (light gray) and predicted (dark grey) between-subject variability. The shaded regions correspond to a ± 1 standard deviation region around the between-subjects mean for each group.

These results suggest that the network produced acceptable predictions for most joints, given that the resultant errors were relatively small and the variability present within the data was tracked across movement time. The next section explores whether these results and discussion translate to the three-dimensional situation.

8.2.2 *Three Dimensions*

The network structure used in this section was based on the two-dimensional network described in Section 6.2, with further inputs to represent the additional angles necessary to define a 3-D posture and to include the strength and anthropometry modifiers (Figure 52). These angles are equivalent to those calculated in Section 5.2.2. The network also added another hidden layer of 100 additional units. This change was made based on pilot tests that indicated this additional layer was needed to aid the convergence process, as compared to a network with additional hidden units within a single hidden layer. While an open area of debate in neural networks research, there is some evidence that the addition of a second hidden layer may be advantageous, from a model flexibility aspect, over the addition of more units to a single hidden layer (Tamura and Tateishi, 1997). The strength and anthropometry inputs are the same as those already discussed on Chapter 7 for the prediction of initial and final posture. These anthropometry and strength inputs provide the network with synthesized (through principal components analysis) information, reducing the overall number of inputs required.

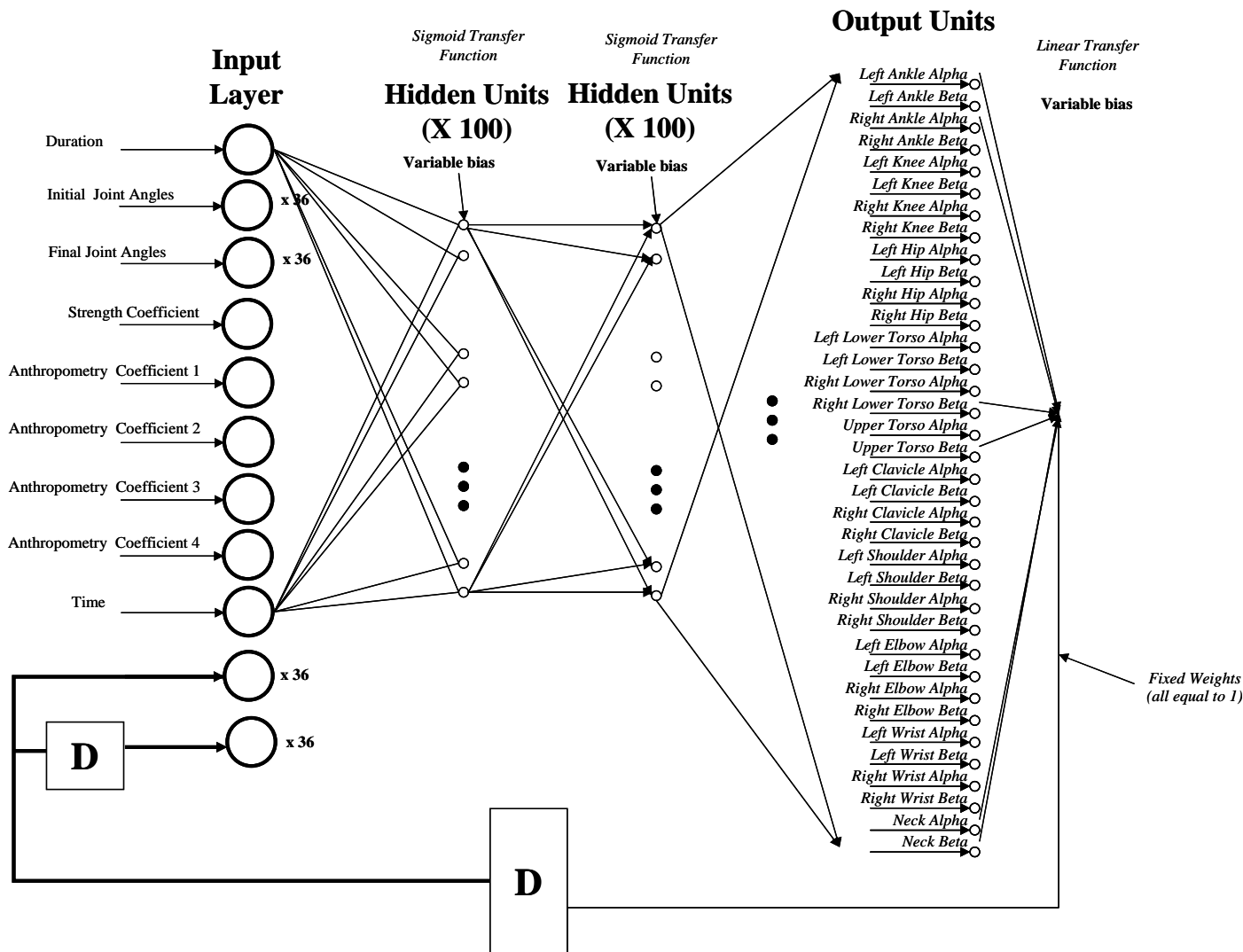


Figure 60. Three-dimensional network structure using joint angles as the input and prediction basis. Although all layers are fully interconnected, some connections are omitted for clarity. Boxes with 'D' represent a single time delay. The 'x 36' next to four of the inputs indicates that each of these nodes represents thirty-six different inputs (each corresponding to one of the outputs).

Given the results obtained for the two-dimensional network, the training set that produced three distinct generalization datasets was used here. This training dataset, referred to in the two-dimensional discussion as the 'second training set', used data from 16 randomly selected participants, but the 'Deliver' and 'Bring back' movements to the near and far Middle Lower and Middle Upper locations performed by these participants were not included in the training dataset. These movements were instead used in the verification dataset. This training approach generated a network that would have to predict motions that were novel to it, supporting (if performance

was adequate) its use as a movement prediction tool. The split in the data allowed three distinct verification sets to coexist. The first verification set would allow for observation of the network's predictive ability for novel movements performed by individuals whose data was used in the training process. The second verification set allowed for observation of the network's predictive ability for novel movements performed by individuals whose data was not used in the training process. The third verification set allowed for observation of the network's predictive ability for familiar movements performed by individuals whose data was not used in the training process.

ANOVA was performed to determine significant differences in prediction error as a function of task characteristics and training or verification dataset. Comparisons were performed in joint position units. Significant differences within significant main effects were determined using Student-Newman-Keuls (SNK) tests. A Type I error of 1% was used across all statistical tests.

As for the posture prediction models, the Jack™ simulation environment was used to predict motion paths for the same empirical tasks used in developing the ANN-based model. This comparison was limited to the 3D model given that the Jack™ environment is fully three-dimensional. The procedure to obtain these predictions was already discussed in the posture prediction chapter. Note that these comparisons were performed in terms of joint angles, since using joint position would have explicitly included in the Jack™ prediction error any inaccuracies in anthropometric scaling for the different participants. Data were not distinguished in terms of training or generalization for these comparisons, as the network performance was similar across these datasets. Note also that the 3DSSPP™ model was not compared against the ANN-based model, since 3DSSPP™ functions in a static environment. For the 3DSSPP™ model to generate motion predictions, the path of the box would have had to be provided, which would have provided 3DSSPP™ with information that was not available to the ANN-based model.

8.2.2.1 Results

The mse threshold for the training set with all data for 16 of the 20 participants and excluding movements to the middle lower and middle upper locations was set at 0.001 rad^2 . Training was manually stopped when the mse approximated 0.042 rad^2 , after the training process had been running for approximately a month on a 2 GHz Pentium-level processor desktop

computer. At this point, the error had not stabilized according to the typical definition used in this document, but its rate of decrease had slowed down considerably. A total of approximately 150,000 epochs had been completed when training was manually stopped.

This 0.042 rad^2 error (which, as before, was calculated across participants, joints, and time samples) represented an rmse of 0.20 rad (11.7°). To compare directly across past models, however, these errors were translated to errors in the prediction of joint positions. The average joint position rmse for the training set was 4.84 cm (range: $0.64\text{-}7.93 \text{ cm}$).

Errors in the training set were dependent on the joint and direction of movement (Figure 61). Error in the antero-posterior axis was higher than error in the left-right axis, which in turn tended to be higher than error in the inferior-superior axis (with the exception of the ankle joints). As observed for two dimensions, errors also tended to increase down the ankle-to-hand kinematic chain. Statistical analysis of error across Movement Type ('Bring back', 'Deliver') and Location showed significant differences as a function of Location ($F(17,234)$, $p < 0.0001$). *Post hoc* tests of the Location factor showed that the Lower Near – and Upper Near – High Rotation locations had the highest rmse levels. Other locations were statistically indistinguishable (Table 28).

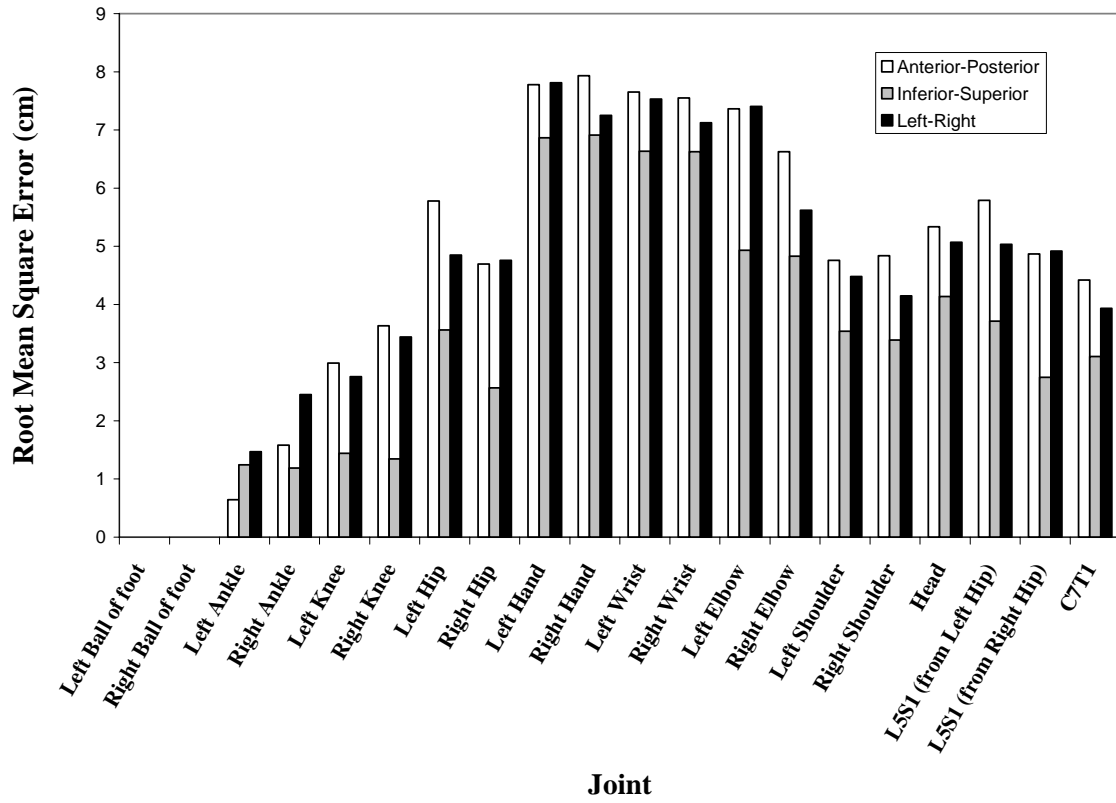


Figure 61. Root mean square error by joint and direction of movement. Training dataset.

Table 28. *Rmse levels across Movement Location. Training dataset.*

Location	rmse (cm)	SNK Letter Rating
Lower Near – High Rotation	9.34	A
Upper Near – High Rotation	9.20	B
Middle Far – High Rotation	5.95	C
Lower Far – No Rotation	5.49	C, D
Upper Far – High Rotation	5.05	C, D, E
Lower Far – High Rotation	5.02	C, D, E
Lower Far – Medium Rotation	4.79	C, D, E
Lower Near – Medium Rotation	4.78	C, D, E
Lower Near – No Rotation	4.67	C, D, E
Upper Far – No Rotation	4.20	C, D, E
Upper Near – Medium Rotation	3.62	D, E
Middle Far – Medium Rotation	3.54	D, E
Upper Near – No Rotation	3.43	D, E
Middle Near – High Rotation	3.40	D, E
Upper Far – No Rotation	3.33	D, E
Middle Far – No Rotation	3.29	D, E
Middle Near – Medium Rotation	2.95	E
Middle Near – No Rotation	2.65	E

Errors in the verification set consisting of additional movements performed by the participants in the training set were also dependent on the joint and direction of movement (Figure 62). Error in the antero-posterior and left-right axes axis again exceeded error in the inferior-superior axis in all cases except the ankle joint. However, for this verification dataset, errors tended to be slightly higher in the left-right axis when compared to the anterior-posterior axis. Errors also increased down the ankle-to-hand kinematic chain. Statistical analysis of error across Movement Type ('Bring back', 'Deliver') and Location showed significant differences as a function of Location ($F(11,150)=12.11, p<0.0001$). *Post hoc* tests of the Location factor indicated that the Middle Lower Far Location with No Rotation group had significantly higher rmse levels than all other locations. Middle Lower locations tended to have higher rmse levels than Middle Upper locations (Table 29).

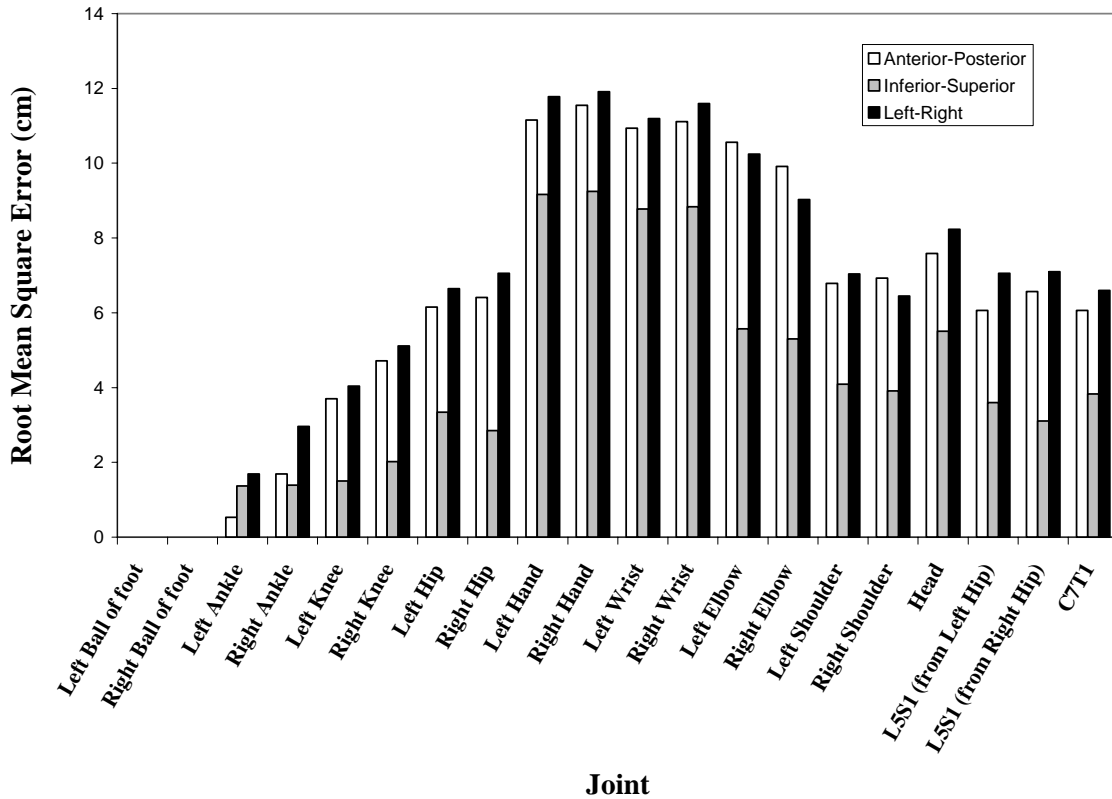


Figure 62. Root mean square error by joint and direction of movement. Verification dataset.

Table 29. Rmse levels across Movement Location. Verification dataset.

Location	rmse (cm)	SNK Letter Rating
Middle Lower Far Location – No Rotation	9.70	A
Middle Lower Near Location – No Rotation	8.13	B
Middle Lower Near Location – High Rotation	7.74	B, C
Middle Lower Far Location – High Rotation	7.65	B, C
Middle Lower Near Location – Medium Rotation	6.74	B, C, D
Middle Lower Far Location – Medium Rotation	6.53	C, D
Middle Upper Far Location – High Rotation	6.50	C, D
Middle Upper Far Location – Medium Rotation	6.17	C, D
Middle Upper Near Location – High Rotation	5.54	D
Middle Upper Near Location – Medium Rotation	5.40	D
Middle Upper Far Location – No Rotation	5.14	D
Middle Upper Near Location – No Rotation	4.87	D

Errors in the verification set consisting of movements in which the network was trained but were performed by a different set of participants showed joint- and direction of movement-dependent errors that were similar to those observed for the training set (Figure 63). Errors for

the left-right and anterior-posterior axes tended to be higher than errors in the inferior-superior axis. Errors in the left-right and anterior-posterior axes were comparable and evenly split in terms of the number of joints for which they represented the highest error. As before, errors also increased down the ankle-to-hand kinematic chain. Statistical analysis of error across Movement Type ('Bring back', 'Deliver') and Location showed significant differences as a function of Location ($F(17,51)=4.19, p<0.0001$). *Post hoc* tests of the Location factor showed that none of the locations were statistically distinguishable from at least a group of other locations (Table 30).

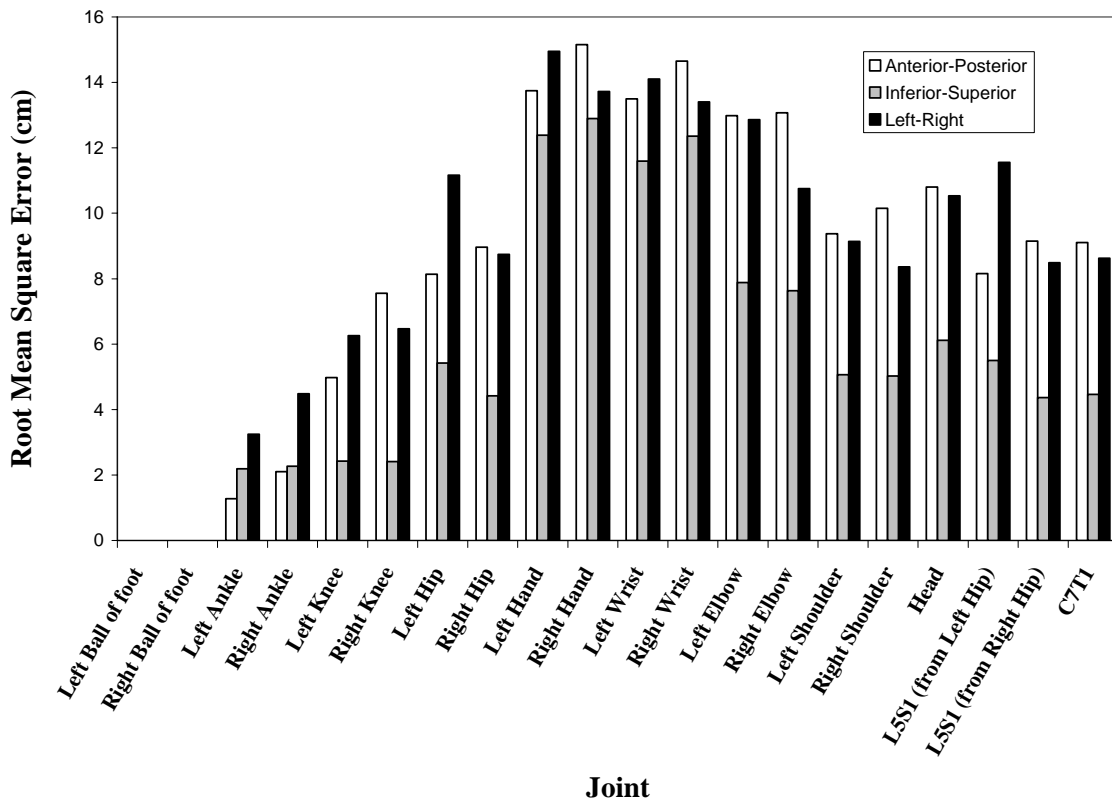


Figure 63. Root mean square error by joint and direction of movement. Verification dataset.

Table 30. *Rmse levels across Movement Location. Training dataset.*

Location	rmse (cm)	SNK Letter Rating
Lower Near – High Rotation	13.39	A
Lower Far – No Rotation	12.22	A, B
Lower Near – No Rotation	11.64	A, B, C
Lower Far – High Rotation	11.00	A, B, C, D
Lower Near – Medium Rotation	10.42	A, B, C, D
Lower Far – Medium Rotation	10.26	A, B, C, D
Upper Far – High Rotation	9.40	A, B, C, D
Upper Near – High Rotation	9.24	A, B, C, D
Middle Near – High Rotation	8.25	B, C, D
Upper Near – No Rotation	7.43	B, C, D
Middle Far – Medium Rotation	7.30	B, C, D
Middle Near – Medium Rotation	7.27	B, C, D
Upper Far – Medium Rotation	6.81	B, C, D
Middle Far – High Rotation	6.71	B, C, D
Upper Far – No Rotation	6.54	B, C, D
Middle Near – Medium Rotation	6.39	B, C, D
Middle Far – No Rotation	5.85	C, D
Middle Near – No Rotation	4.45	D

Errors in the verification set consisting of novel participants and movements were also dependent on the joint and direction of movement (Figure 64). As for the last verification dataset, errors for the left-right and anterior-posterior axes tended to be higher than errors in the inferior-superior axis. Errors in the left-right and anterior-posterior axes were comparable and evenly split in terms of the number of joint for which they represented the highest error. As before, errors also increased down the ankle-to-hand kinematic chain. Statistical analysis of error across Movement Type ('Bring back', 'Deliver') and Location showed no significant differences as a function of Location (Table 31). As observed in the verification set with the same movements but familiar participants, lower target locations tended to have higher rmse levels than higher locations.

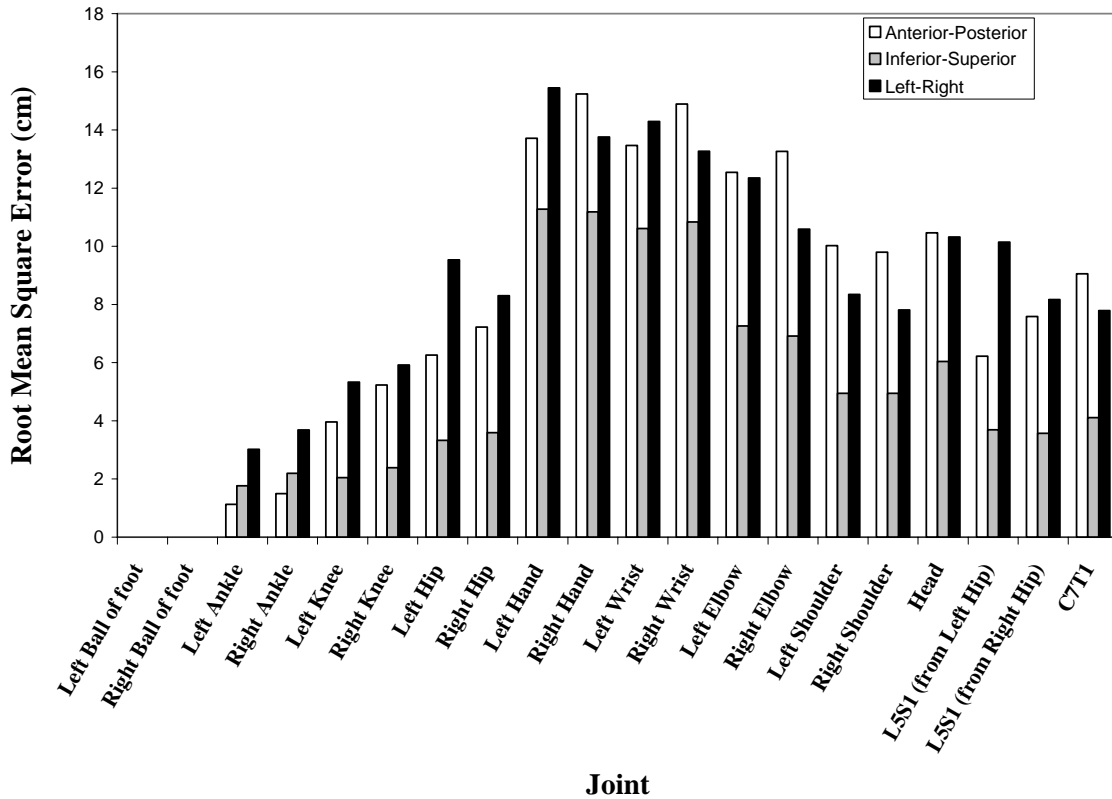


Figure 64. Root mean square error by joint and direction of movement. Verification dataset.

Table 31. Rmse levels across Movement Location. Verification dataset.

Location	rmse (cm)	SNK Letter Rating
Middle Lower Far Location – No Rotation	10.52	A
Middle Lower Near Location – No Rotation	9.82	A
Middle Lower Near Location – High Rotation	9.46	A
Middle Lower Far Location – High Rotation	9.32	A
Middle Lower Far Location – Medium Rotation	8.92	A
Middle Lower Near Location – Medium Rotation	8.56	A
Middle Upper Near Location – High Rotation	8.10	A
Middle Upper Far Location – High Rotation	8.01	A
Middle Upper Far Location – Medium Rotation	7.56	A
Middle Upper Near Location – No Rotation	7.25	A
Middle Upper Far Location – No Rotation	6.71	A
Middle Upper Near Location – Medium Rotation	6.53	A

The generalization abilities of the network were tested statistically by comparing rmse levels across the training and verification datasets. An ANOVA considering the different datasets showed a significant difference in rmse ($F(3,36)=66.60, p<0.0001$) between datasets.

The training dataset had the lowest average rmse level (4.84 cm), with the dataset including novel movements performed by familiar participants having the second lowest average rmse level (6.81 cm). The remaining two datasets, which employed novel participants, were statistically indistinguishable based on their rmse level (range: 8.78 cm – 8.96 cm).

Analysis of rmse levels by subject showed relatively close clustering (Table 32). However, subject 11 appeared to exhibit higher rmse than any other subject, including the other subjects included within the generalization dataset. The generalization subjects also tended to have slightly higher rmse levels than the training subjects.

Table 32. Root mean square error (in degrees) by subject, split in training and generalization groups.

	Subject Number	Rmse (degrees)
Training	2	24.56
	4	19.99
	5	23.51
	6	15.21
	7	17.16
	8	17.48
	9	21.1
	10	19.11
	12	18.46
	13	16.9
	14	15.26
	15	19.38
	17	23.29
Generalization	18	14.09
	19	18.61
	20	16.98
	1	26.51
	3	26.12
	11	29.66
	16	25

Qualitative observation showed that the Jack™ environment resulted in higher average joint prediction errors than the ANN model (Table 33). This difference in prediction errors between models was large enough to be statistically significant ($F(1,38)=912.23, p<0.0001$). The mean rmse for the ANN was 21.0°, whereas the mean rmse for the Jack™ simulation environment was 69.8° (note that rmse levels are now expressed in terms of joint angles). The

interactions of Movement Location X Model and Joint X Model were also significant ($F(29,496)=16.40, p<0.0001$ and $F(35,646)=262.09, p<0.0001$). The interaction between Movement Type and Model could not be tested due to insufficient degrees of freedom.

Table 33. Average network error in comparison to observed average for the JackTM simulation environment.

	Left Ankle Alpha	Left Ankle Beta	Right Ankle Alpha	Right Ankle Beta	Left Knee Alpha	Left Knee Beta	Right Knee Alpha	Right Knee Beta	Left Hip Alpha	Left Hip Beta	Right Hip Alpha	Right Hip Beta	Left Lower Torso Alpha	Left Lower Torso Beta	Right Lower Torso Alpha	Right Lower Torso Beta	Upper Torso Alpha	Upper Torso Beta
ANN	7.7	5.7	15.4	5.9	21.4	5.4	38.2	6.2	30.0	16.2	26.9	7.4	10.9	6.4	13.1	6.3	39.1	9.1
Jack	10.6	11.3	31.8	11.5	65.0	11.3	86.0	10.7	89.4	25.2	72.3	16.3	28.7	15.3	37.9	15.0	101.8	26.9

	Left Clavicle Alpha	Left Clavicle Beta	Right Clavicle Alpha	Right Clavicle Beta	Left Shoulder Alpha	Left Shoulder Beta	Right Shoulder Alpha	Right Shoulder Beta	Left Elbow Alpha	Left Elbow Beta	Right Elbow Alpha	Right Elbow Beta	Left Wrist Alpha	Left Wrist Beta	Right Wrist Alpha	Right Wrist Beta	Neck Alpha	Neck Beta
ANN	11.3	6.9	11.5	6.5	55.8	13.1	45.2	13.2	16.8	13.4	26.2	13.8	17.4	12.2	17.4	12.2	38.0	10.6
Jack	27.3	14.8	36.1	14.7	199.5	31.7	113.7	31.4	47.3	45.0	100.4	44.8	178.0	30.0	145.3	23.6	65.3	47.2

8.2.2.2 Implications of results for motions in three dimensions

The results show that shifting a prediction model from two dimensions to three dimensions is a large step that requires substantial processing power and increases the prediction errors. However, the ANN approach was robust enough to assimilate the training data reasonably well, and prediction errors in the verification datasets, while higher than those for the training set, were not necessarily dismal enough to suggest discarding the ANN modeling approach.

When errors in the first training and verification datasets are specified in terms of angles, they are shown to be smaller than the standard deviations for the between- and within-subject mean movement trajectories (Table 34). This suggests that the errors in network predictions are not beyond the variability in the movement that can be expected when an individual repeats a motion, and strengthens the argument that the network is capable of synthesizing the dataset.

The network also performed well in modeling the amount of variability within the dataset (Figure 65-Figure 67). Note that these plots are based on the complete dataset, not on a specific training or generalization subset. With the exception of a few angles (e.g. right knee α), predicted variability envelopes modeled the bounds set by between-subject variability within a few degrees. This pattern was consistent among different levels of rotation. Note that the movement location depicted in the figures is a lower far location, which typically showed the largest errors observed in the dataset. Figures for a middle lower location are also included (Figure 68). This location was not included within the training dataset and consequently there is less overlap between the predicted and empirical performance envelopes. The concordance between regions, however, is still considerable.

Table 34. Average network error in comparison to observed average between- and within-subject variability. Maximum values are italicized.

	Left Ankle Alpha	Left Ankle Beta	Right Ankle Alpha	Right Ankle Beta	Left Knee Alpha	Left Knee Beta	Right Knee Alpha	Right Knee Beta	Left Hip Alpha	Left Hip Beta	Right Hip Alpha	Right Hip Beta	Left Lower Torso Alpha	Left Lower Torso Beta	Right Lower Torso Alpha	Right Lower Torso Beta	Upper Torso Alpha	Upper Torso Beta
Training Set	6.1	5.1	14.4	4.8	13.4	4.7	26.1	5.1	21.9	12.4	17.7	6.1	8.5	5.4	10.4	5.5	28.5	7.4
Novel Movements, Familiar Subjects	6.7	5.4	13.5	5.9	26.7	5.7	45.8	6.9	32.5	15.2	27.9	7.5	11.7	6.6	14.1	6.1	40.6	9.8
Novel Subjects, Familiar Movements	<i>11.7</i>	<i>7.8</i>	<i>22.5</i>	<i>8.0</i>	<i>28.4</i>	<i>6.9</i>	<i>48.8</i>	<i>7.0</i>	<i>39.5</i>	<i>29.3</i>	<i>38.6</i>	<i>9.4</i>	<i>13.4</i>	<i>7.4</i>	<i>16.5</i>	<i>8.0</i>	<i>53.8</i>	<i>11.2</i>
Novel Subjects and Movements	10.9	6.2	14.2	7.4	22.2	6.1	43.4	7.3	40.3	9.7	39.8	9.2	14.3	8.9	16.3	7.5	53.9	<i>11.3</i>
Between Subjects	9.8	7.3	23.5	7.7	33.3	<i>7.5</i>	73.0	<i>8.3</i>	84.8	22.8	73.4	9.7	<i>19.1</i>	8.3	22.2	8.5	97.4	9.8
Within Subjects	6.6	6.3	<i>26.6</i>	6.7	<i>47.3</i>	6.1	<i>91.3</i>	7.8	<i>95.0</i>	<i>37.1</i>	<i>85.0</i>	9.1	14.3	4.6	16.6	5.0	<i>114.8</i>	10.3

	Left Clavicle Alpha	Left Clavicle Beta	Right Clavicle Alpha	Right Clavicle Beta	Left Shoulder Alpha	Left Shoulder Beta	Right Shoulder Alpha	Right Shoulder Beta	Left Elbow Alpha	Left Elbow Beta	Right Elbow Alpha	Right Elbow Beta	Left Wrist Alpha	Left Wrist Beta	Right Wrist Alpha	Right Wrist Beta	Neck Alpha	Neck Beta
Training Set	9.1	5.8	9.2	5.7	34.6	10.2	32.0	10.5	13.2	10.5	24.6	10.5	12.4	10.1	14.0	10.0	29.8	8.4
Novel Movements, Familiar Subjects	12.2	7.3	12.6	6.6	66.5	13.2	53.6	13.1	18.6	14.7	28.4	15.4	18.3	13.1	18.5	13.4	41.3	11.1
Novel Subjects, Familiar Movements	14.1	8.4	14.3	7.7	70.2	18.0	54.8	18.0	20.5	16.8	28.1	17.8	24.8	15.0	21.6	14.3	51.2	13.5
Novel Subjects and Movements	14.0	8.0	14.0	7.8	76.2	17.4	55.3	17.5	20.5	15.9	23.5	15.9	23.0	14.1	21.5	14.5	41.9	13.7
Between Subjects	<i>16.0</i>	<i>10.4</i>	14.7	9.8	<i>154.5</i>	17.3	84.9	17.4	23.6	19.4	47.6	19.8	26.0	22.7	26.1	22.0	53.6	13.7
Within Subjects	14.4	9.1	<i>15.3</i>	9.7	<i>186.4</i>	<i>19.0</i>	<i>136.8</i>	20.0	25.9	20.8	58.9	20.6	<i>30.4</i>	<i>24.4</i>	26.5	25.3	83.8	<i>14.6</i>

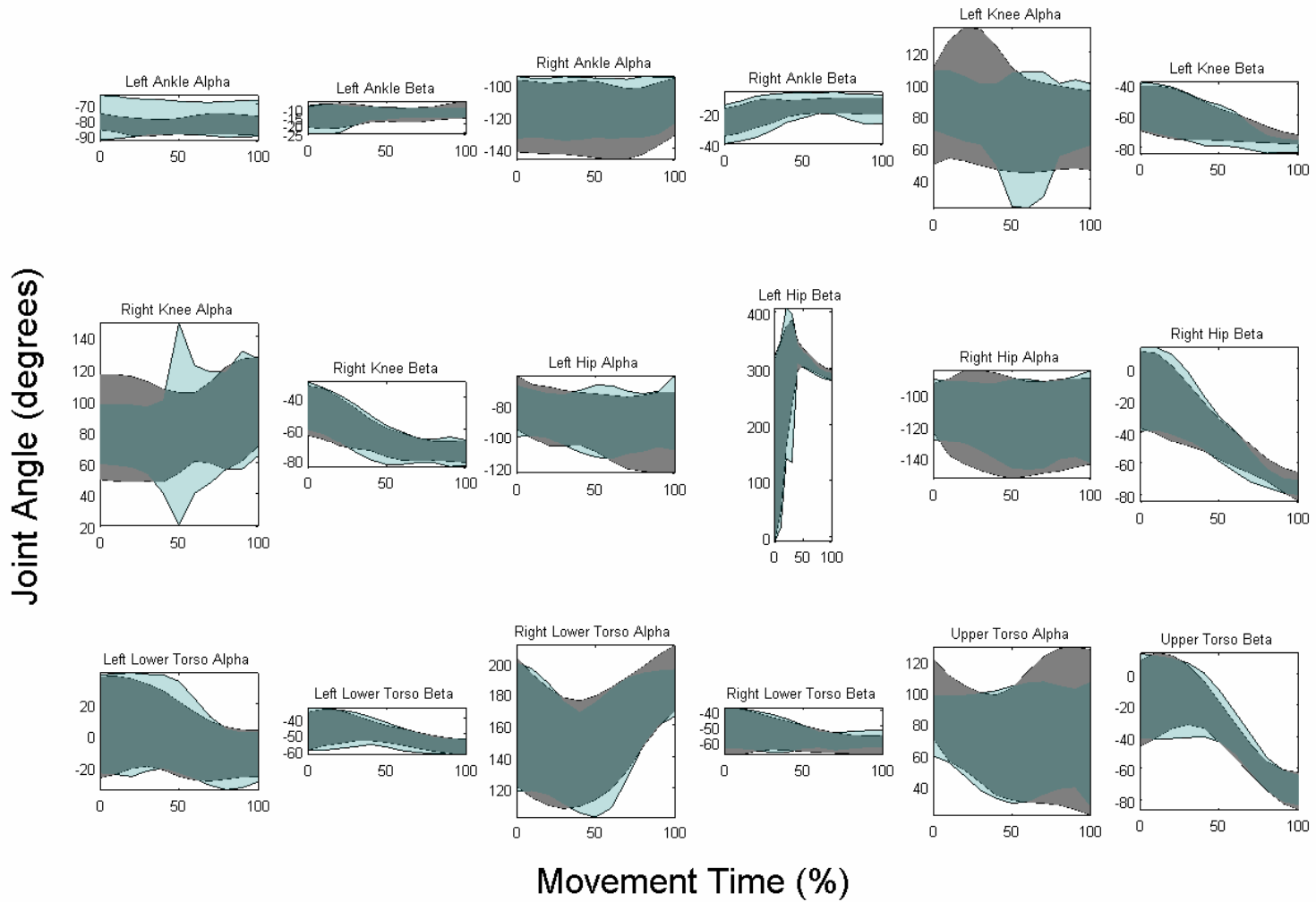


Figure 65. Comparison between target (light gray) and predicted (dark grey) between-subject variability. The shaded regions correspond to a ± 1 standard deviation region around the between-subjects mean for each group. No Rotation.

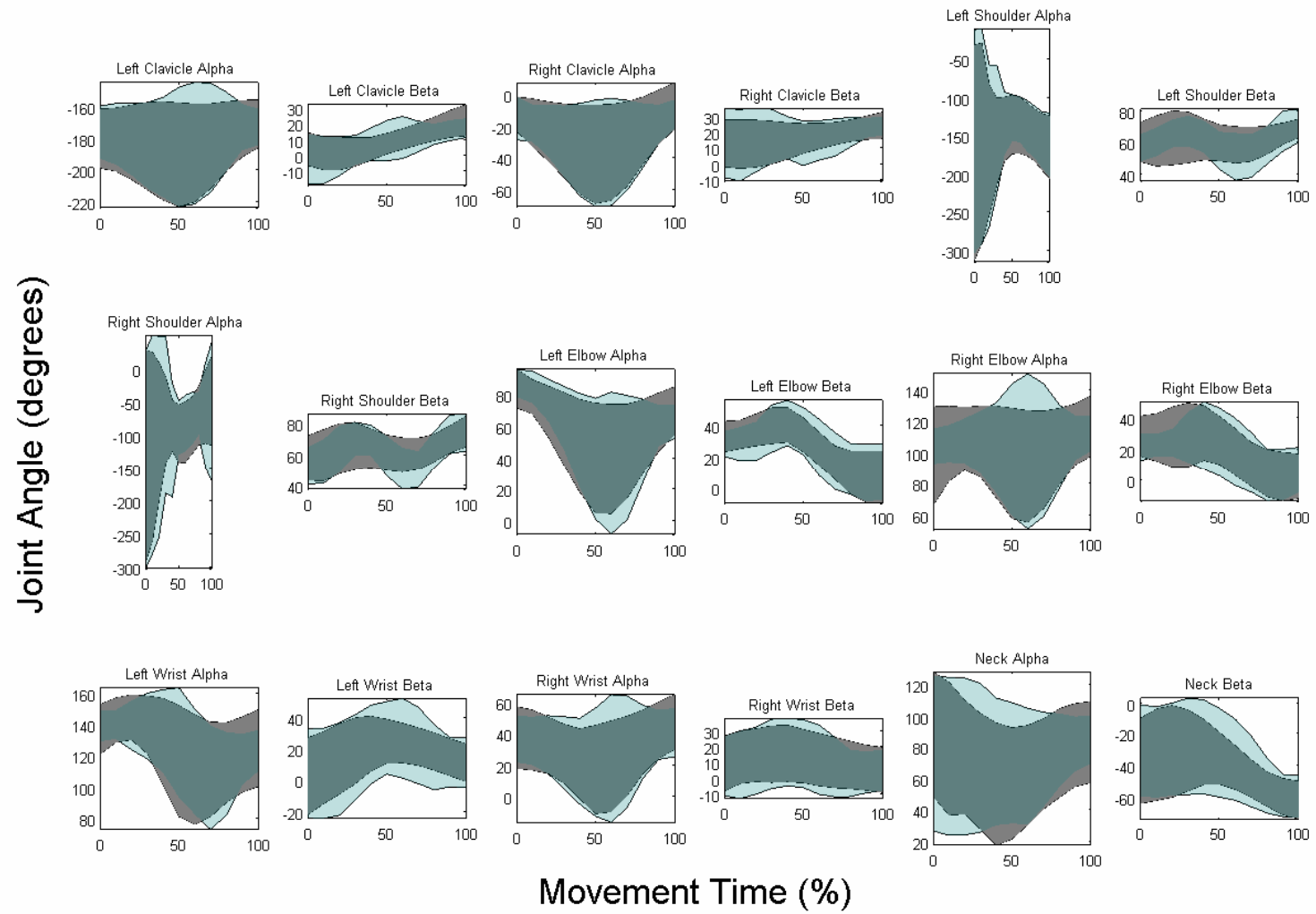


Figure 65 continued.

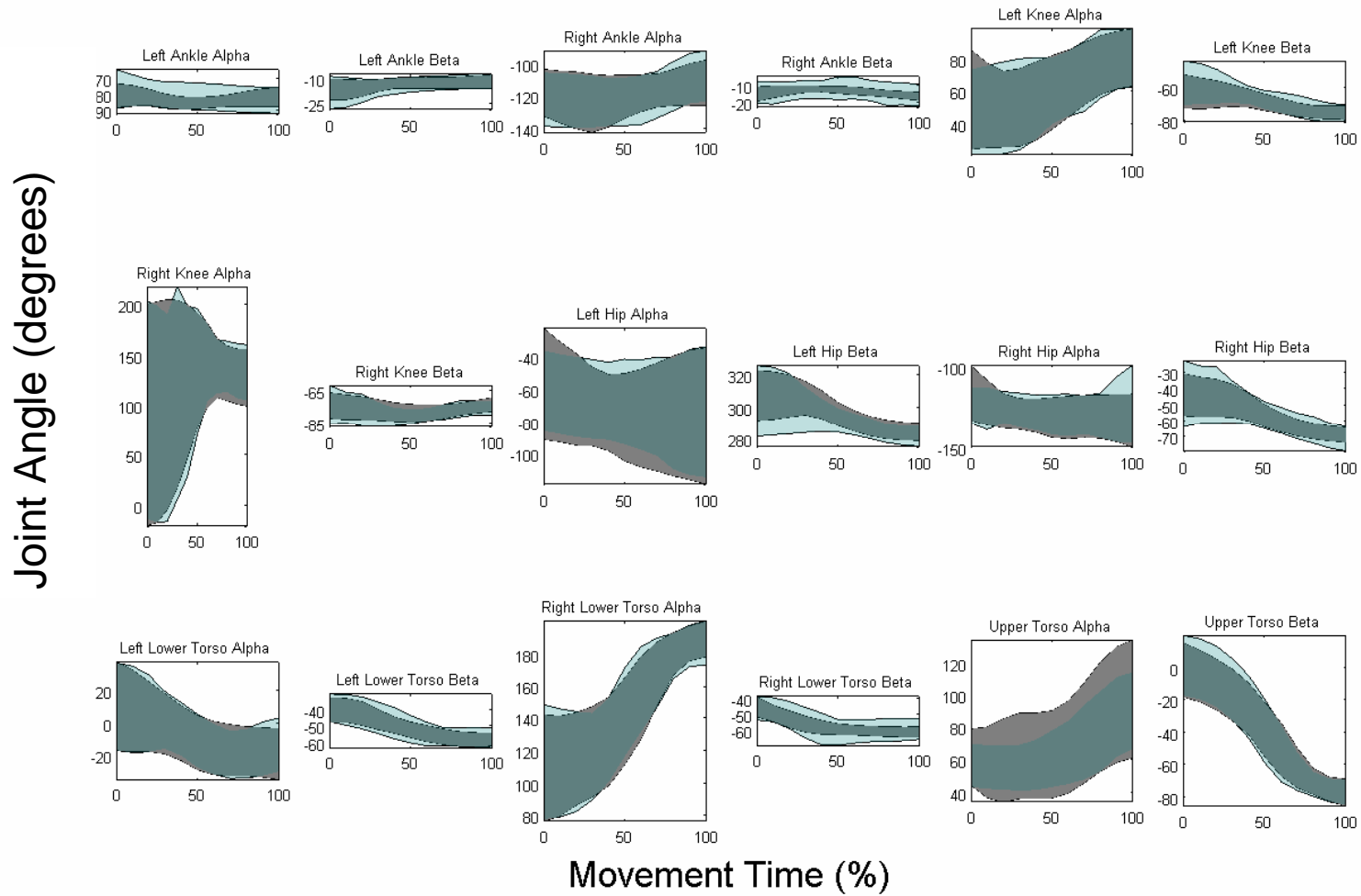


Figure 66. Comparison between target (light gray) and predicted (dark grey) between-subject variability. The shaded regions correspond to a ± 1 standard deviation region around the between-subjects mean for each group. Medium Rotation.

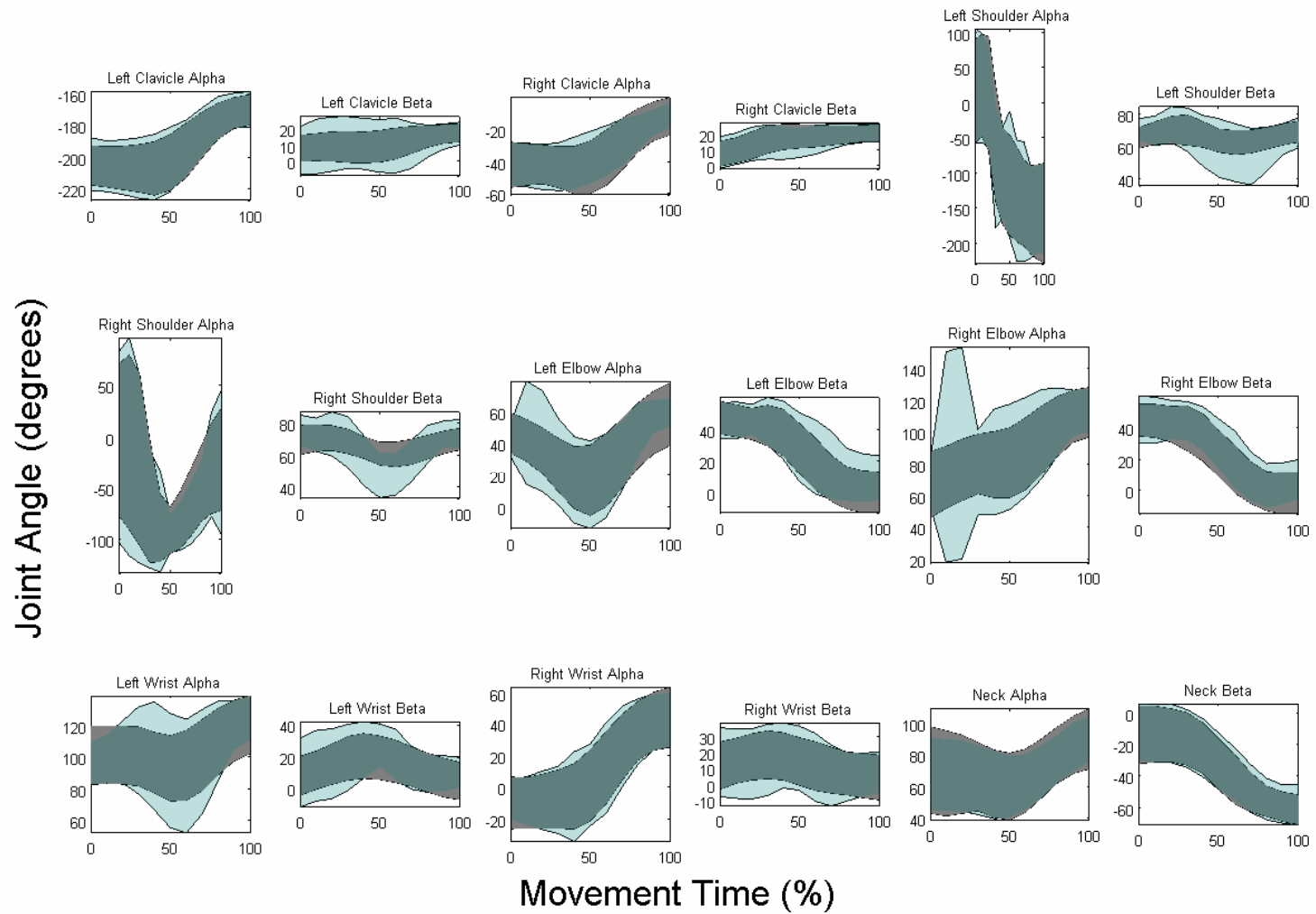


Figure 66 continued.

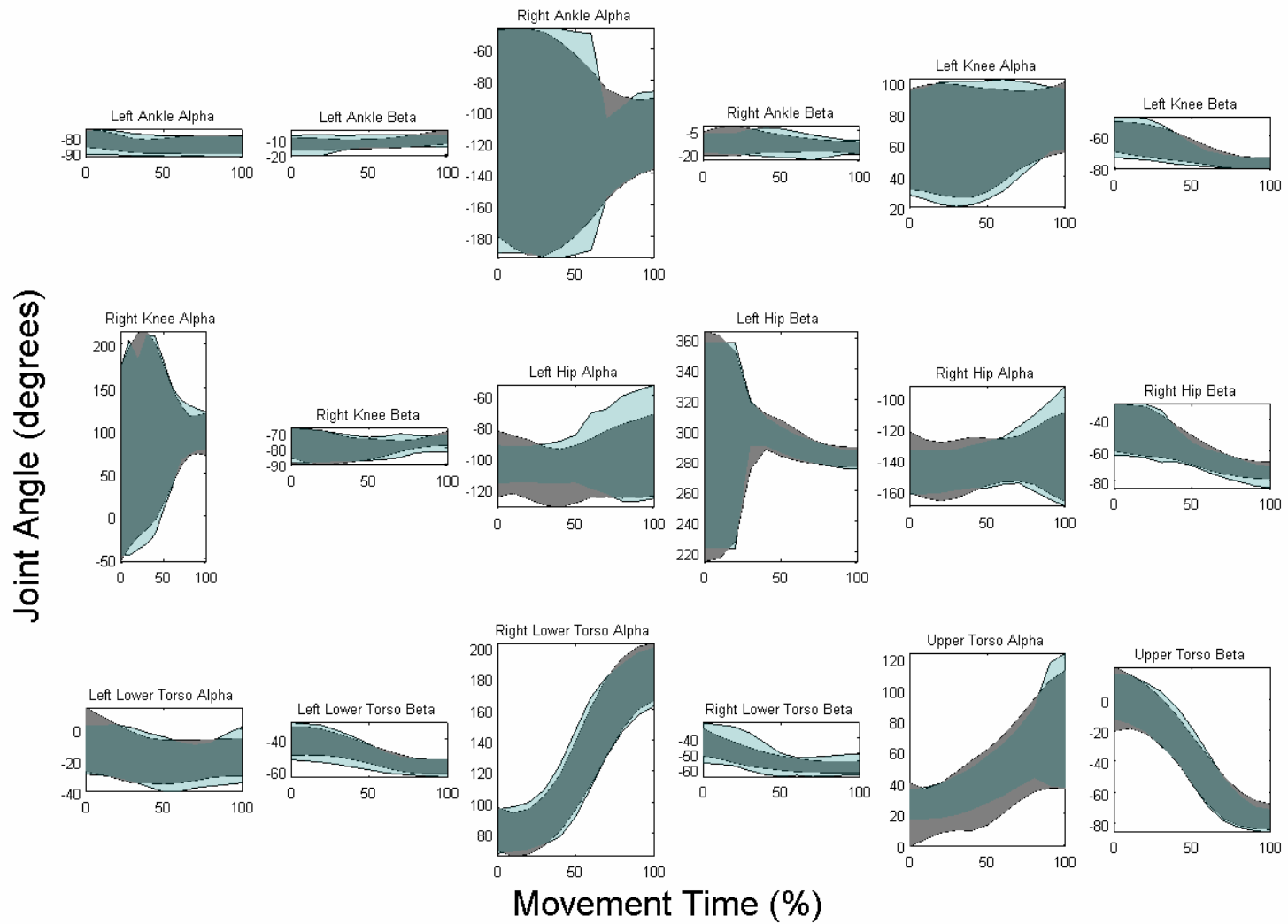


Figure 67. Comparison between target (light gray) and predicted (dark grey) between-subject variability. The shaded regions correspond to a ± 1 standard deviation region around the between-subjects mean for each group. High Rotation.

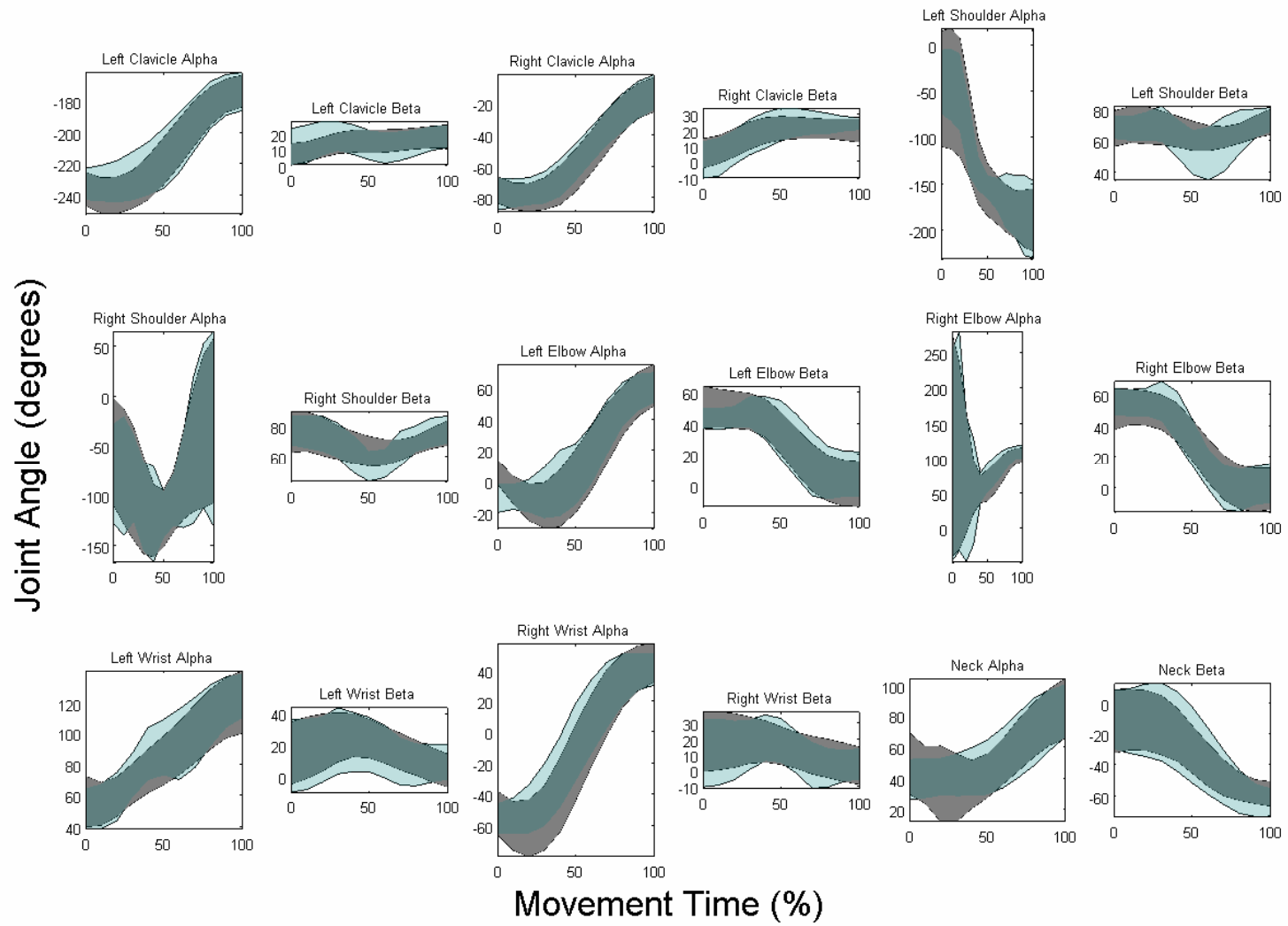


Figure 67 continued.

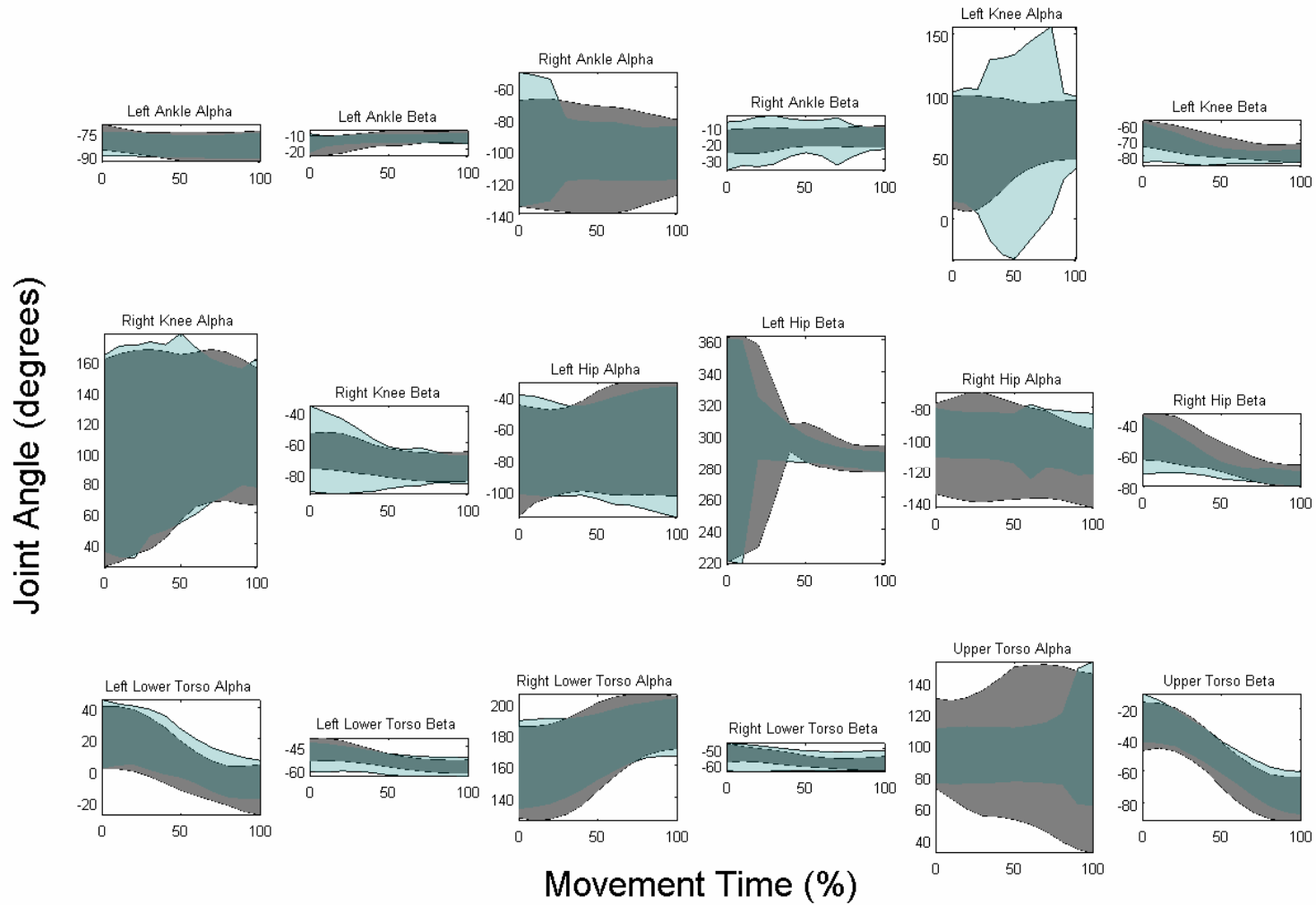


Figure 68. Comparison between target (light gray) and predicted (dark grey) between-subject variability. The shaded regions correspond to a ± 1 standard deviation region around the between-subjects mean for each group. No Rotation.

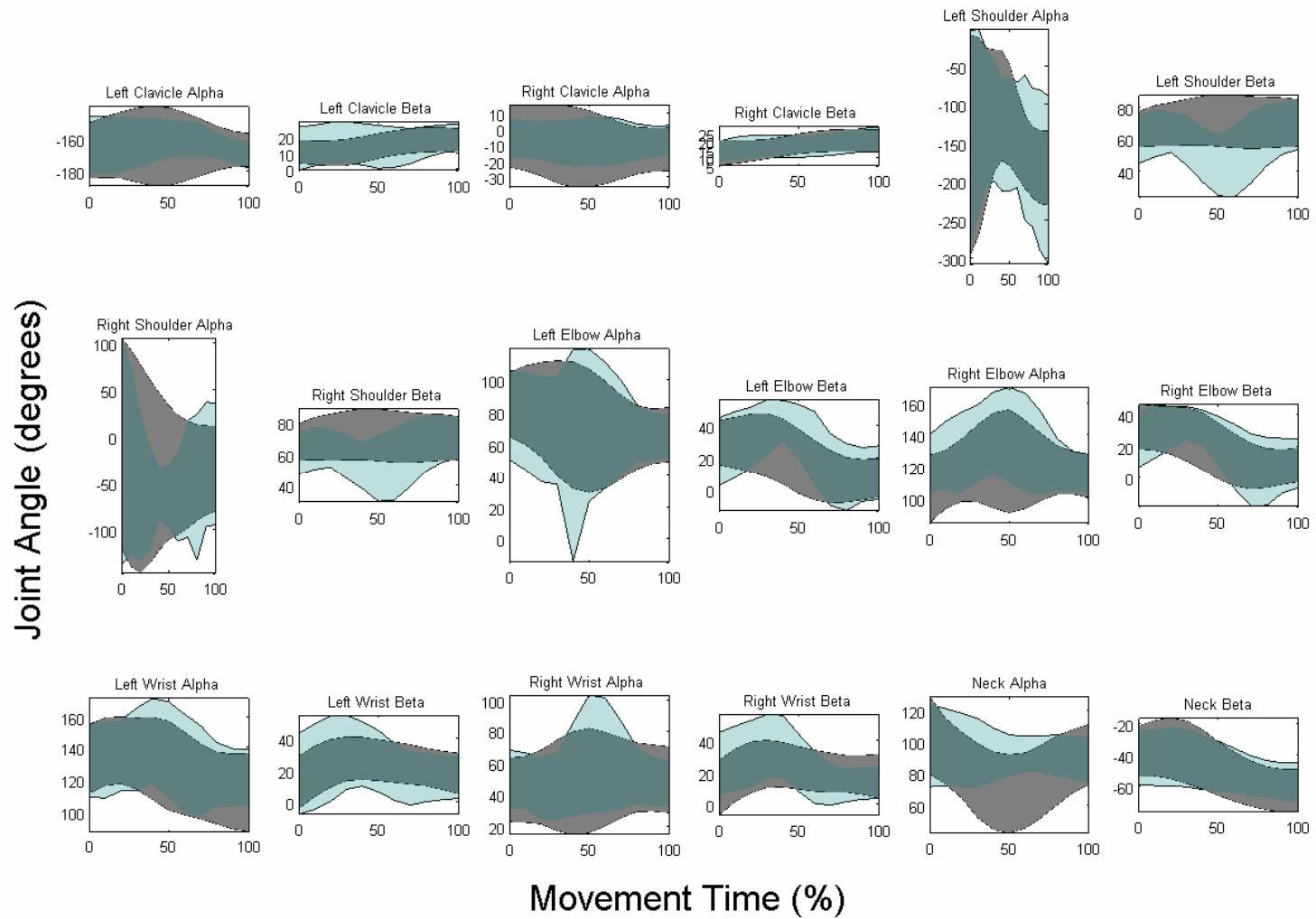


Figure 68 continued.

8.3 Model Characterization

The results suggest that, even though significant differences exist in training and generalization dataset errors (with generalization dataset errors being higher), the errors are low enough to indicate that the network was able to learn reasonably well the patterns that were presented to it and to apply this knowledge towards the prediction of movements from and to novel locations. Overall, it appears that useful predictions were made.

The important question of whether the network acts as a prediction or reproduction tool remains. Based on error analysis alone, the conclusion could be that the network acts as a reproduction tool. The networks tended to provide more accurate predictions for novel movements when they were performed by participants that had been included in the training set than when they were performed by novel participants. This might imply a certain level of over-adaptation of the network towards these participants. It is possible that a reduced training set might reduce this over-adaptation while leaving overall performance levels relatively unaffected, and this is a topic worthy of further research. However, it is important to note that these differences in prediction errors were relatively small and might not hold a substantial amount of practical significance, especially when when consideration is provided to dataset variability. Although the prediction errors tended to increase when novel conditions and/or participants were presented to the network, these errors are within the boundaries set by the dataset itself, and suggest that the network might indeed be acting as a prediction tool.

Perhaps the better question is whether the network can be used to predict movement for particular individuals, and the response to this question is more than likely that it could. Given the large within-subject variability, movements for a particular individual can be expected to vary substantially, and the network predictions tend to fall within this variability envelope. Thus, although the observed errors are not small, they are not large enough to make them implausible.

An alternate issue of importance is the use that the network made of the inputs that were provided. Inputs that were underutilized by the network play little or no role in the predictions and could thus be removed in future iterations to reduce model complexity. With few exceptions, the network inputs contributed evenly to hidden unit input for the case of two-dimensions (Figure 69 - Figure 71). These figures show the relative frequency (in terms of percentage, x-axis) with which particular inputs represented a certain percentage of a hidden unit

input, and are based on the complete dataset. This provides an indication of the relative importance of the input, in lieu of examining transfer functions (as was done in the previous chapter) which would be difficult to represent for this dynamic form of network. In general, a larger shaded area represents larger contributions of the input. Similar figures were also generated for the case of three-dimensions (Figure 72 - Figure 75).

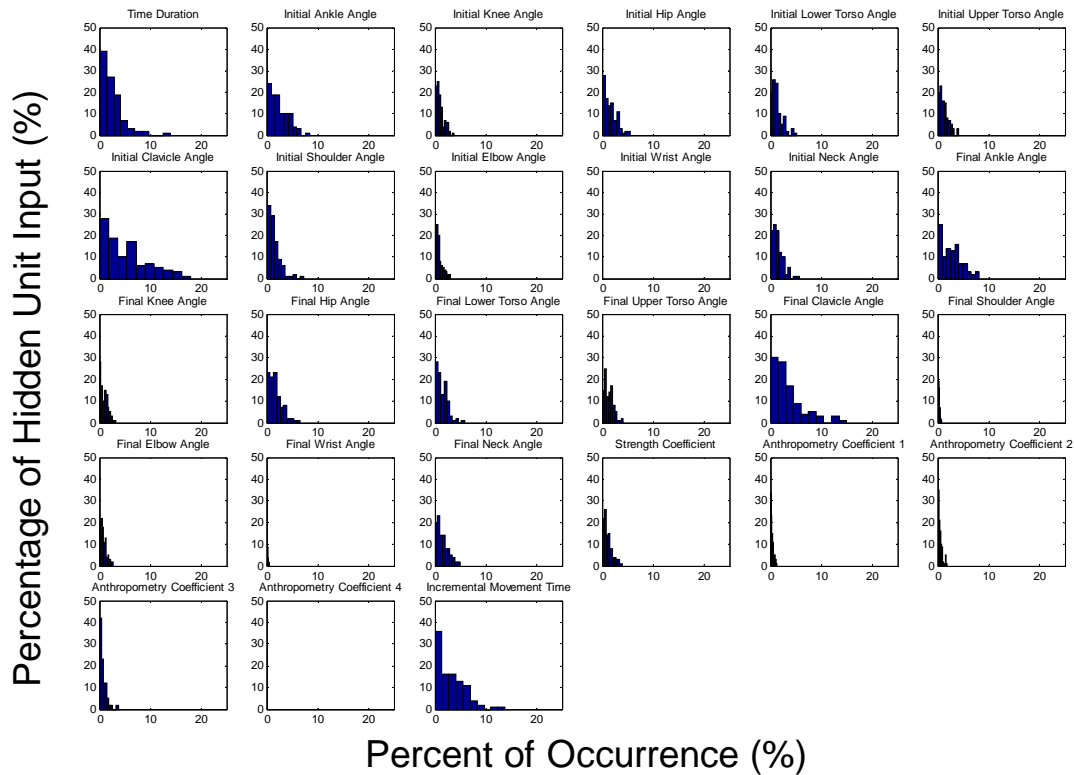


Figure 69. Hidden unit input distributions for inputs that are not delayed (Two dimensions).

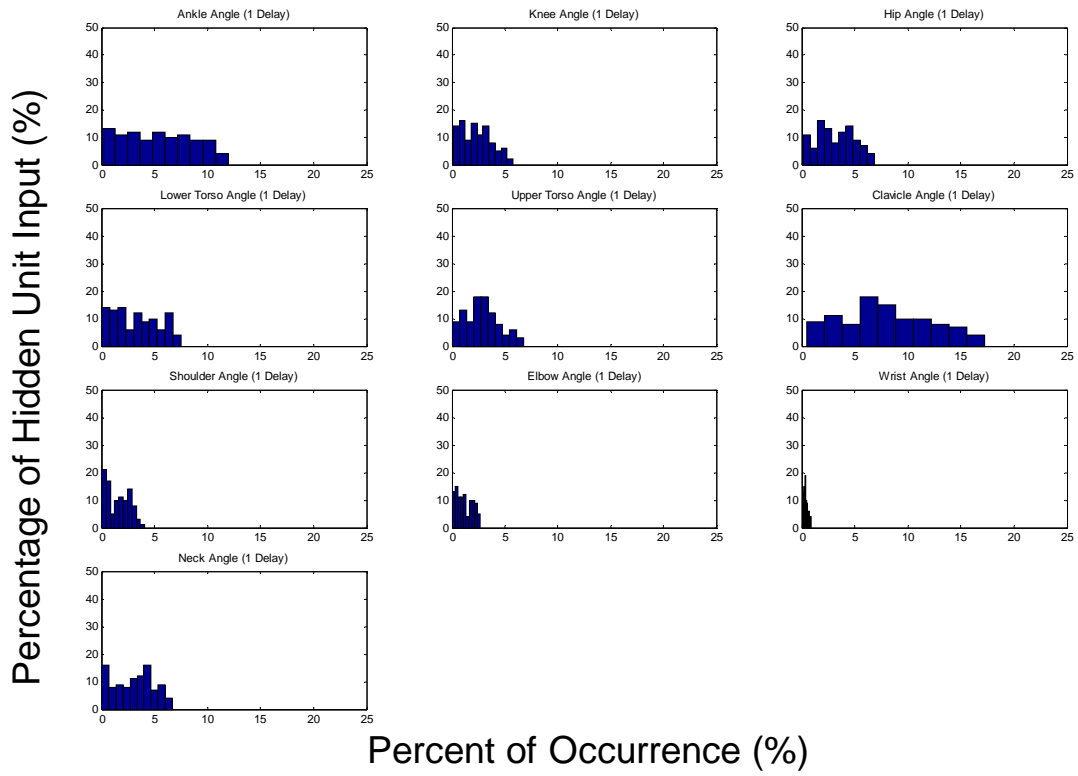


Figure 70. Hidden unit input distributions for inputs that have a single time-step delay (Two Dimensions).

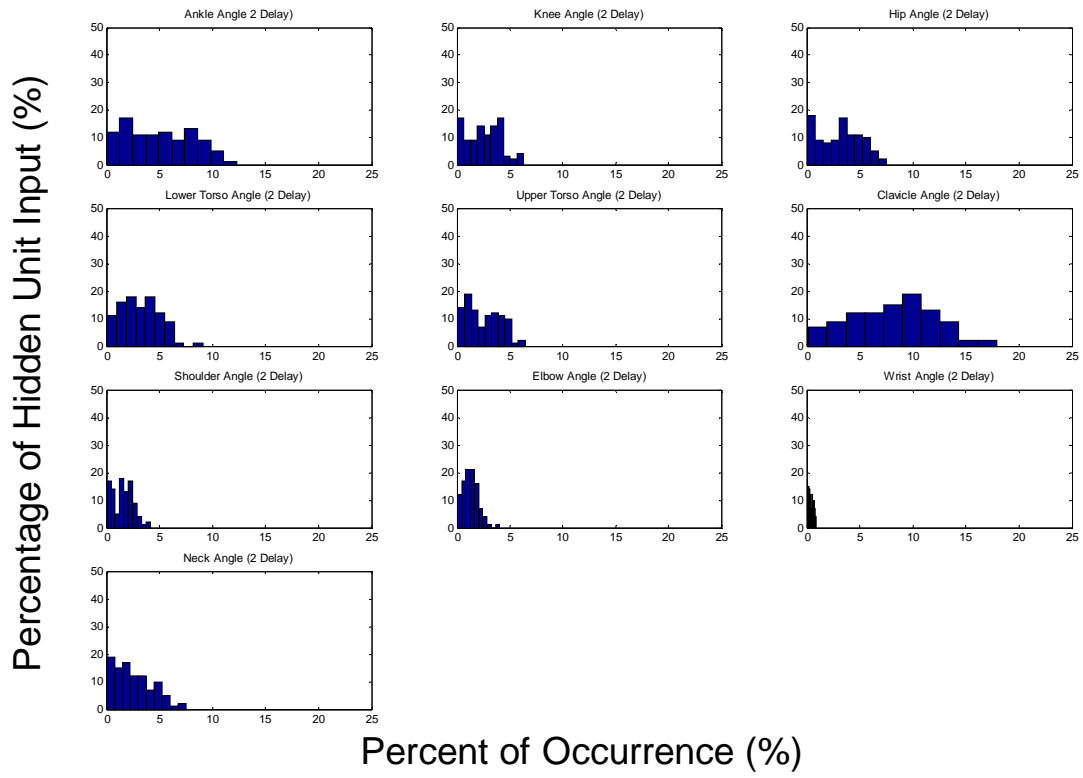


Figure 71. Hidden unit input distributions for inputs that have a double time-step delay (Two Dimensions).

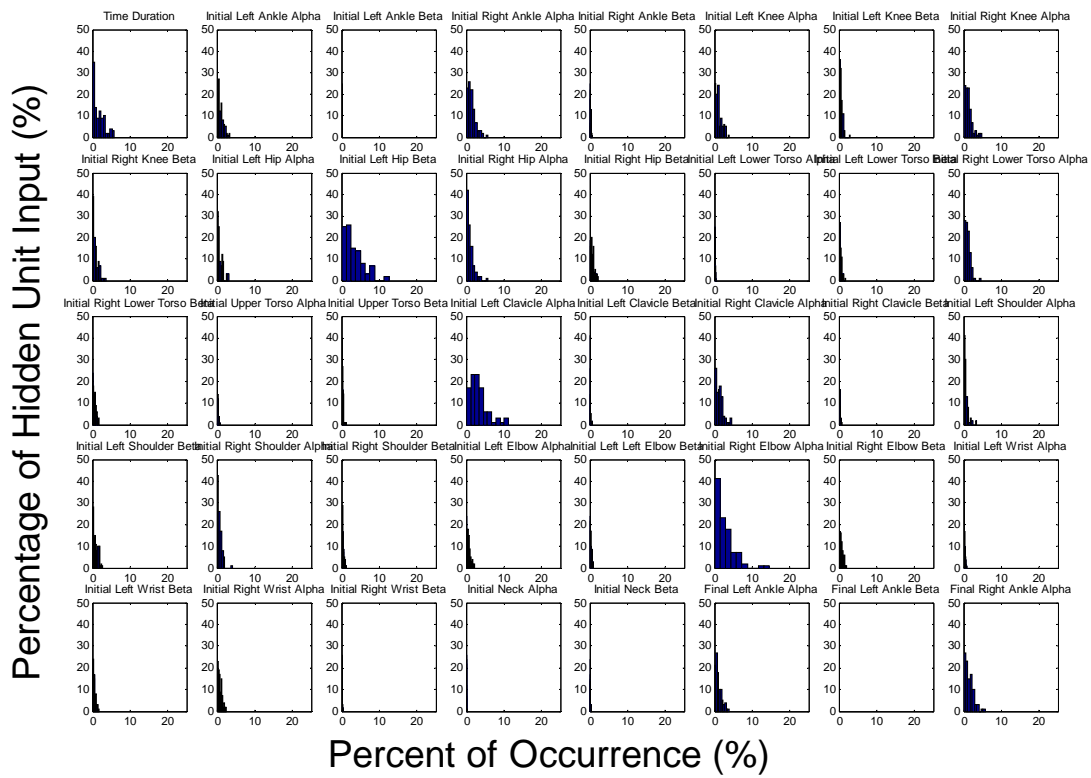


Figure 72. Hidden unit input distributions for inputs that are not delayed – Part 1 (Three dimensions).

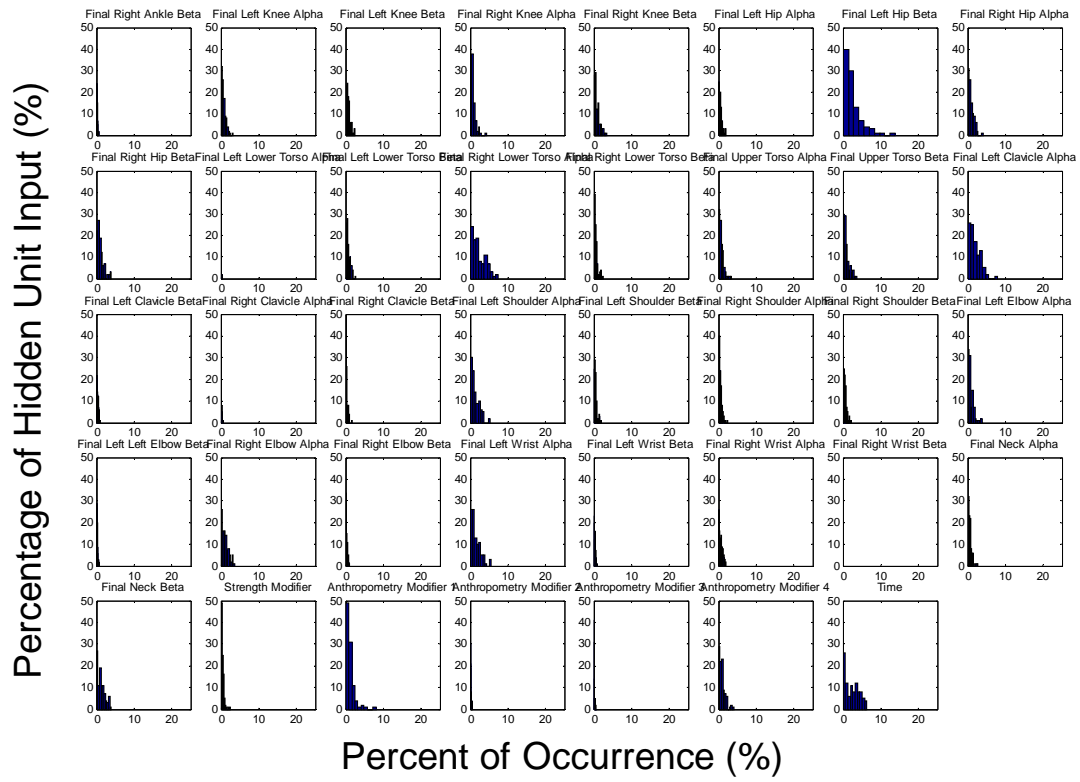


Figure 73. Hidden unit input distributions for inputs that are not delayed – Part 2 (Three dimensions).

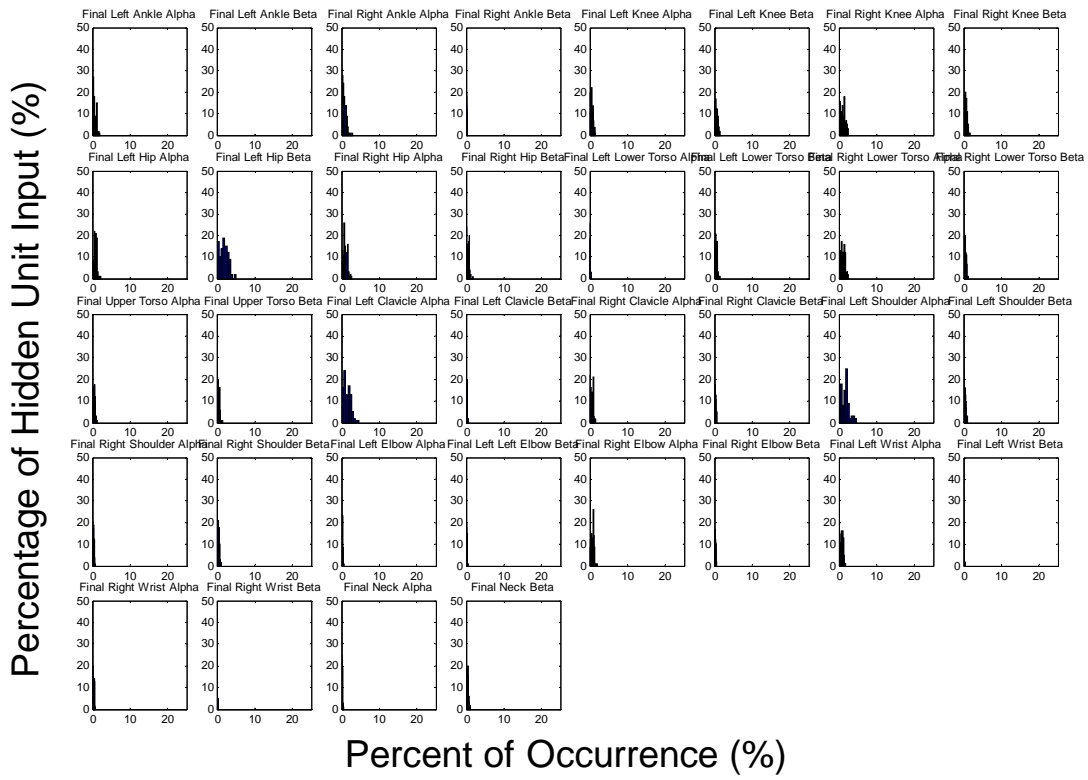


Figure 74. Hidden unit input distributions for inputs that have a single time-step delay (Three Dimensions).

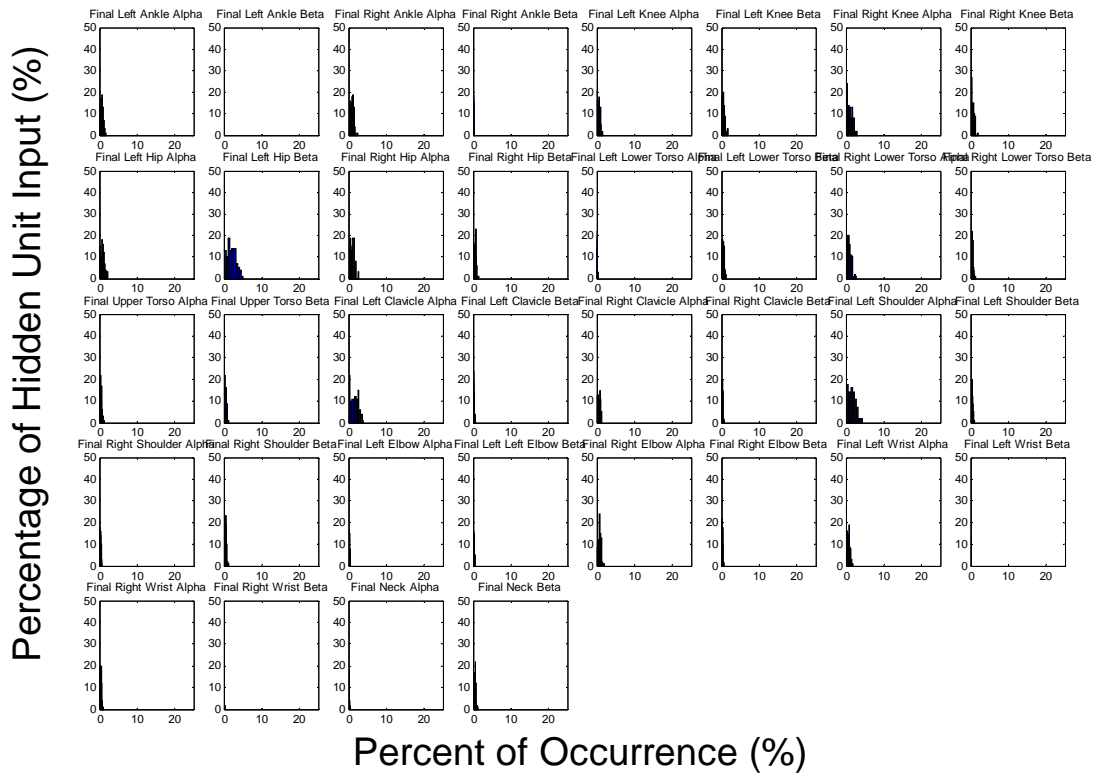


Figure 75. Hidden unit input distributions for inputs that have a double time-step delay (Three Dimensions).

For two dimensions, all of the delayed inputs showed discernible areas in the graphs, indicating that they produced measurable inputs to the hidden units at some point in the simulations. However, for the non-delayed inputs, the initial and final wrist angles, the final shoulder angle, and the fourth anthropometry coefficient showed almost no discernible area. These factors were thus not used very frequently within the network structure. Effects of wrist angles were also small within the delayed inputs.

Clavicle angles showed large areas across all delay conditions, suggesting that the network organized itself to provide a large degree of attention to this input, possibly due to its large variability. Recall that the effect of this angle on final posture is slight, as its projection on two-dimensions is very short compared to other segments. Thus, in this case it would appear that the network is wasting resources in trying to predict this joint. However, this does not necessarily imply inefficiency from the network, but rather a possible improvement in its structural design. The network has no indication of the relative importance of each of the joints, thus, it assigns equal weight to attempting prediction of each of the joints provided. It is possible

that network performance might be improved by removing this particular input in the future. Network complexity would be reduced, and the network could devote the additional resources to reducing errors across other joints that are associated with larger segmental lengths.

For three dimensions, it appeared that the delayed inputs carried a comparatively lower weight than some non-delayed inputs. Various inputs were used sparingly, specially those delayed inputs indicating delayed upper limb angles. It appears that the network focused a substantial portion of its resources into ‘listening’ to non-delayed inputs related to the lower limb, in contrast with the two dimensional case, where substantial network resources were dedicated to the delayed inputs.

Comparison with previous models can also aid in putting the observed errors in perspective. While the prediction errors observed might have been relatively large, these might be less than those observed in the past for other efforts. For example, the work of Lee (1988), employing optimization to predict motion in two dimensions, is also comparable to the current work. In lifts from the floor to knuckle height and based on graphs contained within the work, the ankle, elbow, and shoulder showed maximum absolute errors in the order of 20° , with lower average absolute errors in the 5° to 15° range. The knee and hip joints were slightly better predicted than other joints. This pattern and amount of error were also observed for lifts that transported a container from the floor up to knuckle height. These values are in many cases larger than the prediction errors observed for the 2-D ANN-based model in this chapter.

Lin et al. (1999) report mean square error values for an optimization model that minimizes the square of the joint torque to joint strength ratio, also in a two-dimensional workspace. These researchers also collected a dataset that included factorial combinations of knuckle and shoulder height lifts with various container sizes and weights. The shoulder height (i.e., higher) lifts had what appeared to be higher mse values across joints than the knuckle height lifts. Translated to rmse levels, these values would be 7.44° for the knuckle height lifts and 12.43° for the shoulder lifts for the elbow. The shoulder joint had errors of 15.13° for a knuckle height lift and 17.63° for a shoulder height lift. Equivalent knuckle height lift errors for the hip, knee, and ankle were 7.39° , 16.09° , and 3.87° , respectively. Equivalent shoulder height lift errors for these same joints were 10.11° , 6.17° (which was the sole instance in which the shoulder height lift error was lower than the knuckle height lift error), and 5.17° . These values are comparable in magnitude to the errors observed for the 2D model described in this chapter.

Comparisons in three dimensions generate similar conclusions. For example, Choi and Chung (2003) describe a three-dimensional motion prediction approach employing inverse kinematics. The authors tested empirical motion data for floor to knuckle height and floor to shoulder height at 0°, 45°, and 90° degree asymmetry, which were similar to the range of the motions reported here. Choi and Chung report average root mean square position errors in the 13 cm to 20 cm range, with associated standard deviations in the 6 cm to 11 cm range. These values are at the very least similar, and in some cases larger, than the values observed for the 3D ANN-based model presented in this chapter.

The ANN-based 3D model also compared favorably to the Jack™ simulation environment. The Jack™ environment resulted in higher prediction errors than the ANN-based model. Possible reasons for the lower performance levels observed for the simulation environment were discussed in Chapter 7: Jack™ is not designed for prediction of the ‘most likely’ posture, a knee bending behavior was not implemented, and grasping was not properly achieved. These reasons also apply to the interpretation of these results, and indicate that further development in the Jack™ behaviors is needed before an equitable comparison can be made against it.

As discussed in Chapter 7, note that Jack™ had access the same information that was available to the ANN-based model. This information included the initial and final box locations, anthropometric information for each participant, and the duration of the motion. In some cases, further information could have been provided to the program that might have improved their performance. For example, the orientation of the box as a function of time could have been provided to the Jack™ model. This information was not provided to Jack™ to avoid providing this model with any unfair advantage.

Overall, these comparisons demonstrate that a relatively simple network was able to acquire sufficient knowledge from the training set to allow for reasonable predictions, in light of what other approaches have been able to accomplish. The error levels obtained, however, are still large enough that the model requires improvement in order to be useful in applied settings. Possibilities for these improvements are considered in the next chapter.

Chapter 9 CLOSING DISCUSSION

The main objective of this investigation was to determine the feasibility of performing motion prediction using artificial neural network models. In achieving this objective, five experimental goals were posited in Chapter 4, and the work presented in the previous four chapters was designed with that goal in mind. The two initial goals of the investigation were, first, to determine whether a motion prediction model could be created based on a set of lift posture modifiers and, second, to establish whether a single model would be sufficient. The previous chapters illustrate that such a model can be created and that, other than separating the prediction of posture and motion, a single model is sufficient across a relatively comprehensive set of manual materials handling tasks. The potential ability of artificial neural networks to synthesize patterns of motion and elements of posture within relatively simple and easily solvable structures has been shown. However, these structures specify only a general form that the networks can follow, and it seems improvements are needed before these networks can be reliably used in motion prediction algorithms in more applied environments, especially when dealing with three dimensions.

A third goal of this investigation was to determine the sensitivity of the models to their input parameters, which was tested for both the posture and motion prediction models. For the posture prediction models, network output tended to be more sensitive to the inferior-superior box position. For the motion prediction models, the feedback loops received considerable weight. Across both types of networks, information on participant anthropometry and strength was heavily used.

The fourth goal of the research dealt with the evaluation of the networks. This is discussed later in this chapter, as alternative comparisons between the ANN predictions and the empirical data are performed. Before tackling this goal in more detail, however, it seems appropriate to further discuss some aspects of the final models developed.

First, the degree of difficulty involved in developing existing models to adjust to the situation at hand, especially in the 3-D case, precluded for the most part direct comparison of the ANN models to previous approaches (e.g. optimization-based). The computer platforms on which all of the models had been developed differed substantially from the computer platform employed for this study, and translation of the models would have required substantial work. Furthermore, some of the models had not been developed in the context of lifting, and would

have required considerable extensions on their original development to be made applicable to the current situation. When these efforts were weighted against the potential gains, it was determined that similar information could be obtained using the indirect (i.e. not using the same dataset) comparisons that have been discussed in the previous chapters. Additional comparisons, using a slightly different approach, are discussed later in this section.

Second, the tested ANN models need improvement in terms of accuracy and reliability. This is discussed in more detail at the end of this chapter. An important example, however, are the addition of constraints on the joint angles that limit them to physiologically plausible values. As will be discussed, these improvements are mostly needed in the 3-D situation, where more degrees of freedom were modeled. Without these improvements, it can be expected that ANN performance would be below the standard needed for applied settings.

Third, and last, it is important to note that segment axial rotations were not predicted in the 3D case, given limitations on the information contained within the dataset that was used. This factor has to be considered in comparing ANN predictions with other models that are set to provide segment rotations as part of the 3-D motion prediction process, as these models have been exposed to additional information that was not considered in this investigation.

The reader may recall that errors in this investigation were presented mostly in terms of the rmse for either joint angles or joint positions (or both), as applicable. This approach allowed the establishment of a relative performance measure for each of the models, which in turn allowed certain model structures to be selected, in relatively simple fashion, over others. Whenever a single performance indicator is selected, of course, there is the possibility that the chosen indicator is not sensitive enough to detect important changes between the situations that are compared. This risk was considered low enough in this investigation due to a variety of factors: (1) rmse has been used in the past in a variety of similar studies and is used widely in biomechanics as a performance measure; thus, its sensitivity to the errors typically observed in the field has been empirically shown, (2) the measure increases monotonically as separation between the actual and predicted motion paths increases, (3) differences in rmse between models developed in this investigation were fairly large and physically noticeable; thus, when differences in model performance existed, they were easily observable.

The real risk of describing model performance only in terms of rmse is that it is difficult to examine if differences between actual and predicted motions were due to the ANN implicitly

assuming particular motor control techniques that were not reflected in the empirical data, or vice versa. These possibilities can be tested, however, by defining what these possible motor control techniques may be, determining the adherence of both the ANN and the empirical data to each motor control technique, and analyzing the results of this adherence for systematic differences. A variety of motor control techniques have been suggested on the literature in terms of possible objective functions that are optimized by the motor control system. The following objective functions were selected for this empirical examination:

- Total torque (Dysart, 1994; Woldstad, 1997)

$$\int_0^T \sum |\tau_i| dt$$

- Muscle intensity (Dysart, 1994; Gagnon and Smyth, 1991; Woldstad, 1997)

$$\int_0^T \max \left| \frac{\tau_i}{s_i} \right| dt$$

- Balance (Dysart, 1994; Woldstad, 1997)

$$\int_0^T |\tau_{ball} - \tau_{heel}| dt$$

- Squared Torque (Woldstad, 1997)

$$\int_0^T \sum \tau_i^2 dt$$

- Cubed Intensity (Woldstad, 1997)

$$\int_0^T \sum \left[\frac{\tau_i}{s_i} \right]^3 dt$$

- Mobilization ('Jerk', Flash, 1987; Hsiang and McGorry, 1997)

$$\int_0^T \left[\frac{d^3 y(t)}{dt^3} \right]^2 + \left[\frac{d^3 z(t)}{dt^3} \right]^2 dt$$

- Strength Utilization (Muscle intensity squared, Hsiang and McGorry, 1997)

$$\int_0^T \sum \left[\frac{\tau_i}{s_i} \right]^2 dt$$

In all of these equations, T refers to the duration of the movement, τ_i refers to the torque at the i -th joint, s_i refers to the strength of the i -th joint, t refers to time, and y and z refer to y - and z - axis load positions.

The comparisons were made for two dimensions to simplify the calculations and the need for assumptions regarding weight distributions, locations of centers of mass, location of the center of gravity, and joint strength distributions. Furthermore, past work using similar functions in optimization paradigms has focused on two dimensions. It was also considered likely that result patterns observed for two-dimensions would also apply to the three-dimensional case, given that the kinematics on which these results are based would not be affected..

All of these measures required the calculation of joint torques, joint strengths, and/or joint kinematics with respect to time. The joint torques were calculated using the following equation:

$$\tau_i = M_{Static_i} + M_{CM_Accel_i} + M_{CM_Rotation_i} + M_{I\alpha_i}$$

where M_{Static} refers to the torque at the joint due to static forces, M_{CM_Accel} refers to the torque at the joint due to linear acceleration forces at the segment's center of mass, $M_{CM_Rotation}$ refers to the torque at the joint due to tangential acceleration forces at the segment's center of mass, and $M_{I\alpha}$ refers to the torque at the joint due to the segment's rotational inertia. The M_{Static} was calculated as:

$$M_{Static_i} = \tau_{i-1} + (r_{CM_i} \times W_i) + (r_i \times F_{i-1})$$

where r_{CM} refers to the moment arm from the segment's center of mass (calculated based on Table 3.6 of Chaffin and Andersson, 1991), W_i refers to the segment's weight, calculated based on a percentage of body weight (obtained from Table 3.5 of Chaffin and Andersson, 1991), r_i refers to the moment arm from the previous segment (or load), and F_{i-1} refers to the force at the previous joint.

The M_{CM_Accel} was calculated as $-m_i(r_i \times a_i)$, where m_i is the mass of the segment (based on the weight already calculated to obtain the static torque), and a_i is the linear acceleration of the segment. The $M_{CM_Rotation}$ was calculated as $r_{CM} \times [m_i (r_{CM} \times \alpha_i)]$, where α_i is the angular acceleration of the segment. The $M_{I\alpha}$ term was calculated as $(m_i * C^2 * r_i^2 + m_i * r_{CM_i}^2) \times \alpha_i$, where C is a constant taken from Table 3.13 of Chaffin and Andersson (1991). Velocities and accelerations were obtained using finite difference methods.

Strength distributions were determined using the equations in Table 6.2 of Chaffin and Andersson (1991), re-expressing the angles calculated here into the included angles that are used in that table. Note that these strength distributions are sensitive to male-female differences only;

a search for strength distributions based on a more detailed set of anthropometric criteria was unfruitful.

Comparisons of model predictions and empirical data with respect to the seven objective functions showed a number of statistically significant differences with respect to the data source (i.e. model prediction vs. empirical data).

The total torque objective function varied significantly as a function of movement location and movement type ($F(9,147), p < 0.0001$, $F(1,19), p < 0.0001$, respectively). Lower movement locations tended to have lower total torque measures than higher movement locations (Range: 2250.3 Nm – 13030.9 Nm). Movements of the ‘Deliver’ type had significantly higher average total torque values than ‘Bring back’ movements (‘Deliver’: 7978.7 Nm, ‘Bring back’: 5486.2 Nm). Predicted and empirical motions differed significantly in terms of their total torque ($F(1,19), p = 0.0025$), with predicted motions having slightly higher average total torque values (Predicted: 6849.9 Nm, Empirical: 6622.6 Nm). This difference, however, was dependent on movement location. The lower, middle upper, and upper locations showed no significant differences between predicted and empirical total torque.

The muscle intensity objective function varied significantly as a function of the movement location and the movement type ($F(9,147) = 20.17, p < 0.0001$, $F(1,19) = 50.36, p < 0.0001$, respectively). The far lower movement location required significantly larger average muscle intensity coefficients than other locations (Far Lower Location: 59.0, remaining locations: 5.3 – 27.6). ‘Deliver’ motions required significantly larger average muscle intensity coefficients than ‘Bring back’ motions (‘Deliver’: 22.1, ‘Bring back’: 14.6). No significant differences were detected for this objective function between predicted and empirical movements. Similar trends were observed for the balance objective function and for the mobilization objective function.

Squared torque for the motion was significantly affected by movement location and movement type ($F(9,147) = 46.51, p < 0.0001$, $F(1,19) = 53.56, p < 0.0001$, respectively). The far lower movement location required significantly larger average squared torque than other locations (Far Lower Location: 757766 N²m², remaining locations: 41946 – 538735 N²m²). ‘Deliver’ motions required significantly larger average squared torque than ‘Bring back’ motions (‘Deliver’: 328455 N²m², ‘Bring back’: 235040 N²m²). The interaction between movement location and the data source (i.e. model prediction vs. empirical data) was also significant

($F(9,147)$, $p=0.0020$). This significant interaction appeared to be due to higher squared torque values for empirical motions in the upper locations when compared to their counterparts based on model predictions. This result implies that the model underestimated the squared torque measure for upper locations, but overestimated the measure for lower to middle locations.

No significant differences were observed using the cubed muscle intensity objective function. For the strength utilization objective function, only movement location was found to have a significant effect ($F(9,147)=5.64$, $p<0.0001$). The far lower movement location required significantly larger average strength utilization than other locations (Far Lower Location: 185.71, remaining locations: 2.58 – 48.16). This compares to Bernard et al. (1999), who used a similar objective function to compare the predictions of a posture prediction model employing optimization of the strength utilization objective function. Predicted and actual strength utilization values were highly correlated, although the predicted values were systematically higher. In the current comparison, no significant difference was found between predictions and empirical data, but the average predicted strength utilization value was slightly lower than the corresponding empirical value. Values in Bernard et al. (1999), 1.33 (mean predicted, SD: 0.744) and 1.02 (mean actual, SD: 0.593), were also lower than the values observed here, 30.70 (mean predicted, SD: 125.59) and 32.65 (mean actual, SD: 131.18), suggesting perhaps a different calculation approach or sampling rate. Bernard et al. also employed fewer joints (five) in their calculations.

Thus, it appears that the objective functions dealing directly with torque are more sensitive to differences between empirical and predicted movements. For total torque, the predictions tended to overestimate the measure, suggesting less efficiency for the predicted motion. For squared torque, the data source effect was contained within an interaction, and it appeared that the model overestimated the measure for the lower and middle locations. This sensitivity of torque to differences between predictions and empirical data suggests that even slight changes in motion selection have large effects on torque. In turn, this could be interpreted to imply that torque is an important factor in motion selection.

While this process does not yield any information regarding whether a particular objective function is being optimized, it is informative with respect to establishing functional differences between model predictions and empirical motions. The reader should note that most of the measures were sensitive to changes in movement type and location. Most of these

measures were not sensitive, however, to differences between predicted vs. empirical motions, suggesting that these differences are small when compared against the sources of variability due to task performance (i.e. movement location and movement type).

An alternate goal of this comparison was to determine if the neural network predictions implicitly improved the motion path so that reductions in any of these objective functions were observable. This does not appear to be true, since in the few cases where significance due to data source was observed, model predictions tended to result in higher objective function values. Thus, if participants are providing any consideration (implicit or explicit) to these objective functions in their choice of motion path, the network was likely able to model it considerably well across a variety of tasks. Whether or not this optimization process occurs, however, is a topic for further research and possibly much different methods.

The final goal of this investigation was to relate the models that were obtained to hypotheses of motor control. While the simplicity of the model precludes its direct comparison with very specific motor control hypotheses (which operate at a more detailed level of control than the current approach), comparison to higher level hypotheses can still provide some insights.

The ANN approach for motion prediction advocated in this document uses two distinct feedback loops. These loops were included to attempt to simulate the sequential nature of human motion, where the current state is influenced by previous states. In representing this sequential nature, these loops also eliminated the need to provide information to the network on the joint angle time histories, which represents a huge savings in network complexity. Recall that the motion prediction network was only provided with start and goal locations of a single point and indications of the participants' anthropometry and strength. If feedback loops were ignored by the network while establishing its internal connections, then there would be support for the idea that these feedback loops are of little use to the network. Results showed the opposite, where the feedback loops were of high importance compared to the static network inputs. The relatively good modeling of the movements achieved suggests that this feedback is an important aspect of the type of tasks under study. Physiologically, the feedback loop serves to emulate, at a very high conceptual level, the influence of body sensors such as the eyes (vision and limited proprioception), ears (audition), vestibular system (balance and proprioception), and other receptors (e.g. muscle, joint, cutaneous, typically involved in proprioception). The influence of

these sensors has been well studied and documented (Schmidt and Lee, 1999), and it is reasonable to expect that a motion prediction model could use a similar paradigm in generating useful predictions. Future models could attempt to simulate the distinct functionality provided by these different physiological afferents and their diverse feedback paths. For example, some feedback in the network might be provided directly to the inner layers, or even the output layer itself, and additional delays might be introduced that more closely model actual physiological feedback paths

This discussion on the importance of feedback loops does not intend to suggest that all movements are directly dependent on feedback. Indeed, a substantial body of research exists on deafferentation effects on movement (e.g., Messier et al., 2003), suggesting that ideas such as the response-chaining hypothesis have a certain degree of validity, at least in some movement situations. For these particular situations, a model without a feedback loop might have been sufficient. However, the tasks under study in this investigation, where an object is lifted sporadically and placed in locations that are variable, can be logically expected to need feedback information. This need was empirically verified based on network adaptation and performance. Future research could attempt to use similar model paradigms to predict motions for which feedback is not needed and/or used.

Another aspect of motor control refers to the ‘degrees of freedom problem’, which indicates the difficulty that a central command center would have in controlling all of the degrees of freedom in the human body (Whiting, 1984), especially when considering the large number of actuators that are available. One possible solution to this problem is that higher order centers exist that provide only high-level commands, which in turn activate other structures (e.g., motor programs, Hatze, 1986) that are responsible for the fine-level control. These hypothetical control centers are capable of adapting to particular task situations such as externally imposed joint constraints, required speed, and changes in goal point (Jax et al., 2003). The ANN approach advocated here seems to perform the role of one of these control centers, that adjusts its parameters based on the particular constraints imposed by a unique task that is nevertheless similar in nature to others. While it is not possible to indicate that the relative success of the approach supports the existence of these control centers, it nevertheless shows that such control is possible within the context of lifting and lowering tasks. The ANN approach certainly allowed for achieving goals similar to those presented in Lim et al. (2004), who propose a model that

explicitly considers inter-joint coordination. The advantage of the ANN approach, however, is that it accomplished these goals implicitly.

Certain patterns in bimanual coordination could also be observed from the network's use of its inputs, which relate to past research indicating that certain levels of coordination occur between hands in bimanual movements (Domkin et al., 2002). In the case of the 3D ANN model, similar utilization of inputs was observed between different sides of the body for the lower extremities, but for the upper extremities the frequency with which this symmetry was observed was reduced. This suggests that for this dataset, variability in the upper extremity joints could be modeled employing less information than for the lower extremity, which in turn could suggest that a higher level of coordination is present between the upper extremities when compared against the lower extremities, at least for the lifting and lowering tasks included in the dataset. This finding is supported by research that has found different inter-joint coordination in the left and right sides of the body for the lower limbs (St-Onge and Feldman, 2003).

The extent to which coordination patterns were present likely also influenced the level of variability contained in the dataset, which was quite large, even in within-subject trials. Within-subject variability was generally on par with between-subjects variability. The networks were typically able to model a large portion of the between-subject variability, but had no means for predicting the within-subject variability. Further research into the causes for these within-subject variations is needed that in turn allows for their future modeling. Until such research is available, there are limits on what the prediction capabilities of any model will be. While high degrees of intra-individual constancy have been observed for simple movements (e.g., Alstermark et al., 1993, note that the subjects were cats), this constancy does not seem to translate to more complex movements requiring multi-joint coordination. Furthermore, recent research also points to the possibility that redundant degrees of freedom are allowed to vary more, as long as they don't interfere with the movement goal (Todorov and Jordan, 2002). If this is true, then methods to reproduce this variability will have to be included in future model iterations. In such a model, predictions would be in the form of expected performance envelopes for a particular individual. This approach might in turn aid in the application of the output from these models into musculoskeletal load/injury risk models, which then could output probabilities of injury based on this variability.

Another aspect of coordination can be related to the direction of movement, which seemed to be an important factor to consider, based on the differences observed in direct comparisons of ‘Deliver’ and ‘Bring back’ postures at equivalent movement target points. Donders’ law, which in simple terms posits that posture is unique for a certain state (Soechting et al., 1995; Zatsiorsky, 1998), does not seem to apply for the tasks at hand. This conclusion is also supported by the large amounts of within-subject variability that were observed. This dependency of posture on previous states might have partly resulted in the errors observed for the posture prediction network, since this network’s training and structure did not account for previous state. Perhaps it might be possible to improve the predictive performance of these networks by adding inputs that summarize previous state information. Note that for motion prediction, the current dataset did not allow for a determination of any previous state effects, as all motions started from an equivalent initial state.

Finally, note that artificial neural networks do not explicitly optimize any objective function, other than attempt to maximize the fit between its outputs and the corresponding empirical data. Thus, whether an individual elects to optimize a particular objective function in performing a movement is not relevant to the artificial neural networks discussed in this investigation. The networks will implicitly adapt to that pattern, but not detect it or try to explicitly assimilate it. Formal comparisons between optimization models and the networks in this investigation when both are using the same dataset might be useful in detecting whether any implicit optimization is occurring within the network and would be a possible area of future research.

9.1 Conclusions and further research

The results of this investigation suggest ANNs as a viable motion prediction method. In a recent paper, Chaffin (2005) indicates four criteria to evaluate motion prediction models used for digital human modeling: 1) the motions simulated must be based on real human motion data, 2) models should have extrapolation capability, 3) models should be computationally fast, and 4) models should automatically adapt to and use new motion data. The ANN models presented in this investigation fulfill the first three criteria very well. They could also potentially be complemented by unsupervised training modules that allow the achievement of the fourth criterion.

However, this investigation also showed areas where further development is needed to allow ANNs to reach a level of sophistication that allows their use in practical applications. While prediction errors were smaller on average than errors for other published efforts and for commercially available models, they still may be large enough to result in large effects when these results are input into models that estimate musculoskeletal loads or injury risk.

One possible improvement is based on the addition of constraints in the ANN's predictions that improve performance and prevent unrealistic conditions from being predicted. Examples of these constraints include explicitly limiting the range of motion for certain joint angles and specifying the length of certain segments with a fixed length (e.g. the pelvis). The network might also be outfitted with 'switch' inputs that indicate, for example, whether a movement is a lifting or a lowering activity. This additional input might, without substantially increasing the information required, aid the network in defining differential 'rules' for inherently distinct activities.

Alternatively, rules or strategies that have been hypothesized in the literature could be implemented and tested within a neural network. The approach taken here was a 'bottom-up' approach, where the simplest possible model structure was built-upon to reach networks with sufficient performance levels. Assumptions were not integrated in the model unless absolutely necessary; models had as few constraints as possible. A 'top-down' approach would first build a network that models these principles of movement. Then, the feasibility of each principle would be determined based on the predictive performance of the resultant model. Given the encouraging results obtained in this investigation, it appears that this concept is worthy of future consideration.

The two networks presented here, posture and motion prediction, can be combined sequentially. The results for this combination were not included in this document, since the intent was to consider errors from these networks independently. However, it is possible that a single structure could be created that performs both functions and would require a single training session. Such an approach may result in reduced errors compared to training the models separately and then combining them. Future research should determine whether this is a feasible and/or better approach.

It is also possible to construct a network where joint targets are not used; rather, the object position would be used as a target. This approach would be analogous to the approach

used by Nussbaum, et al. (1996) for the prediction of torso muscle activity. Connections between the joint and the box position layers would use known kinematics relationships. This was attempted in the initial stages of this investigation, but standard recurrent neural networks are not designed to operate in this fashion, and would make typical training algorithms perform very inefficiently. Newer neural network training approaches or more general techniques such as fuzzy logic might be able to provide more efficient means of training these network structures. The advantage of using this approach would be that any output from the network would be entirely predictive, as no empirical data would be required in its training. These networks could potentially be parameterized with sufficient detail to allow for simulation of basic physiological units of motor control.

The use of neural networks for modeling purposes is not without pitfalls. An important consideration when using neural networks is the avoidance of stopping the training process when local minima are reached. In this investigation, this possibility was minimized by using a training function with a low propensity for getting caught at local minima. In addition, a few of the initial network structures were tested under more than one initialization condition to determine if this resulted in different performance levels. None of these tests indicated that local minima were being identified. However, any future use of artificial neural networks in this or similar applications should be cognizant of this potential problem and attempt to minimize the possibility of its occurrence.

Another important consideration is the extrapolation potential of the network. The training sets employed here were created so that extreme data points were included and extrapolation was not required. The dataset used to create these training sets included a large range of exertions that represented in some cases the limits of mobility for the individuals while performing a lifting exertion. Thus, the extrapolation capabilities of the networks discussed in this investigation remain untested. Future research could examine what these capabilities are, and if any improvements in performance are possible by the inclusion of extreme vs. intermediate data points.

In network development, it is also necessary to consider the size of the training set. In this investigation this issue was addressed by including a relatively large portion of the data within the training set. This approach worked well for the exploratory goal of this research, indicating that the networks were able to assimilate most of the information contained in the

training data. Future research might consider the size of the training set and its effect on network performance. It might be possible to use a smaller training set that still results in similar performance levels while avoiding network over-adaptation to certain segments of the data. This over-adaptation was mildly observable in this investigation via differences in network performance between novel movements performed by novel participants and novel movements performed by participants that had been included in the training dataset.

Neural network models of the type discussed here would be very useful in the context of motion simulation. Once trained, as the networks discussed throughout this document are, they can be easily implemented in any software simulation package with a minimal amount of work. Processing requirements of the networks described in this document are also minimal, allowing the simulation of motions in real-time. This is important in allowing task designers the ability to observe tasks in real time. If more accurate posture and motion predictions can be made available within task simulation environments, then it will be possible for these packages to provide task designers with more realistic injury risk estimates that can in turn be used in the creation of more 'human-friendly' tasks.

Chapter 10 REFERENCES

- Abdel-Malek, K., Yu, W., & Jaber, M. (submitted). *Realistic posture prediction*. Paper presented at the SAE Digital Human Modeling and Simulation Conference.
- Adamovich, S. V., Archambault, P. S., Ghafouri, M., Levin, M. F., Poizner, H., & Feldman, A. G. (2001). Hand trajectory invariance in reaching movements involving the trunk. *Experimental Brain Research, 138*(3), 288-303.
- Allread, G. W., Marras, W. S., & Burr, D. L. (2000). Measuring trunk motions in industry: variability due to task factors, individual differences, and the amount of data collected. *Ergonomics, 43*(6), 691-701.
- Allread, W. G., Marras, W. S., & Parnianpour, M. (1996). Trunk kinematics of one-handed lifting, and the effects of asymmetry and load weight. *Ergonomics, 39*(2), 322-334.
- Alstermark, B., Lundberg, A., Pettersson, L. G., Tantisira, B., & Walkowska, M. (1993). Characteristics of target-reaching in cats. I. Individual differences and intra-individual constancy. *Experimental Brain Research, 94*(2), 279-286.
- Amblard, B., Cremieux, J., Marchand, A. R., & Carblanc, A. (1985). Lateral orientation and stabilization of human stance: static versus dynamic visual cues. *Experimental Brain Research, 61*(1), 21-37.
- An, K. N., Kaufman, K. R., & Chao, E. Y. (1989). Physiological considerations of muscle force through the elbow joint. *Journal of Biomechanics, 22*(11-12), 1249-1256.
- Anderson, F. C., & Pandy, M. G. (2001). Dynamic optimization of human walking. *Journal of Biomechanical Engineering, 123*(5), 381-390.
- Anderson, J. A., Otun, E. O., & Sweetman, B. J. (1987). Occupational hazards and low back pain. *Reviews in Environmental Health, 7*(1-2), 121-160.
- Ariens, G. A., Mechelen, W. v., Bongers, P. M., Bouter, L. M., & Wal, G. v. d. (2001). Psychosocial risk factors for neck pain: a systematic review. *American Journal of Industrial Medicine, 39*(2), 180-193.
- Armstrong, T. J. (1986). Ergonomics and cumulative trauma disorders. *Hand Clinics, 2*(3), 553-565.
- Armstrong, T. J., Buckle, P., Fine, L. J., Hagberg, M., Jonsson, B., Kilbom, A., et al. (1993). A conceptual model for work-related neck and upper-limb musculoskeletal disorders. *Scandinavian Journal of Work and Environmental Health, 19*(2), 73-84.
- Armstrong, T. J., Foulke, J. A., Joseph, B. S., & Goldstein, S. A. (1982). Investigation of cumulative trauma disorders in a poultry processing plant. *American Industrial Hygiene Association Journal, 43*(2), 103-116.

- Arndt, R. (1983). Working posture and musculoskeletal problems of video display terminal operators--review and reappraisal. *Am Ind Hyg Assoc J*, 44(6), 437-446.
- Badler, N. I., Phillips, C. B., & Webber, B. L. (1993). *Simulating humans: computer graphics, animation, and control*. New York: Oxford University Press.
- Baker, D. B., & Landrigan, P. J. (1990). Occupationally related disorders. *Medical Clinics of North America*, 74(2), 441-460.
- Barin, K. (1989). Evaluation of a generalized model of human postural dynamics and control in the sagittal plane. *Biological Cybernetics*, 61(1), 37-50.
- Beck, D. J., & Chaffin, D. B. (1992). *An evaluation of inverse kinematics models for posture prediction*. Paper presented at the CAES '92, Tampere, Finland.
- Bellan, Y., Costa, M., Ferrigno, G., Lombardi, F., Macchiarulo, L., Montuori, A., et al. (1999). Artificial Neural Networks for Motion Emulation in Virtual Environments. *Lecture notes in artificial intelligence*, 1537, 83-99.
- Bellan, Y., Gaia, E., & Rizzuto, F. (2000). *ANNIE: standard bio-mechanics and cognitive models for computer aided ergonomics*. Paper presented at the Proceedings of the 44th Annual Meeting of the Human Factors and Ergonomics Society - "Ergonomics for the New Millennium", San Diego, CA.
- Bennett, D. J., Hollerbach, J. M., Xu, Y., & Hunter, I. W. (1992). Time-varying stiffness of human elbow joint during cyclic voluntary movement. *Experimental Brain Research*, 88(2), 433-442.
- Bernard, B., Sauter, S., Fine, L., Petersen, M., & Hales, T. (1994). Job task and psychosocial risk factors for work-related musculoskeletal disorders among newspaper employees. *Scandinavian Journal of Work and Environmental Health*, 20(6), 417-426.
- Bernard, T. M., Ayoub, M. M., & Lin, C. J. (1999). Evaluation of a biomechanical simulation model for sagittal plane lifting. *International Journal of Industrial Ergonomics*, 24(2), 157-171.
- Biguer, B., Jeannerod, M., & Prablanc, C. (1982). The coordination of eye, head, and arm movements during reaching at a single visual target. *Experimental Brain Research*, 46(2), 301-304.
- Bishop, J. B., Szpalski, M., Ananthraman, S. K., McIntyre, D. R., & Pope, M. H. (1997). Classification of low back pain from dynamic motion characteristics using an artificial neural network. *Spine*, 22(24), 2991-2998.
- BLS. (2003). *Workplace injuries and illnesses in 2002* (Report No. No. USDL 03-913). Washington, D.C.: Bureau of Labor Statistics, U.S. Department of Labor.

- Bobick, T. G., Shapiro, R., Blow, C., & Gallagher, S. (1987). Sagittal plane kinematic analysis of a specific simulated low-seam coal mining lifting task. In S. S. Asfour (Ed.), *Trends in Ergonomics/Human Factors IV* (pp. 9-16). Amsterdam: North Holland.
- Bogduk, N. (1995). The anatomical basis for spinal pain syndromes. *Journal of Manipulative and Physiological Therapeutics*, 18(9), 603-605.
- Bonato, P., Boissy, P., Della Croce, U., & Roy, S. H. (2002). Changes in the surface EMG signal and the biomechanics of motion during a repetitive lifting task. *IEEE Transactions on Neural Systems and Rehabilitation Engineering*, 10(1), 38-47.
- Bonato, P., Ebenbichler, G. R., Roy, S. H., Lehr, S., Posch, M., Kollmitzer, J., et al. (2003). Muscle fatigue and fatigue-related biomechanical changes during a cyclic lifting task. *Spine*, 28(16), 1810-1820.
- Bovenzi, M. (1994). Hand-arm vibration syndrome and dose-response relation for vibration induced white finger among quarry drillers and stonecarvers. Italian Study Group on Physical Hazards in the Stone Industry. *Occupational and Environmental Medicine*, 51(9), 603-611.
- Brown, E. W., & Abani, K. (1985). Kinematics and kinetics of the dead lift in adolescent power lifters. *Medicine and Science in Sports and Exercise*, 17(5), 554-566.
- Bruhin, C., Gerdle, B., Granlund, B., Hoog, J., Knutson, A., & Sundelin, G. (1998). Physical and psychosocial work-related risk factors associated with musculoskeletal symptoms among home care personnel. *Scandinavian Journal of Caring Science*, 12(2), 104-110.
- Burg, J. C. v. d., Dieën, J. H. v., & Toussaint, H. M. (2000). Lifting an unexpectedly heavy object: the effects on low-back loading and balance loss. *Clinical Biomechanics*, 15(7), 469-477.
- Burgess-Limerick, R. (2003). Squat, stoop, or something in between. *International Journal of Industrial Ergonomics*, 31, 143-149.
- Burgess-Limerick, R., & Abernethy, B. (1997). Toward a quantitative definition of manual lifting postures. *Human Factors*, 39(1), 141-148.
- Burgess-Limerick, R., & Abernethy, B. (1998). Effect of load distance on self-selected manual lifting technique. *International Journal of Industrial Ergonomics*, 22(4-5), 367-372.
- Burgess-Limerick, R., Abernethy, B., Neal, R. J., & Kippers, V. (1995). Self-selected manual lifting technique: functional consequences of the interjoint coordination. *Human Factors*, 37(2), 395-411.
- Burgess-Limerick, R., Shemmell, J., Barry, B. K., Carson, R. G., & Abernethy, B. (2001). Spontaneous transitions in the coordination of a whole body task. *Human Movement Science*, 20(4-5), 549-562.

- Burgess-Limerick, R., Shemmell, J., Scadden, R., & Plooy, A. (1999). Wrist posture during computer pointing device use. *Clinical Biomechanics*, *14*(4), 280-286.
- Butler, D., Andersson, G. B., Trafimow, J., Schipplein, O. D., & Andriacchi, T. P. (1993). The influence of load knowledge on lifting technique. *Ergonomics*, *36*(12), 1489-1493.
- Byun, S. N. (1991). *A computer simulation using a multivariate biomechanical posture prediction model for manual materials handling tasks*. Unpublished Ph.D. Dissertation, University of Michigan, Ann Arbor, MI.
- Caboor, D. E., Verlinden, M. O., Zinzen, E., Van Roy, P., Van Riel, M. P., & Clarys, J. P. (2000). Implications of an adjustable bed height during standard nursing tasks on spinal motion, perceived exertion and muscular activity. *Ergonomics*, *43*(10), 1771-1780.
- Calvitti, A., & Beer, R. D. (2000). Analysis of a distributed model of leg coordination. I. Individual coordination mechanisms. *Biological Cybernetics*, *82*(3), 197-206.
- Campbell, D. S. (1999). Health hazards in the meatpacking industry. *Occupational Medicine*, *14*(2), 351-372.
- Cats-Baril, W. L., & Frymoyer, J. W. (1991). Identifying patients at risk of becoming disabled because of low-back pain. The Vermont Rehabilitation Engineering Center predictive model. *Spine*, *16*(6), 605-607.
- Chaffin, D. B. (2005). Improving digital human modelling for proactive ergonomics in design. *Ergonomics*, *48*(5), 478-491.
- Chaffin, D. B., & Andersson, G. B. J. (1991). *Occupational Biomechanics*. New York: Wiley.
- Chaffin, D. B., & Erig, M. (1991). Three-dimensional biomechanical static strength prediction model sensitivity to postural and anthropometric inaccuracies. *IIE Transactions*, *23*(3), 215-227.
- Chaffin, D. B., Faraway, J. J., Zhang, X., & Woolley, C. (2000). Stature, age, and gender effects on reach motion postures. *Human Factors*, *42*(3), 408-420.
- Chaffin, D. B., & Page, G. B. (1994). Postural effects on biomechanical and psychophysical weight-lifting limits. *Ergonomics*, *37*(4), 663-676.
- Chaffin, D. B., Stump, B. S., Nussbaum, M. A., & Baker, G. (1999). Low-back stresses when learning to use a materials handling device. *Ergonomics*, *42*(1), 94-110.
- Chang, C. C., Brown, D. R., Blowski, D. S., & Hsiang, S. M. (2001). Biomechanical simulation of manual lifting using spacetime optimization. *Journal of Biomechanics*, *34*(4), 527-532.
- Chen, C. L., Kaber, D. B., & Dempsey, P. G. (2000). A new approach to applying feedforward neural networks to the prediction of musculoskeletal disorder risk. *Applied Ergonomics*, *31*(3), 269-282.

- Chen, Y. L. (2000a). Optimal lifting techniques adopted by Chinese men when determining their maximum acceptable weight of lift. *American Industrial Hygiene Association Journal*, 61(5), 642-648.
- Chen, Y.-L. (2000b). Changes in lifting dynamics after localized arm fatigue. *International Journal of Industrial Ergonomics*, 25, 611-619.
- Choi, K. I., & Chung, M. K. (2003). *Asymmetric lifting posture prediction using inverse kinematics*. Paper presented at the Proceedings of the 2003 Meeting of the International Ergonomics Association, Seoul, South Korea.
- Cholewicki, J., McGill, S. M., & Norman, R. W. (1991). Lumbar spine loads during the lifting of extremely heavy weights. *Medicine and Science in Sports and Exercise*, 23(10), 1179-1186.
- Chou, L.-S., & Song, S.-M. (1992). Geometric work of manipulators and path planning based on minimum energy consumption. *Transactions of the ASME*, 114, 414-421.
- Chow, D. H. K., Man, J. W. K., Holmes, A. D., & Evans, J. H. (2004). Postural and trunk muscle response to sudden release during stoop lifting tasks before and after fatigue of the trunk erector muscles. *Ergonomics*, 47(6), 607-624.
- Corradini, M. L., Gentilucci, M., Leo, T., & Rizzolatti, G. (1992). Motor control of voluntary arm movements. Kinematic and modelling study. *Biological Cybernetics*, 67(4), 347-360.
- Craig, J. J. (1989). *Introduction to robotics: mechanics and control* (2nd ed.). Reading, MA: Addison-Wesley.
- Cruse, H., Bruwer, M., & Dean, J. (1993a). Control of three- and four-joint arm movement: strategies for a manipulator with redundant degrees of freedom. *Journal of Motor Behavior*, 25(3), 131-139.
- Cruse, H., Brüwer, M., & Dean, J. (1993b). Control of three- and four-joint arm movement: strategies for a manipulator with redundant degrees of freedom. *Journal of Motor Behavior*, 25(3), 131-139.
- Cruse, H., Wischmeyer, E., Brüwer, M., Brockfeld, P., & Dress, A. (1990). On the cost functions for the control of the human arm movement. *Biological Cybernetics*, 62(6), 519-528.
- Davis, K. G., & Marras, W. S. (2000). Assessment of the Relationship between Box Weight and Trunk Kinematics: Does a Reduction in Box Weight Necessarily Correspond to a Decrease in Spinal Loading? *Human Factors*, 42(2), 195-208.
- Delisle, A., Gagnon, M., & Desjardins, P. (1996). Load Acceleration and Footstep Strategies in Asymmetrical Lifting and Lowering. *International Journal of Occupational Safety and Ergonomics*, 2(3), 185-195.

- Delisle, A., Gagnon, M., & Desjardins, P. (1999). Kinematic analysis of footstep strategies in asymmetrical lifting and lowering tasks. *International Journal of Industrial Ergonomics*, 23(5-6), 451-460.
- Delisle, A., Gagnon, M., & Sicard, C. (1997). Effect of pelvic tilt on lumbar spine geometry. *IEEE Transactions on Rehabilitation Engineering*, 5(4), 360-366.
- Delmia. (2001). *Welcome to Delmia! - Solutions*. Retrieved December 4, 2001, from <http://www.delmia.com/>
- Dempsey, P. G., & Hashemi, L. (1999). Analysis of workers' compensation claims associated with manual materials handling. *Ergonomics*, 42(1), 183-195.
- Dieën, J. H. v. (1998). Effects of repetitive lifting on kinematics: inadequate anticipatory control or adaptive changes? *Journal of Motor Behavior*, 30(1), 20-32.
- Dieën, J. H. v., Hoozemans, M. J., & Toussaint, H. M. (1999). Stoop or squat: a review of biomechanical studies on lifting technique. *Clinical Biomechanics*, 14(10), 685-696.
- Dieën, J. H. v., Toussaint, H. M., Maurice, C., & Mientjes, M. (1996). Fatigue-related changes in the coordination of lifting and their effect on low back load. *Journal of Motor Behavior*, 28(4), 304-314.
- Dolan, P., & Adams, M. A. (1998). Repetitive lifting tasks fatigue the back muscles and increase the bending moment acting on the lumbar spine. *Journal of Biomechanics*, 31(8), 713-721.
- Domen, K., Latash, M. L., & Zatsiorsky, V. M. (1999). Reconstruction of equilibrium trajectories during whole-body movements. *Biological Cybernetics*, 80(3), 195-204.
- Domkin, D., Laczko, J., Jaric, S., Johansson, H., & Latash, M. L. (2002). Structure of joint variability in bimanual pointing tasks. *Experimental Brain Research*, 143(1), 11-23.
- Dysart, M. J. (1994). *Development and validation of a posture prediction algorithm*. Unpublished Master's Thesis, Virginia Polytechnic Institute and State University, Blacksburg, VA.
- Dysart, M. J., & Woldstad, J. C. (1994). *Development and validation of a posture prediction algorithm for a static lifting task*. Paper presented at the Proceedings of the Triennial Congress of the International Ergonomics Association - IEA '94.
- Dysart, M. J., & Woldstad, J. C. (1996). Posture prediction for static sagittal-plane lifting. *Journal of Biomechanics*, 29(10), 1393-1397.
- EDS. (2001). *PLM Solutions - Jack*. Retrieved December 4, 2001, from <http://www.plmsolutions-eds.com/products/efactory/jack/>

- Ekberg, K., Bjorkqvist, B., Malm, P., Bjerre-Kiely, B., Karlsson, M., & Axelson, O. (1994). Case-control study of risk factors for disease in the neck and shoulder area. *Occupational and Environmental Medicine*, *51*(4), 262-266.
- Elford, W., Straker, L., & Strauss, G. (2000). Patient handling with and without slings: an analysis of the risk of injury to the lumbar spine. *Applied Ergonomics*, *31*(2), 185-200.
- Elman, J. (1990). Finding structure in time. *Cognitive Science*, *14*, 179-211.
- Eom, G. M., Watanabe, T., Futami, R., Hoshimiy, N., & Handa, Y. (2000). Computer-aided generation of stimulation data and model identification for functional electrical stimulation (FES) control of lower extremities. *Frontiers of Medical and Biological Engineering*, *10*(3), 213-231.
- Faraway, J. J. (2000). *Modeling reach motions using functional regression analysis* (SAE Technical Report No. 2000-01-2175). Detroit, MI: Society of Automotive Engineers.
- Faucett, J., & Werner, R. A. (1999). Non-biomechanical factors potentially affecting musculoskeletal disorders. In *Work-Related Musculoskeletal Disorders: Report, Workshop Summary, and Workshop Papers* (pp. 175-199). Washington, D.C.: The National Academy Press.
- Ferguson, S. A., & Marras, W. S. (1997). A literature review of low back disorder surveillance measures and risk factors. *Clinical Biomechanics*, *12*(4), 211-226.
- Ferran, E. A., & Pflugfelder, B. (1993). A hybrid method to cluster protein sequences based on statistics and artificial neural networks. *Computer Applications in the Biosciences*, *9*(6), 671-680.
- Flash, T. (1987). The control of hand equilibrium trajectories in multi-joint arm movements. *Biological Cybernetics*, *22*1, 89-98.
- Frank, J. S., & Earl, M. (1990). Coordination of posture and movement. *Physical Therapy*, *70*(12), 855-863.
- Fraser, D., Potvin, J., & Jones, J. (2000). *Effects of trunk muscle fatigue on spine mechanics during repetitive asymmetrical lifting*. Paper presented at the Ergonomics for the New Millennium. Proceedings of the XIVth Triennial Congress of the International Ergonomics Association and 44th Annual Meeting of the Human Factors and Ergonomics Society, San Diego, CA.
- Fuortes, L. J., Shi, Y., Zhang, M., Zwerling, C., & Schootman, M. (1994). Epidemiology of back injury in university hospital nurses from review of workers' compensation records and a case-control survey. *Journal of Occupational Medicine*, *36*(9), 1022-1026.
- Gagnon, M. (1997). Box tilt and knee motions in manual lifting: two differential factors in expert and novice workers. *Clinical Biomechanics*, *12*(7-8), 419-428.

- Gagnon, M., & Smyth, G. (1991). Muscular mechanical energy expenditure as a process for detecting potential risks in manual materials handling. *Journal of Biomechanics*, 24, 191-203.
- Gallagher, S., & Unger, R. L. (1990). Lifting in four restricted lifting conditions: psychophysical, physiological, and biomechanical effects of lifting in stooped and kneeling postures. *Applied Ergonomics*, 21(3), 237-245.
- Garcia, M., Chatterjee, A., Ruina, A., & Coleman, M. (1998). The simplest walking model: stability, complexity, and scaling. *Journal of Biomechanical Engineering*, 120(2), 281-288.
- Gomi, H., & Kawato, M. (1997). Human arm stiffness and equilibrium-point trajectory during multi-joint movement. *Biological Cybernetics*, 76(3), 163-171.
- Gorelick, M., Brown, J. M., & Groeller, H. (2003). Short-duration fatigue alters neuromuscular coordination of trunk musculature: implications for injury. *Applied Ergonomics*, 34(4), 317-325.
- Gottlieb, G. L., Song, Q., Almeida, G. L., Hong, D. A., & Corcos, D. (1997). Directional control of planar human arm movement. *Journal of Neurophysiology*, 78(6), 2985-2998.
- Gracovetsky, S., Kary, M., Levy, S., Ben Said, R., Pitchen, I., & Helie, J. (1990). Analysis of spinal and muscular activity during flexion/extension and free lifts. *Spine*, 15(12), 1333-1339.
- Granata, K. P., Marras, W. S., & Davis, K. G. (1997). Biomechanical assessment of lifting dynamics, muscle activity and spinal loads while using three different styles of lifting belt. *Clinical Biomechanics*, 12(2), 107-115.
- Granata, K. P., Marras, W. S., & Davis, K. G. (1999). Variation in spinal load and trunk dynamics during repeated lifting exertions. *Clinical Biomechanics*, 14(6), 367-375.
- Granata, K. P., & Sanford, A. H. (2000). Lumbar-pelvic coordination is influenced by lifting task parameters. *Spine*, 25(11), 1413-1418.
- Granata, K. P., & Wilson, S. E. (2001). Trunk posture and spinal stability. *Clinical Biomechanics*, 16(8), 650-659.
- Guez, A., & Ahmad, Z. (1990). Improving the solution of the inverse kinematic problem in robotics using neural networks. *Journal of Neural Network Computing*, 1(4), 21-32.
- Gundogdu, O. (2000). *Quantification and assessment of objective function performance in manual materials handling*. Unpublished Ph.D. Dissertation, Rensselaer Polytechnic Institute, Troy, NY.
- Hagan, M. T., Demuth, H. B., & Beale, M. H. (1996). *Neural network design*. Boston: PWS Publishing.

- Hagberg, M., Silverstein, B., Wells, R., Smith, M. J., Hendrick, H. W., Carayon, P., et al. (1995). *Work related musculoskeletal disorders (WMSDs): a reference book for prevention*. London: Taylor & Francis.
- Hagen, K., Sorhagen, O., & Harms-Ringdahl, K. (1995). Influence of weight and frequency on thigh and lower-trunk motion during repetitive lifting employing stoop and squat techniques. *Clinical Biomechanics*, 10(3), 122-127.
- Hagen, K. B., Hallen, J., & Harms-Ringdahl, K. (1993). Physiological and subjective responses to maximal repetitive lifting employing stoop and squat technique. *European Journal of Applied Physiology*, 67(4), 291-297.
- Hagen, K. B., Harms-Ringdahl, K., & Hallen, J. (1994). Influence of lifting technique on perceptual and cardiovascular responses to submaximal repetitive lifting. *European Journal of Applied Physiology*, 68(6), 477-482.
- Haslegrave, C. M. (1994). What do we mean by a 'working posture'? *Ergonomics*, 37(4), 781-799.
- Hatze, H. (1986). Motion variability - its definition, quantification, and origin. *Journal of Motor Behavior*, 18(1), 5-16.
- Hatze, H. (2000). The inverse dynamics problem of neuromuscular control. *Biological Cybernetics*, 82(2), 133-141.
- Heecheon, Y. (1999). *The development of a risk assessment model for carpal tunnel syndrome*. Unpublished Ph.D. Dissertation, The Pennsylvania State University, University Park, PA.
- Hogan, N. (1984). An organizing principle for a class of voluntary movements. *Journal of Neuroscience*, 4(11), 2745-2754.
- Hogan, N. (1985). The mechanics of multi-joint posture and movement control. *Biological Cybernetics*, 52(5), 315-331.
- Hogan, N., Bizzi, E., Mussa-Ivaldi, F. A., & Flash, T. (1987). Controlling multijoint motor behavior. *Exercise and Sport Sciences Reviews*, 15, 153-190.
- Hoogendoorn, W. E., Poppel, M. N. v., Bongers, P. M., Koes, B. W., & Bouter, L. M. (2000). Systematic review of psychosocial factors at work and private life as risk factors for back pain. *Spine*, 25(16), 2114-2125.
- Hoozemans, M. J., Beek, A. J. v. d., Frings-Dresen, M. H., Dijk, F. J. v., & Woude, L. H. v. d. (1998). Pushing and pulling in relation to musculoskeletal disorders: a review of risk factors. *Ergonomics*, 41(6), 757-781.
- Hsiang, S. H., & Ayoub, M. M. (1994). Development of methodology in biomechanical simulation of manual lifting. *International Journal of Industrial Ergonomics*, 13, 271-288.

- Hsiang, S. H., Brogmus, G. E., & Courtney, T. K. (1997). Low back pain (LBP) and lifting technique - a review. *International Journal of Industrial Ergonomics*, 19, 59-74.
- Hsiang, S. H., Chang, C. C., & McGorry, R. W. (1999a). Development of a set of equations describing joint trajectories during para-sagittal lifting. *Journal of Biomechanics*, 32(8), 871-876.
- Hsiang, S. H., Chang, C. C., & McGorry, R. W. (1999b). *Synthesis of variability of angular trajectories during para-sagittal lifting*. Paper presented at the Proceedings of the Human Factors and Ergonomics Society 43rd Annual Meeting.
- Hsiang, S. H., & McGorry, R. W. (1997). Three different lifting strategies for controlling the motion patterns of the external load. *Ergonomics*, 40(9), 928-939.
- Jaeger, R. J. (1986). Design and simulation of closed-loop electrical stimulation orthoses for restoration of quiet standing in paraplegia. *Journal of Biomechanics*, 19(10), 825-835.
- Jansen-Osmann, P., Richter, S., Konczak, J., & Kalveram, K. T. (2002). Force adaptation transfers to untrained workspace regions in children: Evidence for developing inverse dynamic motor models. *Experimental Brain Research*, 143(2), 212-220.
- Jax, S. A., Rosenbaum, D. A., Vaughan, J., & Meulenbroek, R. G. (2003). Computational motor control and human factors: modeling movements in real and possible environments. *Human Factors*, 45(1), 5-27.
- Johansson, R., & Magnusson, M. (1991). Human postural dynamics. *Critical Reviews in Biomedical Engineering*, 18(6), 413-437.
- Johnson, D. E. (1998). *Applied multivariate methods for data analysts*. Pacific Grove, CA: Duxbury Press.
- Jordan, M. I. (1986). *Serial order: A parallel distributed processing approach* (Institute for Cognitive Science Report No. 8604). San Diego: University of California, San Diego.
- Jorgensen, M. J., Marras, W. S., Gupta, P., & Waters, T. R. (2003). Effect of torso flexion on the lumbar torso extensor muscle sagittal plane moment arms. *The Spine Journal*, 3(5), 363-369.
- Jung, E. S., & Choe, J. (1996). Human reach posture prediction based on psychophysical discomfort. *International Journal of Industrial Ergonomics*, 18, 173-179.
- Jung, E. S., Choe, J., & Kim, S. H. (1994). *Psychophysical cost function of joint movement for arm reach posture prediction*. Paper presented at the Proceedings of the Human Factors and Ergonomics Society 38th Annual Meeting.
- Jung, E. S., Kee, D., & Chung, M. K. (1992). *Reach posture prediction of upper limb for ergonomic workspace evaluation*. Paper presented at the Proceedings of the Human Factors Society 36th Annual Meeting.

- Jung, E. S., Kee, D., & Chung, M. K. (1995). Upper body reach posture prediction for ergonomic evaluation models. *International Journal of Industrial Ergonomics*, 16, 95-107.
- Jung, E. S., & Park, S. (1994). Prediction of human reach posture using a neural network for ergonomic man models. *Computers and Industrial Engineering*, 27, 369-372.
- Jung, E. S., & Park, W. (1997). *Comparison of biomechanical cost functions with weighting factors for posture prediction of human load lifting*. Paper presented at the Proceedings of the Triennial Congress - International Ergonomics Association.
- Kaufman, K. R., An, K. N., & Chao, E. Y. (1989). Incorporation of muscle architecture into the muscle length-tension relationship. *Journal of Biomechanics*, 22(8-9), 943-948.
- Kawato, M. (1999). Internal models for motor control and trajectory planning. *Current Opinion in Neurobiology*, 9(6), 718-727.
- Kerlirzin, Y., Pozzo, T., Dietrich, G., & Vieilledent, S. (1999). Effects of kinematics constraints on hand trajectory during whole-body lifting tasks. *Neuroscience Letters*, 277(1), 41-44.
- Kerry, S., Hilton, S., Dundas, D., Rink, E., & Oakeshott, P. (2002). Radiography for low back pain: a randomised controlled trial and observational study in primary care. *The British Journal of General Practice*, 52(479), 469-474.
- Keyserling, W. M. (2000a). Workplace risk factors and occupational musculoskeletal disorders, Part 1: A review of biomechanical and psychophysical research on risk factors associated with low-back pain. *American Industrial Hygiene Association Journal*, 61(1), 39-50.
- Keyserling, W. M. (2000b). Workplace risk factors and occupational musculoskeletal disorders, Part 2: A review of biomechanical and psychophysical research on risk factors associated with upper extremity disorders. *American Industrial Hygiene Association Journal*, 61(2), 231-243.
- Koike, Y., & Kawato, M. (2000). Estimation of movement from surface EMG signals using a neural network model. In J. M. Winters & P. E. Crago (Eds.), *Biomechanics and Neural Control of Posture and Movement* (pp. 440-457). New York: Springer-Verlag.
- Koozekanani, S. H., Barin, K., McGhee, R. B., & Chang, H. T. (1983). A recursive free-body approach to computer simulation of human postural dynamics. *IEEE Transactions on Biomedical Engineering*, 30(12), 787-792.
- Koozekanani, S. H., Stockwell, C. W., McGhee, R. B., & Firoozmand, F. (1980). On the role of dynamic models in quantitative posturography. *IEEE Transactions on Biomedical Engineering*, 27(10), 605-609.
- Kumar, S. (1994). A conceptual model of overexertion [correction of overexertion], safety, and risk of injury in occupational settings. *Human Factors*, 36(2), 197-209.
- Kumar, S. (2001). Theories of musculoskeletal injury causation. *Ergonomics*, 44(1), 17-47.

- Lariviere, C., Gagnon, D., & Loisel, P. (2000). The effect of load on the coordination of the trunk for subjects with and without chronic low back pain during flexion-extension and lateral bending tasks. *Clinical Biomechanics*, 15(6), 407-416.
- Lavender, S. A., & Andersson, G. B. J. (1999). Ergonomic principles applied on the prevention of injuries to the lower extremity. In W. Karwowski & W. S. Marras (Eds.), *The Occupational Ergonomics Handbook* (pp. 883-893). Boca Raton, FL: CRC Press.
- Lavender, S. A., Shakeel, K., Andersson, G. B., & Thomas, J. S. (2000). Effects of a lifting belt on spine moments and muscle recruitments after unexpected sudden loading. *Spine*, 25(12), 1569-1578.
- Lee, W. A., & Patton, J. L. (1997). Learned changes in the complexity of movement organization during multijoint, standing pulls. *Biological Cybernetics*, 77(3), 197-206.
- Lee, Y. H., & Lee, T. H. (2002). Human muscular and postural responses in unstable load lifting. *Spine*, 27(17), 1881-1886.
- Lee, Y.-H. T. (1988). *An optimization approach to determine manual lifting motion*. Unpublished Ph.D. Dissertation, Texas Tech University, Lubbock, TX.
- Li, J.-H., Michel, A., & Porod, W. (1989). Analysis and synthesis of a class of neural networks: linear systems operating on a closed hypercube. *IEEE Transactions on Circuits and Systems*, 36(11), 1405-1422.
- Lieber, R. L., Loren, G. J., & Friden, J. (1994). In vivo measurement of human wrist extensor muscle sarcomere length changes. *Journal of Neurophysiology*, 71(3), 874-881.
- Lim, S., Jung, E. S., Chung, M. K., & Shin, Y. (1999). *A two-segment trunk model for reach prediction (Paper 123)*. Paper presented at the Proceedings of the International Cyberspace Conference on Ergonomics: CybErg 1999.
- Lim, S., Martin, B. J., & Chung, M. K. (2004). The effects of target location on temporal coordination of the upper body during 3D seated reaches considering the range of motion. *International Journal of Industrial Ergonomics*, 34(5), 395-405.
- Lin, C. J., Ayoub, M. M., & Bernard, T. M. (1999). Computer motion simulation for sagittal plane lifting activities. *International Journal of Industrial Ergonomics*, 24(2), 141-155.
- Lindbeck, L., Karlsson, K., Kihlberg, S., Kjellberg, K., Rabenius, K., Stenlund, B., et al. (1997). A method to determine joint movements and force distributions in the shoulders during ceiling work - a study on house painters. *Clinical Biomechanics*, 12(7-8), 452-460.
- Lindbeck, L., & Kjellberg, K. (2001). Gender differences in lifting technique. *Ergonomics*, 44(2), 202-214.
- Lindstrom, I., Ohlund, C., & Nachemson, A. (1994). Validity of patient reporting and predictive value of industrial physical work demands. *Spine*, 19(8), 888-893.

- Linton, S. J. (2000). A review of psychological risk factors in back and neck pain. *Spine*, 25(9), 1148-1156.
- Loczi, J., & Dietz, M. (1999). *Paper 1999-01-1899: Posture and position validation of the 3-D CAD manikin RAMSIS for use in automotive design at General Motors*. Paper presented at the Proceedings of the Digital Human Modeling For Design And Engineering Conference And Exposition, Hague, The Netherlands.
- MacKinnon, C. D., & Winter, D. A. (1993). Control of whole body balance in the frontal plane during human walking. *Journal of Biomechanics*, 26(6), 633-644.
- Malchaire, J. B., Cock, N. A., & Robert, A. R. (1996). Prevalence of musculoskeletal disorders at the wrist as a function of angles, forces, repetitiveness and movement velocities. *Scandinavian Journal of Work and Environmental Health*, 22(3), 176-181.
- Marach, A., & Bubb, H. (2000). Development of a force-dependent posture prediction model for the CAD human model RAMSIS. In K. H. Landau (Ed.), *Ergonomic Software Tool in Product and Workplace Design* (pp. 105-113). Stuttgart: Verlag ERGON GmbH.
- Marley, R. J., & Duggasani, A. R. (1996). Effects of industrial back supports on physiological demand, lifting style and perceived exertion. *International Journal of Industrial Ergonomics*, 17(6), 445-453.
- Marras, W. S. (2000). Occupational low back disorder causation and control. *Ergonomics*, 43(7), 880-902.
- Marras, W. S., Davis, K. G., Kirking, B. C., & Granata, K. P. (1999). Spine loading and trunk kinematics during team lifting. *Ergonomics*, 42(10), 1258-1273.
- Marras, W. S., Jorgensen, M. J., & Davis, K. G. (2000). Effect of foot movement and an elastic lumbar back support on spinal loading during free-dynamic symmetric and asymmetric lifting exertions. *Ergonomics*, 43(5), 653-668.
- Massone, L., & Bizzi, E. (1989). A neural network model for limb trajectory formation. *Biological Cybernetics*, 61(6), 417-425.
- Matias, A. C., Salvendy, G., & Kuczek, T. (1998). Predictive models of carpal tunnel syndrome causation among VDT operators. *Ergonomics*, 41(2), 213-226.
- McCarthy, J. M. (1990). *An introduction to theoretical kinematics*. Cambridge, MA: The MIT Press.
- McGill, S. M. (1992). A myoelectrically based dynamic three-dimensional model to predict loads on lumbar spine tissues during lateral bending. *Journal of Biomechanics*, 25(4), 395-414.
- McGill, S. M., & Norman, R. W. (1986). Partitioning of the L4-L5 dynamic moment into disc, ligamentous, and muscular components during lifting. *Spine*, 11(7), 666-678.

- Messier, J., Adamovich, S., Berkinblit, M., Tunik, E., & Poizner, H. (2003). Influence of movement speed on accuracy and coordination of reaching movements to memorized targets in three-dimensional space in a deafferented subject. *Experimental Brain Research*, 150(4), 399-416.
- Milosavljevic, S., Milburn, P. D., & Knox, B. W. (2005). The influence of occupation on lumbar sagittal motion and posture. *Ergonomics*, 48(6), 657-667.
- Mirka, G. A., & Baker, A. (1996). An investigation of the variability in human performance during sagittally symmetric lifting tasks. *IIE Transactions*, 28(9), 745-752.
- Mirka, G. A., & Kelaher, D. P. (1995). *The effects of lifting frequency on the dynamics of lifting*. Paper presented at the Designing for the Global Village. Proceedings of the Human Factors and Ergonomics Society 39th Annual Meeting., San Diego, CA.
- Muggleton, J. M., Allen, R., & Chappell, P. H. (1999). Hand and arm injuries associated with repetitive manual work in industry: a review of disorders, risk factors and preventive measures. *Ergonomics*, 42(5), 714-739.
- Murray, W. M., Delp, S. L., & Buchanan, T. S. (1995). Variation of muscle moment arms with elbow and forearm position. *Journal of Biomechanics*, 28(5), 513-525.
- Nashner, L. M., & McCollum, C. (1985). The organization of human postural movements: a formal basis and experimental synthesis. *The Behavioral and Brain Sciences*, 8, 135-172.
- National Institute for Occupational Safety and Health (Ed.). (1997). *Musculoskeletal disorders and workplace factors*. Cincinnati, OH: National Institute for Occupational Safety and Health.
- National Research Council. (1999). *National Research Council Report: work-related musculoskeletal disorders: report, workshop summary, and workshop papers*. Washington, DC: The National Academy Press.
- Neumann, W. P., Wells, R. P., Norman, R. W., Kerr, M. S., Frank, J., Shannon, H. S., et al. (2001). Trunk posture reliability, accuracy, and risk estimates for low back pain from a video based assessment method. *International Journal of Industrial Ergonomics*, 28, 355-365.
- Nordstrom, D. L., Vierkant, R. A., DeStefano, F., & Layde, P. M. (1997). Risk factors for carpal tunnel syndrome in a general population. *Occupational and Environmental Medicine*, 54(10), 734-740.
- Nussbaum, M. A., & Chaffin, D. B. (1996). Evaluation of artificial neural network modelling to predict torso muscle activity. *Ergonomics*, 39(12), 1430-1444.
- Nussbaum, M. A., & Chaffin, D. B. (1997). Pattern classification reveals intersubject group differences in lumbar muscle recruitment during static loading. *Clinical Biomechanics*, 12(2), 97-106.

- Nussbaum, M. A., Martin, B. J., & Chaffin, D. B. (1997). A neural network model for simulation of torso muscle coordination. *Journal of Biomechanics*, 30(3), 251-258.
- Ohlsson, K., Attewell, R. G., Palsson, B., Karlsson, B., Balogh, I., Johnsson, B., et al. (1995). Repetitive industrial work and neck and upper limb disorders in females. *American Journal of Industrial Medicine*, 27(5), 731-747.
- Pandy, M. G., & Anderson, F. C. (2000). Dynamic simulation of human movement using large-scale models of the body. *Phonetica*, 57(2-4), 219-228.
- Pandy, M. G., Anderson, F. C., & Hull, D. G. (1992). A parameter optimization approach for the optimal control of large-scale musculoskeletal systems. *Journal of Biomechanical Engineering*, 114(4), 450-460.
- Pandy, M. G., Zajac, F. E., Sim, E., & Levine, W. S. (1990). An optimal control model for maximum-height human jumping. *Journal of Biomechanics*, 23(12), 1185-1198.
- Park, K. S. (1973). *A control systems simulation approach to a computerized model of human postures during symmetric sagittal plane lifting*. Unpublished Ph.D. Dissertation, The University of Michigan, Ann Arbor, MI.
- Park, W., Martin, B. J., Choe, S., Chaffin, D. B., & Reed, M. P. (2005). Representing and identifying alternative movement techniques for goal-directed manual tasks. *Journal of Biomechanics*, 38(3), 519-527.
- Pierrynowski, M. R., & Galea, V. (2001). Enhancing the ability of gait analyses to differentiate between groups: scaling gait data to body size. *Gait and Posture*, 13(3), 193-201.
- Pineda, F. J. (1987). Generalization of back-propagation to recurrent neural networks. *Physical Review Letters*, 59(19), 2229-2232.
- Prilutsky, B. I., Isaka, T., Albrecht, A. M., & Gregor, R. J. (1998). Is coordination of two-joint leg muscles during load lifting consistent with the strategy of minimum fatigue? *Journal of Biomechanics*, 31(11), 1025-1034.
- Punnett, L., & Beek, A. J. v. d. (2000). A comparison of approaches to modeling the relationship between ergonomic exposures and upper extremity disorders. *American Journal of Industrial Medicine*, 37(6), 645-655.
- Radwin, R. G., & Lavender, S. A. (1999). Work factors, personal factors, and internal loads: biomechanics of work stressors. In *Work-Related Musculoskeletal Disorders: Report, Workshop Summary, and Workshop Papers* (pp. 116-151). Washington, D.C.: The National Academy Press.
- Reed, M. P., Manary, M. A., Flannagan, C. A., & Schneider, L. W. (1999). *Automobile occupant posture prediction for use with human models* (SAE Technical Paper 1999-01-0966). Detroit, MI: Society of Automotive Engineers.

- Reed, M. P., Manary, M. A., Flannagan, C. A., & Schneider, L. W. (2000). Effects of vehicle interior geometry and anthropometric variables on automobile driving posture. *Human Factors*, 42(4), 541-552.
- Richter, B. S. (1998). Illness and injury among female employees at the US Department of Energy. *Journal of Occupational and Environmental Medicine*, 40(11), 994-998.
- Riener, R., & Fuhr, T. (1998). Patient-driven control of FES-supported standing up: a simulation study. *IEEE Transactions on Rehabilitation Engineering*, 6(2), 113-124.
- Rose, D. J. (1997). *A multilevel approach to the study of motor control and learning*. Boston: Allyn and Bacon.
- Ross, J. (1993a). A review of lower limb overuse injuries during basic military training. Part 1: Types of overuse injuries. *Military Medicine*, 158(6), 410-415.
- Ross, J. (1993b). A review of lower limb overuse injuries during basic military training. Part 2: Prevention of overuse injuries. *Military Medicine*, 158(6), 415-420.
- Rossetti, Y., Meckler, C., & Prablanc, C. (1994). Is there an optimal arm posture? Deterioration of finger localization precision and comfort sensation in extreme arm-joint postures. *Experimental Brain Research*, 99(1), 131-136.
- Sato, K. (1981). Dynamic analysis of higher order biological systems. *Advances in Biophysics*, 14, 37-138.
- Schipplein, O. D., Trafimow, J. H., Andersson, G. B., & Andriacchi, T. P. (1990). Relationship between moments at the L5/S1 level, hip and knee joint when lifting. *Journal of Biomechanics*, 23(9), 907-912.
- Schmidt, R. A., & Lee, T. D. (1999). *Motor control and learning: A behavioral emphasis* (3rd ed.). Champaign, IL: Human Kinetics.
- Schmitz, C., Martin, N., & Assaiante, C. (1999). Development of anticipatory postural adjustments in a bimanual load- lifting task in children. *Experimental Brain Research*, 126(2), 200-204.
- Scholz, J. P., & McMillan, A. G. (1995). Neuromuscular coordination of squat lifting, II: Individual differences. *Physical Therapy*, 75(2), 133-144.
- Scholz, J. P., Millford, J. P., & McMillan, A. G. (1995). Neuromuscular coordination of squat lifting, I: Effect of load magnitude. *Physical Therapy*, 75(2), 119-132.
- Schoner, G. (1990). A dynamic theory of coordination of discrete movement. *Biological Cybernetics*, 63(4), 257-270.
- Schouten, A. C., Vlugt, E. d., Helm, F. C. v. d., & Brouwn, G. G. (2001). Optimal posture control of a musculo-skeletal arm model. *Biological Cybernetics*, 84(2), 143-152.

- Seitz, T., & Bubb, H. (1999). *Measuring of human anthropometry, posture, and motion* (SAE Technical Report 1999-01-1913). Detroit, MI: Society of Automotive Engineers.
- Seth, V., Weston, R. L., & Freivalds, A. (1999). Development of a cumulative trauma disorder risk assessment model for the upper extremities. *International Journal of Industrial Ergonomics*, 23, 281-291.
- Smith, J. L., Ayoub, M. M., & McDaniel, J. W. (1992). Manual materials handling capabilities in non-standard postures. *Ergonomics*, 35(7-8), 807-831.
- Soechting, J. F., Buneo, C. A., Herrmann, U., & Flanders, M. (1995). Moving effortlessly in three dimensions: does Donders' law apply to arm movement? *Journal of Neuroscience*, 15(9), 6271-6280.
- Sommerich, C. M., McGlothlin, J. D., & Marras, W. S. (1993). Occupational risk factors associated with soft tissue disorders of the shoulder: a review of recent investigations in the literature. *Ergonomics*, 36(6), 697-717.
- Sparto, P. J., Parnianpour, M., Reinsel, T. E., & Simon, S. (1997a). The effect of fatigue on multijoint kinematics, coordination, and postural stability during a repetitive lifting test. *Journal of Orthopaedic and Sports Physical Therapy*, 25(1), 3-12.
- Sparto, P. J., Parnianpour, M., Reinsel, T. E., & Simon, S. R. (1997b). The effect of fatigue on multijoint kinematics and load sharing during a repetitive lifting test. *Spine*, 22(22), 2647-2654.
- Stitt, J. P., Gaumond, R. P., Frazier, J. L., & Hanson, F. E. (1998). Action potential classifiers: a functional comparison of template matching, principal components analysis and an artificial neural network. *Chemical Senses*, 23(5), 531-539.
- St-Onge, N., & Feldman, A. G. (2003). Interjoint coordination in lower limbs during different movements in humans. *Experimental Brain Research*, 148(2), 139-149.
- Taga, G. (1995a). A model of the neuro-musculo-skeletal system for human locomotion. I. Emergence of basic gait. *Biological Cybernetics*, 73(2), 97-111.
- Taga, G. (1995b). A model of the neuro-musculo-skeletal system for human locomotion. II Real-time adaptability under various constraints. *Biological Cybernetics*, 73(2), 113-121.
- Tamura, S., & Tateishi, M. (1997). Capabilities of a four-layered feedforward neural network: Four layers versus three. *IEEE Transactions on Neural Networks*, 8(2), 251-255.
- Tecmath. (2001). *Human Solutions - ANTHROPOS*. Retrieved December 4, 2001, from http://www.hs.tecmath.de/english/anthropos_eng.shtml
- Thoroughman, K. A., & Shadmehr, R. (1999). Electromyographic correlates of learning an internal model of reaching movements. *Journal of Neuroscience*, 19(19), 8573-8588.

- Todorov, E., & Jordan, M. I. (2002). Optimal feedback control as a theory of motor coordination. *Nature Neuroscience*, 5(11), 1226-1235.
- Touretzky, D. S., & Pomerleau, D. A. (1989). What's hidden in the hidden layers? *Byte*, 227-233.
- Trafimow, J. H., Schipplein, O. D., Novak, G. J., & Andersson, G. B. (1993). The effects of quadriceps fatigue on the technique of lifting. *Spine*, 18(3), 364-367.
- Tulder, M. W. v., Assendelft, W. J., Koes, B. W., & Bouter, L. M. (1997). Spinal radiographic findings and nonspecific low back pain. A systematic review of observational studies. *Spine*, 22(4), 427-434.
- van Schaik, C. S., Hicks, A. L., & McCartney, N. (1994). An evaluation of the length-tension relationship in elderly human ankle dorsiflexors. *Journal of Gerontology*, 49(3), B121-127.
- Vaughn, M. L., Cavill, S. J., Taylor, S. J., Foy, M. A., & Fogg, A. J. B. (2000, May 13-16, 2000). *The use of a knowledge discovery method for the development of a multi-layer perceptron network that classifies low back pain patients*. Paper presented at the Artificial Neural Networks in Medicine and Biology - Proceedings of the ANNIMAB Conference, Goteborg, Sweden.
- Vender, M. I., Kasdan, M. L., & Truppa, K. L. (1995). Upper extremity disorders: a literature review to determine work-relatedness. *Journal of Hand Surgery - American*, 20(4), 534-541.
- Verriest, J. P., Trasobt, J., & Rebiffe, R. (1991). *MAN3D: a functional and geometrical model of the human operator for computer aided ergonomic design*. Paper presented at the Advances in Industrial Ergonomics and Safety III.
- Vingard, E., Alfredsson, L., Hagberg, M., Kilbom, A., Theorell, T., Waldenstrom, M., et al. (2000). To what extent do current and past physical and psychosocial occupational factors explain care-seeking for low back pain in a working population? Results from the Musculoskeletal Intervention Center-Norrtaälje Study. *Spine*, 25(4), 493-500.
- Wang, X. (1999). A behavior-based inverse kinematics algorithm to predict arm prehension postures for computer-aided ergonomic evaluation. *Journal of Biomechanics*, 32(5), 453-460.
- Warren, N., Dillon, C., Morse, T., Hall, C., & Warren, A. (2000). Biomechanical, psychosocial, and organizational risk factors for WRMSD: population-based estimates from the Connecticut upper-extremity surveillance project (CUSP). *Journal of Occupational Health Psychology*, 5(1), 164-181.
- Weisman, G., Clark, A. A., Haugh, L. D., & Pope, M. H. (1992). Assessing variability in isokinetic strength through a range of motion. *International Journal of Industrial Ergonomics*, 9(2), 117-126.

- Werness, S. A., & Anderson, D. J. (1984). Parametric analysis of dynamic postural responses. *Biological Cybernetics*, 51(3), 155-168.
- Westgaard, R. H., Jensen, C., & Hansen, K. (1993). Individual and work-related risk factors associated with symptoms of musculoskeletal complaints. *International Archives of Occupational and Environmental Health*, 64(6), 405-413.
- Whiting, H. T. A. (Ed.). (1984). *Human motor actions: Bernstein reassessed* (Vol. 17). Amsterdam: North Holland.
- WHO. (1995). *Global Strategy on occupational health for all: the way to health at work*. Geneva, Switzerland: World Health Organization.
- Wiker, S. F. (1992). Posturally-mediated perceptions of strain encountered when lifting: a preliminary analysis of the basis and value in predicting worker posture. In M. Mattila & W. Karwowski (Eds.), *Computer Applications in Ergonomics, Occupational Safety and Health* (pp. 497-509). Amsterdam: North-Holland.
- Williams, R. J., & Zipser, D. (1989). A learning algorithm for continually running fully recurrent neural networks. *Neural Computation*, 1, 270-280.
- Windhorst, U. (1996). On the role of recurrent inhibitory feedback in motor control. *Progress in Neurobiology*, 49(6), 517-587.
- Windt, D. A. v. d., Thomas, E., Pope, D. P., Winter, A. F. d., Macfarlane, G. J., Bouter, L. M., et al. (2000). Occupational risk factors for shoulder pain: a systematic review. *Occupational and Environmental Medicine*, 57(7), 433-442.
- Winter, D. A., MacKinnon, C. D., Ruder, G. K., & Wieman, C. (1993). An integrated EMG/biomechanical model of upper body balance and posture during human gait. *Progress in Brain Research*, 97, 359-367.
- Woldstad, J. C. (1997). *Further evaluations of a revised posture prediction algorithm for static lifting*. Paper presented at the Advances in Occupational Ergonomics and Safety II.
- Yang, J. F., Winter, D. A., & Wells, R. P. (1990a). Postural dynamics in the standing human. *Biological Cybernetics*, 62(4), 309-320.
- Yang, J. F., Winter, D. A., & Wells, R. P. (1990b). Postural dynamics of walking in humans. *Biological Cybernetics*, 62(4), 321-330.
- Young, M. F. (1995). *An heuristic approach to upper limb posture prediction and analysis*. Unpublished Master's Thesis, The University of Utah.
- Zatsiorsky, V. M. (1998). Kinematics of human motion (pp. 432). Champaign, IL: Human Kinetics.

- Zhang, X., & Buhr, T. (2002). Are back and leg muscle strengths determinants of lifting motion strategy? Insight from studying the effects of simulated leg muscle weakness. *International Journal of Industrial Ergonomics*, 29, 161-169.
- Zhang, X., & Chaffin, D. B. (2000). A three-dimensional dynamic posture prediction model for simulating in- vehicle seated reaching movements: development and validation. *Ergonomics*, 43(9), 1314-1330.
- Zhang, X., Chaffin, D. B., & Thompson, D. (1997). *Development of dynamic simulation models of seated reaching motions while driving* (No. Progress with human factors in automotive design: seating comfort, visibility, and safety; SP-1242). Warrendale, PA: Society of Automotive Engineers.
- Zhang, X., Kuo, A. D., & Chaffin, D. B. (1998). Optimization-based differential kinematic modeling exhibits a velocity- control strategy for dynamic posture determination in seated reaching movements. *Journal of Biomechanics*, 31(11), 1035-1042.
- Zhao, J., & Badler, N. I. (1994). Inverse kinematics positioning using nonlinear programming for highly articulated figures. *ACM Transactions on Graphics*, 13(4), 315-336.